

Disclaimer

This Report, including the data and information contained in this Report, is provided to you on an “as is” and “as available” basis at the sole discretion of the Government of Alberta and subject to the terms and conditions of use below (the “Terms and Conditions”). The Government of Alberta has not verified this Report for accuracy and does not warrant the accuracy of, or make any other warranties or representations regarding, this Report. Furthermore, updates to this Report may not be made available. Your use of any of this Report is at your sole and absolute risk.

This Report is provided to the Government of Alberta, and the Government of Alberta has obtained a license or other authorization for use of the Reports, from:

Shell Canada Energy, Chevron Canada Limited. and Marathon Oil Canada Corporation, for the Quest Project

(collectively the “Project”)

Each member of the Project expressly disclaims any representation or warranty, express or implied, as to the accuracy or completeness of the material and information contained herein, and none of them shall have any liability, regardless of any negligence or fault, for any statements contained in, or for any omissions from, this Report. Under no circumstances shall the Government of Alberta or the Project be liable for any damages, claims, causes of action, losses, legal fees or expenses, or any other cost whatsoever arising out of the use of this Report or any part thereof or the use of any other data or information on this website.

Terms and Conditions of Use

Except as indicated in these Terms and Conditions, this Report and any part thereof shall not be copied, reproduced, distributed, republished, downloaded, displayed, posted or transmitted in any form or by any means, without the prior written consent of the Government of Alberta and the Project.

The Government of Alberta’s intent in posting this Report is to make them available to the public for personal and non-commercial (educational) use. You may not use this Report for any other purpose. You may reproduce data and information in this Report subject to the following conditions:

- any disclaimers that appear in this Report shall be retained in their original form and applied to the data and information reproduced from this Report
- the data and information shall not be modified from its original form
- the Project shall be identified as the original source of the data and information, while this website shall be identified as the reference source, and
- the reproduction shall not be represented as an official version of the materials reproduced, nor as having been made in affiliation with or with the endorsement of the Government of Alberta or the Project

By accessing and using this Report, you agree to indemnify and hold the Government of Alberta and the Project, and their respective employees and agents, harmless from and against any and all claims, demands, actions and costs (including legal costs on a solicitor-client basis) arising out of any breach by you of these Terms and Conditions or otherwise arising out of your use or reproduction of the data and information in this Report.

Your access to and use of this Report is subject exclusively to these Terms and Conditions and any terms and conditions contained within the Report itself, all of which you shall comply with. You will not use this Report for any purpose that is unlawful or prohibited by these Terms and Conditions. You agree that any other use of this Report means you agree to be bound by these Terms and Conditions. These Terms and Conditions are subject to modification, and you agree to review them periodically for changes. If you do not accept these Terms and Conditions you agree to immediately stop accessing this Report and destroy all copies in your possession or control.

These Terms and Conditions may change at any time, and your continued use and reproduction of this Report following any changes shall be deemed to be your acceptance of such change.

If any of these Terms and Conditions should be determined to be invalid, illegal or unenforceable for any reason by any court of competent jurisdiction then the applicable provision shall be severed and the remaining provisions of these Terms and Conditions shall survive and remain in full force and effect and continue to be binding and enforceable.

These Terms and Conditions shall: (i) be governed by and construed in accordance with the laws of the province of Alberta and you hereby submit to the exclusive jurisdiction of the Alberta courts, and (ii) ensure to the benefit of, and be binding upon, the Government of Alberta and your respective successors and assigns.



Heavy Oil

Controlled Document

Quest CCS Project

Second Annual Status report to AER

Project	Quest CCS Project
Document Title	Second Annual Status report to AER
Document Number	07-3-AA-5706-0006
Document Revision	0
Document Status	Issued for Information
Document Type	5706 – Assurance plan
Control ID	NA
Owner / Author	Mauri Smith
Issue Date	2014-01-31
Expiry Date	None
ECCN	EAR 99
Security Classification	Unclassified
Disclosure	None


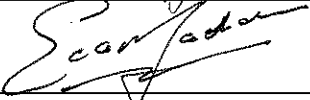
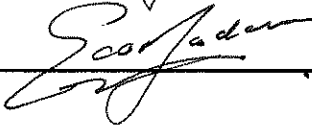
Revision History shown on next page

Revision History

REVISION STATUS			APPROVAL		
Rev.	Date	Description	Originator	Reviewer	Approver
0	2014-01-31	For information	Mauri Smith	Sean McFadden	Sean McFadden

- All signed originals will be retained by the UA Document Control Center and an electronic copy will be stored in Livelink

Signatures for this revision

Date	Role	Name	Signature or electronic reference (email)
	Originator	Mauri Smith	
	Reviewer	Sean McFadden	
	Approver	Sean McFadden	

Summary

Keywords

07-3-AA-5706-0006		0
Heavy Oil		

SHELL CANADA LIMITED

Quest Carbon Capture and Storage Project

SECOND ANNUAL STATUS REPORT

Prepared By:
Shell Canada Limited
Calgary, Alberta

January 31, 2014

Page Intentionally Blank

The Second Annual Status Report addresses the AER application approval referenced in the Carbon Dioxide Disposal Approval No. 11837A, issued on August 8th 2013 to Shell Canada Limited [1]. This report addresses the Conditions 10 and 14 required by January 31, 2014. Outstanding information regarding BCS fall-off test results required to complete Condition 11c is also included here-in.

In addition, test results of the CO₂ entry pressure tests are included as Appendix F as per Condition 5 in the letter received by Shell from the AER on December 3, 2013 due January 31, 2014 [2].

Page Intentionally Blank

Table of Contents

PREPARED BY:.....|

TABLE OF CONTENTS.....|

1. SPECIFIC REQUIREMENTS 1

2. CONSTRUCTION AND SCHEME OPERATIONS UPDATE4

 2.1. Capture and Pipeline Construction4

 2.2. Project Wells.....5

 2.3. Well Workovers & Treatments8

 2.3.1. *Injection Wells Completions*..... 8

 2.3.2. *Deep Monitoring Wells Completions*..... 9

 2.3.3. *Groundwater Wells Completions* 9

3. INJECTION AND GROUNDWATER WELL SUMMARY11

 3.1. Injection Wells Geology Update11

 3.2. Deep Monitoring Wells.....14

 3.2.1. *Geologic Summary*..... 14

 3.3. Groundwater Wells16

 3.3.1. *Geologic Summary*..... 16

 3.3.2. *Petrophysical Summary*..... 16

4. BCS RESERVOIR PRESSURE ANALYSIS17

 4.1. IW 5-35 Production Test17

 4.2. IW 7-11 Production Test18

 4.3. Well Test Results Summary19

 4.4. Pressure Transient Analysis.....20

 4.5. Well Test PTA Derivative Plots.....21

 4.5.1. *Permeability Comparison of Well Tests and Core Results* 23

5. RESERVOIR MODELLING25

 5.1. Model Updates25

 5.2. Future Static Model Updates.....25

 5.3. Dynamic Model Updates.....25

 5.3.1. *Pressure Prediction*..... 25

 5.3.2. *Plume Prediction* 26

6. MMV PLAN ACTIVITIES, PERFORMANCE AND RESULTS27

 6.1. Summary of MMV Operations and Maintenance Activities.....27

 6.1.1. *Atmospheric Monitoring – LightSource* 27

 6.1.2. *Biosphere Monitoring Activities*..... 28

 6.1.3. *Hydrosphere Monitoring Activities* 28

 6.1.4. *Geosphere Monitoring Activities* 29

 6.1.5. *In-Well Monitoring Activities* 31

Table of Contents

6.2. MMV Performance or Plan Issues	31
6.3. New MMV Data Collected	32
6.4. Proposed Changes to Current MMV Plan.....	33
6.4.1. Atmosphere – LightSource	33
6.4.2. Biosphere	33
6.4.3. Hydrosphere	34
7. MONITORING WELLS	37
7.1. Need for Monitoring Wells near Periphery of Pressure Build-up	37
7.2. Need for Additional Monitoring Wells near Legacy Wells.....	37
7.3. Monitoring at Injection wells.....	37
8. STAKEHOLDER ENGAGEMENTS.....	39
8.1. Government Authority Updates.....	39
8.2. Public Information Sessions	39
8.3. MMV plan community involvement through CAP	40
9. CONSTRUCTION AND IMPLEMENTATION TEST RESULTS	41
REFERENCES	44
APPENDIX A: BCS CORE DESCRIPTIONS FOR IW 5-35 AND IW 7-11	XLVII
APPENDIX B: DETAILED FORMATION EVALUATION FINDINGS	XLVIII
APPENDIX C –PETROPHYSICAL EVALUATION OF GROUNDWATER WELLS	XL
APPENDIX D –ARTIFICIAL TRACER INTERIM FEASIBILITY REPORT	XLI
APPENDIX E – GOLDER HBMP RESULTS FALL 2012 TO END 2013.....	XLI
APPENDIX F – MCS CO2 ENTRY PRESSURE RESULTS FOR IW 8-19.....	XL

1. Specific Requirements

1. SPECIFIC REQUIREMENTS

The following Table 1-1 lists the requirements for Annual Reporting as listed in the AER QUEST Project Approval No 11837A, and the corresponding Section in this report:

Table 1-1 Concordance Table

Requirement as listed in the ERCB Quest Project Approval No 11837A	Section
10) The Approval Holder must provide annual status reports and presentations. The reports must be aligned with the most current MMV plan and submitted to ResourceCompliance@aer.ca. The report must be in metric units and include:	
a) a summary of scheme operations including, but not limited to,	2, 2.1
i) any new project wells drilled in the reporting period,	2.2
ii) any workovers/treatments done on the injection and monitoring wells including the reasons for and results of the workovers/treatments,	2.3
iii) changes in injection equipment and operations,	2.3.1
iv) identification of problems, remedial action taken, and impacts on scheme performance.	6.2
b) complete pressure analysis including but not limited to stabilized shut-in formation pressures and a discussion on how the pressure compares with the formation pressure expected for the cumulative volume of CO ₂ injection, along with an updated estimate of what the actual cumulative injection volume will be at the maximum shut-in formation pressure specified in clause 5) a),	4.0
c) discussion of the overall performance of the scheme, including: how the formation pressure is changing over time; updated geological maps; and updated CO ₂ plume extent and pressure distribution models, if needed. The updated models should be based on all new data obtained since the last model run including the cumulative CO ₂ injected to the end of the reporting period.	5.0
d) a summary of MMV Plan activities, performance and results in the reporting period, including, but not limited to:	6.0
i) a report on any event that exceeded the approved operating requirements or triggered MMV activities,	N/A
ii) comparison of measured performance to predictions,	N/A
iii) summary of operations and maintenance activities conducted,	6.1

1. Specific Requirements

Requirement as listed in the AER Quest Project Approval No 11837A	Section
iv) details of any performance or MMV Plan issues that require attention,	6.2
v) pressure surveys, corrosion protection, fluid analyses, logs and any other data collected that would help in determining the success of the scheme, and	3.1, 6.3
vi) discussion of the need for changes to the MMV plan.	6.4
e) a table for all wells listed in clause 3)(1) a), showing the following injection data for each month of the reporting period:	N/A
i) mole fraction of the CO ₂ and impurities in the injection stream,	N/A
ii) volume of the CO ₂ injected at standard conditions,	N/A
iii) formation volume factor of the injected CO ₂ stream,	N/A
iv) cumulative volume of the injected CO ₂ at standard conditions following the commencement of the scheme,	N/A
v) volume of the CO ₂ injected at reservoir conditions,	N/A
vi) hours on injection,	N/A
vii) maximum daily injection rate at standard conditions,	N/A
viii) average daily injection rate at standard conditions,	N/A
ix) maximum wellhead injection pressure (MWHIP) and corresponding wellhead injection temperature,	N/A
x) average wellhead injection pressure, corresponding average wellhead injection temperature,	N/A
xi) maximum bottom hole injection pressure (MBHIP) at the top of injection interval and the corresponding bottom hole injection temperature, and	N/A
xii) average bottom hole injection pressure at the top of injection interval and the corresponding average bottom hole injection temperature.	N/A
f) a table showing the volumes of injected CO ₂ on a monthly and cumulative basis,	N/A
g) Hall Plots of constant average reservoir pressure where unexplained anomalous injection rate and pressure data could indicate fracturing.	N/A
h) a plot showing the following daily average data at standard conditions versus time since the commencement of CO ₂ injection:	N/A
i) daily CO ₂ injection rate,	N/A
ii) wellhead and bottom hole injection pressure, and	N/A

1. Specific Requirements

Requirement as listed in the AER Quest Project Approval No 11837A	Section
iii) estimated or measured average reservoir pressure in the BCS formation.	4.5
i) the potential need for installing additional monitoring towards the periphery of the pressure build up area later in the project life,	7.1
j) evaluate the need for additional deep monitoring wells adjacent to the four legacy wells in the approval area. Based on the information provided the ERCB may require the Approval Holder to drill one or more such deep monitoring wells, and	7.2
k) discussion of stakeholder engagement activities in the reporting period.	8
11 c) the initial baseline BCS fall-off test analyses of 00/08-19-059-20W400 and any other drilled injection wells.	4.5
14) The Approval Holder must provide its second annual status report by January 31, 2014. The report must include all the relevant requirements listed in clause 10). As well, this report must include updates, conclusions, and reviews of:	
a) geology update from new injection wells	3.1
b) initial injection well drilling and testing, and need for additional injection wells, and	4.3
c) any testing results in relation to construction and implementation activities	9
Appropriate requirement as listed in the AER pre-baseline MMV approval Dec.3 2013 [7]	Section
5) Shell must submit the results of the CO₂ entry pressure tests which were not available at the time of submission of the October 15, 2012 Special Report #1.	Appendix F
7) b) The Approval Holder must submit the initial fall-off test analysis of the 00/08-19-059-20W400 well as per Approval Condition 11c (above).	4.5

N/A means that the specific requirement is not applicable at this time.

2. CONSTRUCTION AND SCHEME OPERATIONS UPDATE

2.1. Capture and Pipeline Construction

Overall progress for Capture and Pipeline as of December 31, 2013 includes the following:

- Engineering: 99% complete
- Procurement: 96% complete
- Module fabrication: 55% complete
- Capture site Construction: 30% complete
- Pipeline construction : 34% complete
- Approximately 1.03 million Construction field man hours to date (including the module yard), with 2 medical aid incidents and 19 First Aids
- 957 engineering work packages issued for construction in capture areas and all drawing issued for construction for the pipeline. Majority (or 84%) of major equipment has been received at site or at the module yard.
- D 56 regulatory approve received for the pipeline laterals. .
- Horizontal drill under the North Saskatchewan River is complete. Pipeline construction has cleared, graded and strung pipe for the full right of way including laterals. Welding has completed 21 kilometers, installed and backfilled 4.5 kilometers.
- 42 of 336 crossing are complete on the pipeline
- Early works site construction completed the underground cooling water, CO2 pipeline, firewater and potentially oily water server line installations as well as the underground electrical cable installation. All piling and concrete foundations are installed.
- Flue gas Recycle in HMU #2 steam methane reformer was installed and tested
- During the 2013 turnaround in HMU #2 low NOx burners were installed, the fill replaced in the pressure swing absorbers and all tie-ins for the project were completed.
- 9 pipe rack modules have been received and set at site, with addition three modules ready to ship and 33 others in various stages of erection.

Current schedule forecasts show that mechanical completion will occur in Q1 of 2015. Commissioning and start up activities will follow in Q2 2015 as well as the final shutdown of the HMU #1 area and Base Upgrader allowing the final tie-ins to those areas. The capture unit and HMU3 absorber will start up late in Q2 2015. Filling of the

pipeline and first injection will come from HMU3 in early Q3 2015. HMU1 and 2 absorbers will be commissioned next and full production is expected Q4 of 2015.

2.2. Project Wells

Shell has completed drilling all the wells (Table 2-1) currently planned for the operations phase of the Project. The third deep monitoring well, 102-07-11-059-20W400 (DMW 7-11) was drilled from January 23rd to February 5th 2013 and hence not included in the first annual status report submitted on January 31, 2013. In addition, the four remaining shallow project groundwater wells, 2 located at each of the injection well pads 5-35-59-21W4 and 7-11-59-20W4, were drilled in February 2013. Table 2-1 is a synopsis of all the completed drilling activity for the Quest Project. Only wells drilled/completed in 2013 are discussed herein. No more wells are expected to be drilled for this Project unless required as per the Conditions in AER approval 11837A [1].

Post drilling, Shell identified surface casing vent flows in all deep monitoring and injection wells as well as gas migrations in injection wells IW 7-11 and IW 5-35 (Table 2-1). See Section 6.2 for further details.

2. Construction And Operations Updates

Table 2-1 Quest Well Summary

UWI	Well type	Well name in this report	Spud date [d/m/y]	Rig release [d/m/y]	Total Depth [m MD]	TD formation
1AA/11-32-055-21W400	Appraisal (Abandoned)	Redwater 11-32	10/11/2008	02/01/2009	2240.6	Precambrian
100/03-04-057-21W400	Observation	Redwater 3-4	23/01/2009	18/03/2009	2190.0	Precambrian
100/081905920W4/00	Injection	IW 8-19	01/08/2010	08/09/2010	2132.0	Precambrian
102/081905920W4/00	Deep Monitoring	DMW 8-19	30/09/2012	15/10/2012	1696.0	Ernestina Lake
102/053505921W4/00	Injection	IW 5-35	21/10/2012	20/11/2012	2143.0	Precambrian
100/053505921W4/00	Deep Monitoring	DMW 5-35	24/11/2012	06/12/2012	1710.0	Ernestina Lake
103/071105920W4/00	Injection	IW 7-11	14/12/2012	20/01/2013	2105.0	Precambrian
102/071105920W4/00	Deep Monitoring	DMW 7-11	23/01/2013	05/02/2013	1664.5	Ernestina Lake
1F1/081905920W4/00	Groundwater	GW 1F1/8-19	08/12/2010	08/01/2011	201	Lea Park
UL1/081905920W4/00*	Groundwater	GW UL1/8-19	14/01/2011	17/01/2011	101.0	Foremost
UL2/081905920W4/00*	Groundwater	GW UL2/8-19	12/01/2011	13/01/2011	62.8	Foremost
UL3/081905920W4/00*	Groundwater	GW UL3/8-19	09/01/2011	10/01/2011	37.5	Foremost
UL4/081905920W4/00*	Groundwater	GW UL4/8-19	11/01/2011	11/01/2011	20.0	Oldman
1F1/053505921W4/00	Groundwater	GW 1F1/5-35	08/02/2013	17/02/2013	200	Lea Park
UL1/053505921W4/00*	Groundwater	GW UL1/5-35	17/02/2013	18/02/2013	23	Foremost
1F1/071105920W4/00	Groundwater	GW 1F1/7-11	19/02/2013	26/02/2013	180	Lea Park
UL1/071105920W4/00*	Groundwater	GW UL1/7-11	26/02/2013	27/02/2013	30.7	Foremost

Legend: *: well name used in Shell but not official UWIs as these wells do not require a well licensed because they are less than 150m depth

- DMW 7-11
 - UWI: 102/071105920W4/00
 - Well type: Deep Monitoring Well
 - Spud date: January 23, 2013
 - Rig release: February 5, 2013
 - TD – depth, formation: 1664.5m MD, Ernestina Lake
 - Logging program: TLD-HNGS-ECS-AIT, GR-GPIT-Sonic Scanner-PPCX2-UBI, CMR-APS-HNGS, XPT, MDT
 - Core: 1261 – 1279 mMD, Moberly, 100% recovery
 - Fluid/gas sampling
 - MDT: Glauconite Sandstone at 778.0 mMD and Cooking Lake at 1138.8 mMD

- GW 1F1/5-35
 - UWI: 1F1/05-35-059-21W4/00
 - Well type: Groundwater Monitoring Well
 - Spud date: February 8, 2013
 - Rig release: February 17, 2013 (rig moved to location UL1/05-35)
 - TD – depth, formation: 200 mMD, Lea Park
 - Logging program: Induction imager (AIT), lithodensity (TLD), compensated neutron (CNL), gamma ray (GR), 4-arm caliper (PPC), and borehole compensated sonic (BHC) – Open Hole. USIT/CBL – Within 178mm casing
 - Fluid/gas sampling:
 - Water sample: 116.44 m below ground surface (Well Screen Midpoint)
 - Isotube (mud gas): at selected depths while drilling from surface to TD

- GW UL1/5-35
 - Unlicensed well name: UL1/05-35-059-21W4/00
 - Well type: Groundwater Monitoring Well
 - Spud date: February 17, 2013
 - Rig release: February 18, 2013 (rig moved to location 1F1/07-11)
 - TD – depth, formation: 23.5 mMD, Foremost
 - Fluid/gas sampling:
 - Water sample: 21.5 m below ground surface (Well Screen Midpoint)
 - Isotube (mud gas): at selected depths while drilling from surface to TD

- GW 1F1/7-11
 - UWI: 1F1/07-11-059-20W4/00
 - Well type: Groundwater Monitoring Well
 - Spud date: February 19, 2013
 - Rig release: February 26, 2013 (rig moved to location UL1/07-11)
 - TD – depth, formation: 180 mMD, Lea Park
 - Logging program: Induction imager (AIT), lithodensity (TLD), compensated neutron (CNL), gamma ray (GR), 4-arm caliper (PPC), and borehole compensated sonic (BHC) – Open Hole. USIT/CBL – Within 178mm casing
 - Fluid/gas sampling:
 - Water sample: 125.9 m below ground surface (Well Screen Midpoint)
 - Isotube (mud gas): at selected depths while drilling from surface to TD

- GW UL1/7-11
 - Unlicensed well name: UL1/07-11-059-20W4/00
 - Well type: Groundwater Monitoring Well
 - Spud date: February 26, 2013
 - Rig release: February 27, 2013
 - TD – depth, formation: 31 mMD, Foremost
 - Fluid/gas sampling:
 - Water sample: not collected due to extremely low recovery however sampled were recovered in following sample campaigns associated with the Hydrosphere Biosphere Monitoring Program (HBMP).

2.3. Well Workovers & Treatments

2.3.1. Injection Wells Completions

The final completion in the injection wells was executed this year in the following sequence: IW 8-19, IW 5-35 and then IW 7-11. There were no complications encountered during the completion operations. However, post-completion a perforation depth error in IW 5-35 was identified (see Section 6.2). The IW 5-35 and IW 7-11 were production tested and then suspended with a plug in the packer tail and a column of inhibited fluid (KCl). All three injection wells, IW 8-19, 7-11 and 5-35 are currently suspended as per the above.

Although it was originally proposed to complete the injection wells with a temporary 3 ½" J55 tubing for testing purposes and subsequently suspend the wells and complete them at a later date (2014) with up to 4 ½" inch tubing, the preliminary log analysis indicated that the reservoir quality had sufficiently high permeability that the 3 ½" J55

tubing could be left as the final completion. The packer assembly (packer + packer tail + on-off tool) are IPC 3000 coated, which is suitable for (wet) CO₂ service. After D-51 approval, the wells will be unsuspending and conditioning for injection by pumping them full of CO₂ prior to commencement of injection in 2015.

There have been no changes in the injection operations plan since the 2013 annual status report submission.

2.3.2. *Deep Monitoring Wells Completions*

The current preferred MMV formation is the Cooking Lake Formation (CKLK). The DMW 5-35 and DMW 7-11 wells were perforated and equipped with a permanent downhole pressure gauge in order to acquire baseline pressure data in the Cooking Lake. These gauges are hooked up to a surface read-out and recording device, but do not have power. The gauges are expected to have power supplied and start continuously recording data in Q1 2014. The DMW 8-19 is expected to be completed in the CKLK in Q3 2014. Furthermore, the Redwater 3-4 well is proposed to be completed in both the CKLK and BCS in Q2 2014. The addition of the CKLK interval in Redwater 3-4 for pressure monitoring is conditional on the outcome of further regional CKLK studies and Alberta Energy approval to monitor the CKLK formation in addition to the BCS in that well.

2.3.3. *Groundwater Wells Completions*

The groundwater wells 1F1/05-35-059-21W4/00 and 1F1/07-11-059-20W4/00 were completed as soon as the pilot boreholes at each of those locations were drilled, evaluated, and the target screen interval was selected. A portion of the borehole was abandoned (backfilled) using time delayed bentonite pellets (peltonite) and a retrievable bridge plug. Sand was then tremied above both the retrievable bridge plug and the selected screen interval. This was followed by reaming the pilot borehole and installment and cementing in place of the casing. After the cement shoe and sand pack were drilled out, a six inch telescope pre-pack 316 L stainless steel wire wrap screen, five inch ID stainless steel blank sections, and two K-packers were installed. After the screen installation, the screen was washed using a jetting tool.

The target depth of the boreholes for groundwater wells UL1/05-35-059-21W4/00 and UL1/07-11-059-20W4/00 was selected based upon evaluation of the nearby 1F1 wells on each pad. After reaching the target borehole depth, a pipe based screen and casing were run into the hole. The screen consisted of 304 L stainless steel wire wrap screen. The screen and casing were suspended so that the screen was at the target interval. Sand was then tremied around the screen. Time delayed bentonite pellets (peltonite) were tremied above the sand. The casing was then bentonite grouted to 1.5 mbgs and cement grouted

to 1 mbgs. The grout was allowed to set and the wells were developed by washing the screen using a jetting tool and by pumping.

3. INJECTION AND GROUNDWATER WELL SUMMARY

3.1. Injection Wells Geology Update

No new injection wells were drilled in this reporting period. However, it is confirmed based on 2012 drilling that the stratigraphic framework within the QUEST project area is as expected. Table 3-1 provides a summary of the formation thicknesses within the BCS storage complex and selected overlying formations up to the top of the Quest Sequestration Lease rights for IW 8-19, IW 5-35 and IW 7-11. The formation thicknesses observed within the 'new' injection wells IW 5-35 and IW 7-11 are very similar (almost identical) to those that were observed in IW 8-19. For instance, the BCS has a thickness of 47m in IW 8-19 versus 43 m in IW 5-35, and the MCS has a thickness of 52 m in IW 8-19 versus 51 m in IW 5-35. The differences between actual depth and prognosed (prog) formation thickness are also shown for the new IW 5-35 and 7-11 and are as expected.

With regards to the BCS reservoir properties, good agreement was observed between core analyses and log data (Figure 3-1). For a detailed description of the BCS Formation reservoir properties (e.g. porosity), please refer to Appendix A and B of the First Annual Status Report [2] and Appendix A attached hereto for the core descriptions. This report only provides the additional updated information not available at time of the previous submission.

Table 3-1 Summary of zone thicknesses for Quest Sequestration rights interval

Injection Wells			thickness (m) & actual vs prog (m)				
			8-19	5-35		7-11	
Seal	Prairie Evap./ Lo Prairie Evap.	126	122	+5	127	-4	
	Winnipegosis/ Contact Rapids	75	72	-7	70	-4	
BCS Storage Complex	Seal	Upper Lotsberg	84	83	0	89	+3
	Seal	Lower Lotsberg	35	36	+2	36	+1
	Seal	MCS	52	51	+1	50	-4
		LMS					
	Injection Target	BCS	47	43	-4	42	-6
	PreCam						

3. Injection and Groundwater Summary

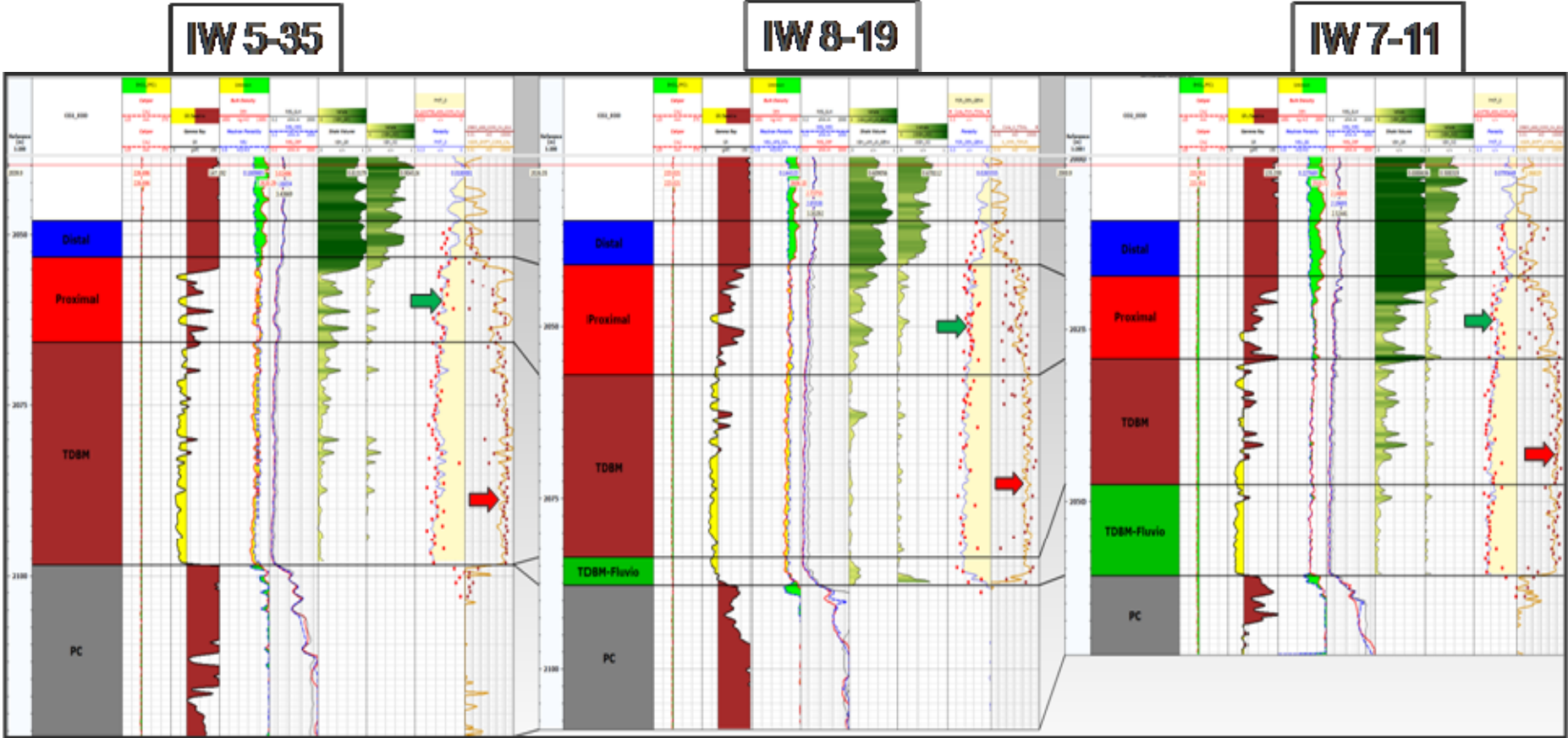


Figure 3-1 Comparison of log response over the BCS formation and the corresponding core analysis results in all three injection wells. The green arrows are pointing to the porosity track, very good correspondence between the core porosity and log porosity. The red arrows are pointing at the permeability track, a good agreement between the log and core permeability in IW 5-35 whereas the correspondence is better in IW 7-11

Based on the IW 5-35 and IW 7-11 BCS cores, the depositional environment was interpreted to be consistent with IW 8-19, as illustrated in Table 3-2 and Appendix A.

Table 3-2: Depositional Environment in LMS-BCS for the injection wells from core data.

Depositional Paleo-Environment	IW 8-19, thickness (m)	IW 5-35, thickness (m)	IW 7-11, thickness (m)
Distal Bay	11*	5*	8*
Proximal Bay	10	12	11
Tide Dominated Bay Margin (TDBM)	25	30	17
TDBM (Fluvial Influenced)	4.5	2.4	13

* Based on core data only – log data indicates that that Distal Bay is significantly thicker.

Consistency was also observed with regards to the geochemical composition of the BCS Formation brine from IW 5-35 and IW 7-11 compared to IW 8-19, as illustrated in Figure 3-2.

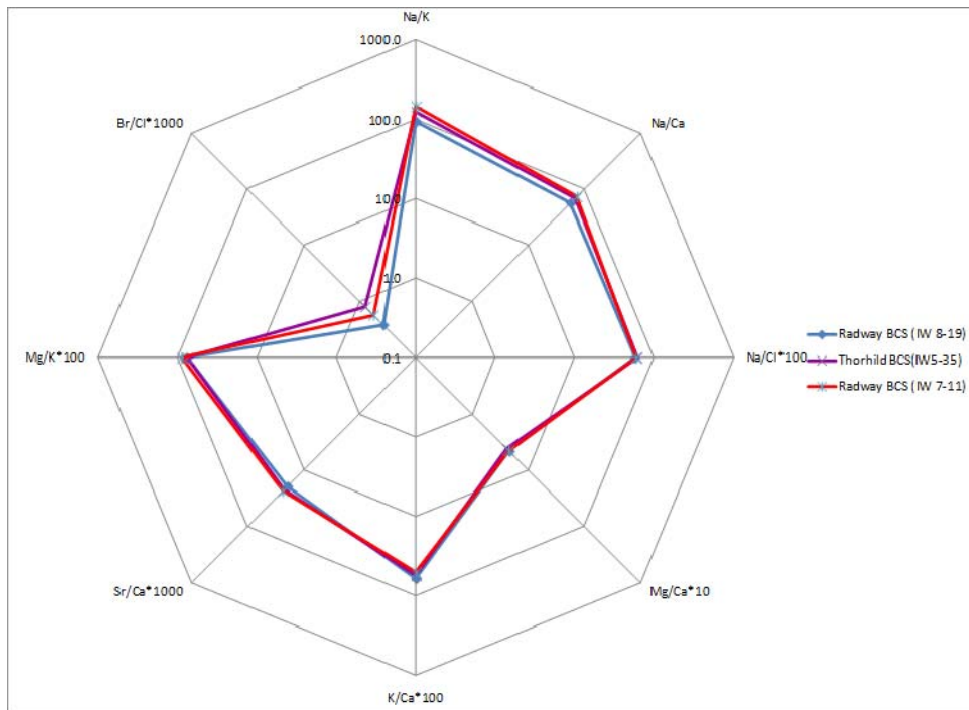


Figure 3-2: Ion Ratio plot of BCS Formation brine waters from IW 8-19 (sampled in 2010), IW 5-35 (sampled in 2012) and IW 7-11 (sampled in 2013).

3.2. Deep Monitoring Wells

3.2.1. Geologic Summary

Formation thicknesses for some key formations in DMWs 5-35, 8-19, and 7-11 are shown in Figure 3-3. Overall the geological tops for DMW 7-11 were within expectation. As expected, formation thicknesses were similar between adjacent DMWs and IWs. For instance, the Winnipegosis/ Contact Rapids Formation thickness was 71 m in DMW 7-11 compared to 70 m in IW 7-11 and the Prairie Evaporite/Lower Prairie Evaporite Formation thickness was 127 m, as was observed in IW 7-11. A summary of all the reservoir properties for each of these formations observed in the three DMW and three IW is given in Tables 3-3 to 3-6. For detailed information on the formation evaluation of DMW 7-11, please refer to Appendix B.

Table 3-3: Average Contact Rapids Properties (Vsh and Porosity cut-offs applied)

Well	Zones	Top	Bottom	Gross	Net	Net to Gross	Av_Shale Volume	Av_Porosity
100053505921W400	Contact Rapids	1630	1694	64.2	23.2	0.36	0.364	0.064
100081905920W400	Contact Rapids	1614	1682	68	37.8	0.56	0.151	0.076
102053505921W400	Contact Rapids	1630	1694	64.2	31	0.48	0.326	0.071
102081905920W400	Contact Rapids	1615	1675	60	31.3	0.52	0.305	0.068
103071105920W400	Contact Rapids	1584	1638	54	33.1	0.61	0.324	0.071
102071105920W400	Contact Rapids	1585	1640	54.7	30.5	0.56	0.345	0.067
Average				62.1	31.3	0.51	0.294	0.070

Table 3-4: Average Winnipegosis Fm. Properties (Vsh and Porosity cut-offs applied)

Well	Zones	Top	Bottom	Gross	Net	Net to Gross	Av_Shale Volume	Porosity
100053505921W400	Winnipegosis	1612	1629.8	17.7	15.9	0.9	0.13	0.085
100081905920W400	Winnipegosis	1598.5	1614	15.5	5.9	0.39	0.038	0.108
102053505921W400	Winnipegosis	1612.1	1629.8	17.7	5.7	0.32	0.077	0.103
102081905920W400	Winnipegosis	1600	1615	15	8.3	0.55	0.019	0.107
103071105920W400	Winnipegosis	1568	1584	16	6.6	0.41	0.045	0.108
102071105920W400	Winnipegosis	1570	1585.3	15.3	14.3	0.94	0.064	0.093
Average				16.4	8.5	0.514	0.062	0.102

Table 3-5: Average Moberly member properties (Vsh and Porosity cut-offs applied)

Well	Zones	Top	Bottom	Gross	Net	Net to Gross	Av_Shale Volume	Av_Porosity
100053505921W400	Moberly	1274	1355	81	1.07	0.01	0.035	0.087
100081905920W400	Moberly	1264	1338	74	7.01	0.1	0.016	0.098
102053505921W400	Moberly	1280	1354	74	3.4	0.05	0.054	0.098
102081905920W400	Moberly	1267	1340	73	7.9	0.11	0.007	0.097

103071105920W400	Moberly	1231	1303.7	72.7	11.2	0.15	0.042	0.098
102071105920W400	Moberly	1231	1305	74	3.9	0.05	0.05	0.116
Average				74.9442	6.1154	0.083	0.0308	0.0956

Table 3-6: Average Cooking Lake Fm. Properties (Vsh and Porosity cut-offs applied)

Well	Zones	Top	Bottom	Gross	Net	Net to Gross	Av_Shale Volume	Porosity
100053505921W400	Cooking Lake	1166	1250	84	39.6	0.47	0.018	0.110
100081905920W400	Cooking Lake	1148.6	1231	82.4	31.2	0.38	0.000	0.122
102053505921W400	Cooking Lake	1165.5	1248	82.5	51.4	0.62	0.045	0.125
102081905920W400	Cooking Lake	1148	1232.5	84.5	31.4	0.37	0.011	0.121
103071105920W400	Cooking Lake	1107	1190	83.1	53.1	0.64	0.034	0.144
102071105920W400	Cooking Lake	1107	1192	85	44.3	0.52	0.036	0.137
Average				83.3	41.4	0.5	0.022	0.124

The MDT data acquired in the Cooking Lake in DMW 7-11 confirm the fluid mobility seen in previous DMWs (Appendix B) and therefore support the proposed use of the Cooking Lake as a pressure monitoring zone (see Section 5.4 of the 2013 Annual Status Report for comparison to previously drilled wells [2]). Figure 3.3 summarizes the final conclusion on the potential use of the Winnipegosis, Contact Rapids/Lower Winnipegosis, Moberly, and Cooking Lake Formations as a deep pressure monitoring zone.

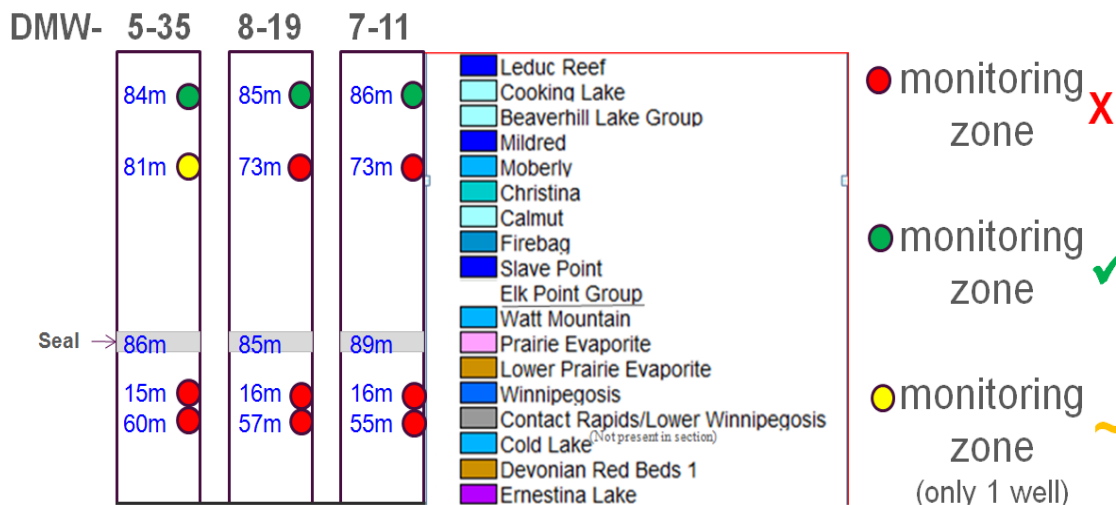


Figure 3-3: Stratigraphic thickness (blue font) for selected formations within the DMW 5-35, 8-19, and 7-11. Also indicated is the potential of the Winnipegosis, Contact Rapids/Lower Winnipegosis, Moberly, and Cooking Lake Formations to be used as a deep monitoring formation based on XPT/MDT tests.

3.3. Groundwater Wells

3.3.1. Geologic Summary

Overall, the geology encountered while drilling GW 1F1/5-35 and GW 1F1/7-11 was within expectation. The information from GW 1F1/5-35 and GW 1F1/7-11 were used to decide Total Depth (TD) and screening interval positioning for GW UL1/5-35 and GW UL1/7-11.

Table 3-3 lists the formation tops for the Belly River Group and Lea Park in GW 1F1/5-35 and GW 1F1/7-11, which are key units with regards to the base of the groundwater protection zone. No logs were acquired in any of the shallow, unlicensed wells.

Table 3-3: Top Belly River and Lea Park Formation in GW 1F1/5-35 and GW 1F1/7-11

Formation	Log Depth MD (m)	
	GW 1F1/5-35	GW 1F1/7-11
Belly River Group	109.0	113.5
Lea Park	122.5	137.0

3.3.2. Petrophysical Summary

Petrophysical logs were run as part of the drilling operations of GW 1F1/5-35 and GW 1F1/7-11. Please refer to Appendix C for a copy of the logs used in the petrophysical evaluation. The key observations from the logging operations are:

- Cement bond logs show good cement for both GW 1F1/5-35 and GW 1F1/7-11.
- The sands encountered in the Belly River of GW 1F1/5-35 are of slightly higher quality than those in 1F1-07-11-059-20W4 (Table 3-4).

Table 3-4: Belly River reservoir properties based on petrophysical log interpretation.

Well	Gross Thickness (m)	Net sand (m)	Net/Gross	Shale Volume (%)	Porosity (v/v)	Water Saturation (%)
GW 1F1/5-35	13.4	10.8	0.81	15	0.32	88
GW 1F1/7-11	23.7	16.2	0.75	25	0.28	74

4. BCS RESERVOIR PRESSURE ANALYSIS

As the Quest Project does not start up until 2015, there will not be any pressure data to compare to forecast until the January 2016 annual report submission. Recent well test results from IW 5-35 and IW 7-11 support high injectivity and low associated bottom hole well pressure. These results support better reservoir quality than the expectation case from the Gen-4 report.

The expectation remains the same as stated in the January 31, 2013 report that the Quest Project will not raise the stabilized reservoir pressure at any injector to the AER approved 26 MPa limit within the life of the project. As there is no expectation for the flowing bottomhole pressure to exceed 26MPa, the associated stabilized pressure will be less. Therefore the full 27 Mt of CO₂ is expected to be sequestered without ever approaching the maximum shut-in formation pressure specified in clause 5) a) of AER Approval 11837A [1].

4.1. IW 5-35 Production Test

A water production test was performed in the second injection well, IW 5-35, to validate BCS initial injectivity. Coil tubing was run in the hole on March 19th, 2013 and started to inject nitrogen at midnight. In addition to nitrogen a small amount of methanol water blend was circulated to mitigate both scale build up in the production system and the -30°C temperatures.

Net brine production was estimated from measurements at the flow meter just downstream of the separator. As water hauling trucks were able to keep the holding tanks at low volumes, the test was extended for an extra 12 hrs and was followed by an extended build up. Figure 4-1 illustrates the flow rates recorded per half hour.

The water was produced over 36 hours, of which an average rate of approximately 342 m³/d was maintained at a BHP of 20.2 MPa. With an interpreted average reservoir pressure MPP of 20.5 MPa this estimates a productivity index (PI = q/dP) of 1140 m³/d/MPa.

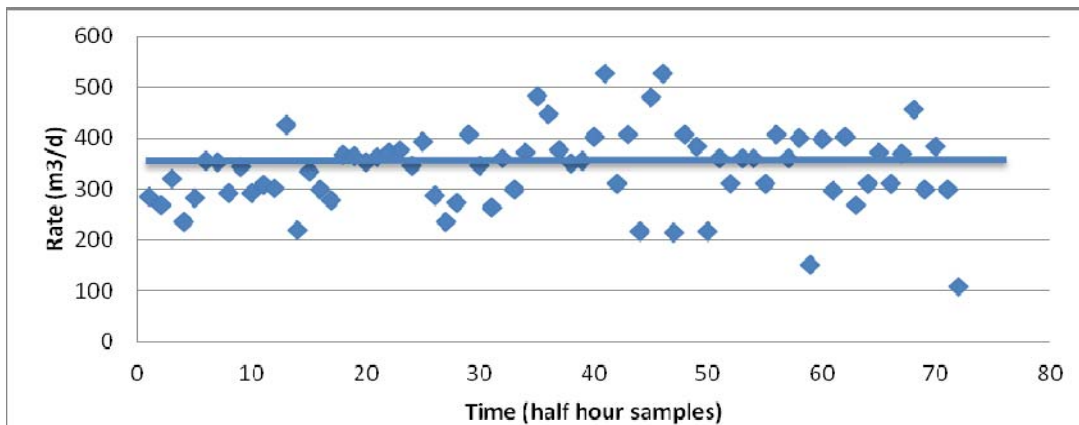


Figure 4-1 Daily rate equivalent half hour flow measurements for IW 5-35

4.2. IW 7-11 Production Test

A water production test was performed in the third injection well, IW 7-11, to validate BCS initial injectivity. Coil tubing was run in the hole on June 29th, 2013 and started to inject nitrogen at noon. Due to operational issues the production test was separated into 3 flow periods as illustrated in Figure 4-2.

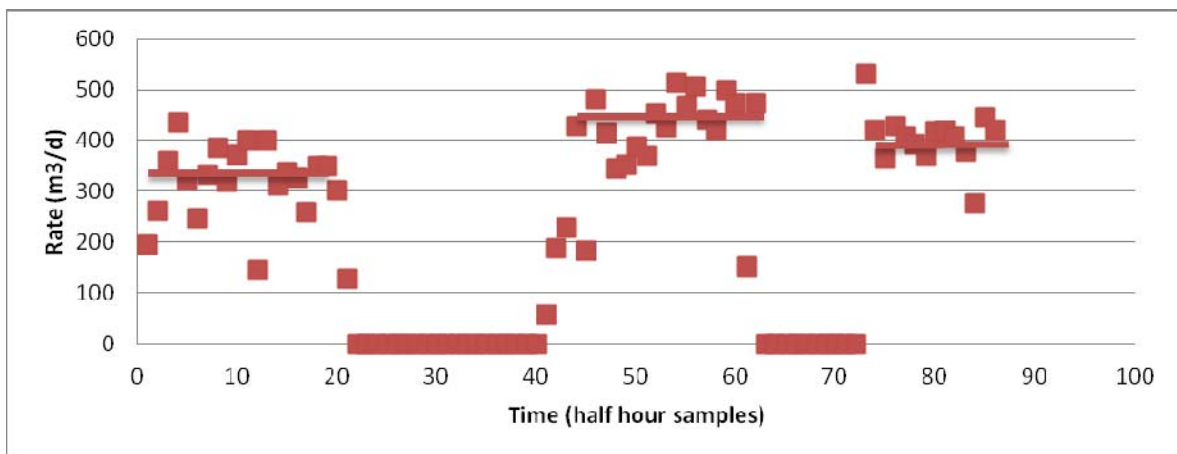


Figure 4-2 Daily rate equivalent half hour flow measurements for IW 7-11

Flow Period # 1: An average rate 327 m³/d flowed for 9 hours; at that time, for safety, it was decided to pull out of hole after observing a thunderstorm approaching for the last hour, and lightning around the lease area. The associated build up lasted 9.5 hours.

The water was produced over 9 hours, of which an average rate of approximately 327 m³/d was maintained at a BHP of 19.8 MPa. With an interpreted average reservoir pressure MPP of 20.0 MPa this estimates a productivity index (PI=q/dP) of 2181m³/d/MPa.

Flow Period # 2: The second flow period was 12.5 hours. The water was produced over 5 hours, of which an average rate of approximately 467m³/d was maintained at a BHP of 19.8 MPa. With an interpreted average reservoir pressure MPP of 20.0 MPa this estimates a productivity index (PI=q/dP) of 2594 m³/d/MPa.

Flow Period # 3: The third flow period averaged a rate of 396 m³/d for 8 hours. This rate continued to flow until the 24hr shut-in time derived from the start of flow period #2. An extended build up followed.

The water was produced over 8 hours, of which an average rate of approximately 396m³/d was maintained at a BHP of 19.8 MPa. With an interpreted average reservoir pressure MPP of 20.0 MPa this estimates a productivity index (PI=q/dP) of 2085 m³/d/MPa. It is generally fair to assume that the final PI is the most representative for predictive performance.

4.3. Well Test Results Summary

The project requires an initial water PI greater than 380 m³/d/MPa to confidently inject 1.08Mt/a of CO₂ to meet project objectives. The results of the well test support initial PI's of each individual injection well (IW 7-11, IW 5-35, IW 8-19) greater than the full project requirement. Table 4-1 summarizes the PI assessments for all of the wells tested in the BCS.

Table 4-1: Summary of all PI assessments in the BCS Formation

Well Name	Rate m³/d	DeltaP kPa	Injectivity m³/d/MPa
IW 7-11	396	0.19	2085
IW 5-35	342	0.33	1036
IW 8-19	360	0.95	379
Redwater 11-32	492	12.13	41

With similar petrophysical log responses in IW 5-35, IW 7-11 and IW 8-19 it can be inferred that the initial PI in IW 8-19 is understated. As it was an injection test with known near well bore formation damage it is likely that the PI for IW 8-19 is a minimum initial PI. The IW 8-19 5th injection test more than likely still had significant formation damage. The project total initial PI can be calculated as 9 times the quoted requirement of 380 m³/d/MPa.

- Project initial PI = 379+1036+2085 = 3500 m³/d/MPa of water.
- Average Initial PI = 1167 m³/d/MPa of water

It is very probable that the project will be capable of sustaining PI's greater than the 380 m³/d/MPa for the duration of the project life; therefore no further well development should be required for injectivity requirements.

4.4. Pressure Transient Analysis

The total initial injectivity reported from the previous section of 9 – 18 times the project requirement is only valid initially. Beyond initial injection rates a dynamic model is required to predict the average reservoir pressure. Therefore it is desirable to revise the numerical model with updated reservoir properties to accurately forecast the reservoir pressure.

Pressure Transient Analysis (PTA), is an excellent way of estimating the effective permeability of the formation over an appreciably greater investigation radius than core or log analysis. Furthermore, estimates of net skin, mechanical and dynamic, and boundaries can be interpreted. The derivative plots for all three well test build-ups are reviewed and the results are then tabulated. In addition, the interpreted permeabilities are compared to the results of core measurements.

Furthermore, the baseline pressure data Shell is currently collecting needs to be effective in fulfilling the condition set by the AER for the Quest Storage Scheme Approval [1] as follows:

15. Conduct additional fall-off test with pressure transient analyses after two years of injection, in all injection wells, for comparison with the baseline pressure analysis of the 8-19 well. [351]

As elaborated in AER (formerly the ERCB) Decision number 351 [3]:

'[351] The Board understands that accurate and timely reservoir pressures that meet ERCB Directive 40: Pressure and Deliverability Testing Oil and Gas Wells stabilized pressure requirements, and that are taken at the injectors and test wells, would greatly enhance understanding of plume movement. Following an initial baseline pressure analysis of the fall-off data from the 8-19 well, the Board requires an additional fall-off test with pressure-gradient analysis, after two years of injection in all injection wells, for comparison with the baseline data. These data will provide stabilized shut-in reservoir pressures and information on any indication of fracture flow. Based on the results of each fall-off test the Board may require Shell to conduct further fall-off test in order to better understand plume movement.

The above condition requires Shell to demonstrate that the injection operations have not fractured the reservoir as observed by a significant interpretable increase in permeability. As a comparison of a fall off test after two years of CO₂ injection to a short term water injection test can be very difficult to interpret Shell plans to perform

an initial fall off test for each well during the first 3 months of operation in 2015 with at least a week of CO₂ injection per well. As additional baseline comparison data, the following section includes BCS fall off test analysis for all the injection wells as per Approval Condition 11c and AER pre-baseline monitoring plan approval # 7b [7]; it also includes build up test analysis for IW 7-11 and IW 5-35.

4.5. Well Test PTA Derivative Plots

The derivative plot, log-log scale of pressure and equivalent time, is able to display many separate formation characteristics in a single plot. Although this type of analysis is highly interpretive it illustrates some possible reservoir character. There is no evidence of the presence of boundaries and compartmentalization that would lead to premature pressure build up.

Figure 4-3 illustrates that the IW 5-35 build-up experienced an infinite acting radial flow period, depicted on derivative plot as a zero slope, highlighted by the yellow box. It then appears to transition into a constant pressure boundary as indicated by the continuously decreasing dashed purple arrow. This supports the interpretation that the formation is acting as a well connected highly permeable infinite aquifer.

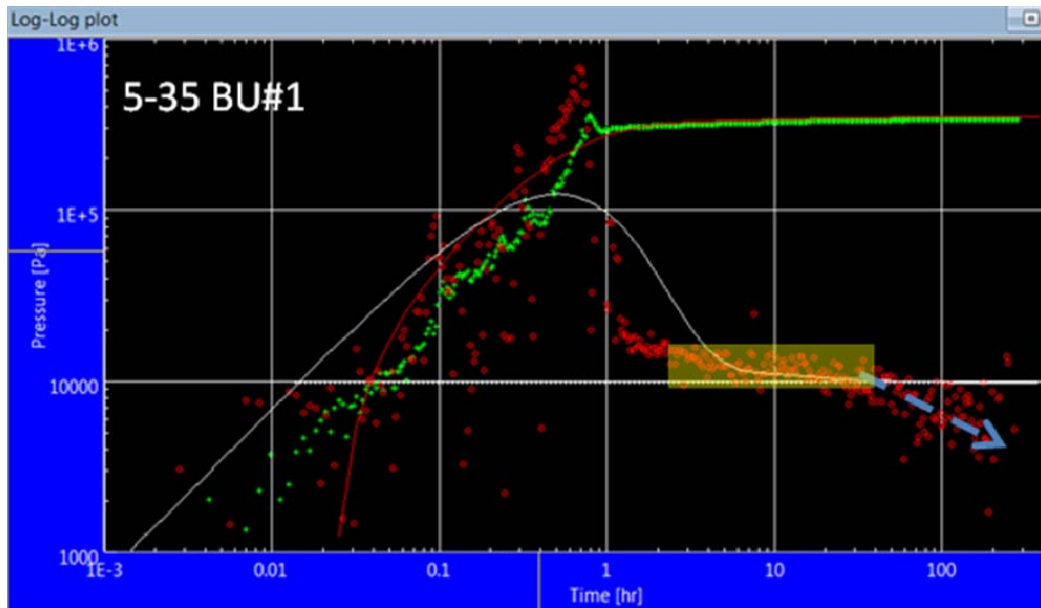


Figure 4-3: IW 5-35 PTA Derivative Plot

Figure 4-4 illustrates that the IW 7-11 build-up #3 experienced an infinite acting radial flow period, depicted on derivative plot as a zero slope, highlighted by the yellow box. It then has a peculiar sudden unit slope noted with the orange arrow, that then abruptly falls back down to the previous level; it is well known in well testing that any abrupt changes are not reservoir behavior, therefore this is likely an unexplained

wellbore or equipment artifact. After the anomaly the remaining data has too much scatter to be interpretable. Overall, the test supports the interpretation that the formation is acting as a well connected highly permeable infinite aquifer.

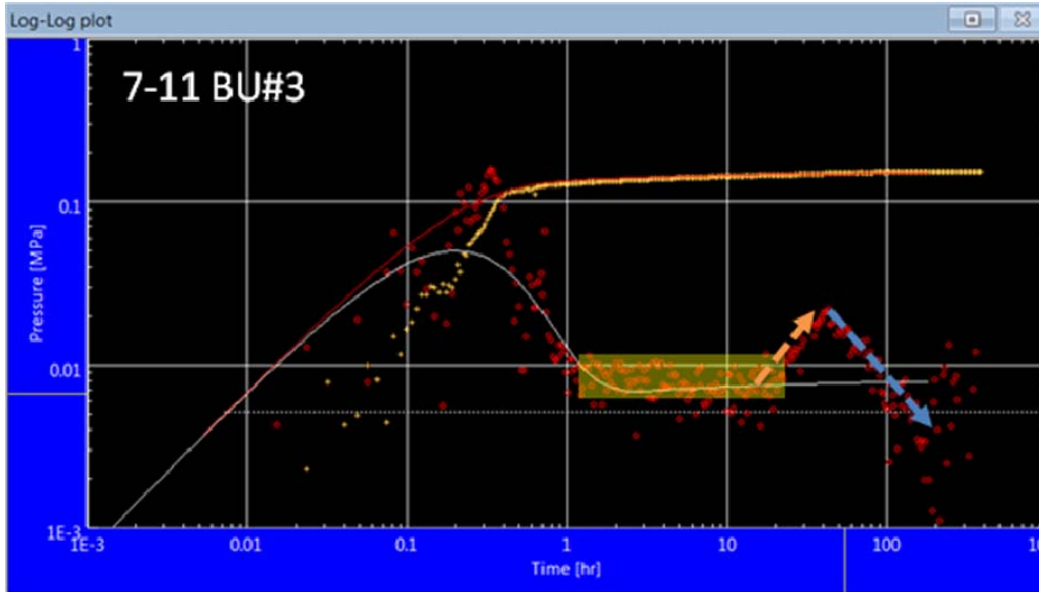


Figure 4-4: IW 7-11 PTA Derivative Plot

Figure 4-5 illustrates that the IW 8-19 fall-off #5 experienced an infinite acting radial flow period, depicted on derivative plot as a zero slope, highlighted by the yellow box. It then takes a small dip and builds back as indicated with the dashed orange and purple arrows; this dip is likely due to noise in data and cannot be interpreted as any reservoir effects. The IW 8-19 pressure data was not recorded long enough to illustrate the far field constant pressure depicted in the two build-ups above. The skin interpreted for 8-19 is considerably higher than the other two wells; indicates that the formation damaged caused during the earlier injection test was not sufficiently cleaned up.

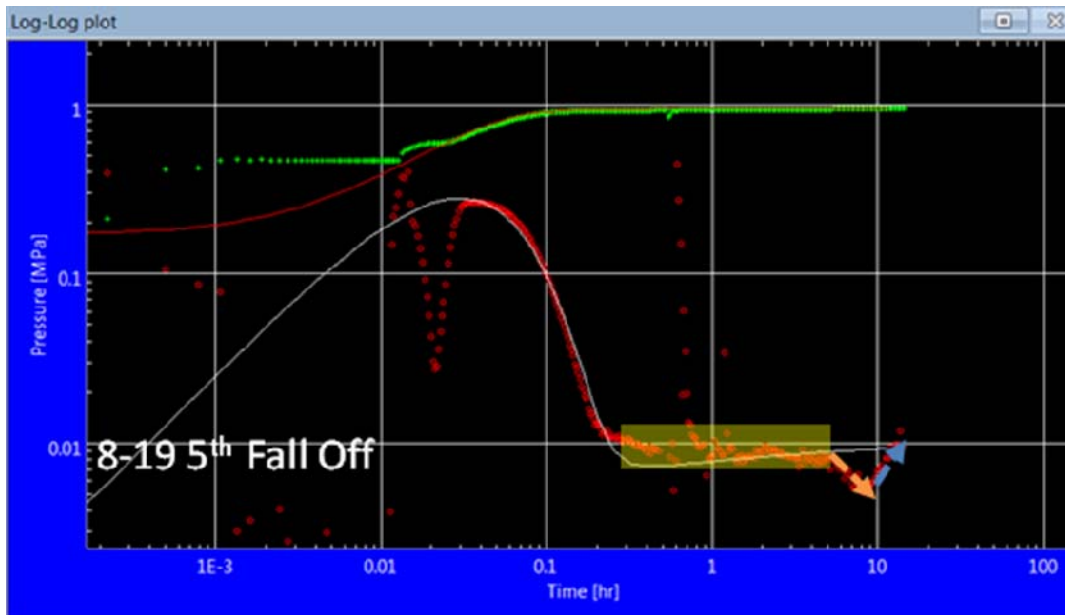


Figure 4-5: IW 8-19 PTA Derivative Plot

Vertical homogeneous infinite acting reservoir models were used to fit the data and estimate reservoir properties. The solid white lines in the above plots illustrate the effectiveness of the models. Overall it appears that reasonable fits could be obtained with these fairly basic assumptions. Table 4-2 summarizes the key outputs of the analyses.

Table 4-2: Summary of PTA Interpreted Reservoir Properties

Well	Pi (MPa)	Skin	Mid $k_{eff} (D)^2$
IW 8-19	20.4	40	0.8
IW 5-35	20.2	10	1.0
IW 7-11	20.0	5	1.8

In conclusion, the well test interpretation supports permeability of one Darcy or greater. The IW 7-11 in particular has evidence of two Darcy effective permeability. Overall, the results support the interpretation that the formation is acting as a well connected highly permeable infinite aquifer. The results of Table 4-2 should be used for the initial baseline test results to comply with AER Approval conditions 11c [1] and 7b [7].

4.5.1. Permeability Comparison of Well Tests and Core Results

As the results of the PTA interpretations of permeability are significantly higher than previously considered, it is necessary to cross check the results with the values

calculated from the core measurements. Table 4-3 summarizes the core and PTA permeability interpretations. Both the core average permeability and the mid-case effective permeability average approximately one Darcy across the wells. It is important to note that the high-case effective permeabilities, interpreted through PTA, are considerably less than the core maximum permeability for each well. This allows the effective permeability to be considerably higher than the average permeability in the IW 7-11 as the flow is likely dominated by a subset of net pay with a higher than average permeability.

Table 4-3: Summary of BCS Permeability Interpretations

Well	Core Avg k (D)	Core Max k (D)	Low K _{eff} (D)	Mid k _{eff} (D) ²	High k _{eff} (D) ³
8-19	0.5	3.6	0.5	0.8	1.1
5-35	0.9	2.2	0.8	1.0	1.3
7-11	0.9	2.9	1.2	1.8	2.0

Inspection of the permeability histograms in Figure 4-6 illustrates that IW 7-11 has a narrow cluster of high permeability that would explain the above average effective permeability interpreted to be associated with the increased amount of fluvial influenced TDBM facies.

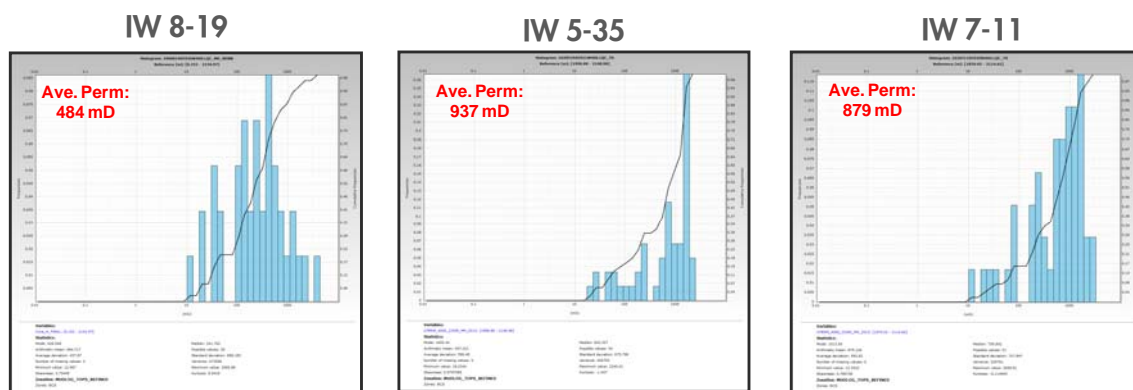


Figure 4-6: BCS Reservoir Core Permeability

In conclusion, the core results support the well test interpretation of one or greater Darcy permeability. The IW 7-11 in particular has evidence of two Darcy effective permeability. Although we will only be able to minimize the uncertainty of far field connectivity after approximately 6 to 12 months of injection the well test results present considerable evidence of high reservoir quality throughout the Quest Injection area.

5. RESERVOIR MODELLING

5.1. Model Updates

The fourth generation (Gen-4) of BCS full field static reservoir models describes the range of subsurface uncertainty in terms of reservoir quality and reservoir connectivity [2]. These are both key uncertainties that influence the maximum achievable injection rates into the reservoir, the plateau length of that injection rate and the total amount of CO₂ that can be injected. The ability to maintain injection rate over time and successfully inject the required total volume depends largely upon the pore volume in the reservoir and the pressure build up over time around injector wells.

At the time the Gen-4 models were built, it was still uncertain on whether the IW 8-19 results were representative of the mid or high end of the range of uncertainty for reservoir properties. As a result, the Gen-4 models maintained a conservative approach in the scenarios presented for the static model. However, the results of the recent drilling campaign suggest that all three well results are representative of the mid or high end of the range of uncertainty for reservoir properties. Therefore, the low case presented in Gen-4 does not exist at the location of the injection wells and is a low probability of occurring away from these wells due to the consistent regional geology. A fifth generation (Gen-5) of modeling is currently under construction; the results of which will be submitted as part of the January 2015 annual report.

5.2. Future Static Model Updates

In 2013, Shell completed the BCS core descriptions and associated paleo-depositional environment updates for IW's 7-11 and 5-35 (Section 3.1). The results are in line with pre-drill expectation and will be incorporated into the Gen-5 static model update.

The results of the Gen-5 model and the associated impact on modeled plume and pressure predictions will be submitted in the January 2015 Third Annual Status Report to AER.

5.3. Dynamic Model Updates

5.3.1. Pressure Prediction

The injection wells are currently suspended; prior to conditioning the wells for start-up there will not be any measured data on formation pressure or CO₂ plume extents. The Gen-4 dynamic model results, as presented in the 2013 status report, indicate that the pressure build up in the BCS is expected to be less than 2 MPa of DeltaP at the perforations of the injection wells while flowing at the end of the project life [2]. Recent well results from IW 5-35 and IW 7-11 support this forecast and indicate an even

5. Reservoir Modelling

lower DeltaP may occur. However, an updated pressure forecast will be included in the January 2015 submission following the fifth generation of modeling.

5.3.2. *Plume Prediction*

Detailed Gen-4 CO₂ plume migration modeling of a 3 injection well scheme concluded a P50 CO₂ plume length of 4100m at the end of injection in 2040. The range of uncertainty is large and is heavily driven by the range of uncertainty in the relative permeability. A revision of this estimate will be reported in the January 2015 annual report as we are currently developing the Gen-5 models. This latest model will incorporate new well control, but the uncertainty on relative permeability will remain until post start-up.

6. MMV PLAN ACTIVITIES, PERFORMANCE AND RESULTS

6.1. Summary of MMV Operations and Maintenance Activities

Recent activities associated with the MMV Plan are described in the following sections. A summary overview of Hydrosphere Biosphere Monitoring Plan (HBMP) activities can be seen in Table 6-1.

Table 6-1: Summary overview of HBMP activities completed to-date.

a)												
Discrete GW well sampling (Landowner & Project Wells)												
Sampling event	Jan	Feb	Mar	Apr	May	Jun	Jul	Aug	Sep	Oct	Nov	Dec
Q4-2012												
Q1-2013												
Q2-2013												
Q3-2013												
Q4-2013												
b)												
Continuous GW well sampling (Project Wells only)												
Sampling event	Jan	Feb	Mar	Apr	May	Jun	Jul	Aug	Sep	Oct	Nov	Dec
2013												
c)												
Soil Gas/Flux Sampling & Remote Sensing Calibration Data Acquisition												
Sampling event	Jan	Feb	Mar	Apr	May	Jun	Jul	Aug	Sep	Oct	Nov	Dec
Q4-2012												
Q1-2013												
Q2-2013												
Q3-2013												
Q4-2013												

In addition to baseline data acquisition, Shell doing a significant amount of work towards implementation of the supporting Infrastructure which will transmit all data types between well sites, Scotford Upgrader, Calgary office and relevant external parties.

6.1.1. Atmospheric Monitoring – LightSource

A LightSource field trial was successfully completed between September 8th and 13th, 2013. In addition, Boreal laser delivered a new enhanced performance single line-of-sight CO₂ sensor which was successfully tested in this field trial. Compilation of the field trial data is ongoing along with final hardware (laser) and software development work. The information from the field trial is being used as input to calibrate the monitoring system and to help set final detection thresholds that will be used for LightSource atmospheric CO₂ monitoring. These detection thresholds will be confirmed in the pre-injection MMV Plan Update 2015.

6.1.2. *Biosphere Monitoring Activities*

6.1.2.1. Soil and Vegetation Sampling for Remote Sensing Calibration

14 soil and vegetation plots were sampled over 3 different field events in the spring, summer and fall timeframes with an additional soil survey carried out later in the fall. A summary of the campaign completed to date, is provided in Appendix E. A similar baseline campaign will be undertaken in 2014.

6.1.2.2. Soil Gas and Soil Surface CO₂ Flux Sampling

A significant soil gas and soil surface CO₂ flux sampling program has been carried out since Q3-2012 in order to support the baseline monitoring program. The first soil gas and soil surface CO₂ flux sampling campaign took place in Q3-2012 and was followed by 4 sampling campaigns in 2013, distributed throughout the year.

A summary of the soil gas and soil surface CO₂ flux sampling campaign completed to date is provided in Section 3.6 of Appendix E. Another baseline soil gas and soil surface CO₂ flux sampling campaign will be undertaken in 2014, which will complete the soil gas and soil surface flux CO₂ data gathering program.

6.1.3. *Hydrosphere Monitoring Activities*

6.1.3.1. Artificial and Natural Tracers

PFC tracer feasibility studies are ongoing – preliminary results are available in Appendix D and final results will be submitted by June 2014. The aim of this study is to identify potential scavenging and losses of the PFC tracer due to the interaction of the parent fluid, i.e. CO₂, with different rock matrices and other subsurface fluids. The experimental study for this research was conducted in collaboration with The Commonwealth Scientific and Industrial Research Organization (CSIRO). The preliminary conclusion is that PFCs may remain in sufficient detectable amounts in its parent CO₂ phase at shallow depth in the hydrostratigraphic column. The data confirm that PFCs have very low solubility in water and are not retained at significant/critical amounts during migration by matrices prone to adsorb organic compounds such as clays. Hence, experimental data obtained so far suggest that PFCs are a suitable reliable passive/conservative tracer of injected CO₂. Experimental measurements are continuing to explore the behavior of organic substrate adsorption and CO₂/water/hydrocarbons partitioning.

In addition to the artificial PFC tracer study, the use of the natural abundance C isotopic composition of CO₂ is being investigated as a potential natural tracer. As part of the HBMP activities, the isotopic composition of CO₂ in soil gas and well gas

are being determined. Samples from the Scofford Upgrader are also being collected for analysis. Furthermore, the University of Calgary was contracted to undertake laboratory and modelling studies to assess whether or not the isotopic composition of the injection gas may change along the stratigraphic column in case of a hypothetical leakage event. Draft reports for the laboratory and modelling studies have been received, and are currently under review. A potential extension to these studies is also being investigated.

6.1.3.2. Water Well Sampling

A significant groundwater sampling program has been carried out since Q4-2012 in order to support the baseline monitoring program. The first groundwater sampling campaign took place in Q4-2012 and was followed by 4 sampling campaigns in 2013, distributed throughout the year.

A summary of the water well sampling campaign completed to date is provided in Section 4.0 of Appendix E. Another baseline water well sampling campaign will be undertaken in 2014.

In April 2013, Alberta Innovates – Technology Futures (AITF) started a study entitled ‘GROUND WATER STUDY FOR QUEST CCS PROJECT’ to support the HBMP. During 2013, the main focus has been on revising and updating the conceptual geological model from surface to the Lea Park Formation for the QUEST Sequestration Lease area. A key focus of this study is to assess the characteristics of potable groundwater aquifers across the Quest project area and to evaluate potential trigger conditions which may suggest a deviation from established baseline conditions. Final observations from the AITF study are expected by the end of 2014.

6.1.4. Geosphere Monitoring Activities

6.1.4.1. DAS/DTS

The optical fibers that have been previously cemented within the injection wells on each well pad will be used for these technologies. These fibers were successfully deployed and initial testing shows that they are functional. Shell will test the fibers again prior to implementing hardware associated with DAS or DTS data collection. Studies completed to date support DTS/DAS for the use in the following:

- DTS as a temperature log that can be used to for hydraulic isolation testing across the BCS storage complex when the well has been shut-in for a short period of time
- The DAS system in Quest has been demonstrated to be similar quality to a conventional walkaway VSP and Shell plans to use DAS for the baseline 3D VSP's that will be acquired in Q4 2014.

The remaining feasibility work is focused on the ability to use DTS/DAS to detect potential leaks real time while injection is occurring.

6.1.4.2. Microseismic

Shell received approval on November 29th 2013 for the Special Report #1 and MMV plan [Ref.]. This approval recognizes that no requirements are needed at this time for revisions or changes to the planned downhole microseismic monitoring (DHMS) and contingency monitoring in the deep observation wells. The microseismic array will be installed in DMW 8-19 as per the MMV plan, though the well used for DHMS may be adjusted based on observed injection performance. Shell has been working to finalize a vendor contract to construct and deploy the microseismic array which will be complete by Q1 2014. Guidelines for an appropriate vendor include their ability to supply instruments that can handle high salinity environments and an array that can be installed using magnets. C&P activities are on-going for this contract with a plan for installation to occur in June/July 2014. This planned timing for installation will allow Shell to record baseline seismicity prior to 2015 injection.

6.1.4.3. 3D VSP

Shell is in the process of designing the 3D VSPs scheduled for 2014 by modeling the response for different shot spacing and locations. The information gained from that modeling will be aimed at optimizing processing and reservoir imaging.

The baseline survey is planned to be acquired October/November 2014 after the farmers have harvested their crops. This will help to reduce stakeholder impact and complete a baseline survey prior to the 2015 injection. It is not advantageous to do this survey earlier in 2014 due to unnecessary noise attributed to heavy construction on the sites.

6.1.4.4. InSAR

Shell acquired 15 RadarSat2 satellite images for InSAR baseline data in 2013 and will continue through 2014. The full set of images acquired as of Q3 2014 will be re-processed, in a similar process as used in 2012, prior to the start of injection to complete the baseline phase. In addition, in 2013 Shell received Approval from the AER on October 4, 2013 that corner reflectors are not required for InSAR monitoring subject to the following:

- When InSAR section is revisited in annual status reports, Shell must confirm a data-processing method has been used that captures sufficient natural coherent targets within the AOI(SLA) and,
- Confirm they are keeping track of how fast the area of deformation at the surface is expanding. If it appears it will extend beyond the AOI (SLA) in the lifetime of the project, Shell shall either demonstrate the existence of adequate

natural stable targets outside the AOI, or revisit the question of whether artificial corner reflectors may be required.

6.1.5. *In-Well Monitoring Activities*

6.1.5.1. DMW Pressure Monitoring

Discrete pressure measurements were acquired in the Cooking Lake in all Deep monitoring wells through MDT/XPT sampling while drilling.

In 2013, the Cooking Lake was perforated in DMW 5-35 and DMW 7-11 and gauges installed. Continuous baseline pressure data acquisition will start in Q1 2014 to assist in determining the detection thresholds to be submitted as part of the pre-injection MMV plan update in January 31, 2015.

6.2. **MMV Performance or Plan Issues**

MMV performance and plan issues for the year of 2013 have been identified as follows:

- 1) Surface Casing Vent flows were identified in all Shell injection and deep monitoring wells as well as gas migrations in IW 5-35 and IW 7-11. All activities and information has been disclosed by Shell to the AER in 2013 and discussed with AER in additional documents [8,9]. Associated changes to the MMV plan are discussed in Section 6.1.4.1.
- 2) After completion of the injection wells, Shell determined that the DTS cables in IW 7-11 and IW 5-35 only extend 2 m above and 11 m above the top of the MCS, respectively. Therefore, the DTS cannot be used to detect leaks across the first seal, the MCS. However, there are still DTS cables extending over the lower and Upper Lotsberg salts, to ensure containment within the BCS storage complex. Shell has updated the MMV plan address the AER approval condition 5i to report Co₂ entry into the MCS or above as discussed in Section 7 of the February 14, 2014 MMV plan submission to the AER [1,11].
- 3) Due to an operation error, the 5-35 injection well was perforated off-depth 3.4m downward into the Precambrian basement. Shell submitted a self-disclosure to the AER concerning the out of zone perforation on November 25, 2013 [10] with additional information submitted to AER January 20, 2014 [12]. It is Shell's interpretation that this will have no impact on the project as there is negligible permeability in the granite basement.
- 4) Distributed Acoustic Sensing (DAS) – in the Oct.15 2012 MMV plan it was stated that DAS along an optical fibre deployed alongside the DTS fibre may provide an independent means of verifying cement bond integrity and the absence of fluid flow outside the casing. In the unexpected event of a loss of

cement bond integrity, any upward migration of fluids outside the casing will generate acoustic noise that reaches the adjacent portion of the DAS fibre.

However, it is not known what magnitude of leak would be required to generate a detectable level of noise. Testing of acoustic levels during the injection period will be used to validate the potential of using DAS acoustic monitoring for leak detection. Other applications of the DAS technique for detection of small changes are currently being developed by third parties (e.g. OptaSense) and appropriate technologies will also be tested during the injection period.

- 5) The feasibility study on the use of RadarSat2 imagery for biosphere monitoring for increased soil salinity in the case of a BCS brine leak has been postponed to early 2014. The reason being that HBMP baseline soil sampling procedures must be altered to take a grid sampling of various soils on each sample plots as opposed to a composite sample so that variations across a single the plot can be detected and interpreted. As a result, only the October 2013 image can be calibrated and processed in 2013 and one in spring 2014. However, this should be sufficient to finalize feasibility studies for the technology.

There is a delay in hooking up the power to the BCS pressure gauge in IW 8-19 until trenching associated with the pipeline is complete and cables can be installed. This has no impact to the ability to attain appropriate baseline monitoring data.

6.3. New MMV Data Collected

New MMV data collected and or interpreted in 2013 are included as follows:

- 1) Updated Core descriptions for the IW 7-11 and IW 5-35 completed in 2013 (Appendix A)
- 2) Well data associated with the drilling of the final deep monitoring well (Section 3.2 and Appendix B)
- 3) Well data associated with the four project groundwater wells that were not completed by the time of the previous annual report Section 3.3 and Appendix C
- 4) Artificial Tracer interim report – Appendix D
- 5) HBMP program results compiled from fall 2012 to end 2013 (Appendix E).
- 6) CO₂ entry pressure core analysis results for 100/08-19-059-20W400 not available at time of submission of Special Report #1 as per AER Condition 5 [7] (in Appendix F)

6.4. Proposed Changes to Current MMV Plan

Shell is submitting an updated MMV plan on February 14, 2014 in fulfillment of the conditions for AER approval [7] of the pre-baseline MMV plan submitted October 15, 2012 [5]. Included in the update are the changes required as per the conditions stated in the AER approval [7] as well as changes associated with issues addressed in Section 6.2 above. In addition, the MMV plan was updated to take into account the fact that all injection wells have been drilled and that this will be a 3 well injection scheme unless more wells are required in future to meet Project obligations. Furthermore, some changes to sampling procedures (i.e. flow through sampling device for gas sampling) have been implemented already to ensure proper sampling is occurring in the 2014 baseline period. Additional changes, outside the AER approval conditions, included in the February 14, 2014 MMV plan, are as follows:

6.4.1. Atmosphere – LightSource

There was an errata in the October 15, 2012 MMV Plan update in Section 9.1 addressing the intervention indicator for emitted mass of CO₂ to ensure accurate CO₂ inventory measurement. The text should read:

Emitted mass of CO₂

- **Monitoring:** LightSource (Line-of-sight CO₂ flux metering)
- **Intervention Indicator:** Controlled release tests, planned during regular service visits using small “fire extinguisher” calibration tests are not detected.
- **Control Options:** Recalibrate or, if necessary, replace sensors.
- **Response Time:** 1-3 months.

6.4.2. Biosphere

6.4.2.1. Soil Gas / Flux Component

The original sampling sites for soil gas and soil surface CO₂ flux measurements included:

- near injection well pads: 3 sites in total
- at permanent soil plots: 2 sites in total
- at transient soil plots: 10 sites in total.

as outlined in Section 3.4.2 of Appendix A of Special Report #1 submitted October 15th 2012 [5]. Note that in 2013, it was decided not to use transient plots for baseline monitoring and instead use semi-permanent plots, as explained in the response to the September 5th, 2013 IR [6].

6.4.2.2. Remote Sensing RIA for brine leak detection

The number of images processed and calibrated in 2014 will be reduced to 1 image in the Spring as this is what is required to complete the final technical feasibility study. However, images will continue to be acquired at same frequency as InSAR images every 24 days.

6.4.3. Hydrosphere

6.4.3.1. Tracers:

An emphasis will be placed upon identification and possible selection of natural tracer(s) to help identify an unlikely leakage event from the storage complex as a potential alternative to artificial tracers.

6.4.3.2. Water Well Sampling

1) In the response to the AER information request received March 28th, 2013 [4], it was noted that the 2013 sampling program was modified based on observations from the Q4-2012 sample event results. Similarly, the 2014 sampling program has been revised compared to the proposed plan presented in Section 2.5.1 of Appendix A of Special Report #1 submitted October 5th 2012 [5]. Table 6-2 shows a summary of updated 2014 hydrosphere sampling plan which is explained in detail in the February 14, 2014 MMV Plan Update [11].

Table 6-2: Summary of changes to 2014 hydrosphere sampling program

	Tier 2, total # of wells	Tier 3, total # of wells
"October 15 th , 2012" sampling plan for 2014	75	33
"revised" sampling plan for 2014*	266	115

* Not all planned wells may be sampled as this depends upon a number of factors, such as consent from private well owners, or well status (accessibility, functioning pump).

2) In 2012 and 2013, Tier 3 included the following analyses:



Based on evaluation of the data collected during 2012 and 2013, it has been decided to remove, for redundancy reasons, the following two analyses from the Tier 3 suite of analyses:

$\delta^{81}\text{Br}$ & $\delta^{11}\text{B}$

- 3) As noted in the 2012 Annual report, groundwater well conditions (e.g. presence of tubing, electrical wires) impacted the success of collecting well headspace gas (WHG) samples. During 2013, the WHG sampling protocol was modified to help improve the success rate of gas collection at a groundwater well by including a diffusing baffle rather than an airtight seal at the wellhead to prevent airflow from entering the well. Furthermore in Q4-2013, a flow-through sampling device for gas collection at a select number of wells was tested for gas collection in addition to the established WHG sampling protocol. Based upon evaluation of the Q4-2013 data, gas sampling at a groundwater well will be done using a flow-through sampling device during 2014.
- 4) Based on current baseline data collected as part of the HBMP 2012 and 2013 program, the mean baseline pH and EC values and threshold values will be finalized at the end of the HBMP pre-injection (baseline) sampling program and potentially differ across the Sequestration Lease area.
- 5) During the injection phase (starting 2015), the frequency and number of landowner wells monitored within the Sequestration Lease area will most likely be reduced compared to the baseline (pre-injection) phase and monitoring will most likely only focus on wells near the injection well pads.

6.4.3.3. SCVF and Gas Migration Monitoring

The following AER conditions [7, 8] have been integrated as changes in the February 14, 2014 MMV plan update [11]:

- Annual SCVF testing as per AER ID 2003-01 for non-serious SCVF, until time of well abandonment or until SCVF dies out.
- Annual Gas Migration testing as per procedure given in AER Directive 020, Appendix 2, until time of well abandonment or until the GM disappears.
- Annual monitoring using existing project groundwater monitoring wells on each injection pad, including head gas composition, and until time of well abandonment, as per the project HBMP. Monitoring technologies must include the ability to detect contamination due to SCVF's and GM's.
- Annual reporting to the AER of the results of the monitoring activities as long as both issues exist on the wells must be submitted to the AER.
- Should any environmental, public safety, water contamination issue or landowner concern arise at any time due to these SCVF or GM issues, the AER will be notified and the SCVF or GM remediation will be immediately initiated.

6.4.3.4. Pressure Monitoring in Deep Monitoring Wells

In the 2013 First Annual Status Report [2] Shell proposed changing of the deep monitoring target to the Cooking Lake Formation. Additional information supporting that decision that was not presented previously is summarized below.

As presented in Section 3.2 of this report, the Cooking Lake is a well developed aquifer system that shows consistent properties throughout the area. A good quality interval can be correlated at the base of Cooking Lake Formation and occurs in all wells. In addition, the XPT results in DMW 5-35 and DMW 8-19, as well as the successful MDT fluid samples attained in those wells, support the use of the Cooking Lake as a viable option for deep pressure monitoring.

It should be noted that since the data acquisition from the recent well campaign, Shell has acquired the rights to perforate, sample and monitor the Cooking Lake Formation in DMW 81-9, DMW 7-11 and DMW 5-35. It is important to establish a pressure baseline in the Cooking Lake to understand the pressure variability induced primarily by far field production from the Leduc Reef.

Baseline pressure data could be acquired from any one of the three DMW's. Since the primary discriminator on the Cooking Lake baseline data assessment will be the quality of data collected it is advisable to collect data from more than one point source. Therefore, the recommendation was made to get permanent down-hole pressure gauges installed in the 7-11 and 5-35 DMW's in September 2013. As the 8-19 DMW is going to have a micro-seismic array installed and that program is still under development it was decided to not complete and install gauges in the 8-19 DMW until impacts to microseismic are fully understood.

Upon connection to power at DMWs 7-11 and 5-35, the wells will commence data collection with the Cooking Lake as the primary deep pressure monitoring interval. However, Shell will review the results of the pressure baseline of the Cooking Lake to confirm that it will ultimately be acceptable for monitoring purposes.

7. Monitoring Wells

7. MONITORING WELLS

7.1. Need for Monitoring Wells near Periphery of Pressure Build-up

Approval No. 11837A Condition 10i, requires that each annual status report address the need for additional monitoring wells towards the periphery of the pressure build up area later in the project life.

There has been no change since submission of the 2013 first annual report [2]. At this time, Shell considers additional monitoring wells (BCS wells, Deep Monitoring wells or Groundwater Wells) situated towards the periphery of the pressure build up zone and near legacy wells unnecessary. There is no indication, from well data, that BCS pressure will increase to levels that would provide a threat to containment (see Section 4). Therefore, Shell considers the current pressure monitoring program adequate until future, injection information indicates otherwise. The Redwater 3-4 well is proposed to be completed in both the CKLK and BCS in Q2 2014 dependant on the outcome of further study and regulatory approval to monitor the CKLK formation in that well.

7.2. Need for Additional Monitoring Wells near Legacy Wells

Approval No. 11837A Condition 10j, requires that each annual status report evaluate the need for additional deep monitoring wells adjacent to the four legacy wells in the approval area (Imperial Eastgate 100-01-34-057-22W400, Imperial Egremont 100-06-36-058-23W400, Imperial Darling #1 100-16-19-062-19W400 and Westcoast et al Newbrook 100-09-31-062-19W40). Based on the information provided, the AER may require the Approval Holder to drill one or more deep monitoring wells.

At this time, Shell considered monitoring wells near the legacy wells to be unnecessary, as there is no indication, from well data, that BCS pressure will increase to levels that would provide a threat to containment near the legacy wells (see Section 4).

7.3. Monitoring at Injection wells

In accordance with Condition 2 of the AER Approval received by Shell December 3, 2013 for the October 15, 2012 MMV plan, Shell will use IW 7-11 and IW 5-35 as temporary BCS monitoring wells until injection starts as per Shell's original plan.

Shell plans to use each of the three injection wells as pressure monitoring wells when feasible. At start-up, the first injector (IW 8-19) will be progressively ramped up in 2015 until stable injectivity is achieved. An interference test will follow with pressure in the BCS being monitored at IW 7-11 and IW 5-35. Afterwards, the other IWs will be

7. Monitoring Wells

started sequentially to ensure they all reach stable injectivity before the end of 2015 so that the contractual obligation for sustained operations can be achieved before the deadline of end 2015.

Furthermore, Shell plans to monitor the BCS pressures across the AOR, in the BCS, continuously at the three injection wells (IW 8-19, IW 7-11, and IW 5-35 and one observation well (Redwater 3-4) as well as through InSAR monitoring. This long-term continuous pressure monitoring within the wells will be the basis for history matching dynamic reservoir models.

8. Stakeholder Engagements

8. STAKEHOLDER ENGAGEMENTS

Stakeholder engagement activities for Quest continued throughout 2013. Activities fell into three main categories:

- 1) Updates to town, city and county councils through regularly scheduled meetings,
- 2) Project information sessions to the public, and
- 3) Community involvement in the Measurement, Monitoring and Verification (MMV) plan development and communication of results through participation in the Community Advisory Panel (CAP).

8.1. Government Authority Updates

Bi-annual updates were given to town and county authorities at their council sessions to provide the most recent Project progress information. Specifically, updates were provided to the following municipalities:

- April 16, 2013 – Redwater Town Council
- April 17, 2013 – Bruderheim Town Council
- May 2, 2013 – Lamont County Council
- May 7, 2013 – Strathcona County Council
- May 28, 2013 – Fort Saskatchewan City Council
- May 28, 2013 – Sturgeon County
- July 23, 2013 – Thorhild County Council

Shell's updates to the above councils were well received. No major issues were raised and all questions posed by each of the councils were general in nature and answered immediately at the council sessions. Council updates will continue through out 2014.

8.2. Public Information Sessions

To provide the broader public with the opportunity to hear the most recent updates on the Project and to provide a forum for questions and answers, open houses were held in the Quest impacted areas. These sessions were as follows:

- October 28, 2013 – Thorhild Community Center
- October 29, 2013 – Radway Agricentre
- October 30, 2013 – Bruderheim Community Hall

The open houses were advertised to the greater public through local advertising and were also promoted in the Quest Newsletter which was sent to over 2500 residents in the communities of Thorhild, Radway, Abee and Redwater. Residents living within the

8. Stakeholder Engagements

450m emergency planning zone of the pipeline were sent invitations to the open houses.

These open houses were generally well received with the attendees primarily looking for updates to the Project. No major concerns or objections were raised with respect to the Project at any of these public information sessions and any concerns that were raised have been addressed. There are no outstanding issues. The Project team is currently reviewing the plan for timing of open houses or other types of public information forums for 2014.

8.3. MMV plan community involvement through CAP

To involve the greater public in the development of the MMV plan, a Community Advisory Panel (CAP) was formed in 2012. The CAP comprises local community members including educators, business owners, emergency responders and medical professionals as well as academics and AER representation. The mandate of the panel is to provide input to Quest on the design and implementation of the MMV program on behalf of the broader community and to help ensure that results from the program are communicated in a clear and transparent manner.

In 2013 each meeting started with a project update followed by specific topics summarized below:

- March 7, 2013 – MMV plan presentations continued from first CAP meeting November 1, 2012.
- April 10, 2013 – MMV Plan presentation and education continued
- May 1, 2013 – SCVF and GM presentation and information session
- June 12, 2013 - Emergency Response Plan and update on SCVF and GM issues
- September 18, 2013 – CAP visit of North Saskatchewan River Cross during the directional drilling campaign and tour of the pipeline and Scotford Capture Facilities
- October 23, 2013 – Update on baseline monitoring progress to date.

CAP meetings will be continued in 2014.

9. CONSTRUCTION AND IMPLEMENTATION TEST RESULTS

A summary of the wells drilled in 2013 are listed in Table 2-1 and any major issues associated with the subsurface (MMV and wells) are discussed in Section 6.2. This Section is focused on construction and implementation activities related to capture and pipeline.

The main activities as related to construction and implementation for capture and pipeline in 2013 included finishing engineering, procuring equipment and advancing construction. Testing results relevant to this stage are focused around meeting regulatory requirements and Shell standards primarily related to pressure piping and equipment. A summary of such results are outlined in Table 9-1.

One part of the Project, however, was commissioned in 2013: the flue gas recycle (FGR) unit (FGR) on hydrogen manufacturing unit (HMU) 2. Due to the novelty of using FGR with an HMU, the potential risk of its operation impacting the Upgrader and the opportunity to access the process unit, the Project completed an accelerated installation of this unit during a scheduled Scotford Upgrader shut down. A process performance test was completed on this unit and a summary of the results is provided in Table 9-2.

Table 9-1: Summary of construction and implementation tests completed in 2013 for Quest CCS Project.

Test	Capture		Mod Yard	Pipeline	
	Piping ¹	Civil/Structural			
Total Butt Welds	76	647	6751	1097	
Total Socket Welds	11	-	-	-	
Total Cooling Water Butt Welds	133	-	-	-	
Total Fillet Welds	-	9 ²	-	-	
Welding Tests	Radiography (RT)	76 (Butt) 81 (Cooling Water) ³	NA	992 ⁴	1097
	Magnetic Particle Examination (MT) ⁵	64 (Butt) 11 (Socket)	9	4863	316
	Liquid Penetration Inspection (LPI)	2	NA	1393	NA
	Hardness	2 ⁶ (Butt)	NA	807	NA
	Ultrasonic Inspection (UT)	NA	647	See Note 4	NA
	Positive Material Identification (PMI)	21	NA	8077	NA
	Optical Emission Testing	NA	NA	98	NA
Other	Pneumatic and Hydrotests (Accepted)	Firewater Lines – 2 Instrument Air – 2 Vessels/Exchangers – 2	Piping Spools – 618 Vessels - 42	Preliminary integrity testing for bore section under the NSR. Accepted on October 28, 2013 Will be tested again with entire pipeline - 2014	
	Infiltration Test	Manholes and storm drains – 5	NA	NA	
	Process Performance Test	FGR (HMU2)	NA	NA	
	Functional Tests	FGR (HMU2) – 38 instrumentation devices and associated control loops	NA	NA	

¹ Piping welds include those on the main CO₂ pipeline located within the Scotford Complex and those completed on other equipment associated with Quest.

² Fillet welds are completed on the lifting lugs.

³ RT on cooling water line welds was completed on 100% of underground welds and on a sampling on those above ground

⁴ This total includes both RT and UT results.

⁵ MT testing is done on 100% of the main CO₂ pipeline Butt Welds and on a sampling of welds on other equipment.

⁶ Hardness Testing is done on a percentage of total Butt Welds by line class

⁷ PMI testing is completed on a prescribed percentage of welds based on material type.

The process performance test completed on the FGR of HMU2 provided the engineering and operations community the opportunity to test the equipment prior to installation of the other two FGRs on HMU1 and 3 and prior to changing the operating conditions to “carbon capturing”. The objectives of this test included to establish the functionality of FGR and to obtain the learnings for the installation in HMU 1 and HMU 3. This test also served to test the performance of the newly installed low NO_x burners.

Overall, testing of the FGR fan was successful and has shown that no major design changes are needed to move forward with the completion of FGR 1 & 3. A summary of the detailed results are found in Table 9-2 below.

Table 9-2: Testing results from FGR2 Performance Test

Testing Objectives	Conclusions
Operability	The fan performed as per expectations, and had limited impacts on the operation of the reformer
Fan Ramp Up	FGR fan was successfully ramped up and down, with limited impacts on HMU operations. Natural Gas flows were increases to burners to compensate for flow of colder FGR gas into combustion air stream. This occurred as expected
Continuous Operation	The goal of operating the FGR fan continuously for 24hr was not achieved do to operational constraint set by base plant. Due to the success of the testing and the limited impact that FGR has on the HMU operation, there may be an opportunity at a later date to retest the fan for a longer period of time.
NO _x Levels	The NO _x came down from 30.7ppm just prior to the test to 17.6ppm at 36000sm ³ /h of FGR flow (further increases are difficult to compare due to process flow changes). This was a significant decrease that was not expected based on design data. The NO _x levels have remained 25% below normal operating levels during CO ₂ rich operations (no FGR).
FGR Operating parameters	All other operating parameters were as expected including O ₂ content in the combustion air, FGR flows, convection bank temperatures, FGR and FD fan power consumption, as well as pressures associated with fan operation.
Test Flame Scanners	The flame scanners that were being tested on the reformer showed inconsistent performance. Prior to the shutdown, both test instruments gave highly variable readings (compared with the current flame scanners that have a consistent signal), and after start up the signals from both new scanners was going in and out of Bad Signal readings. These tested flame scanners should not be considered acceptable for installation without further testing and evaluation.

REFERENCES

- [1] Carbon Dioxide Disposal Approval No. 11837A, AER, August 8, 2013.
- [2] Shell Quest Carbon Capture and Storage Project: First Annual Status Report. Submitted to AER January 31, 2013 as per Carbon Dioxide Disposal Approval 11837A Conditions 10 and 11.
- [3] Energy Resources Conservation Board Decision 2012 ABERCB 008: Shell Canada Limited, Application for the Quest Carbon Capture and Storage Project, Radway Field. Energy Resources Conservation Board, Calgary Alberta. July 10, 2012.
- [4] Energy Resources Conservation Board. Quest Carbon Capture and Storage Project Radway Field & Surrounding Areas ERCB Approval No. 11837, ERCB Decision 2012 ABERCB 008 Information Request to Shell. Received March 28, 2013.
- [5] Quest Carbon Capture and Storage Project Radway Field & Surrounding Areas AER Approval No. 11837A, AER Decision 2012 ABERCB 008 Special Report #1 & Pre-baseline MMV Plan. Submitted to AER October 15, 2012.
- [6] Quest Carbon Capture and Storage Project Radway Field & Surrounding Areas AER Approval No. 11837A. Information Request #3 RE: November 2012 MMV plan submitted with Application No. 1670112, Special Report #1 October 15, 2012 Appendix: Measurement Monitoring and Verification Plan, Shell April 23, 2013 Response to ERCB April 17, 2013 IR. Received by Shell September 5, 2013.
- [7] Alberta Energy Regulators. Quest Carbon Capture and Storage Project Radway Field & Surrounding Areas AER Approval No. 11837A, AER Decision 2012 ABERCB 008 Special Report #1 & Pre-baseline MMV Plan October 15, 2012 Submission. Updated Approvals and Conditions. Received December 3, 2013.
- [8] Shell Canada Energy: Proposed Resolution for the Surface Casing Vent Flows and Gas Migrations on the wells SCL 102/05-35-059-21W4/00 and SCL 103/07-11-059-20W4/00. Letter submitted to AER August 28, 2013.

References

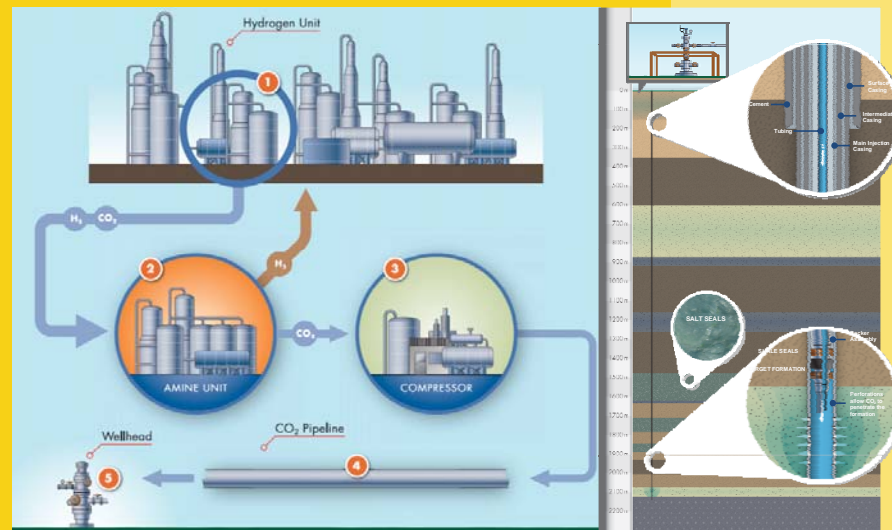
- [9] Surface Casing Vent Flow (SCVF) and Gas Migration Repair (GM) – Deferral Request. AER Approval and Conditions. Received by Shell September 4, 2013.
- [10] Shell Canada Limited Quest Carbon Capture and Storage Project (the “Project”) Approval No. 11837A (the “Approval”) Carbon Sequestration Lease Approvals: 5911050001, 5911050002, 5911050003, 5911050004, 5911050005, 5911050006 (the “Leases”) letter of self-disclosure of out of zone perforation. Submitted to AER November 25, 2013.
- [11] Shell Quest Carbon Capture and Storage Project Measurement Monitoring and Verification Plan February 14, 2014 Update. Submitted to AER February 14, 2014.
- [12] Shell Canada Limited Quest Carbon Capture and Storage Project Approval No. 11837A submission of additional information regarding off-depth perforations in injection well 102-05-35-059-21W400. Submitted to AER January 20, 2014.

APPENDIX A: BCS CORE DESCRIPTIONS FOR IW 5-35 AND IW 7-11



QUEST CCS PROJECT – Core Description Summary of the Basal Cambrian Sand

January 15, 2014



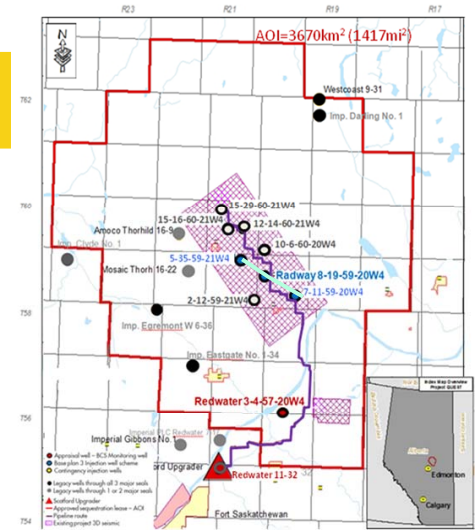
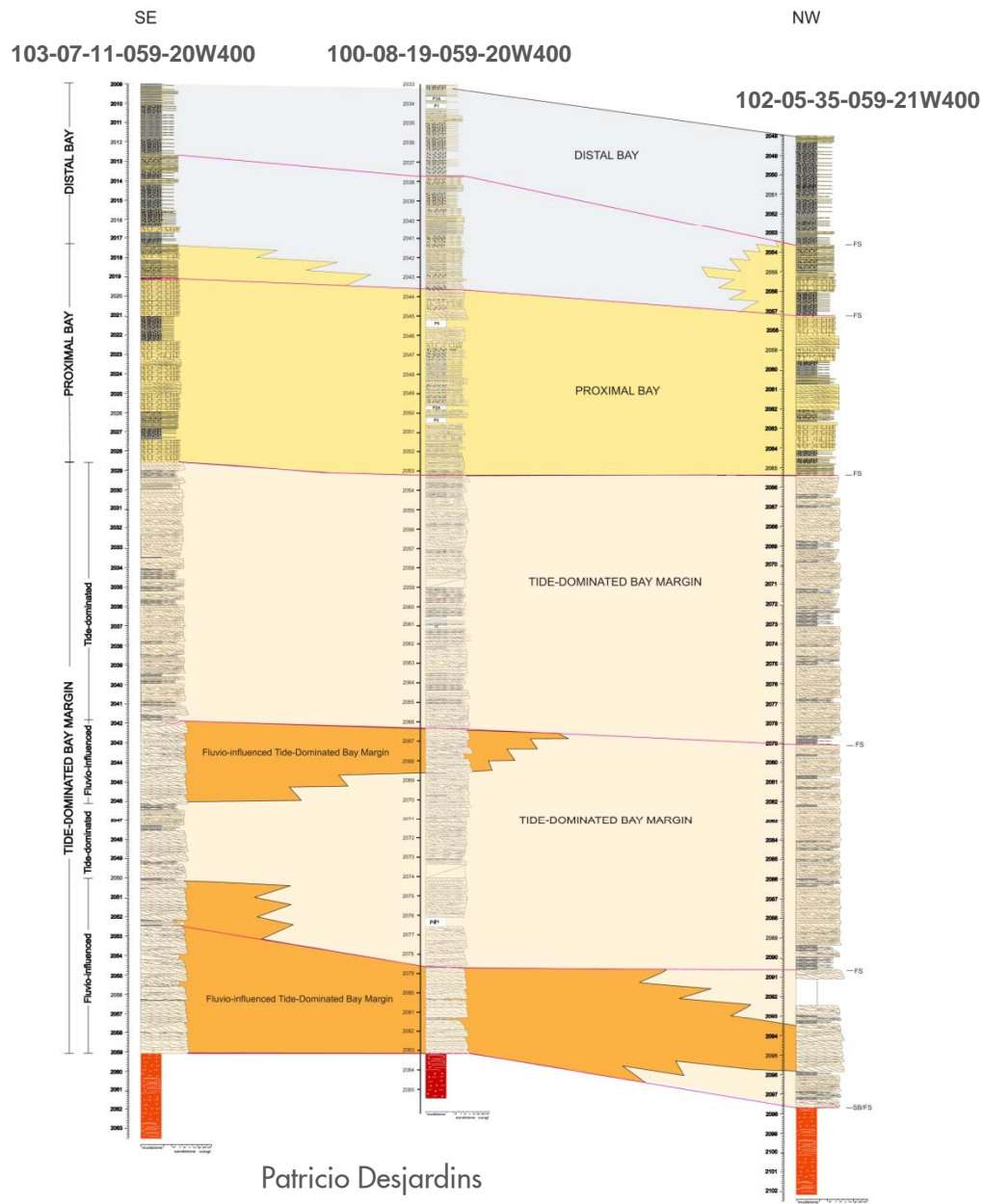
Patricio Desjardins

Summary of Quest Wells with Core Interpretations

- The new cores interpreted in 2013 were the IW 7-11 and IW 5-35 cores. A summary of how these cores relate to previously interpreted core descriptions for the BCS is presented here-in.

UWI	Well type	Well name in this report	Spud date [d/m/y]	Rig release [d/m/y]	Total Depth [m MD]	TD formation
1AA/11-32-055-21W400	Appraisal (Abandoned)	Redwater 11-32	10/11/2008	02/01/2009	2240.6	Precambrian
100/03-04-057-21W400	Observation	Redwater 3-4	23/01/2009	18/03/2009	2190.0	Precambrian
100/081905920W4/00	Injection	IW 8-19	01/08/2010	08/09/2010	2132.0	Precambrian
102/053505921W4/00	Injection	IW 5-35	21/10/2012	20/11/2012	2143.0	Precambrian

Correlation Parallel to Depositional Dip



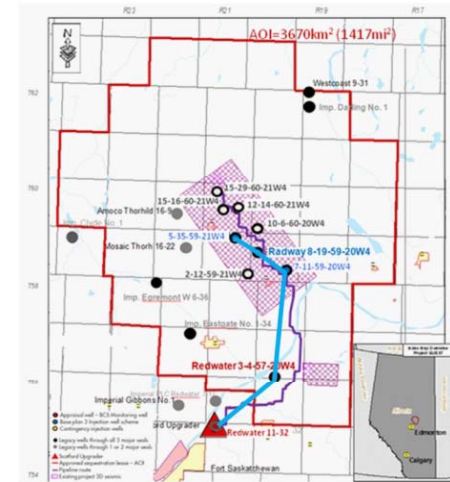
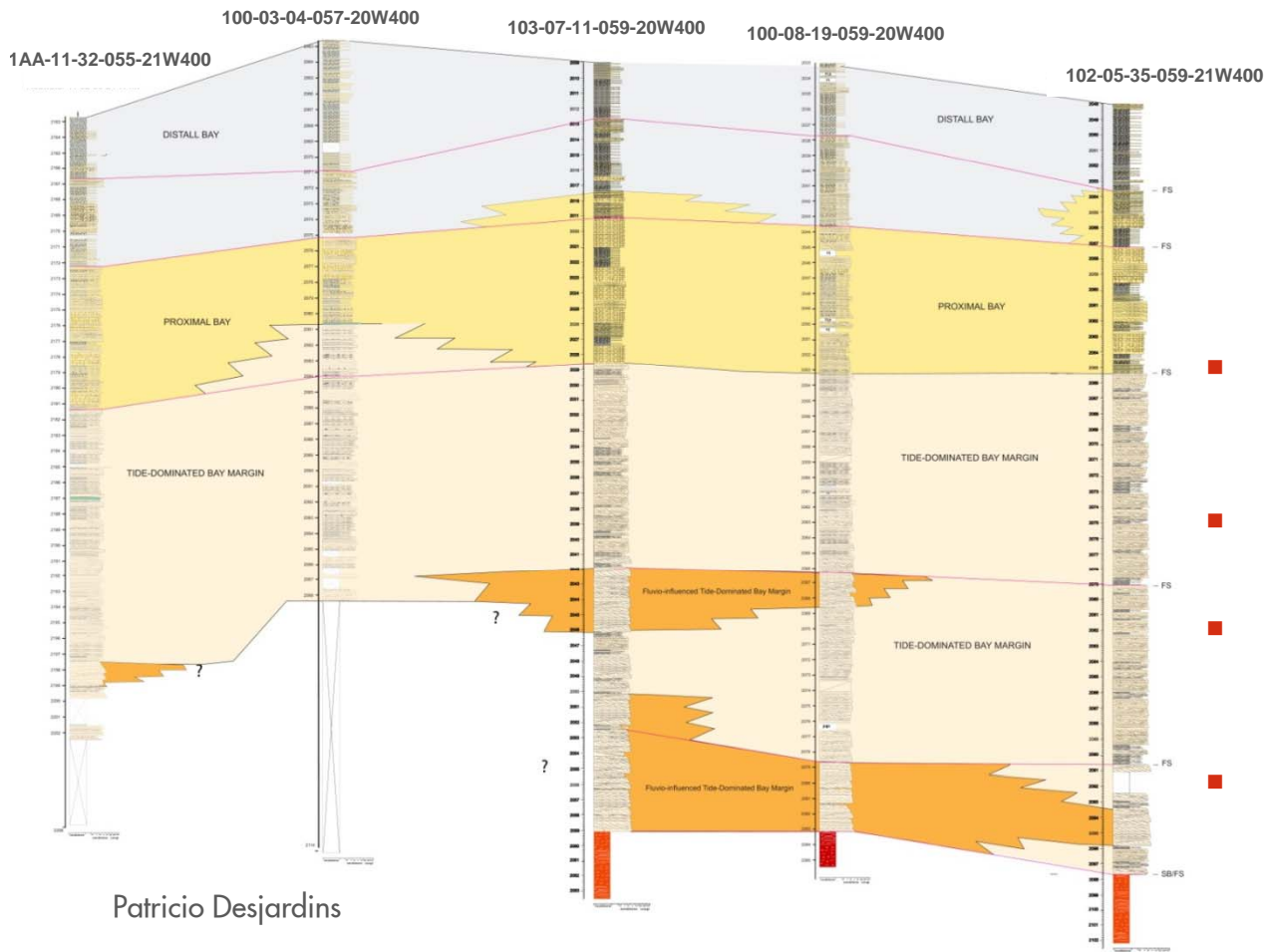
- Major flooding surfaces were used to correlate between wells
- Overall, the cores become coarser grained to the East where the Tide Dominated bay margin has a greater influence by fluvial systems. This confirms the proximal-distal trends in the reservoir model
- The Proximal Bay and Distal Bay settings do not have a clear proximal-distal trend as the TDBM, as this environment is dominated by large compound dunes fields (sandsheets) that are internally more heterogeneous
- The compound dunes in the Proximal Bay are the product of reworked sands by tidal current that can create a non-uniform sandstone distribution on the sea-floor surface
- The thicker development of Proximal Bay deposits in IW 5-35 suggest that the sandstones in this environment do not follow the trends of the Tide-Dominated Bay Margin

January 15, 2014

Correlation Using All Cores

CAMBRIAN BASAL SANDSTONE CROSS SECTION

author: Patricio Desjardins



- The correlation between all cores suggests that IW 5-35 and Redwater 11-32 are located in the most distal position with respect to the shoreline
- IW 7-11 is possibly most proximal of all cores as it has the thickest Fluvio-influenced interval
- However, the Redwater 3-4 well has the thickest of TDBM interval. The lower portion of the BCS was not cored.
- No major unconformity or facies changes have been identified that would required a major change to the current reservoir model

Conclusion

- Lithofacies and facies associations in these new cores are similar to those described before
- The vertical stacking of lithofacies and facies associations is also similar to the other wells, with tide-dominated bay margin deposits , follow by proximal bay sediments which are capped by fine-grained lithologies recording the distal bay environment
- The analysis of the IW 7-11 and IW 5-35 cores have confirmed the lateral continuity of the same types of sandstone lithologies as observed in previous cores
- These additional cores have also confirmed the proximal versus distal trends built into the Gen-4 static model. The core from IW 7-11, located in the most eastern part of the SLA, has the coarsest lithologies as predicted by the geologic model
- Like in IW 8-19, in IW 7-11 at the base of the BSC there is an coarse-grained sandstone interval interpreted as high-energy dunes deposited within channels of fluvio-influenced tide-dominated bay margin
- Based on the study of these new cores no major modifications related to the environments of deposition are required in the upcoming Gen-5 static model update

APPENDIX B: DETAILED FORMATION EVALUATION FINDINGS

1. Monitoring Well 102-07-11-059-21W400 (DMW 7-11)

The logging program in DMW 7-11 was designed to acquire data in the reservoirs overlying the BCS storage complex in order to reduce uncertainty in rock properties (porosity, permeability, net reservoir, lithology, lateral extent, vertical connectivity) and enable selection of the zone to be used for pressure monitoring. The sampling program was also designed to obtain fluid samples for geochemical analysis. The well had an extensive wireline data and fluid collection program, as described below.

Logging and coring programs were designed accordingly.

a. TD Section DMW 7-11 (420-1667 m MD)

- Logging runs
 - TLD-APS-HNGS-ECS-AIT
 - GR-GPIT-SSCAN-PPCX2-UBI
 - Wireline magnet (Cancelled)
 - CMR PLUS-GR-APS-CNL
 - XPT-GR
 - MDT-GR (Dual Packer Module for fluid sampling)
- Log Quality and Findings Summary:
 - All logs are good quality
 - Glauconitic Sandstone: 11.3 meters TVD of net reservoir @ 19.5 p.u. average porosity
 - Cooking Lake: 44.3 meters TVD of net reservoir @ 13.7 p.u. average porosity
 - Moberly: 3.9 meters TVD of net reservoir @ 11.6 p.u. average porosity
 - Winnipegosis: 14.2 meters TVD of net reservoir @ 9.3 p.u. average porosity
 - Contact Rapids: 30.5 meters TVD of net reservoir @ 6.7 p.u. average porosity.
 - Formation fluid was recovered from two aquifers
 - Glauconitic Sandstone Fm.: 6 MPSR bottles were filled at 778 m MD
 - Cooking Lake Fm.: 6 MPSR bottles were filled at 1138.8 m MD
 - Winnipegosis / Contact Rapids were not pressure tested as the log response showed the same tight response. (low perm estimation from the CMR)

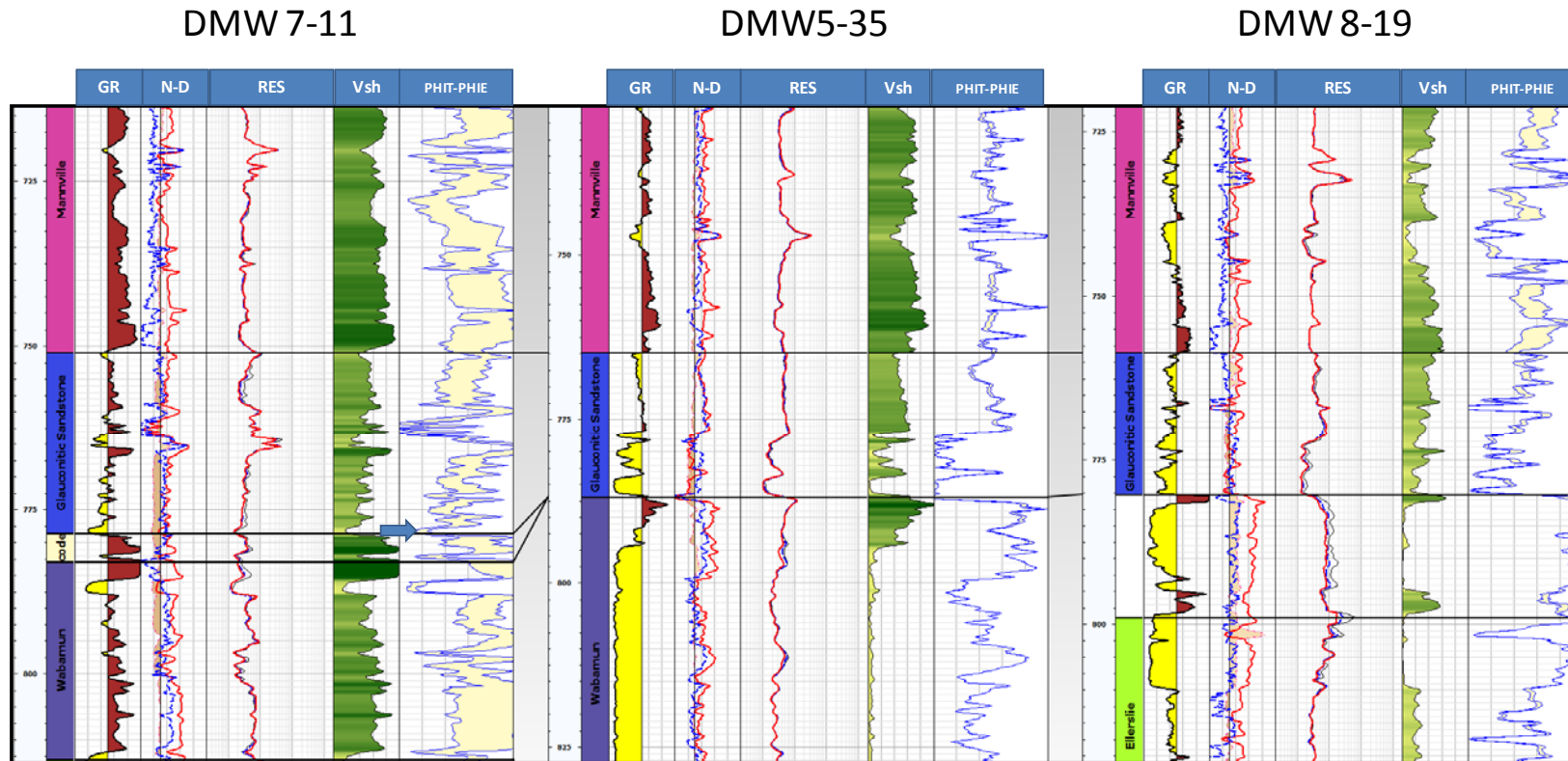


Figure 3-1: MDT fluid sample depth in the Glauconitic Sandstone Formation for the DMW 7-11. Sample depth: 778 m MD (the blue arrow is pointing to the sample depth)

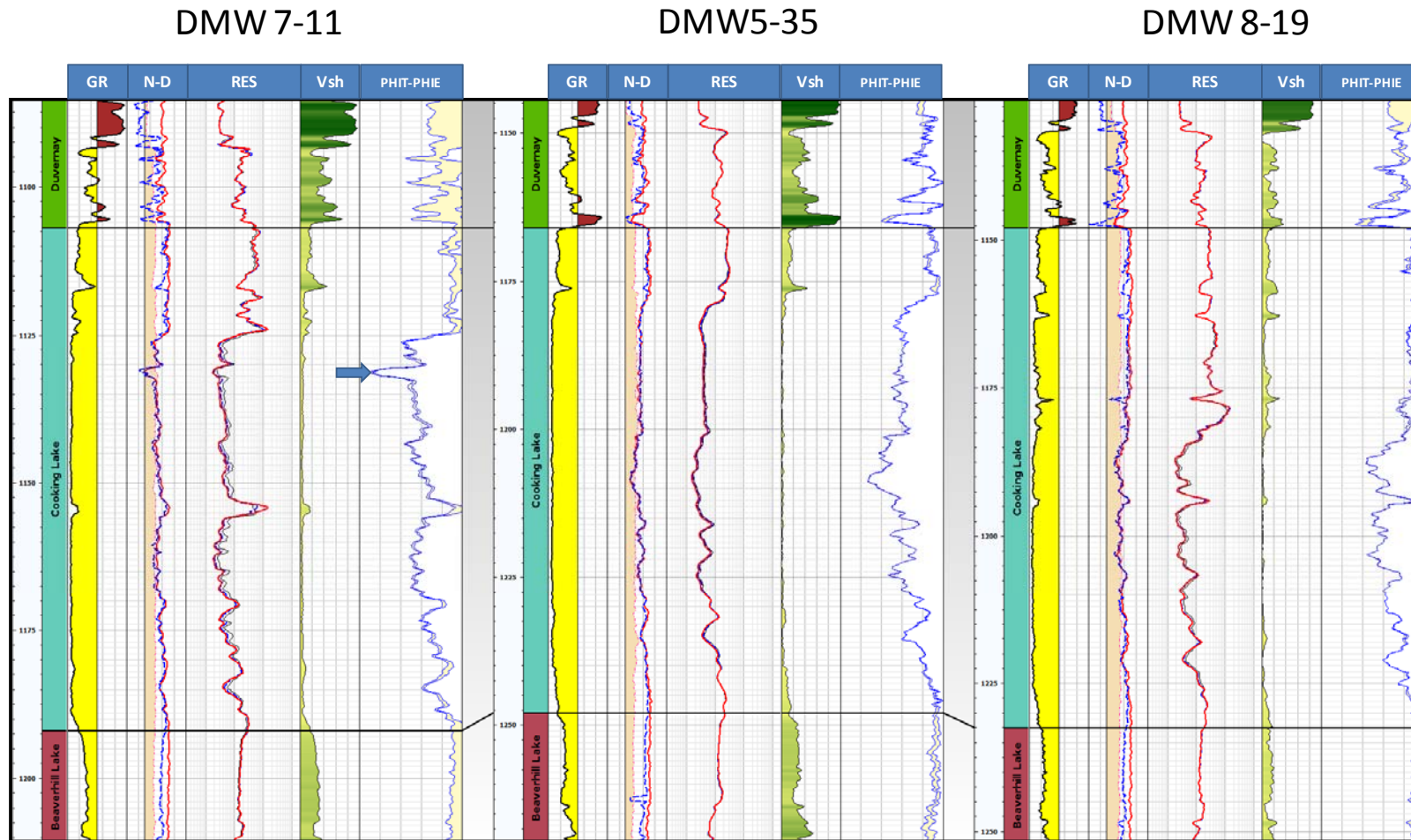


Figure 3-2: MDT fluid sample depth in the Cooking Lake Formation for the DMW 7-11. Sample depth: 1338.8 m MD (the blue arrow is pointing to the sample depth).

Appendix B

Field: Radway

Well: SCL RADWAY 7-11-59-20W4 (DMW 7-11)

Mud Weight = 1050.0 kg/m3

KB (m) = 641.41

Field Engineer(s): Derek Woods / Duane Gillis (+1-780-518-7655)

Ground Level (m) = 636.25

Wellsite Witness: Larry Haynes (+1-403-512-6643)

Bit size = 216 mm

FEAST Engineer: Melton Hows / Tushar Prasad

Logging Date = 3/4-Feb-2013

Test No.	File No.	Depth MD (m)	Depth TVD (m)	Depth SSTVD (m)	Mud Before (kPaa)	Mud After (kPaa)	Last Read (kPaa)	Good P (kPaa)	EMW (kg/m3)	Temp (degC)	Mob (md/cp)	Zone	G	T	D	LS	SC	Remarks	MW (kg/m3)	MW (ppg)			
4	2	753.80	753.80	112.4	8102.8	8102.4	4689.26		634.3	29.21	0.98	Glauconitic SS						5@30, 5@12. Incorrect call	1096.1	9.148			
7	3	753.79	753.79	112.4	8103.8	8103.2	4692.07	4692.07	634.7	29.58	0.50	Glauconitic SS	1					5@30, 2x1@15	1096.3	9.149			
11	4	755.50	755.50	114.1	8123.1	8123.4	4713.87	4713.87	636.2	29.75	1.37	Glauconitic SS	1					5@30, 2x1@15, 2@6. Good	1096.4	9.150			
14	5	756.99	756.99	115.6	8141.9	8139.5	4728.20	4728.20	636.9	29.86	1.41	Glauconitic SS	1					5@30, 2x 2@6. Good	1096.8	9.153			
16	6	772.79	772.79	131.4	8311.8	8308.8	5220.36		688.8	30.00	0.32	Glauconitic SS					1	5@30, 1@6. Very slow BU. Maybe SC.	1096.8	9.153			
18	7	774.99	774.99	133.6	8334.7	8331.8	5579.60		734.2	30.10	0.21	Glauconitic SS					1	1@6, 0.5@3. Very slow BU. SC.	1096.7	9.152			
22	8	778.09	778.09	136.7	8367.2	8365.5	4936.76	4936.76	647.0	30.19	179.6	Glauconitic SS	1					1@6, 5@15, 2x5@30. Good	1096.6	9.151			
25	9	786.71	786.71	145.3	8460.8	8458.1	4987.45	4987.45	646.5	30.46	284.8	Eilerslie	1					1@6, 2x5@30. Good	1096.7	9.152			
26	10	796.80	796.80	155.4	8568.1	8568.8	5117.51		654.9	30.44	0.13	Eilerslie					1	1@6. Tight, slow BU. Aborted	1096.5	9.151			
32	11	827.60	827.60	186.2	8901.0	8893.0	5389.59	5389.59	664.1	30.71	0.36	Nisku	1					2x1@6, 1@3, 3x2@3. Possible SC	1096.7	9.153			
36	12	841.01	841.01	199.6	9038.3	9033.8	5526.87	5526.87	670.1	30.87	0.41	Nisku	1					3x1@6, 2@3.	1095.9	9.146			
37	13	846.50	846.50	205.1	9094.9	9092.9				31.00		Nisku					1	1@6 Dry test	1095.6	9.143			
38	14	858.30	858.30	216.9	9220.8	9219.0				31.10		Nisku					1	1@6 Dry test	1095.5	9.142			
41	15	1126.11	1126.11	484.7	12041.4	12032.8	8906.72		806.5	37.68	0.08	Cooking lake	1					1@6, 2x1@3. Low mob. Probably SC.	1090.4	9.100			
45	16	1131.61	1131.61	490.2	12096.1	12093.9	8963.70	8963.70	807.7	38.11	8.4	Cooking lake	1					1@6, 5@6, 2x5@30	1090.0	9.097			
49	17	1138.79	1138.79	497.4	12169.2	12168.0	9042.05	9042.05	809.7	38.16	10.1	Cooking lake	1					1@6, 5@6, 2x5@30	1089.7	9.094			
53	18	1143.41	1143.41	502.0	12219.3	12215.0	9089.44	9089.44	810.6	38.78	0.26	Cooking lake	1					2x1@6, 2@6, 2@3.	1089.7	9.094			
54	19	1160.41	1160.41	519.0	12394.2	12392.6	9160.10		804.9	39.03	0.05	Cooking lake		1				1@6. Very tight aborted.	1089.1	9.089			
57	20	1167.11	1167.11	525.7	12465.4	12461.5	9355.02		817.4	39.29	0.15	Cooking lake					1	2x1@6, 1@3. Slightly SC	1089.1	9.089			
60	21	1173.00	1173.00	531.6	12524.9	12522.3	9448.76		821.4	39.59	0.12	Cooking lake					1	1@6, 2x1@3. Low mob. SC.	1088.8	9.087			
62	22	1184.59	1184.59	543.2	12645.2	12644.0	9644.72		830.2	39.77	0.18	Cooking lake					1	1@6, 1@3. Low mob. SC	1088.5	9.084			
63	23	1265.81	1265.81	624.4	13492.2	13492.7				41.63		Moberly					1	1@6 Dry test	1086.9	9.071			
64	24	1275.20	1275.20	633.8	13589.8	13589.0				41.72		Moberly					1	1@6 Dry test	1086.7	9.069			
65	25	1280.20	1280.20	638.8	13642.6	13642.8				41.86		Moberly					1	1@6 Dry test	1086.7	9.069			
66	26	1291.49	1291.49	650.1	13761.3	13761.0				42.00		Moberly					1	1@6. Very tight. Classify as Dry test	1086.5	9.068			
67	27	1347.80	1347.80	706.4	14347.0	14347.1				42.56		Calmut					1	1@6 Dry test	1085.5	9.059			
68	28	1349.30	1349.30	707.9	14362.1	14361.4				43.02		Calmut					1	1@6 Dry test	1085.4	9.058			
69	29	1351.00	1351.00	709.6	14379.1	14378.5				43.30		Calmut					1	1@6 Dry test	1085.3	9.057			
												TOTAL	18	11	1		6						

Figure 3-3: Summary of the XPT results for DMW 7-11.

Appendix B

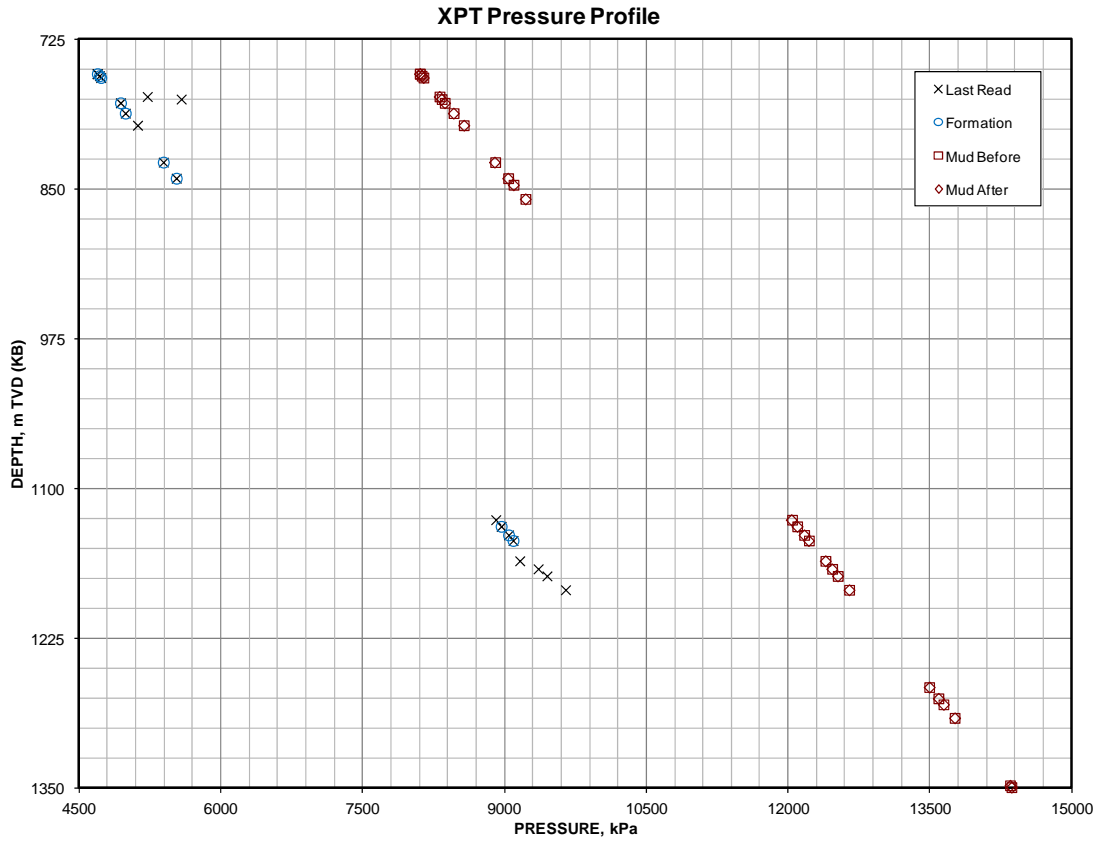
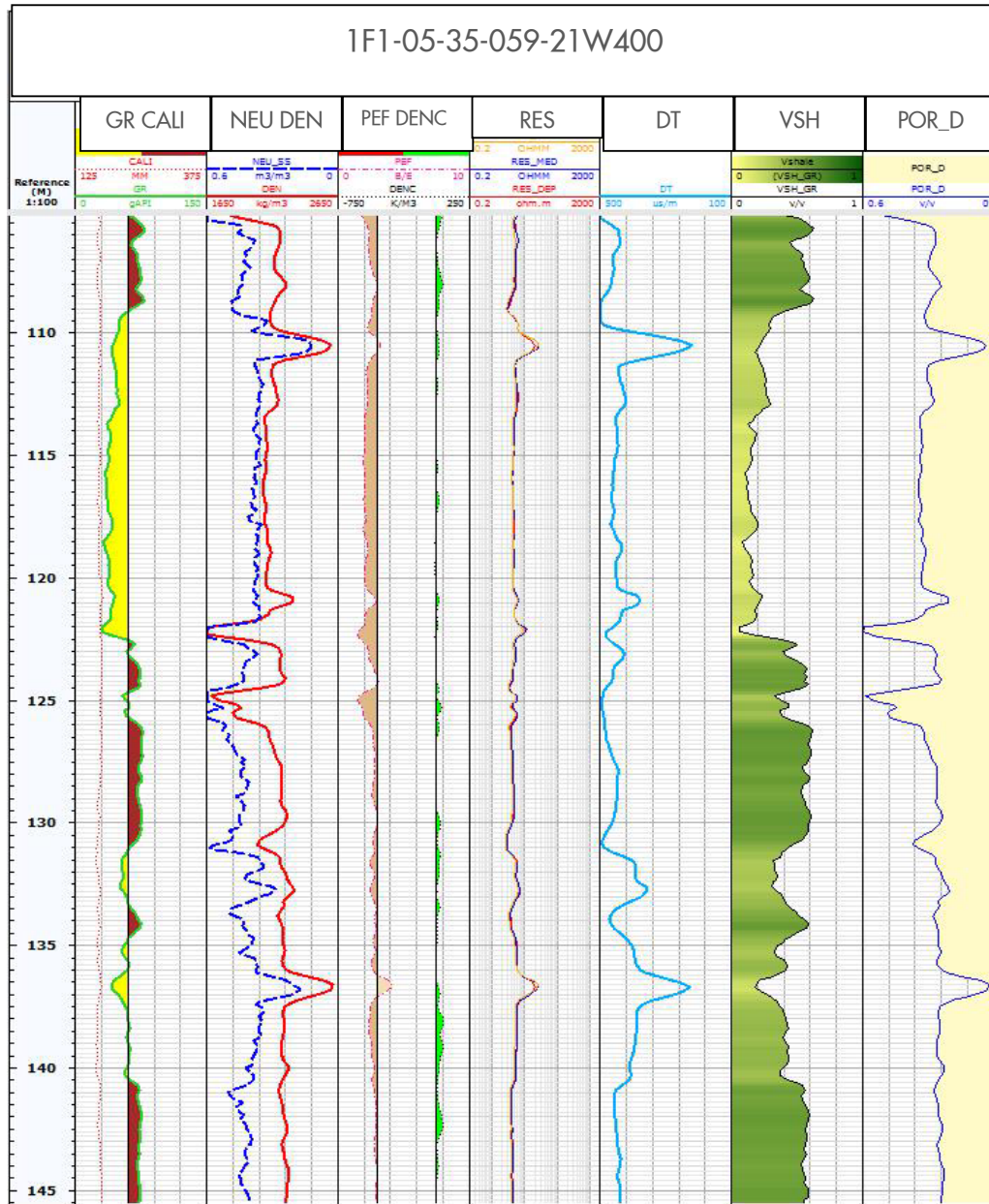


Figure 3-4: XPT pressure-depth cross plot for DMW 7-11.

Appendix C

APPENDIX C –PETROPHYSICAL EVALUATION OF GROUNDWATER WELLS

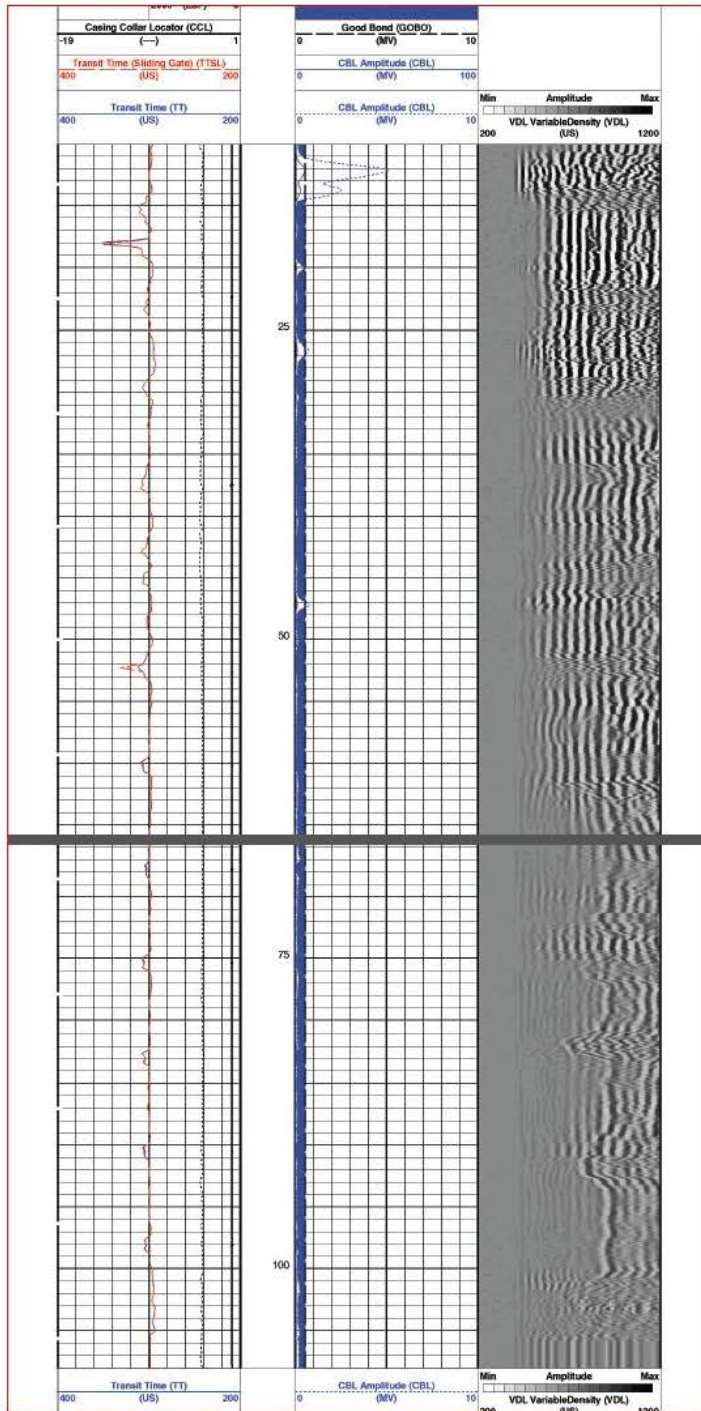
2. Well 1F1-05-35-059-21W400



Appendix C

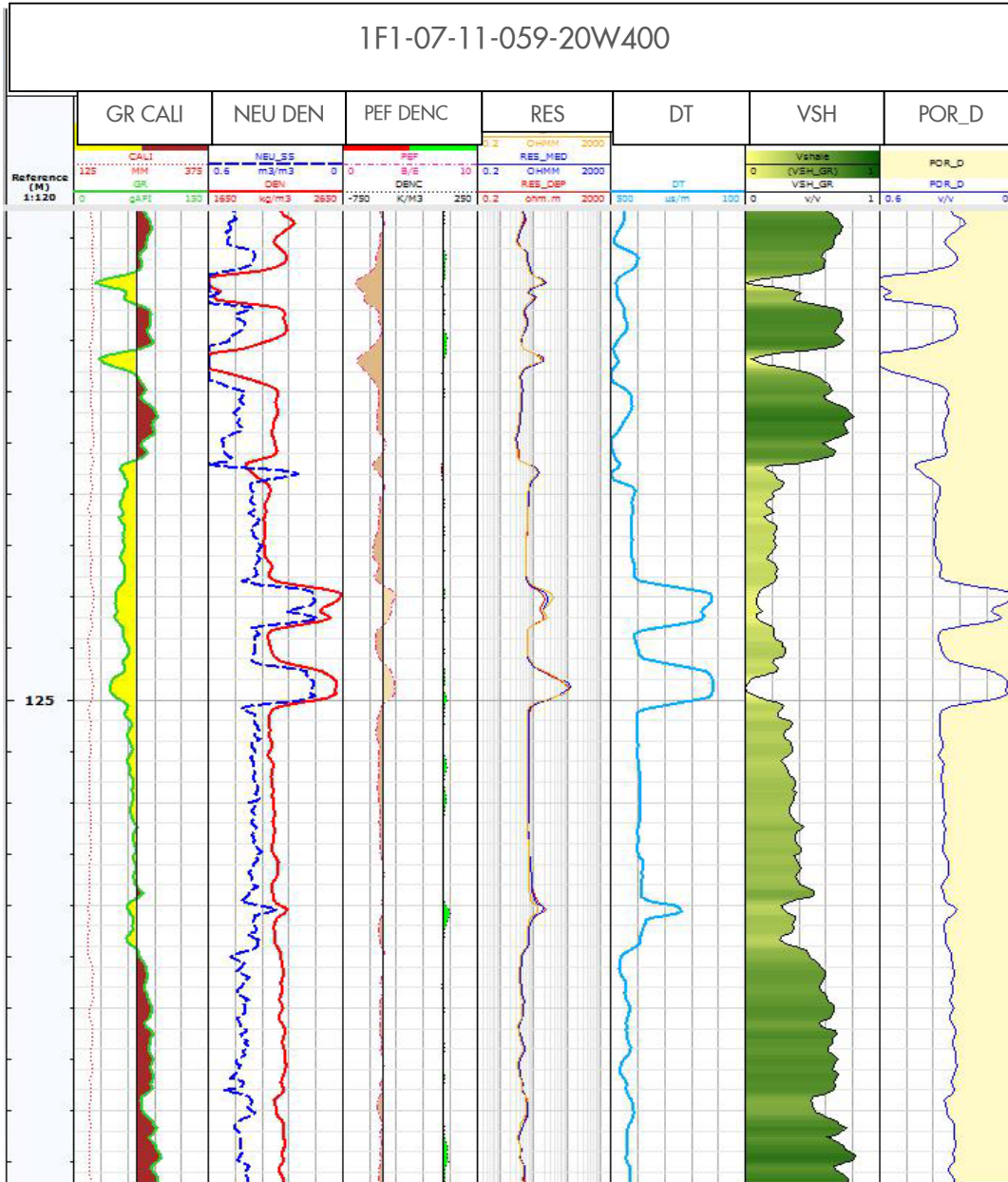
1F1-05-35-059-21W400

CBL



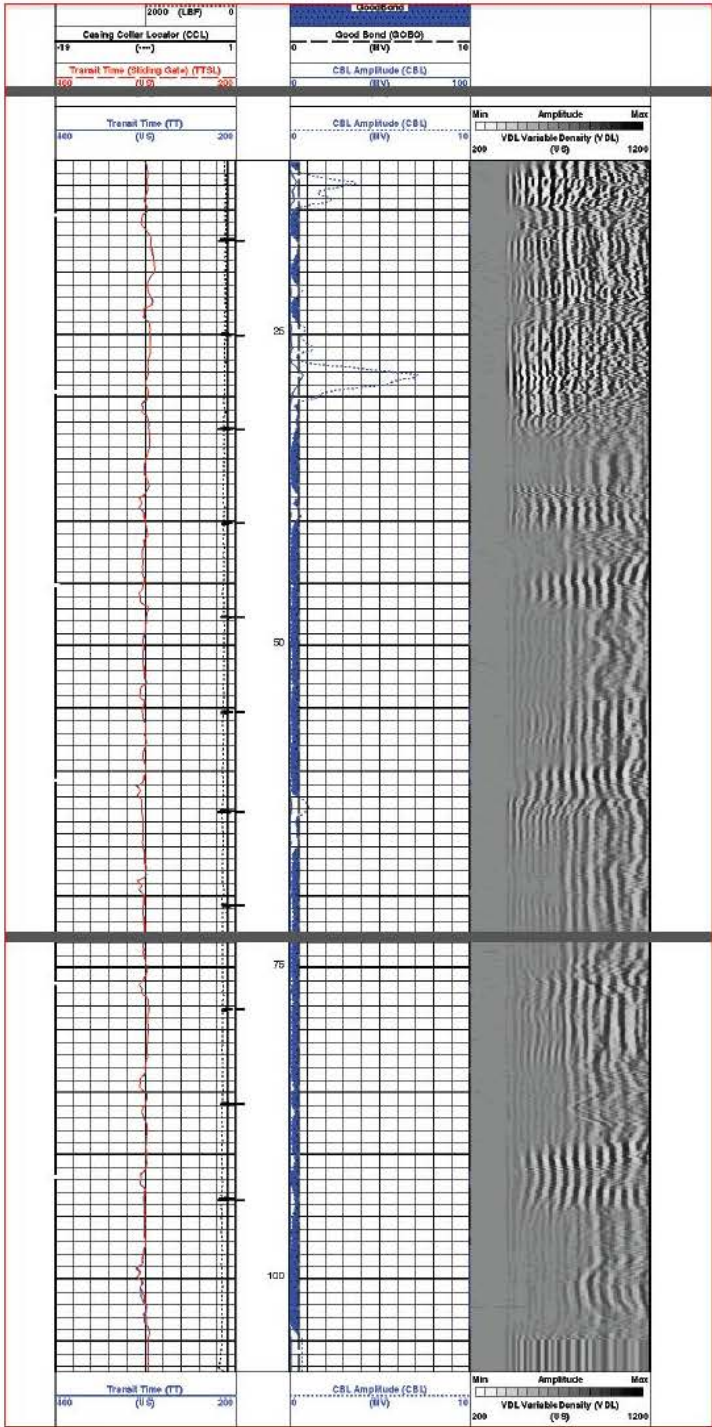
Appendix C

3. Well 1F1-07-11-059-20W400



Appendix C

1F1-07-11-059-20W400
CBL



APPENDIX D –ARTIFICIAL TRACER INTERIM FEASIBILITY REPORT

Unrestricted

SR.14.

Interim Report

**Perfluorocarbon Tracers Technology applied
to
CCS Quest Project**

**by
H.Peters (PTI/RC)**

This document is unrestricted.

Shell Global Solutions International B.V., Rijswijk

Further electronic copies can be obtained from the Global Information Centre.

Executive summary

In this research, the suitability of perfluorinated organic compounds (PFCs) as passive tracers in long term CCS-MMV applications is being evaluated. The aim is to identify potential scavenging and losses of the tracer due to the interaction of the parent fluid, i.e. CO₂, with different rock matrices and other subsurface fluids.

The research at this stage is closely linked to the QUEST project which is operated by Shell Canada Ltd. Therefore, the main focus is primarily on lithologies and fluid inventories associated with the QUEST project. Fluids range from freshwater, NaCl dominated up to NaCl saturated brines. Lithologies comprise arkose type sandstones, clay and coal rich siliciclastics and carbonates.

The perfluorinated compounds include various methylated, ethylated cyclic and straight chain perfluorocarbons ranging from C₄ to C₆ backbones. These are assessed in terms of their partitioning behavior with other fluids and their retention/scavenging with respect to certain rock matrices. Until now, pure silica, pure sandstones and sandstones with certain amounts of clay (kaolinite) and organic substrates (i.e. matured coals) were studied in their ability to retain or adsorb PFCs in 1D displacement scenarios of supercritical CO₂ displacing water/brine.

The experimental study for this research is conducted in collaboration with The Commonwealth Scientific and Industrial Research Organisation (CSIRO), and the Institute for Energy Technology (IFE). The partitioning behavior, which includes the effects of temperature, pressure and salinity, is investigated using a classical batch reactor setup. The retention and/or adsorption behavior is assessed using a slim tube apparatus.

The preliminary conclusion is that PFCs may remain in sufficient detectable amounts in its parent CO₂ phase at shallow depth in the hydrostratigraphic column. The data confirm that PFCs have very low solubility in water and are not retained at significant/critical amounts during migration by matrices prone to adsorb organic compounds like clays and coal. Hence, experimental data obtained so far suggest that PFCs are a suitable reliable passive/conservative tracer of injected CO₂. Experimental measurements are continuing to explore the behavior of organic substrate adsorption and CO₂/water/hydrocarbons partitioning.

Table of contents

Executive summary	II
1. Introduction	1
2. Aim of Perfluorocarbon tracer feasibility study	3
3. History of PFC chemical tracers applied to CO ₂ sequestration projects	5
3.1. K12B project	7
3.2. Frio Brine Project	8
3.3. San Juan CBM Project	11
3.4. The West Pearl Queen site	14
3.5. ZERT site Bozeman, Montana	16
3.6. Synopsis	18
4. PFC - Petroleum reservoir studies	19
4.1. Synopsis	25
5. Perfluorocarbon tracer properties	26
5.1. Physical and Chemical properties of Perfluorocarbon Tracers	26
5.2. Partitioning and adsorption characteristics of PFCs	30
6. Environmental fate of perfluorocarbons	31
6.1. Reactivity of PFCs	31
6.2. Atmospheric background of PFCs	32
6.3. Greenhouse Gas Potential of PFCs	35
6.4. Solubility of PFCs	36
6.4.1. <i>Synopsis</i>	42
6.5. Detection of PFCs	43
6.5.1. <i>GC-ECD – electron capture detection method</i>	44
6.5.2. <i>GC-MS - Mass spectrometry detection technique</i>	45
7. Laboratory study to understand subsurface behavior of Perfluorocarbon Tracers	49
7.1. Laboratory setup of batch and slim tube experiments	49
7.1.1. <i>Loading procedure</i>	49
7.1.2. <i>Sampling procedures</i>	49
7.1.3. <i>Gas Phase sampling</i>	50
7.1.4. <i>Water phase sampling</i>	50
7.2. Slim tube experimental setup description	50
7.2.1. <i>Sampling procedure</i>	51

7.2.2. <i>GC Sample Injection Procedure Using Packed Glass Tube</i>	51
8. Batch reactor experimental results	52
9. Slim tube experimental results	54
9.1. GC response curves for PFC concentration ranges	54
9.2. Retention behavior – scCO ₂ vs. water/brine	58
9.3. Retention behavior – synthetic quartz vs. clay content	62
10. Preliminary Conclusion	65
11. Outstanding experimental work	66
References	67
Bibliographic information	71

List of tables

Table 1:	PFC travel times of the three separate injections and calculated saturation of CO ₂ (adapted from [12])	10
Table 2:	Perfluorocarbon tracer compounds considered in research initiative with CSIRO, Australia.	27
Table 3:	Perfluorocarbons commercially available (status 2003) including amines and ethers (adapted from [22] Gladysz & Emnet 2004).	27
Table 4:	Adapted from Tsai (2009) – physical properties of perfluorocarbons	29
Table 5:	Characteristics of TD-GC-NICI detection of PFCs (after [67])	46
Table 6:	Data acquired for scCO ₂ /H ₂ O partitioning of various PFC compounds (first attempt)	53
Table 7:	Summary of GC response calibration curves for multiple PFCs in a concentration range from 0.08 to 6 nl	56
Table 8:	Scheduled slim tube experiments under supercritical CO ₂ conditions	57

List of figures

Figure 1:	K12B reservoir 3D and 2D maps with locations of injection and production wells (adapted from [5])	7
Figure 2:	Breakthrough curves of PMCP and 1,3 PDMCH at K12 B1 well (Aug 2005) and K12 B5 (June 2006) vs. CO ₂ breakthrough and cumulative CO ₂ production (adapted from [5])	7
Figure 3:	Interwell setup of tracer tests used by NETL during Frio Brine I phase [6]	8
Figure 4:	Tracer amounts, injection time, duration and travel times of tracers at Frio Brine phase I [11]	9
Figure 5:	Summary of PFC tracer concentrations of all injections normalized to their initial conc. vs. travel times in hours (from [11])	9
Figure 6:	Site description of San Juan CCS project White cross = injection site; Red crosses = offset/ observation wells (from [8])	11
Figure 7:	Tracer breakthrough data monitored at three offset wells (adapted from [8])	12
Figure 8:	Tracer plume migration monitoring using atmospheric and soil gas monitoring sites; Left picture: atmospheric detection during injection, yellow to red concentration scales are in the order of 350 to 400 fl/l, bluish colours are background concentrations of a few fl/l; Right picture: 2 months later soil gas monitoring detection; values in big print close to SW offset well; red colours indicating 500 to 600 fl/l conc. (adapted from [8])	12
Figure 9:	Lithology profile at West Pearl Queen shallow injection site with gamma ray detection (LEFT); CATS locations (yellow squares) and injection site (red square) highlighted (adapted from [14])	14
Figure 10:	PDCH(left) and PDCB (right) concentrations measured during a 54 days exposure after injection (after [14])	15
Figure 11:	Soil gas and tracer detection installations along the horizontal well of the second ZERT release test (adapted from [9])	16
Figure 12:	Cummulative soil–gas tracer concentrations at 1 m depth along the horizontal release test after 2.5 days exposure; pink and red colours indicate relative high concentrations, bluish colours represent minimum concentrations, measurement locations marked by black dots (after [9])	16
Figure 13:	Tracer concentrations measured at various depths (0.2 to 1m) at certain distance from the horizontal well taken at consecutive days after injection (after [9])	17
Figure 14:	Tracer compound mix at Snorre field; indicated are tracer injection data and recovery (adapted from [16])	19
Figure 15:	Tracer profile compared to GOR at Snorre Oilfield, adapted from [16]	20
Figure 16:	Tracer concentrations in CFB Snorre field study, adapted from [17]	20
Figure 17:	Production well P-29 tracer concentration profiles vs. GOR (gray bars) of the produced fluids (from [17])	21

Figure 18:	Total mass balance of all PFC tracer injected into the Snorre field (from Huseby et al 2008)	22
Figure 19:	Equation to calculate S_{or} , residual oil saturation, using the different retention times of the partitioning tracers applied; K-factors are calculated as ratio of immobile vs. mobile phase partitioning; right side: formula using an ideal tracer mixed with a partitioning one and the time difference of arrival (adapted from [19])	23
Figure 20:	Gas Tracer breakthrough curve; normalized and partition coefficients of tracers measured in static experiments with Ekofisk oil, from [19]	23
Figure 21:	Simulated vs. measured tracer breakthrough curves (adapted from [19])	24
Figure 22:	Retention behavior of tracer due to partitioning effect (adapted from [19])	24
Figure 23:	Birch reduction mechanism to exchange fluorine for hydrogen under catalytic conditions using a Zirconium complex (from Amii & Uneyama, 2009)	31
Figure 24:	Perfluorohexane and-heptane concentrations in the atmosphere (adapted from Laube et al. 2012)	32
Figure 25:	Mean “heavy” PFC mole fractions and estimated growth rates in the atmosphere (adapted from Ivy et al. 2012)	33
Figure 26:	Mean measured concentrations of n-C6F14 and the annual growth rates (from Ivy et al. 2012)	33
Figure 27:	Estimated and rounded background concentrations of PFCs chosen for CCS MMV purposes; above: generalized background values in ppqv; below: complementary measured data from various past years and atmospheric monitoring campaigns (adapted from Watson & Sullivan (2011); Watson et al. (2007))	34
Figure 28:	Global Warming Potential of PFCs (adapted from [44])	35
Figure 29:	Corresponding cumulative GWP of all heavy PFCs reflected in mass of CO ₂ (adapted from [43])	35
Figure 30:	Partition coefficient on molar basis on the left side measured by GC counts and taking into account different sample volume correction vs. conversion to mole fraction based units on the right side using densities and molecular weights of the solvents (from [46])	36
Figure 31:	Van’t Hoff plot – illustration of temperature dependency of an equilibrium constant/partition coefficient	36
Figure 32:	Octanol/water vs. solid organics/water partitioning of organic compounds (from [49])	37
Figure 33:	Solubility of perfluorohexane in the hydrocarbon phase as open squares for measured data and a solid line for the CPA predicted values; Perfluorohexane solubility in the water phase as stippled line – calculated (from [1]).	39
Figure 34:	Octanol/water constants calculated after Lyman 1982 and water solubility estimated; taken from [51]	39

Figure 35:	Calculated logK for octanol/water of straight chain PFC (from [54] EPA GOV report No. 201-13244)	40
Figure 36:	Perfluorobenzene solubility estimates using various modelling approaches ([53])	41
Figure 37:	Water solubility of fluorobenzenes ($C_6H_{(6-y)}F_y$) calculated and experimentally determined, from left to right fluorination increases, from [53]	41
Figure 38:	Water solubility of perfluorobenzene vs. ethylbenzene, from [52] Freire et al. (2005)	42
Figure 39:	Gas standard used with TD-GC-ECD methodology by [63]	45
Figure 40:	Conceptual chromatogram with elution time of major PFCs reported in [67]	47
Figure 41:	Corresponding GC-ECD trace from CSIRO experiments – first PFC batch	48
Figure 42:	Corresponding GC-ECD trace from CSIRO experiments – second lower boiling PFC mix	48
Figure 43:	Partitioning of PFCs into the water/brine phase – van’t Hoff plot	52
Figure 44:	GC-desorption method related response of PFCs used in the experiments in a linear interval	55
Figure 45:	GC-desorption method related response of PFCs used in the experiments in a linear interval	55
Figure 46:	Summary plot of tracer response from all experiments listed in Table 8 except 10% brine of PMCH and PDCH; focus is on the variation regarding the different PFC tracer	58
Figure 47:	Slim tube tracer response curve for 10% brine of PCMH, 1,2 PDCH and 1,3 PDCH	59
Figure 48:	Comparison of 20% salinity vs. 0% salinity of high boiling tracer mix	60
Figure 49:	Comparison of low boiling tracer mix with sand matrix	61
Figure 50:	Summary of High and low boiling tracer mix response curves, sand + clay (kaolinite matrix)	62
Figure 51:	Summary of High Boiling PFC Mix vs. sand+clay (kaolinite) matrix response curves	63
Figure 52:	Summary of “Low” Boiling tracer Mix vs. sand + clay (kaolinite) response curves	64

1. Introduction

Tracing/fingerprinting sequestered CO₂, its dynamics and flow paths in the subsurface in a reliable and consistent way is the ultimate goal of a measuring, monitoring and verification (MMV) program for carbon containment and storage (CCS). Geochemical techniques use generally a mix of tracer technologies in order to trace either the CO₂ itself or various interactions of the CO₂ with subsurface fluid inventories. The range of tracers that can be considered is wide. They cover natural and artificial ones, passive and active compounds, and conventional (tracer for simple fingerprinting) vs. process (tracer for a particular chemical process) driven ones. A complete tracer program may include stable and radiogenic isotope tracers, hydrological tracers, and passive / inert tracers for fingerprinting the CO₂. The latter category is part of this research project which aims to elucidate the suitability of perfluorinated organic compounds for long term CCS-MMV applications.

In order to determine, if a tracer stays in sufficient measurable amounts with its parent fluid (i.e. sequestered CO₂), its (a)partitioning, (b)retention, (c)dispersion and (d)adsorption behaviors in the subsurface need to be studied. The tracer qualification for CCS applications consists of verifying detectability of PFC in the injected CO₂ in case of a leakage event, its inertness, stability and interaction potential with various matrices and fluids. Perfluorocarbon (PFC) molecules are a compound class which is tested as a candidate to successfully fingerprint CO₂ in the subsurface in the extremely unlikely event of a loss of containment up to the shallow subsurface, above the base of the groundwater protection zone. Mixes of PFC tracers which are liquid under atmospheric conditions are considered.

Perfluorocarbon tracers are a unique class of man-made organic compounds which are used in several industry branches. Its widest application in the subsurface is leak detection, such as leaks related to underground screened cable laying and across a barrier in waste management. Interwell tests in the oil and gas business also use PFCs to determine connectivity of reservoir intervals and tracing EOR related fluid injection. However, there are several shortcomings in the quantitative characterization of these tracers proposed for CO₂ MMV geosequestration programs. Up to date, there is no long term storage demo test applied on these tracers to determine their fate in the subsurface. The use of PFCs in CCS applications is a patent pending R&D 100 awarded technology introduced by researchers of the National Energy Technology Laboratory (NETL) in 2009 called the SEQUIRE Tracer program.

Shell is undertaking a research laboratory based program to test and re-define the subsurface behavior of perfluorocarbons with the following two key project aims:

1. Partitioning in water/brine vs. supercritical CO₂(scCO₂) systems and water/brine/oil vs. supercritical CO₂ systems at subsurface pressure, temperature and salinity ranges using a batch reactor setup
2. Adsorption behavior with respect to different solid matrices, including hydrophilic and hydrophobic surfaces using a slim tube apparatus. Slim tube experiments are set up to study potential interactions with matrices in the subsurface under realistic fluid inventory conditions (multiphase, i.e. brine/water/oil/CO₂) to investigate retention and dispersion of PFCs in the sub-surface.

A collaboration has been setup with CSIRO in Perth, Australia to undertake the majority of the laboratory experiments. In addition, collaboration with IFE, Norway, has been set up to act as a

second, independent vendor using a different detection technique and different slim tube setup for comparison.

This report provides background information on PFCs, summarizes the current status of the experimental work, and describes outstanding analyses needed to achieve the project aims. A preliminary assessment of the application of perfluorocarbons to be used as a tracer to tag CO₂ for monitoring activities at CCS sites will also be given.

2. Aim of Perfluorocarbon tracer feasibility study

As eluded to in the Introduction, the aim of this study is to test the suitability of PFCs as a conservative, passive geochemical tracer applicable for the injection of supercritical CO₂ into the subsurface. This study is seen as an integral part of Shell's assessment of techniques available for a Measuring, Monitoring and Verification (MMV) program at Carbon Capture and Storage (CCS) sites. In MMV programs, geochemical PFC tracer technology focuses on the detection of injected CO₂ leakage within the shallow subsurface hydrosphere and biosphere, in essence the zone above the base of the groundwater protection zone.

Compared to geophysical methods, which are utilized for plume tracking within the subsurface containment structure, PFC tracers aim to detect and mitigate CO₂ leakage and breakthrough scenarios before they reach significant irregularities in the subsurface, which are of environmental concern. Therefore, false positive (e.g. contamination) and false negative (e.g. tracer retardation) detection of PFC tracers in leakage scenarios must be understood and ruled out. From a technical point of view, an ideal passive/conservative tracer is: of artificial origin, therefore exhibits a negligible background concentration elsewhere; inert, i.e. thermally and chemically stable; non-biodegradable; non-toxic; easily identified with analytical tools, exhibits low detection limits; has no detrimental environmental potential; and have little or no tendency to distribute/partition between immiscible phases. Here, PFCs were verified to cover all of the aforementioned characteristics to a very large extent, which uniquely qualify them to distinguish injected CO₂ vs. native CO₂ sources in containment assurance monitoring.

Uncertainties regarding the properties of PFC compounds are related to the partitioning behavior with aqueous and non-aqueous fluids/gases including the dependency of temperature, pressure and salinity. PFC compounds have been regarded as having very low solubility in water which is a challenge to measure quantitatively. So far, only a reported modeled solubility of common PFCs tracers in the C-6 to C-8 carbon backbone range exists in relation to water/brines. The computed solubility, i.e. liquid-liquid equilibria between the perfluorocarbon in the supercritical CO₂ (scCO₂) and aqueous phase, for cyclic and straight chain liquid perfluorocarbons is on the order of 10⁻⁹ to 10⁻¹¹ at room temperature [1]. Perfluorocarbon tracer dispersed in the supercritical CO₂ phase will even have a lower solubility taking into account non-ideal behavior. It is expected that PFCs have increased partitioning at higher temperatures on the order of 10⁻⁸. Furthermore, the partitioning is often denoted as octanol/water partition coefficients which are not suitable with respect to true scCO₂/water partition coefficients. In relation to amounts of sequestered CO₂ and interactions with subsurface brines, it is vital to identify even a very low solubility with sufficient confidence. This study will provide data to judge on the final solubility of perfluorocarbons in the water phase at reservoir (i.e. saline aquifer) conditions.

The second major uncertainty with regards to subsurface conditions is the interaction with various solid matrices regarded as adsorption. "Adsorption is the net accumulation of matter on the solid phase at the interface with an aqueous solution or a gas phase" [2]. For this study hydrocarbon fluids with an increased ability to scavenge perfluorocarbons are of minor interest (petroleum reservoir scenario) Adsorption would remove PFC from the bulk phase and therefore alter the PFC subsurface behavior. Adsorption is generally been described in relation to its concentration using adsorption isotherms. Prominent models to describe such adsorption phenomena are from Langmuir or Brunauer, Emmett & Teller (BET model, [3]). In this study, adsorption or retention behavior of tracer compounds are assessed using a slim tube setup which resembles a 1D displacement experimental technique to study miscible, and here in particular, immiscible phase behavior. The scenarios investigated include a) CO₂ with added PFC tracer

displacing a water/brine phase during injection into a saline aquifer (CSIRO study), and b) CO₂ with added PFC tracer displacing a brine/hydrocarbon mixture during injection into a gas/oil field (IFE study). The main focus is on the first scenario, which is relevant for the QUEST project in Alberta, Canada.

3. History of PFC chemical tracers applied to CO₂ sequestration projects

This chapter gives a brief overview of recent CCS demonstration projects in which PFC chemical tracers were tested as part of their measuring, monitoring and verification (MMV) program. In Salah, Algeria, is the only reported long term commercial scale project which included PFCs in its monitoring strategy. Due to limited data on PFC usage for this project, it will not be discussed any further in this report.

The pilot scale CCS projects of interest are:

1. ZERT (Zero Emission Research and Technology), Bozeman, Montana, USA – shallow hydrosphere
2. SECARB Frio Brine I, Texas, USA – multiple tracer mix including PFCs
3. K12B, offshore The Netherlands – produced CO₂ reinjection into a depleted gas field
4. San Juan Basin, Pump Canyon Station, New Mexico, USA – Coal Bed Methane (CBM) CO₂ sequestration project
5. West Pearl Queen, New Mexico, USA – low boiling tracer PDCB included

Note that in the next chapter a few of the numerous other examples in which PFCs were used in subsurface petroleum reservoir applications are described. General interest of using PFCs in reservoir studies was to monitor flow paths of the parent fluid or to derive saturation profiles. Dugstad et al. (1993) started to use PFCs in hydrocarbon reservoir surveillance projects to determine compartmentalization and get a better understanding of reservoir dynamics. [4]. However, there is currently no demonstration project in which a CO₂ leak path through a significant overburden rock column with changing lithologies using PFC tracers has been investigated.

The timeline of the five demonstration projects highlighted here are as follows:

1. West Pearl Queen was conducted in 2003
2. Frio I and K12B projects injected perfluorocarbons in 2005, monitored between 2006 to 2008
3. ZERT in Montana and San Juan CO₂ pilot test site injected PFCs in late 2008/early 2009 as part of their atmospheric and soil gas monitoring strategies; the monitoring period extended from several weeks up to 2 years using a rectangular array of permanent installations.

Currently, ongoing PFC chemical tracing strategies including demos with extensive MMV programs attached are mostly part of the CCS Mustang project. Push-pull well tests are conducted at Hontomin, Spain and Heletz, Israel. In the Mustang projects, the PFC tracer technology is often part of an extensive geochemical monitoring program using native conservative and non-conservative tracers like pH, alkalinity, bulk gas compositions, noble gases and stable isotope signatures of various gases and groundwater. Yet, the project outcomes are not published in sufficient detail, which is the reason why those are only mentioned to consolidate ongoing PFC usage in CCS demonstration projects.

In order to put the various projects into a perspective in terms of their scale, i.e. volumes of CO₂ sequestered, and purpose of PFC tracers, the volumetrics are quickly highlighted.

At K12B depleted oilfield test site, the aim to use PFC tracers was to distinguish injected CO₂ from produced one and the partitioning of CO₂ in CH₄ as major constituent of the hydrocarbon gases. The PFC tracer should “mimic” the methane behaviour[5]. Up to **30 million tones**

equivalent of CO₂ were re-injected into K12B reservoir site which is at 3850m depth underlying a massive Zechstein salt seal. Current reservoir temperature is 127 °C.

The Frio Brine project used PFCs in order to determine CO₂ breakthrough and potential flow paths within the targeted reservoir [6], [7]).

The Frio Project injected only **1600 tons** of CO₂ into the 1540m deep salt dome adjacent Frio Formation sandstone and monitored CO₂ breakthrough at a well 31meters up-dip from injection.

San Juan Basin project injected **16700 tons** CO₂ into three 5 to 10 meters thick highly permeable coal seams of the prominent Upper Cretaceous Fruitland coals in the High Rate Fruitland production fairway [8] (Wells et al. 2013). The depth of the Fruitland Formation is about 900 meters.

In the West Pearl Queen pilot test, **2100 tons** of CO₂ were injected into the Shattuck sandstone member of the Permian Queen Formation. Tracers injected with the CO₂ were detected within a few days of injection.

ZERT site at Bozeman, Montana, had the purpose to improve NETL's shallow monitoring techniques and therefore made investigations at very shallow depth [9], [10] . Phase one was a vertical well drilled 2.5 meters into the shallow subsurface in 2006, Phase 2 consists of a 80 meter long horizontal well drilled at 6 ft depths in 2007 and divided by packers into six equal length sections. During Phase 2, CO₂ was released at **300 kg/day over a period of 12 days** along the entire well and at a rate of 50kg/day in the NETL zone (packer 4) which was relevant for the PFC tracer tests. Sorbent tubes were installed at defined distances from the well at depths of 0.3, 0.6 and 1 meter for soil gas measurements. For atmospheric monitoring, 90 installations were installed NW and SE of the well in a vertical 10m/20m grid at a height of 4 ft above ground.

ZERT and San Juan projects were more inclined to soil gas and atmospheric monitoring techniques and sampled the PFCs within the biosphere-hydrosphere zone. Therefore, different levels of PFCs were targeted. Here, femtoliter (10⁻¹⁵) to picoliter (10⁻¹²) levels were detected compared to 10⁻¹⁰ to 10⁻⁹ liters at K12B. At Frio Project, the initial PFC vs. CO₂ injected molar concentrations relate to the recovered PFC vs. CO₂ fraction. With the PFCs also other gas tracers, namely Sulfurhexafluoride (SF₆) and the noble gas Krypton were used.

3.1. K12B project

At K12B, perfluoromethylpentane (PMCP) and 1,3 perfluorodimethylhexane (1,3 PDMCH) as PFC tracers were added to the sequestered CO₂ (mix of 92% CO₂ and 6% CH₄ + impurities) in the K12-B6 injector well (Fig.1). Breakthrough was detected at B1 and B5 producers after 130 days and 463 days respectively. K12 B1 showed during this interval a steady increase in CO₂ production from 13 to 25 mol% compared to B5 producer with constant 13 mol% CO₂.

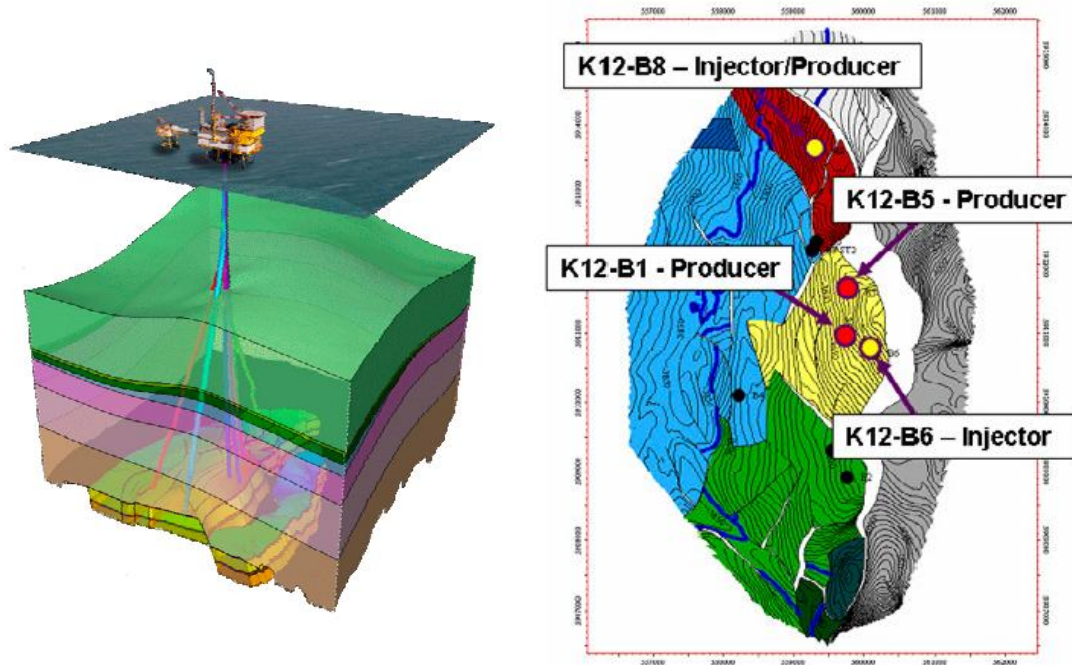


Figure 1: K12B reservoir 3D and 2D maps with locations of injection and production wells (adapted from [5])

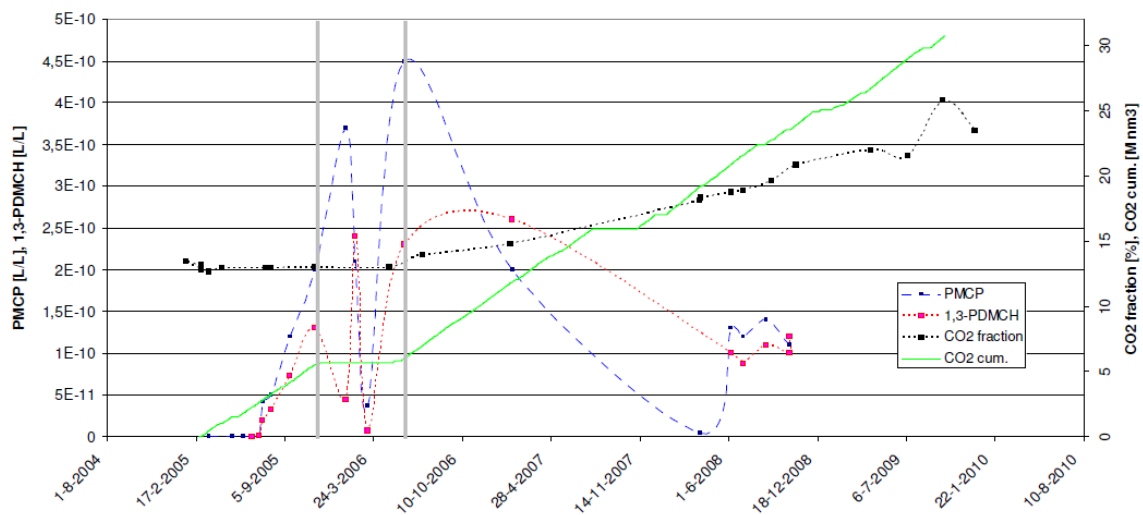


Figure 2: Breakthrough curves of PMCP and 1,3 PDMCH at K12 B1 well (Aug 2005) and K12 B5 (June 2006) vs. CO₂ breakthrough and cumulative CO₂ production (adapted from [5])

The tracer breakthrough curves (Fig.2) indicate a faster movement compared to the CO₂ (black stippled line) as it travels with the injected CH₄ preferentially to the B1 monitoring site. Retention compared to the initial CO₂ breakthrough at well K12 B5 is minor.

1,3 PDMCH exhibit a smaller concentration compared to PMCP in the breakthrough. However, the first maximum of PMCP does not coincide with the one of PDMCH which is likely due to the different travel times of the two compounds. PDMCH as the larger molecule is retarded compared to PMCP due to its different molecular conformation, hence velocity and potentially stronger adsorption behavior. The sharp peak of PMCP at B1 determines a low dispersion profile. The initial double peak of PDMCH corresponds to a different CO₂ flow paths with different adsorption phenomena resulting in a higher retardation compared to PMCP. After 463 days, peak concentrations of both tracers were recognized at B5 production well. The broad bleed off of the PDMCH tracer is linked to higher CO₂ saturations, a more pronounced interaction with connate formation waters and higher dispersivity compared to PMCP which commences much faster. Higher percent of CO₂ fraction in the saturation profiles (right Y-Axis in Fig.2) immediately is reflected by higher tracer concentrations which are a hint of a fully dispersed tracer after two and a half years.

3.2. Frio Brine Project

At Frio Brine Phase I, multiple tracers including perfluorocyclopentane and -hexane backbones were injected by two parties: Oak Ridge National Lab and National Energy and Technology Lab [6]. The PFCs used were perfluoromethylcyclopentane (PMCP), perfluoromethylcyclohexane (PMCH), Perfluorodimethylcyclohexane (PDCH), and perfluorotrimethylcyclohexane (PTCH). PFCs were detected using field based mass spectroscopy (MS) and laboratory based GC-ECD analysis.

The setup in this interwell test is that the injection and monitoring wells are 31 meters apart with the latter being 24 meters updip (Fig. 3).

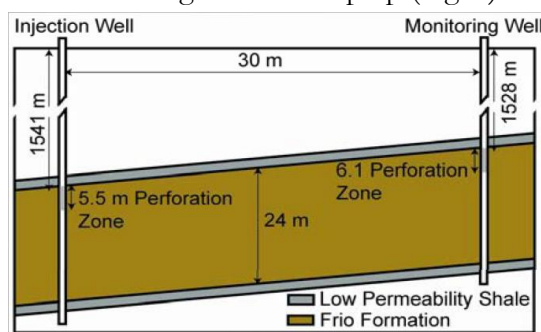


Figure 3: Interwell setup of tracer tests used by NETL during Frio Brine I phase [6]

McCallum et al. (2004) [6] noted that travel times of injected tracers compared with CO₂ breakthrough times exhibit slight retardation during second and third injection of PFCs (Fig.4). The “heavier” PFC mix of methylated perfluorohexanes travels significantly slower which results in a 2.5 hrs time difference to the perfluorocyclopentane. The faster travel time and similar breakthrough compared to the CO₂ of the primary PFC injection can be explained with the limited interactions of the PFCs with the surrounding matrix and the complete solubility in CO₂. However, it cannot be ruled out that PFC move in a single phase flow rather than fully dispersed into CO₂ due to the small travel distance. The follow up injections (see Fig.4) are better dosed compared to the injected CO₂. Between the heavier PFCs and heavy noble gas/SF₆ tracer only small differences or even similar travel times were recorded. This similar behavior of the various

tracers can be interpreted as no significant interactions with rock matrices, no partitioning into an aqueous phase and very good solubility in the CO₂ phase.

Component	Mass Injected	Injection Time (Rel. time hr.)	Injection Duration (hr)	Arrival Time (Rel. time hr.)	Peak Time (Rel. time hr.)	Travel time (hr.)
CO ₂	3 kg/s*	4 Oct 11:34 (0.00±0.0/-2.0)	N/A	6 Oct 14:28 50.90±0.0/-2.0	N/A	50.9±0.0/-2.0
PMCH, PTCH	3.1 kg	4 Oct 13:26 (1.87)	3.9	6 Oct 14:28 50.90±0.0/-2.0	6 Oct 15:20 (51.8±0.9)	48.0±0.9
PMCP, PDCH	0.3 kg	8 Oct 18:19 (102.75)	1.0	10 Oct 15:32 (147.97±0.5)	10 Oct 22:52 (155.3±0.5)	50.22±0.5
PMCH, PTCH	0.3 kg	9 Oct 11:37 (120.05)	1.0	11 Oct 11:42 (168.13±0.5)	11 Oct 18:36 (175.03±0.5)	52.67±0.5
SF ₆	< 200g [†]	9 Oct 11:37 (120.05)	0.58	11 Oct 10:26 (166.87±0.5)	11 Oct 18:22 (174.80±0.5)	52.63±0.5
Kr	83.8 g	9 Oct 12:39 (121.08)	0.13	11 Oct 10:37 (167.05±0.5)	11 Oct 20:01 (176.45±0.5)	53.47±0.5

Figure 4: Tracer amounts, injection time, duration and travel times of tracers at Frio Brine phase I [11]

Important to state is the so called peak broadness of the three different injections (Fig.5). The first injection around 50 hrs highlighted in dark gray has the narrowest PFC peak with respect to time. The period of time PFCs were recorded was for the first peak 14 hrs, the second is intermediate with 20hrs and the third lasted 24 hrs. The C/C_{no} data on the Y-axis determines the difference of PFC vs. CO₂ in initial sample vial vs. the “dilution” at production well using MS detection. The value is decreasing an order of magnitude from around 0.25 onwards. Therefore, the concentration gets more and more diluted in the later tracer tests. Especially in test 2 and 3 in which the similar mass of PFCs was used, the dispersion is significantly higher for the perfluorohexanes.

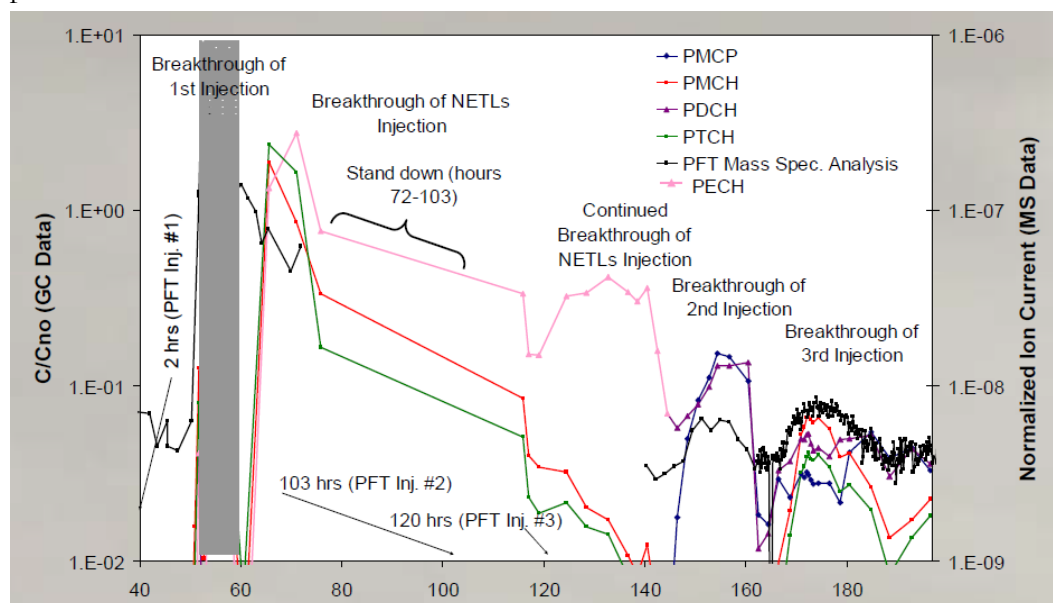


Figure 5: Summary of PFC tracer concentrations of all injections normalized to their initial conc. vs. travel times in hours (from [11])

The stable travel times of the PFCs highlighted in Fig.4 and Fig. 5 are an indicator of the stability of the CO₂ flow path during the experiment. No significant deviation from the flow path would result also in a stable saturation state of the CO₂, because of reduced interactions with the wetting aqueous fluid. The attempt was made to calculate residual CO₂ saturations using a simple radial disk model and the travel times of the PFC tracers [12]. Results are shown in Table 1.

Table 1: PFC travel times of the three separate injections and calculated saturation of CO₂ (adapted from [12])

Injection #	Travel time (hrs)	Estimated CO ₂ Saturation (SCO ₂)
#1 (PMCH/PTCH)	50.3	17
#2 (PMCP/PDCH)	51.7	17
#3 (PMCH/PTCH)	51.2	17

3.3. San Juan CBM Project

The San Juan demo site was targeting the Fruitland coals for CO₂ injection including PFC tracers [8]. It is a collaborative project of the Southwest Regional Partnership (SWP) together with Conoco Phillips' Carbon Sequestration Group. The aim of the project was to identify CO₂ movement in the coal seams and to test monitoring techniques. This makes it an important demo experiment for PFC tracer testing regarding adsorption behavior on organic substrates. PFCs are regarded as having the potential to be adsorbed by CO₂ wetted, hydrophobic surfaces present in high organic matter soils and coal environments. However, natural coal samples are not comparable with activated coals in the CATS sampling tubes which have been burned, graphitized and therefore have a much more increased active surface area.

The question, if organic matter solid surfaces would scavenge PFCs to a large extent, and therefore act as a major threat for any CCS project associated with such lithologies, can be discussed in such an attempt and potentially verified.

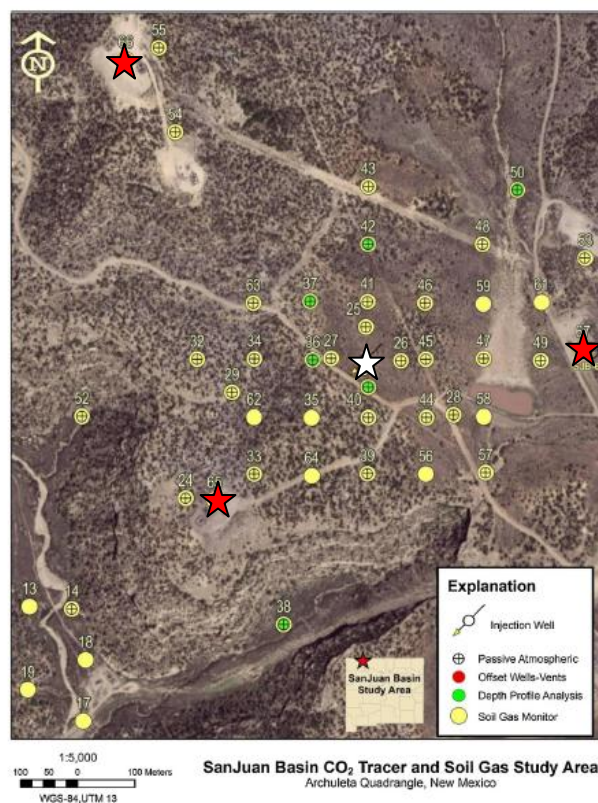


Figure 6: Site description of San Juan CCS project
White cross = injection site; Red crosses = offset/ observation wells (from [8])

PFC tracers were co-injected with CO₂ during the second month after the start of injection at the San Juan site. Two separate, 3 week-long, 20 liter sequential additions of perfluorocarbon (PFC) tracers to CO₂ were made at the wellhead. In the passive monitoring mode, soil-gas or atmosphere was sampled by exposing 3 inch (7.62 cm) long glass tubes (Gerstel tubes) containing Amborsorb[®] to collect the tracer. The tubes were exposed for periods of approximately 2 months and collected as a set, which was returned to the NETL laboratory for GC/negative ion MS analysis at the femtoliter/liter level. The PFC gas analysis was conducted on an Agilent 6890N Gas Chromatograph (GC). The GC had a 5975 inert MSD (Mass Spectrometer Detector) with a CI (Chemical Ionization) source. The samples were dried and then introduced to the GC with a Gerstel MPS 2L Twister desorption system [8].

The first tracer batch consisted of 90% PMCH and 10% PTCH, and was injected from September 18, 2008 till October 8, 2008. The second tracer batch consisted of 100% PTCH and was injected from October 18, 2008 through November 12, 2008. The weight of tracer mixture (90% PMCH) injected during the first tracer injection run was 31 kg. The weight of tracer (PTCH) injected during the second tracer injection run was 39 kg. The ratio of tracer to CO₂ injected during tracer injection was regulated in continuous injection mode at 1 g of tracer (or tracer mixture) for every 40 kg of CO₂ [13]. Tracer signals were seen only at the two production wells closest to the injection well (highlighted by red stars in Fig.6, white star = injection well).

Tracers reach the east offset well about 90 days after injection. The southwest offset well saw tracer production after about 240 days. No breakthrough of PFC tracer to the Northwest offset production well was observed (Fig.7).

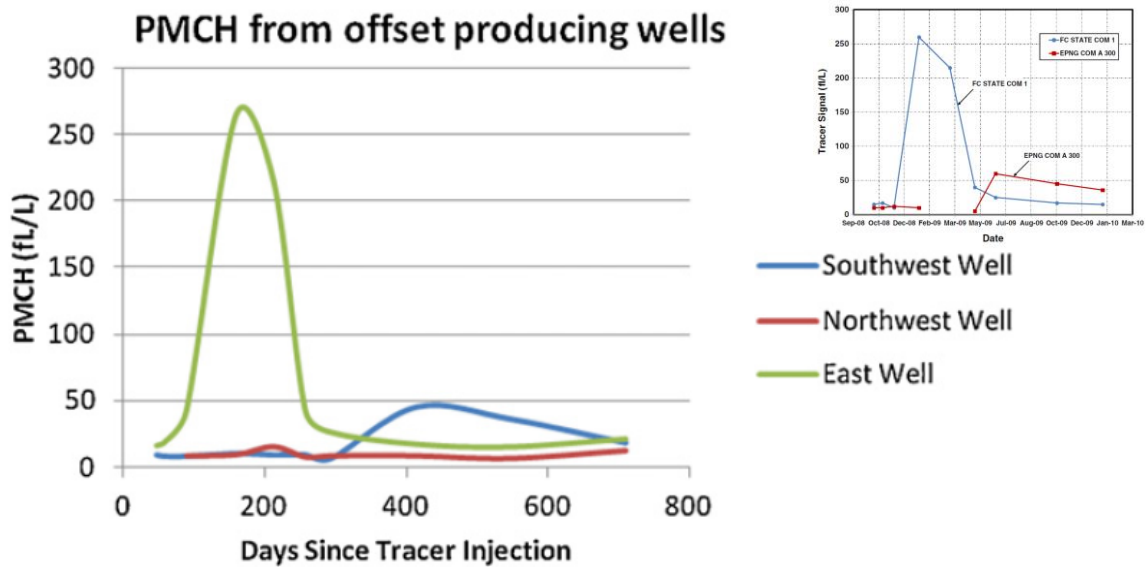


Figure 7: Tracer breakthrough data monitored at three offset wells (adapted from [8])

The excessive monitoring plan allowed the researchers to track tracer migration fronts on the atmospheric and soil gas levels throughout the release test period (Fig.8).

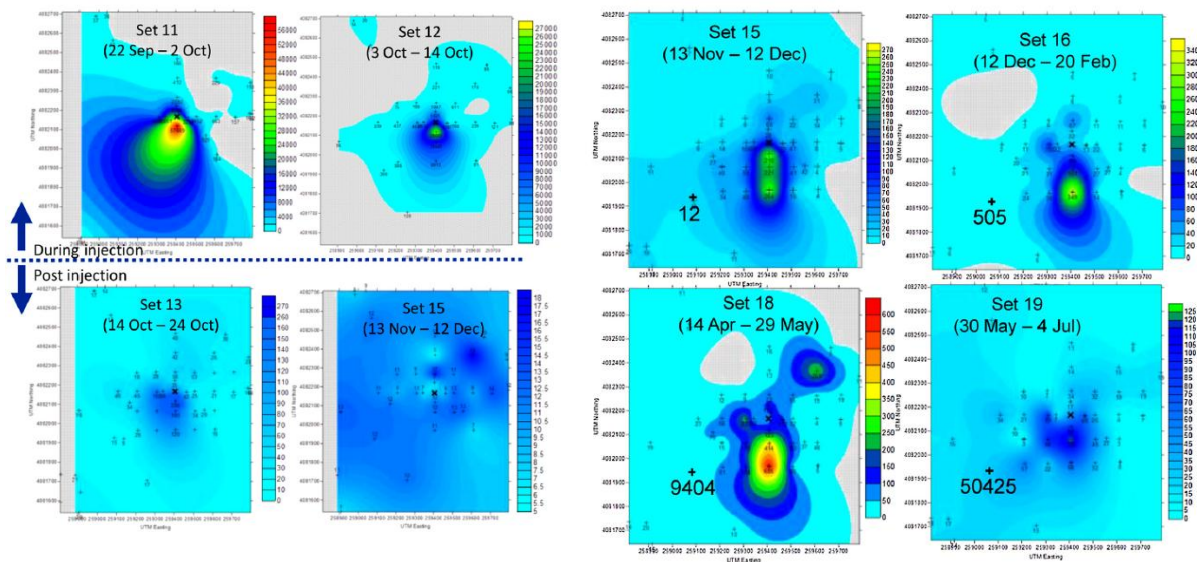


Figure 8: Tracer plume migration monitoring using atmospheric and soil gas monitoring sites; Left picture: atmospheric detection during injection, yellow to red concentration scales are in the order of 350 to 400 fl/l, bluish colours are background concentrations of a few fl/l; Right picture: 2 months later soil gas monitoring detection; values in big print close to SW offset well; red colours indicating 500 to 600 fl/l conc. (adapted from [8])

The PFC tracers were added to the injected CO₂ together with nitrogen gas (N₂). The PFCs and the N₂ were monitored in the production wells simultaneously. An offset related to the CO₂ is expected as CO₂ adsorption affinity on coal is higher in the field case as tracers and the N₂ preferentially would use fractures in the coal seam to migrate and therefore limit their interaction with the matrix. This behaviour indicates preferential flow paths and reflects on the heterogeneity of poroperm in the subsurface reflected in the absence of the tracer in the North and increased recovery with increased CO₂ concentrations in the East of the injection well. In Fig. 8 the atmospheric monitoring devices detected a clear southward migration of the tracer plume initiated during tracer injection (left pictures). Susequently, the PFCs also interacted with the soil gas due to barometric pumping(right pictures) resulting in higher concentrations directly south of the injection site. The tracer concentrations went back to normal after several months.

Timing of breakthrough could not be determined in relation to CO₂ measurements, but the signal could have been missed with the background concentration of CO₂ in the production stream gas generally running between 20 and 30%. Also the tracer breakthrough is likely to precede CO₂ breakthrough again referring to the K12B scenario due to the high affinity of CO₂ for coal. A few months later also PFCs reached the SW located offset well. The difference in porosity and permeability of the coal seams indicates a high anisotropy of the “containment”. Apart from reservoir dynamic investigations, a leakage at a well pad was confirmed using PFC concentration measurements which followed up by CO₂ and CH₄ soil gas measurements to confirm the leakage. All measurements were able to locate the leak from an underground pipe used for soil gas monitoring close to the well pad.

3.4. The West Pearl Queen site

Leakage detection experiments conducted at the pilot site were designed and undertaken by Art Wells and Rod Diehl (Pittsburgh NETL). The pilot site consists of an extensive Caliche horizon, the Mescalero Caliche acting as a barrier and sandwiched by sandstones (Fig.9, left picture). The two researchers positioned capillary adsorption tube samplers (CATS) in a radial pattern centered about the injection well (see Fig.9 right picture). Ultimately, 40 CATS were placed at the site. Individual CATS were placed in metal tubes at depths of approximately 2 m. The CATS were specially designed to detect minute amounts (10-13 liters) of perfluorocarbon tracers injected with the CO₂. The base of the each tube was left open to allow for diffusion of soil gas into the sampler. CATS were left in the ground for different periods to measure changes in tracer concentration as a function of time throughout the CO₂ injection process.

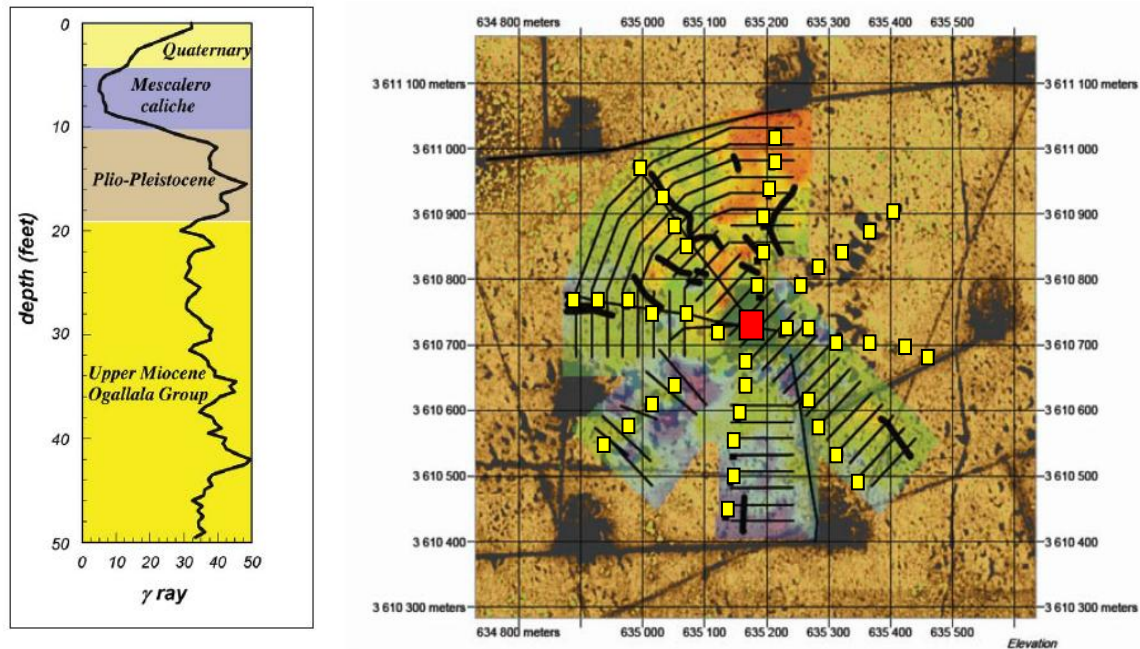


Figure 9: Lithology profile at West Pearl Queen shallow injection site with gamma ray detection (LEFT); CATS locations (yellow squares) and injection site (red square) highlighted (adapted from [14])

Three different perfluorocarbon tracers were injected into the CO₂ stream: perfluorodimethylcyclohexane (PDCH), perfluorotrimethylcyclohexane (PTCH), and perfluorodimethylcyclobutane (PDCB).

CATS exposed for a 54-day period revealed the presence of anomalies in the distribution of tracers detected around the injection well. Elevated concentrations of PDCH (Fig. 10) and PTCH (not shown) were detected by CATS located northwest of the injection well. Elevated concentrations of PDCB (Fig. 10) were detected by CATS located southwest of the injection well. The PDCH tracer was added 24 hours after CO₂ injection was initiated. PTCH was added nine days after injection started, and the PDCB tracer was injected into the CO₂ stream 21 days after CO₂ injection commenced. Measured concentrations of PDCH (the first tracer injected into the CO₂ stream) at 6, 10, and 54 days following injection revealed that tracer release was incremental through the injection period. PDCB concentrations reported in this study are for the total of 54 day exposure time. CATS placed at the site during the soaking period following CO₂ injection reveal a decline in concentration for all tracers. This decline was most significant for the

PDCBs. PDCB, which has the highest diffusion constant among PFC tracers, tends to be present in larger amounts, and drops to background levels more rapidly than the other tracers.

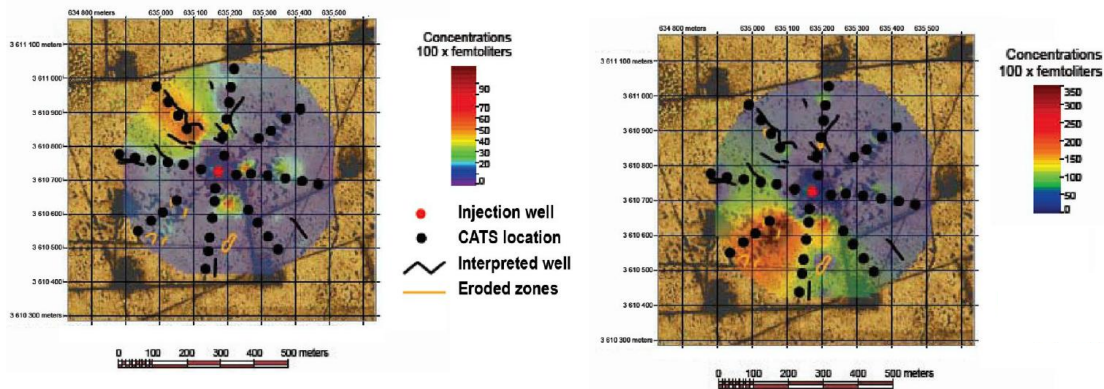


Figure 10: PDCH(left) and PDCB (right) concentrations measured during a 54 days exposure after injection (after [14])

At the West Pearl Queen site, the vadose zone, the region of the subsurface that is located near the ground surface and is above the water table (i.e., not saturated with water), is about 60 m deep. The primary mechanism of transport in the vadose zone is diffusion unless significant pressure changes occur at or near the surface—e.g., a leak in a pipe or a rapid change in atmospheric pressure. Diffusion of CO₂ and tracer can occur both radially outward from the injection well and upward from leaks below the water table. However, diffusion coefficients cannot explain the large travel distances of the tracer which is most likely enhanced by high permeability streaks either in the caliche (carbonate cemented, ancient soil level) or on top of it[14] .

Analysis of remote sensing imagery revealed prominent lineament trends (NW-SE and NE-SW) in the thin veneer of sands that blanket the entire area of the experiment. The radar survey revealed significant discontinuity and structure within the near-surface late Pleistocene Mescalero Caliche. That fits with the observations from the PFC tracer experiment[14] .

3.5. ZERT site Bozeman, Montana

The last review example of applying PFC tracer technology in the field is from the ZERT site at Bozeman, Montana. This was regarded as one of the most extensive vadose zone monitoring program test sites which was specifically aimed to test for shallow MMV strategies. Here, the contributions of NETL researchers in a horizontal and vertical CO₂ test release including PFC tracers is reflected. The test site was equipped with multiple tracer monitoring stations (Fig.11).

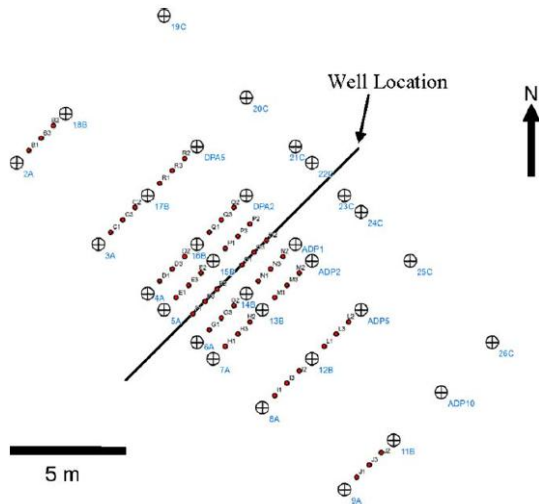


Figure 11: Soil gas and tracer detection installations along the horizontal well of the second ZERT release test (adapted from [9])

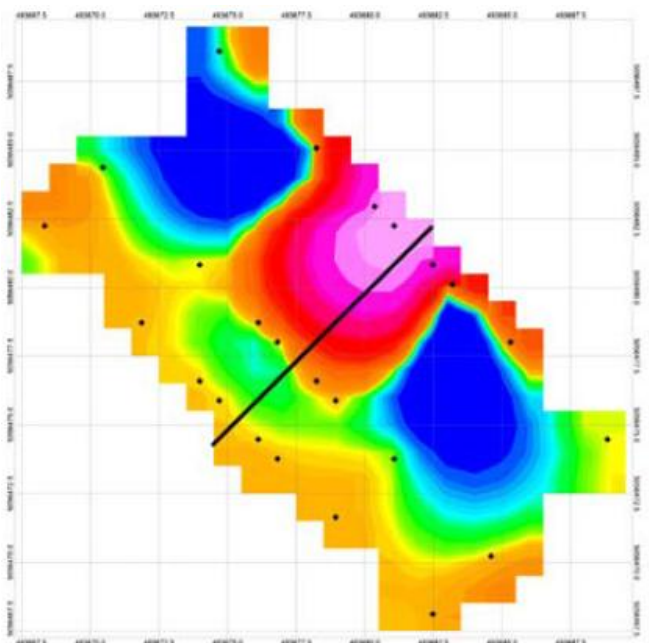


Figure 12: Cummulative soil–gas tracer concentrations at 1 m depth along the horizontal release test after 2.5 days exposure; pink and red colours indicate relative high concentrations, bluish colours represent minimum concentrations, measurement locations marked by black dots (after [9])

Fig. 12 indicates a cumulative concentration profile along the horizontal well release test marked by the black line. Tracer “hot spot” migration was skewed slightly to the north indicated by the

red and pinkish colours labeling high tracer concentrations. An almost radial distribution with a slight offset of the tracer from the centered well location could be observed which reflects the good and homogeneous soil pattern in the area of interest. The other minimum hot spot, also slightly skewed to the North is indicated by the greenish/bluish colours and resulted from higher CO₂ flux in the area in the western section of the horizontal well. The increased dissolution in the CO₂ lower overall concentrations significantly.

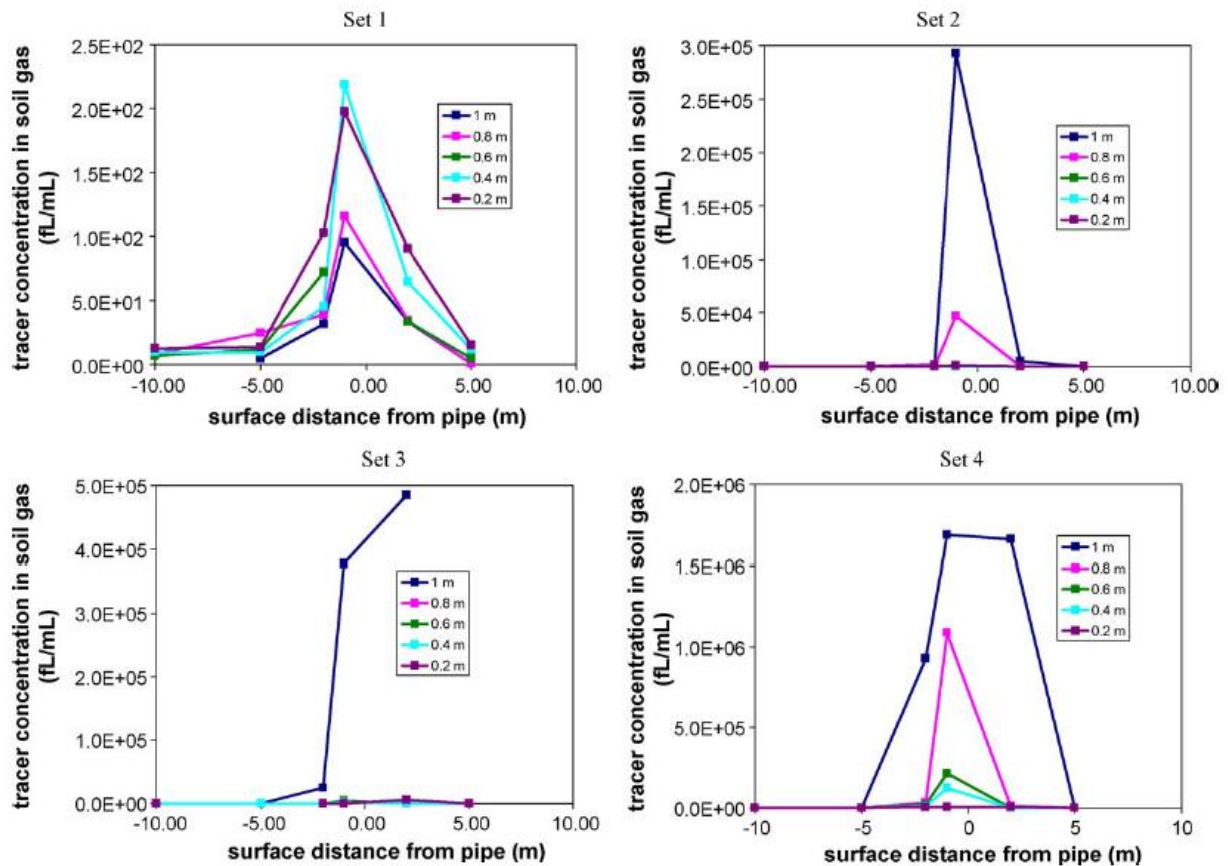


Figure 13: Tracer concentrations measured at various depths (0.2 to 1m) at certain distance from the horizontal well taken at consecutive days after injection (after [9])

All of the depth profile sets (Fig. 13) monitored the highest tracer concentrations at 1 and 2 m from the horizontal well. Tracer concentrations are increasing with soil–gas depth. The researchers mention that sets 2 to 4 are the results of tracer reservoir depletion after injection. Presumably this reservoir of tracer had not reached the depth profiling line during the first profile set. For sets 2–4, it is possible that significant barometric pumping of tracer resulted in the loss of tracer at shallower depths. Barometric pumping might be enhanced due to extensive rooting and animal burrows dissections.

3.6. Synopsis

Various qualitative and semi-quantitative retentions/retardation of the tracer vs. the CO₂ breakthrough were addressed in the above described demonstration projects. These data act as complementary information for the comparison of laboratory based 1D displacement experiments in this experimental study.

To conclude from the various PFC tracers demonstration test sites, most applications aimed to use the tracer qualitatively to study reservoir dynamics and CO₂ flow paths to account for reservoir heterogeneity. The more quantitatively used tracer data was successful in calculating CO₂ saturations from the different tracer breakthrough timing and therefore enabled to link tracer movements directly to the CO₂ movement path. Breakthrough times and curves were studied and were able to describe subsurface behaviour of PFCs qualitatively regarding dispersion or adsorption. Interpretation of these profiles relates to the various dilutions with increased travel time, tracer configuration and residual CO₂ saturations. CO₂ trapping was inferred in comparison with slightly more water soluble noble gas tracers (Frio I experiment).

The take away message from the pilot tests so far is that there is a consistent lack of quantitative data for tracer-water-rock interactions, scavenging of the tracer, wettability issues and a more sophisticated and consistent study on CO₂ flow paths and tracer recovery is needed which can be achieved through laboratory studies. A full mass balance and recovery was difficult to achieve in these field studies.

4. PFC - Petroleum reservoir studies

After petroleum business related laboratory studies with PFCs involving slim tube experiments by Dugstad et al ([14] [15]), gas tracers were applied in future petroleum reservoir field studies including well tests. Highlighted here is the Snorre field study by Dugstad (1999)[16] and Huseby et al. 2008 [17]. Further tracer studies are summarized in Senum et al. (1992)[18].

PFC tracer injection was part of a water alternating gas (WAG) EOR reservoir study at Central Field Block of the Snorre field in the North Sea. The main effect of testing WAG was to sweep parts of the reservoir that will not be swept by water, such as oil attics, and to reduce the residual oil saturation in the swept areas. PFCs were part of an extensive chemical tracer program conducted in the years 1994, 1995 and 1998 which involved in total ten different tracer compounds (such as referenced in Fig. 14, Table 2.).

Table 1 Tracer injected in the WAG program at the Snorre field

Inj. date	Tracer	Well	Amount
09.03.93	HTO	P-25	5430 GBq
28.03.94	PMCH	P-25	20 kg
13.06.95	PMCH	P-25	20 kg
05.07.95	4-FBA	P-25	40 kg
02.04.98	PMCH	P-25	5 kg
23.03.93	SCN ⁻	P-28	797 kg
28.09.94	PDMCB	P-28	10 kg
05.07.95	1,3-PDMCH	P-28	100 kg
22.03.97	SF ₆	P-28	150 kg
09.03.93	S ¹⁴ CN ⁻	P-34	50,5 GBq

Table 2 Explanation of tracer names

Tracer	Type	Full name
HTO	W	Tritiated water
S ¹⁴ CN ⁻	W	14C labelled thiocyanide
SCN ⁻	W	Thiocyanide
4-FBA	W	4-fluoro benzoic acid
PMCH	G	Perfluoromethylcyclohexane
PDMCB	G	Perfluorodimethylcyclobutane
1,3-PDMCH	G	1,3-perfluorodimethylcyclohexane
SF ₆	G	Sulphurhexafluoride
C ₂ H ₅ T	G	Tritiated ethane

Inj. Date	Tracer	Amount:	Well produced	Breakthrough (days)	Recovery * %
09.03.93	HTO	5430 GBq	P-13	368	0,27
			P-18	1785	0,03
			P-29	707	0,23
			P-40	671	0,21
05.07.95	4-FBA	40 kg	P-13	330	16,9
			P-18	937	0,25
			P-29	643	31,6
			P-40	767	3,6
28.03.94	PMCH	20 kg	P-13	n.d	-
13.06.95	PMCH	20 kg	P-18	37	13,7
02.05.98	PMCH	5 kg	P-29	184	14
			P-40	590	-

n.d= not detected , n.m = not measured *until April 1998

Figure 14: Tracer compound mix at Snorre field; indicated are tracer injection data and recovery (adapted from [16])

20 to 100 kg of PFC tracer compound was injected and monitored after production well breakthrough. PFC tracers had a stable recovery of around 15% (Fig.14) of injected volumes up to 1998 compared to more water soluble tracer like fluorbenzoic acid (4-FBA). The latter was recovered with a huge spread due to its injection proximity to the water table and partition losses in residual water saturation. The comparison of a passive tracer (PFC) and a more reactive tracer which is soluble in polar solvents like water (4-FBA) enabled to calculate residual oil/water saturations and therefore sweep efficiency.

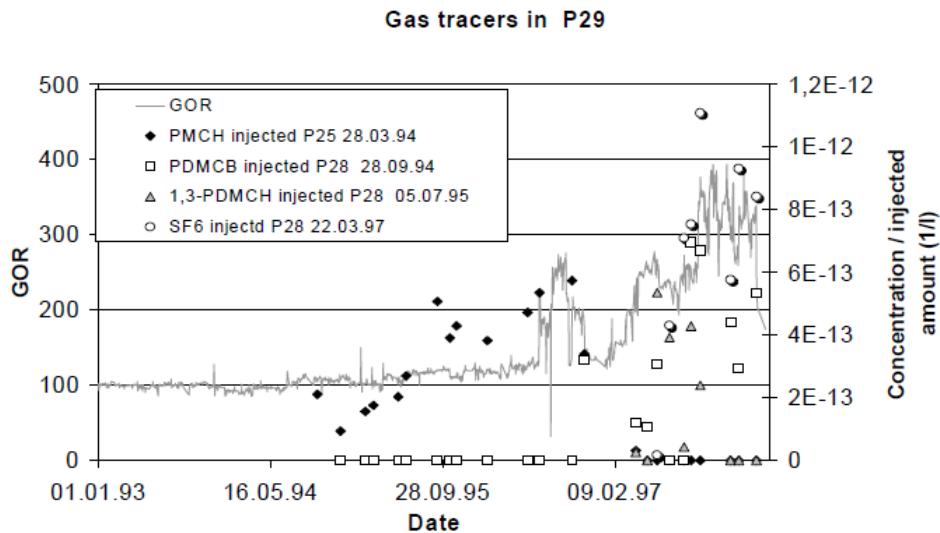


Figure 15: Tracer profile compared to GOR at Snorre Oilfield, adapted from [16]

Tracer knowledge has been advanced considerably after 50 tracer campaigns in 14 years. Objectives in that period included proof of communication between injector and producer, foam assisted WAG in single well tests and determination efforts of residual oil saturations in high permeable streaks. A comparison of gas to oil ratio (GOR) vs. tracer concentration monitoring was evaluated and showed good, positive correlation. That proofed the PFC tracer’s affinity to the produced hydrocarbon gas (see Fig.15).The clear link of the GOR vs. tracer recovery in Fig.15 confirms a preferential solubility in volatile hydrocarbon gases compared to higher carbon chain length hydrocarbons.

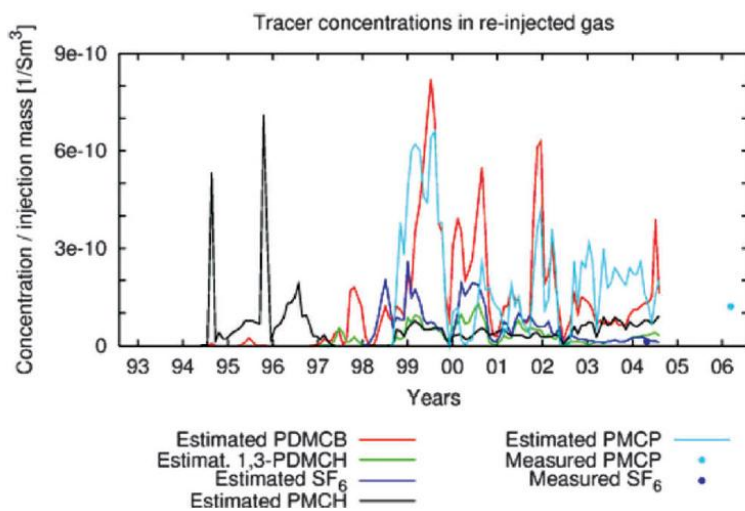


Figure 16: Tracer concentrations in CFB Snorre field study, adapted from [17]

In the past years, produced gas was re-injected at Snorre Oilfield, and therefore also tracer mass balance got disturbed which put the tracer evaluation to an end.

Divided by injection mass, the overall estimated tracer concentrations were calculated (Fig.16). Two measurements in 2004 and 2006 for SF₆ and PMCP were in the correct ballpark of the estimated amounts. However, large uncertainties with respect to the tracer response and mass balances remain.

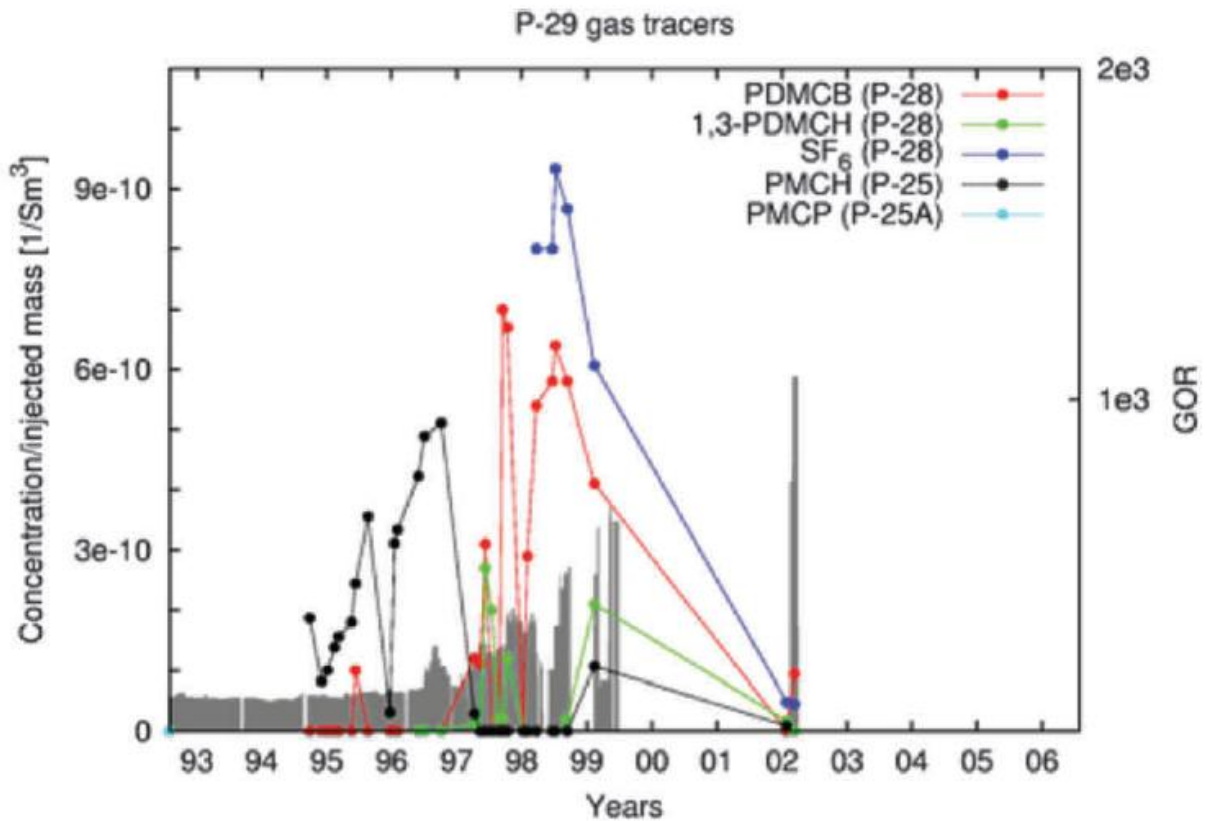


Figure 17: Production well P-29 tracer concentration profiles vs. GOR (gray bars) of the produced fluids (from [17])

The correlation within the tracer compound mix is related to the boiling point of the tracer and the higher partitioning into the gas vs. fluid phase. This is evident in Fig.17 which highlights tracer concentration profiles in production well P-29. Here, PDMCB and SF₆ are nicely correlated with GOR as well as PMCH in a previous injection and earlier elution time. The higher boiling tracer 1,3 PDMCH indicates less good recovery.

TABLE 3—CUMULATIVE TRACER AMOUNTS IN PRODUCERS IN THE SNORRE FIELD CFB FOR GAS TRACERS 1,3-PDMCH, PDMCB, PMCH, PMCP, AND SF ₆ , INJECTED IN P-25, P-25A, AND P-28					
Tracer	Injection Well Date/Amount	Producer	Cumulated Produced Mass (kg)	Produced Mass Divided by Injected Mass	Allocation Factor*
PDMCB	P-28,	P-04	0.14	1.4 %	2%
	28/9-94 /	P-13	1.35	13.5 %	24%
	10 kg	P-18A	2.33	23.3 %	41%
		P-29	0.48	4.8 %	9%
		P-40	1.33	13.3 %	24%
Total all wells			5.63	56.3 %	-
1,3-PDMCH	P-28,	P-04	0.26	0.3 %	3%
	6/6-95 /	P-13	0.70	0.7 %	7%
	100 kg	P-18A	1.97	2.0 %	21%
		P-29	1.09	1.1 %	12%
		P-40	5.38	5.4 %	57%
Total all wells			9.40	9.4 %	-
SF ₆	P-28,	P-04	1.22	0.8 %	5%
	22/3-97	P-09	2.62	1.7 %	10%
	150 kg	P-13	0.97	0.6 %	4%
		P-18A	6.09	4.1 %	23%
		P-29	6.58	4.4 %	24%
	P-40	9.59	6.4 %	35%	
Total all wells			27.1	18.0 %	-
PMCH	P-25,	P-04	0.37	0.8 %	4%
	28/3-94 /	P-13	2.05	4.6 %	20%
	20 Kg	P-18A	1.07	2.4 %	10%
	P-25,	P-18	2.81	6.2 %	27%
	15/5-95 /	P-29	2.76	6.1 %	27%
	20 Kg	P-40	1.33	3.0 %	13%
	P-25,				
	2/4-95 /				
	2 kg				
Total all wells			10.4	23.1 %	-
PMCP	P-25A,	P-09	0.10	2.1 %	4%
	3/8-98 /	P-13	1.12	22.4 %	43%
	5 kg	P-18A	1.31	26.1 %	51%
	P-40	0.06	1.1 %	2%	
Total all wells			2.59	51.7%	-

* Allocation factor: Total produced tracer mass in a well divided by the total produced mass in all wells.
 The amount relative to the injected mass is an indication of how good the communication is between the injector and the producer.

Figure 18: Total mass balance of all PFC tracer injected into the Snorre field (from Huseby et al 2008)

The summary table of all tracer injections and ultimate recovery reflects (Fig.18) the different partitioning and thermophysical properties of PFC tracer mix. The low boiling tracers PDCB and PMCP have recoveries in the 50% range whereas the high boiling ones, larger ones reach only recoveries of 9.4% and 3%. Recovery of tracers might be reflected in the different phase behavior and adsorption losses including dissolution into residual oil phase, as they are incompatible with aqueous phases.

Another slim tube study investigated residual oil saturations from tracer injection profiles ([19] Chatzichristos et al 2000). The study highlights the attempt to calculate residual oil saturations with a combined passive tracer test using tracers with different partitioning behavior.

The retention time of the ideal vs. the non-ideal, partitioning tracer can be used in a simple formula to derive residual saturations:

$$\overline{S_{or}} = \frac{R - 1}{R - 1 + K_2 - RK_1}$$

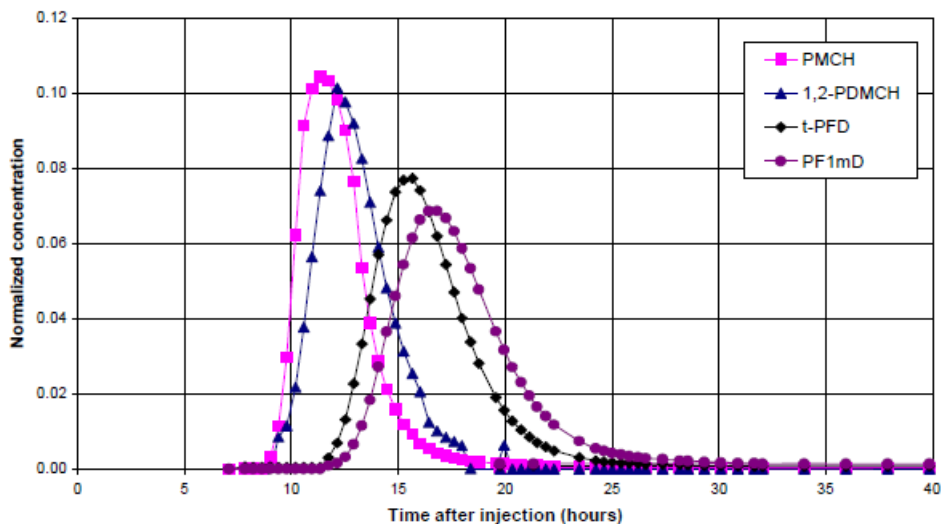
$$\text{where: } R = \frac{\Delta t_2}{\Delta t_1}$$

$$\overline{S_{or}} = \frac{\frac{\Delta t}{t_0}}{\frac{\Delta t}{t_0} + K}$$

Figure 19: Equation to calculate S_{or} , residual oil saturation, using the different retention times of the partitioning tracers applied; K-factors are calculated as ratio of immobile vs. mobile phase partitioning; right side: formula using an ideal tracer mixed with a partitioning one and the time difference of arrival (adapted from [19])

Breakthrough time has been calculated using the peak method being independent of physical dispersion (Fig.19). Parameters affecting the arrival time of the partitioning tracer are oil saturation and the partition coefficient. The latter is an intrinsic property which depends on temperature, pressure, salinity and fluid composition.

In a slim tube experiment, PFC gas tracers were tested using a 6m long slim tube with Ottawa sand as the matrix component. The slim tube was conditioned using Ekofisk oil and a remaining oil saturation of 0.27. Synthetic wet gas was flushed through the slim tube until a steady state was observed. Tracer pulse was immediately injected and retention times were monitored including partition coefficients between oil and gas (Fig.20).



Pressure (Bars)	PMCH	1,2-PDMCH	1,3-PDMCH	c-PFD	t-PFD
150	1.04	1.49	1.29	2.53	2.38

Figure 20: Gas Tracer breakthrough curve; normalized and partition coefficients of tracers measured in static experiments with Ekofisk oil, from [19]

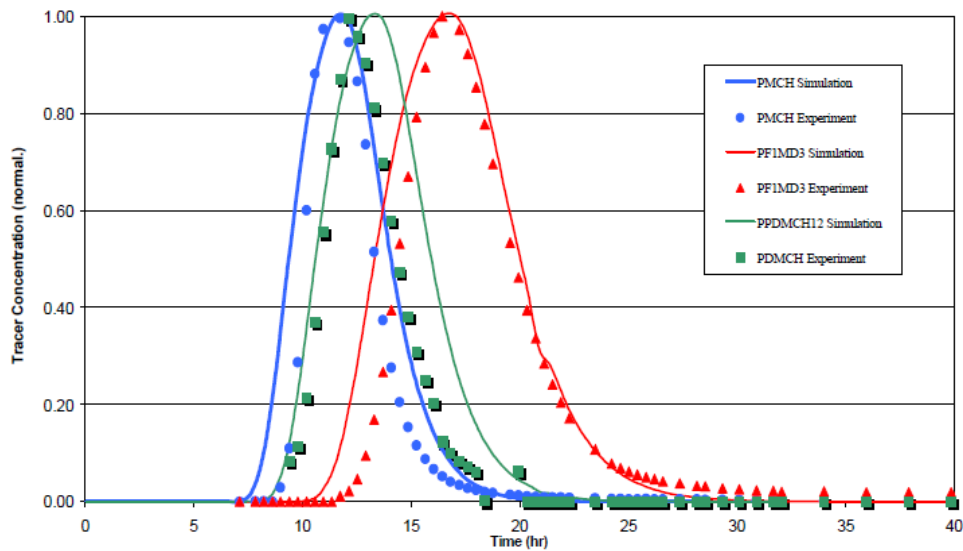


Figure 5: Comparison of the simulated with the experimental results for the gas tracers.

Figure 21: Simulated vs. measured tracer breakthrough curves (adapted from [19])

The comparison of the static experiments were also modelled with good agreement of the modelling efforts with the experimental results (Fig.21). In the next step, simulation of tracer flow was mimicked taking into account tracer flow velocities, partitioning, adsorption and full tensor dispersion. Fig.22 highlights the effect of partition coefficient on tracer flow and this is reflected in PFC arrival times.

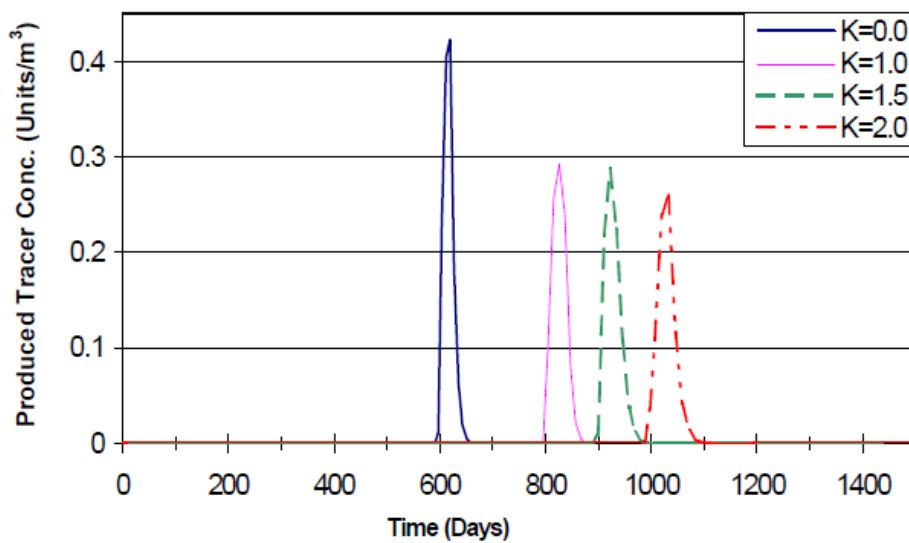


Figure 22: Retention behavior of tracer due to partitioning effect (adapted from [19])

4.1. Synopsis

The petroleum reservoir modelling demonstration projects using PFC tracers mainly as gas tracers to verify communication, flow paths and study the subsurface behaviour of the tracer in multiphase fluid environments was successful to that point that qualitatively, PFC tracer performance was reliable. The proof of PFCs acting as a true passive tracer was reflected in the high stable recoveries compared to other tracers like fluorinated benzoic acids and similar to SF₆. A good indication of tracer movement in the presence of hydrocarbon phases was demonstrated in positive correlations with GORs of the hydrocarbon fluids investigated.

Slim tube experiments have shown that in miscible displacement and mimicking WAG, the PFC tracer predictability due to its inertness and limited interactions was good.

The link of the partitioning between the residual oil and the gas phase indicated by the different partition coefficient had a clear impact on the retention of the tracer and its mobility. Therefore, this data could be used for saturation calculations.

The link to use slim tube in partial to miscible displacement studies was verified and known in the petroleum research community. A more reliable testing on the role of the matrix has so far not been studied nor established.

5. Perfluorocarbon tracer properties

5.1. Physical and Chemical properties of Perfluorocarbon Tracers

The objective of this chapter is to summarize the most important aspects of the physical, chemical and structural aspects of fluorine chemistry. The logical sequence to reveal the behaviour of fluorocarbons as pure compounds and in mixtures is to state their fundamental molecular properties, which are linked to their physical properties (density, viscosity, molar volumes, heat capacities, free energies etc.).

Per-fluorocarbon is a common name for the chemical compound class of perfluoroalkanes termed after The International Union of Pure and Applied Chemistry (IUPAC) nomenclature. Perfluorocarbons are saturated compounds solely consisting of carbon and fluorine.

Perfluoroalkanes are systems with an empirical formula (C_nF_{2n+2}). Cyclic perfluoroalkanes (C_nF_{2n}) are usually denoted with a fluorine symbol in the centre of the ring which indicates that all unmarked bonds to carbon are fluorine. For aliphatics of C_1 to C_4 still the greek or latin nomenclature is used to state fully fluorinated molecules like octafluoropropane for C_3F_8 . The prefix “perfluoro” is used for C_{5+} fully fluorinated carbon chains.

It is important to state that all hydrogen is replaced by fluorine as physicochemical properties and phase properties differ tremendously compared to only partly fluorinated compounds like hydrofluorocarbons and other halogenated hydrocarbons.

PFCs are generally regarded as ‘chemically inert’ substances which have some unusual chemical characteristics derived from its carbon-fluorine (C-F) bond activation. Although fluorine’s size replaces hydrogen without changing the overall dimensions of a molecule, its high electronegativity, with 4.0 the highest in the periodic system, leads to very different chemical behaviour compared to hydrogen.

In association with carbon and due to this high electron affinity, the C-F bond is highly polarized with fluorine being partially negatively and carbon positively charged, $F^{\delta-}$ and $C^{\delta+}$. The energy of a C-F bond reads in between 450 - 560 kJ/mol and makes it a very short and one of the strongest bonds in chemistry. In that large threshold, the bond energy increases with the degree of fluorination. $D^0(C-F) = 108.3 \text{ kcal mol}^{-1}$ in CH_3F , 119.5 for CH_2F_2 , 127.5 for CHF_3 and 130.5 kcal mol^{-1} in CF_4 (Smart, 1995)

The three lone pairs in the fluorine molecule are tightly bound to the nucleus and are therefore not reactive, although highly polarized leaving all the electron density close to the fluorine atom. This makes the C-F bond a weak hydrogen-bond acceptor. Due to the strong attraction of the electrons around the fluorine, it tears so effectively that behind the carbon a free anti-bonding orbital acts as the corresponding exceptional function of C-F bonds [30]. The repulsion of the free electron pairs of the adjacent fluorine atoms also has geometric and steric implications. The different conformations of F-alkyl chains compared to H-alkyl chains result in a common all trans helical steric configuration of perfluorinated molecules in relation to a planar/zig-zag H-alkyl chain structure ([20] Jang et al 2003).

Commercially available perfluorocarbons, which are of interest for Shell’s tracer experiments comprise linear and cyclic perfluoroalkanes. Amines and ethers are not considered yet in future CCS tracer pilots. Aromatic perfluoroalkanes differ in reactivity and solubility due to their higher polarity caused by

π -system attached fluorine and are therefore discarded as tracers (see [21] Dunitz 2003 for a review on this subject). However, they are intended to be used as a benchmark for water solubility in the batch experiments.

The PFC tracers chosen to be included in the PFC tracer study with CSIRO are:

Table 2: Perfluorocarbon tracer compounds considered in research initiative with CSIRO, Australia.

perfluoro(methylcyclopentane) (bp 48 °C)	perfluoro-2-methyl-3-ethylpentane (bp 103°C)
perfluoro(methylcyclohexane) (bp 76 °C)	perfluorooctane, mixture (bp 103.4 °C)
perfluoro-1,2-dimethylcyclohexane (bp 102 °C)	perfluorobutane (bp -1.6 °C)
perfluoro-1,3-dimethylcyclohexane (bp 102 °C)	perfluorohexane (bp 57 °C)
perfluoro-1,4-dimethylcyclohexane (bp 102 °C)	Perfluorodimethylcyclobutane (PDCB) (bp 45°C)
Perfluoroethylcyclohexane (bp 101.7 °C)	Perfluoro-3-ethylpentane (bp 84°C)*
Perfluorocyclobutane (PCB) (bp -6°C)	

A compilation of perfluorocarbon molecules common for industrial manufacturing are (Table 3):

Table 3: Perfluorocarbons commercially available (status 2003) including amines and ethers (adapted from [22] Gladysz & Emnet 2004).

Entry	Solvent	Formula	bp (°C)	mp (°C)	Density (g/mL)	Common name (trade name family)	CAS #	2003 Vendors ^a
1	perfluorohexane ^{e,c}	C ₆ F ₁₄	57.1	-90	1.669	FC-72 (Fluorinert)	[355-42-0]	a-e,g,h,m
2	perfluoroheptane ^{b,d}	C ₇ F ₁₆	82.4	-78	1.745	-	[335-57-9]	a-d,g,h,m
3	perfluorooctane ^{e,g,h}	C ₈ F ₁₈	103-104	-25	1.766	-	[307-34-6]	a-e,g,m
4	perfluoromethylcyclohexane	CF ₃ C ₆ F ₁₁	76.1	-37	1.787	PFMC	[355-02-2]	a-e,g,i,m
5	perfluoro-1,2-dimethylcyclohexane	C ₈ F ₁₆	101.5	-56	1.867	PP3 (Flutec(R))	[306-98-9]	a-d,g,m
6	perfluoro-1,3-dimethylcyclohexane	C ₈ F ₁₆	101-102	-55	1.828	-	[335-27-3]	a-e,g,h,m
7	perfluoro-1,3,5-trimethylcyclohexane	C ₉ F ₁₈	125-128	-68	1.888	-	[374-76-5]	a-d,m
8	perfluorodecalin	C ₁₀ F ₁₈	142	-10	1.908	-	[306-94-5]	a-c,e,g-i,m
9	1-bromoperfluorooctane	C ₈ F ₁₇ Br	142	6	1.930	-	[423-55-2]	a-e,g,h
10	perfluoro-2-butyltetrahydrofuran	C ₈ F ₁₆ O	99-107	-88	1.77	FC-75 (Fluorinert)	[335-36-4]	a-e,h,m
11	perfluoropolyether ^f	MW ≈ 340	57	-	1.65	HT55 (Galden)	-	l
12	perfluoropolyether ^f	MW ≈ 410	70	-	1.68	HT70 (Galden(R))	[69991-67-9]	c,l,m
13	perfluoropolyether ^f	MW ≈ 460	90	-	1.69	HT90 (Galden(R))	-	c,l,m
14	perfluoropolyether ^f	MW ≈ 580	110	-	1.72	HT110 (Galden(R))	-	c,l,m
15	perfluorotriethylamine ^{b,d}	C ₁₂ F ₂₇ N	178	-	1.883	FC-43 (Fluorinert)	[311-89-7]	a-e,g,h,k,m
16	perfluorotripropylamine ^{b,h}	C ₁₅ F ₃₃ N	212-218	-	1.93	FC-70 (Fluorinert)	[338-84-1]	a-e,k,m
17	perfluorotrihexylamine	C ₁₈ F ₃₉ N	250-260	33	1.90	FC-71 (Fluorinert(R))	[432-08-6]	a-c,m

^aCodes for vendors are as follows: a = Oakwood Products (<http://www.oakwoodchemical.com>); b = ABCR (<http://www.abcr.de>); c = Fluorochem (http://www.fluorochem.co.uk/index2_n.s.asp); d = Lancaster (<http://www.lancastersynthesis.com>); e = Acros Organics (<http://www.acros.be>); f = 3M (<http://www.3m.com>); g = Aldrich (<http://www.sigmaaldrich.com/Brands/Aldrich.html>); h = Fluka (http://www.sigmaaldrich.com/Brands/Fluka_Riedel_Home.html); i = Merck (<http://ph.merck.de/servlet/PP/menu/1001723/index.html>); j = Oxychem (<http://www.oxychem.com>); k = Sigma (<http://www.sigmaaldrich.com/Brands/Sigma.html>); l = Solvay Solexis (<http://www.solvaysolexis.com>); m = Apollo Scientific Ltd. (<http://www.apolloscientific.co.uk>). ^bSeveral fluoruous solvents are available in technical grades that have distinct CAS numbers and/or common names. ^c[86508-42-1], FC-72 [Fluorinert(R)], PP1 [Flutec(R)], a, c, f, m. ^d[86508-42-1], FC-84 [Fluorinert(R)], a, c, f, m. ^e[86508-42-1], [52623-00-4], [52923-00-4], FC-77 [Fluorinert(R)], a, c, e, f, h, k, m. ^fGeneral formula CF₂((OCF(CF₃)CF₂)_n(OCF₂)_m)OCF₃. ^g[86508-42-1], FC-43 [Fluorinert(R)], a, c, f, m. ^h[86508-42-1], FC-70 [Fluorinert(R)], f, m.

Tables 2 and 3 provide a good overview of what boiling point ranges and molecular weights will be covered in the perfluoroalkanes of interest. The high densities due to the high fluorine content compared with the low boiling points makes perfluoroalkanes a unique class of organofluorine compounds.

Physical properties of PFCs are closely associated with the fundamental properties of fluorine and the interactions of fluorine introduced in an aliphatic and cyclic carbon skeleton/backbone.

Good overviews and summaries for a wealth of physical properties and the link to PFC's unique molecular properties are compiled especially by [23] [24] [25] Smart (1994, 1995, 2001), [21] [26] Dunitz (2003, 2004), [27] Gladysz & Jurisch (2012); [22] Gladysz & Emnet (2004); [28] Krafft & Ries (2009); [29] Sandford (2003); [30] Hunter (2010); [31] O'Hagan (2008) and [32] Tsai (2009). [33] Varanda et al. (2008) ; [34] [35] Dias et al (2006, 2009); [36] Morgado et al. (2011) and numerous co-workers in the field of fluorine chemistry have concise, short introductory summaries, which mostly link back to the aforementioned detailed review articles/book chapters.

The low molecular polarizability (related to the C-F bond characteristics) of fluorocarbons relative to their molecular weights and volumes fits in with their low surface tension and low boiling points relative to their molecular weights (the very similar boiling points of hydrocarbons and corresponding fluorocarbons point to similar cohesive energies per mole). Since polarizability α has the same dimension as volume V , the ratio $Q=\alpha/V$ is a dimensionless quantity. Among the elements commonly present in organic compounds, fluorine has the smallest value of Q . "...large molecules tend to have large polarizabilities, while small molecules have small ones. Each additional atom in a molecule adds to the molecular volume and to the molecular polarizability, keeping Q roughly constant. Only replacement of hydrogen by fluorine results in an increase in molecular volume without any concomitant change in molecular polarizability, besides changing the sign of the local charge." – from J.D. Dunitz: - "Organic Fluorine: Odd Man Out"[26] .

The above cited statement discusses the interaction between physical properties and their chemical "expressions", which serves as a thorough understanding of the behaviour of the peculiar compound class. Smart (1995, 2001)[24] [25] and Dunitz (2003)[21] in their reviews lists the unique patterns of PFC's various physical properties as follows:

- PFCs boil only 25 to 30°C higher than noble gases of similar molecular weight
- Branching has little effect on boiling point in contrast to the corresponding alkanes which points to low intermolecular interactions
- Boiling points correlate well with the molecular dipole (in hydrofluorocarbons)
- PFCs have very high thermal stabilities (depends only on C-C bond strength) except perfluorocyclopropanes which are unusually thermolabile
- PFCs have the lowest refractive index at surface temperature
- PFCs have the lowest surface tension at surface temperature
- PFCs have the lowest dielectric constant at surface temperature
- PFC liquids wet any surface
- PFCs demonstrate high compressibility
- PFCs show high vapour pressures
- PFCs are poor solvents for organics due to their characteristics as:
 - Non polar molecules
 - Having low polarizability
 - Exhibit small inter-and intramolecular forces

To put some numbers to the different physical properties, [37] Pottof (2009) and [38] Hallwell (2010) provide a wealth of compiled data of gaseous and liquid perfluorocarbons. Tsai (2009) summarizes physical properties from literature [32] (Table 4):

Table 4: Adapted from Tsai (2009) – physical properties of perfluorocarbons

Property	Units	C ₅ F ₁₂	C ₆ F ₁₄	C ₇ F ₁₆	C ₈ F ₁₈	C ₉ F ₂₀	Ref.
Molecular weight	–	678-26-2	355-42-0	335-57-9	307-34-6	375-96-2	
Boiling point at 1 atm	g/mol	288.04	338.04	388.05	438.06	488.07	
Freezing point at 1 atm	°C	29.3	57.2	82.3	103.5	125.3	Poling et al. (2001)
	°C	-120	-86	-51	-25	-16	(Oliver et al. 1951; Stiles and Cady, 1952)
Critical temperature	K	421.4	450.6	475.3	502.20	542.35	(Vandama et al., 1994;
Critical pressure	MPa	2.037	1.877	1.62	1.548	1.450	Marsh et al., 2007)
Critical volume	cm ³ /mol	465	545	636	718	– ^a	
Liquid molar volume	cm ³ /mol	177.8	198.9	223.9	246.5	269.5	(Poling et al., 2001;
	20 °C	178.9	201.6	224.3	248.2	271.2	Duce et al., 2007)
	25 °C	178.9	201.6	224.3	248.2	271.2	
Pitzer acentric factor	–	0.415	0.513	0.561	0.619	0.635	Poling et al. (2001)
Density	g/cm ³	1.620	1.691	1.732	1.777	1.800	(Dias et al., 2004; Dias et al.,
	20 °C	1.604	1.676	1.706	1.765	1.788	2005; McCabe et al. 2003;
	25 °C	1.604	1.676	1.706	1.765	1.788	Sakka and Ogata, 2005)
Surface tension	mN/m	9.89	12.97	14.09	14.92	15.82	(Sakka and Ogata, 2005;
	20 °C	9.89	12.97	14.09	14.92	15.82	Freire et al., 2006)
	25 °C	9.4	12.23	13.55	14.47	15.39	Freire et al. (2008)
Kinetic viscosity at 25 °C	mPa s	0.465	0.700	0.938	1.256	1.789	
Dynamic viscosity at 25 °C	mm ² /s	0.290	0.417	0.543	0.712	1.001	
Vapor pressure	kPa	71.39	23.58	7.89	2.85	0.94	(Crowder et al., 1967; Dias
	20 °C	86.89	29.28	10.17	3.74	1.29	et al., 2004; Dias et al., 2005;
	25 °C	86.89	29.28	10.17	3.74	1.29	Duce et al., 2007)
Refractive index	–	1.2383	1.2558	1.2690	1.2740	1.2781	(Haszeldine and Smith, 1951;
	20 °C	1.2380	1.2526	1.2670	1.2720	1.2760	Qiu and Dhir, 1999)
	25 °C	1.2380	1.2526	1.2670	1.2720	1.2760	
Heat of vaporization at 25 °C	kJ/mol	27.3	31.73/32.47	36.36	39.88/40.96	45.27	(Dias et al., 2004; Dias et al.,
	20 °C	27.3	31.73/32.47	36.36	39.88/40.96	45.27	2005; Duce et al., 2007)

^a No available data.

Gladysz and Jurisch (2012)[27] add to the statements of Smart(1994,1995)[23] [24] in comparing the PFCs with alkanes. They summarize the interaction as follows:

- PFCs have no tendency to engage in hydrogen bonding
- Close to corresponding alkanes are the following properties of PFCs
 - Enthalpies of vaporization
 - Boiling points
 - Molecular polarizabilities
- Totally different compared to the corresponding alkane are:
 - Atomic number
 - Molecular weight
 - Molecular volume
 - Density
 - Viscosity

In comparison to alkanes, Krafft & Riess (2009)[28] state the following characteristics of PFCs:

- much lower cohesive energy density in condensed state induces much higher vapour pressures and non-ideal behaviour in mixing
- higher critical temperatures
- a much narrower “liquid domain”
- large discrepancies of molecular weights and boiling points
- the aforementioned surface energies contribute to very low surface tensions
- the low refractive index correlates well with the low polarizabilities
- much higher hydrophobicity resulted from a larger surface area

5.2. Partitioning and adsorption characteristics of PFCs

Of particular interest in the subsurface behavior of PFCs are its partitioning and adsorption characteristics. Its comparison with hydrocarbons, their hydrogenated counterparts highlights its unique properties compared to non fluorinated solvents.

PFCs are regarded as being very hydrophobic, i.e. having very low polarities. Polarity is generally described with a dielectric constant, Hildebrand parameter, or the so called Spectral Polarity Index (P_s), which relates to adsorption of a perfluoroheptyl related dye ([22] Gladysz & Emnet 2004; [69] Freed et al. (1990)). On all three scales, the perfluorocarbon exhibits a less polar behavior than the corresponding alkane with values for example on the Hildebrand scale of less than 13([22] Gladysz & Emnet, 2004; [23] Smart, 1994; [39] Rabai et al. 2006). For comparison, water has a Hildebrand parameter value of 48 and alkanes range in Hildebrand parameter values from 14 to 17 MPa^{1/2}. Regarding the P_s index, perfluoroalkanes exhibit values in the range of $P_s = 0$ for perfluorohexane, $P_s = 0.58$ for perfluoro-1,3,-dimethylcyclohexane (PDCH) to $P_s = 0.99$ for perfluorodecalin. Perfluorobenzene has a value of $P_s = 4.53$. Corresponding hydrocarbons range in P_s values from 2.56 for n-hexane to 6.95 for benzene. Decalin exhibit a value of $P_s = 4.07$. The entropies of vaporization were also determined for both classes. A comparison revealed a larger entropy of vaporisation by about 1 cal mol⁻¹ °K⁻¹ ([40] Funk & Prausnitz, 1971). Perfluorohexane to -octane measured surface tension is in the range of $\gamma = 12.8$ to 14.5 Nm/m +/-0.1 at 20°C[70] which describes PFCs as a surfactant and therefore more prone to adsorption. True adsorption of PFCs has only been reported under laboratory conditions and used in analytical protocols. True adsorption of PFCs is linked to carbonaceous substrates. Activated charcoal is a prominent absorbent widely used for this purpose; hence, capillary adsorption tubes (CATS) tubes are utilized to adsorb PFCs for analysis. For the inert PFC compounds, physisorption (physical adsorption) is the most likely mechanism which reflects van der Waals forces compared to the more covalent character of chemisorptions processes. However, the hydrophobic character of the PFCs has a strong impact on the solid/solvent partitioning behavior due to the incompatibility of the PFCs to dissolve in a polar solvent. The solution enthalpy is considered to be very high as a measure of immiscibility. On the other hand, the very low surface energy “disturbance” on wetting solid surfaces described above as low surface tension reflects this property as well.

Characteristics of organic solutes and, even more, for organofluorine solutes are the adsorption onto non-polar surfaces like organic particles. Organic particles, depending on their surface structure, can exhibit a high surface/volume ratio which is extreme for activated coals in which due to combustion, volatiles which would block and coagulated particles are removed. An adsorbed hydrophobic molecule does not disturb the polar solvent like water in such a way a dissolved organic molecule would. This determines its affinity to be adsorbed. Water molecules tend to minimize electrostatic repulsion forces and orient themselves accordingly, so that the interaction energy between the solute and the solvent is minimized. The presence of a large hydrophobic molecule is therefore energetically unfavorable which is reflected in its high difference in solution enthalpy ΔH_{sol} and a large ΔG_{sol} . On the contrary, the higher the solution enthalpy and Gibbs energy wrt. to polar solvents, the more likely is the state of adsorption onto hydrophobic solids. Therefore, the PFCs are very good surfactants and have very low surface tensions as described previously. That increases the affinity of the PFCs to stick on hydrophobic surfaces. Chiou et al (1979)[68] compared solid/water partition coefficients with water solubilities of halogenated organic molecules and describes the negative correlation of this relationship.

6. Environmental fate of perfluorocarbons

The environmental fate of perfluorocarbons focuses on the inertness of this compound class. The atmospheric distribution is important to determine a background of certain PFCs which limits their detection in the hydro-/biosphere. The extrapolation of this background needs to be estimated for the future to determine changes in levels of detection for the next decades. Finally, the greenhouse gas potential of PFCs is discussed.

6.1. Reactivity of PFCs

Saturated perfluorocarbons are exceptionally “inert” due to the tightly bond electrons in fluorine. However, there are exceptions to the commonly referred non-reactivity of PFCs.

PFCs and HFCs are susceptible to defluorination by reducing agents ([41] Amii & Uneyama, 2009). Strong reducing agents loose electrons or more often considered in organic chemistry “hydrogen”. Alkali metals and low valent metal ions are prone reducers and sodium is especially advantageous. The Birch reduction uses sodium and an alcohol to hydrogenize aromatic compounds, sodium naphthalide etches perfluoropolymers and dipotassium benzoin dianion is known for its ability to introduce carboxylic groups to PTFE already at 50 °C.

The reaction of 1-fluorohexane with a Zirconium complex, i.e. Cp*₂ZrH₂, at ambient temperature for 2 days produces hexane and Cp*₂ZrHF in quantitative yields (Fig.23). Also, fluorocyclohexane undergoes hydrodefluorination at 120 °C.

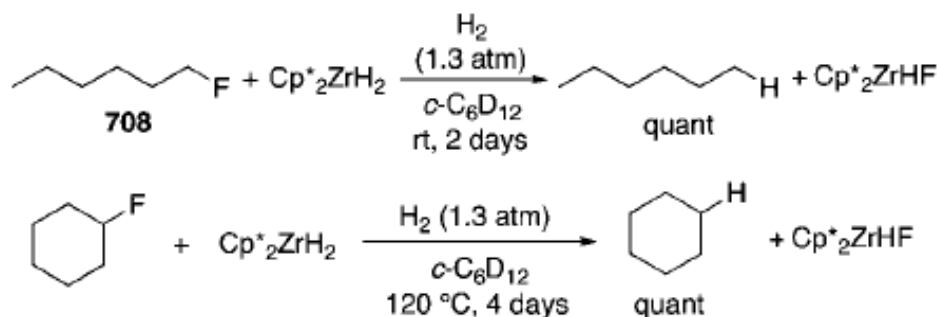


Figure 23: Birch reduction mechanism to exchange fluorine for hydrogen under catalytic conditions using a Zirconium complex (from Amii & Uneyama, 2009)

The high affinity for electrons accounts mostly for the chemical behaviour of perfluorocarbons. Defluorination is induced by “one electron transfer” mechanism which destabilizes the C-F bond and dissociates into a carbon centred radical and F⁻. PFCs with relatively weak tertiary C-F sigma* orbitals can be reduced even more efficiently by organic sodium sulfides. So far, in the subsurface under natural conditions, reducing agents are rather mild and special metal complexes involving Zirconium are very rare. Nevertheless, this has not been studied in full detail, if there is a potential risk of PFCs being oxidized during prolonged exposure to reducing environments like oil and gas reservoirs. From our subsurface knowledge so far, the danger of chemical alteration of PFCs is regarded as negligible.

Biotransformation of fluorinated molecules are more common for fluoroaromatic molecules and fluorinated acetate and carboxylic groups ([42] Murphy,2010). Perfluorobutane to –hexane molecules have not been reported yet to degrade via microbial enzymatic pathways.

6.2. Atmospheric background of PFCs

Atmospheric background concentrations have been assessed from recent academic literature. The highest emitter of PFCs is the semiconductor industry. Perfluoromethane (CF_4) has the highest reported concentrations in the atmosphere with 75 ppt followed by C_2F_6 with 0.11 ppt. C_3F_8 is not detectable due to its exceptional labile configuration for cosmic radiation. PFCs are regarded as very inert and do undergo degradation through high energy radiation very slowly. CF_4 has a calculated lifetime of 32000 years, perfluorohexane, $n\text{-C}_6\text{F}_{14}$, still remains with 3200 yrs lifetime a very stable molecule[44] . SF_6 has comparable lifetimes with perfluorohexane.

Laube et al (2012)[43] reported on perfluorohexane/-heptane concentrations in the atmosphere (Fig. 24).

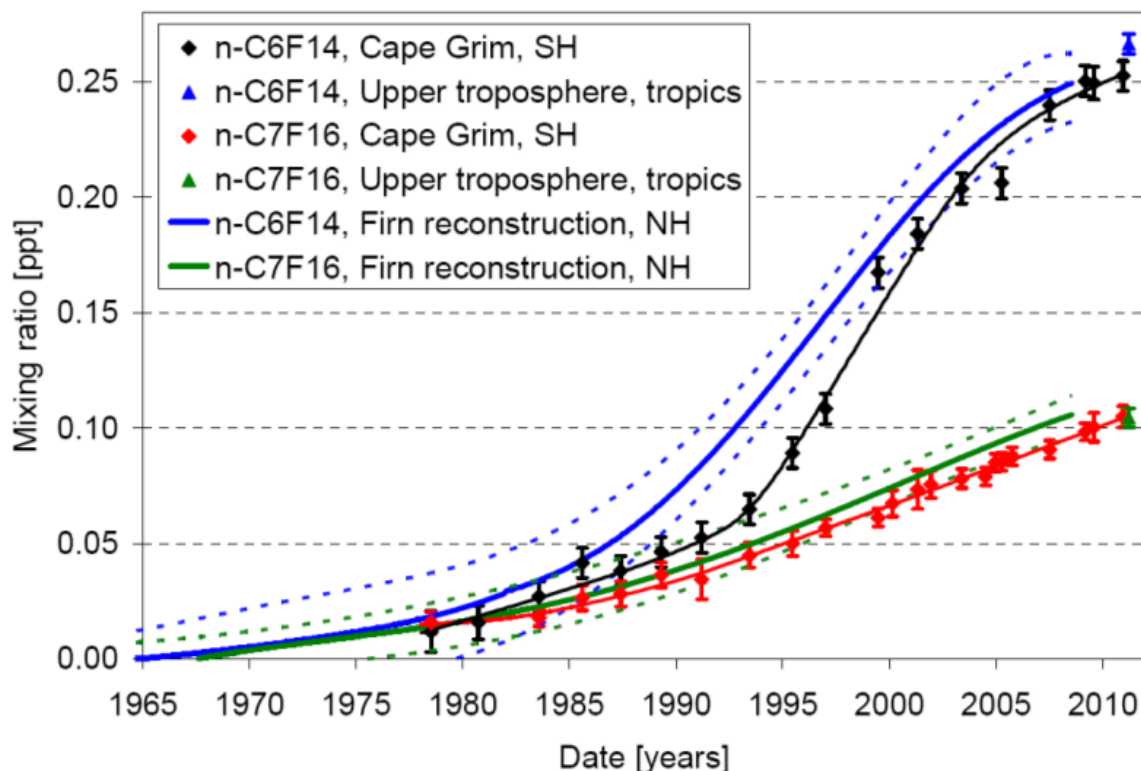


Figure 24: Perfluorohexane and-heptane concentrations in the atmosphere (adapted from Laube et al. 2012)

The increase of PFCs since 1980 to 2010 is due to the increased industrial use as refrigerant replacing chlorinated halocarbons and hydrofluorocarbons (CFCs, HFCs).

Ivy et al. (2012)[44] reported on mean growth estimates for the heavy PFCs in the atmosphere which are the most suitable PFCs for spiking the injected CO_2 (Fig.25).

Species	Mean Mole Fractions [ppt]	Mean Growth Rate [ppq yr ⁻¹]	2011 Mole Fractions [ppt]	2011 Radiative Forcing [mW m ⁻²]
C ₄ F ₁₀	0.101	4.58	0.18	0.059
C ₅ F ₁₂	0.072	3.29	0.12	0.049
C ₆ F ₁₄	0.119	7.50	0.28	0.137
C ₇ F ₁₆	0.053	3.19	0.12	0.058
C ₈ F ₁₈	0.043	2.51	0.09	0.051

Figure 25: Mean “heavy” PFC mole fractions and estimated growth rates in the atmosphere (adapted from Ivy et al. 2012)

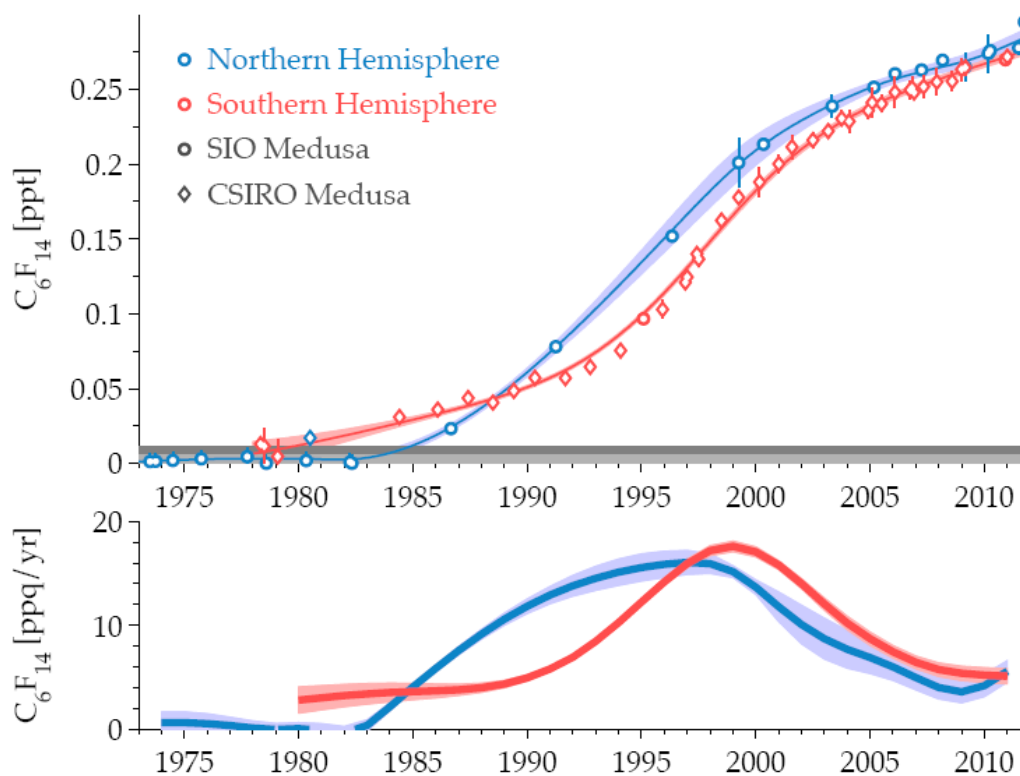


Figure 26: Mean measured concentrations of n-C₆F₁₄ and the annual growth rates (from Ivy et al. 2012)

Ivy et al. (2012)[44] summarized the PFC growth rates for the last 30 years which reflects on a declining annual growth since 1998 where it peaked with an annual increase of around 18 to 20 ppq split in both hemispheres (Fig.26).

	PDCB	PMCP	PMCH	oPDCH	ptPDCH	
Bkgrd (ppqv)	3	8	8	1	7	
Total Atmospheric load (metric tons)	140	430	500	71	500	
	PDCB	PMCP	PMCH	oPDCH	PTCH	ptPDCH
1986 (36)	0.34 ± 0.01	3.22 ± 0.03	4.6 ± 0.05	0.30 ± 0.10	0.07	3.4 ± 1.0
ANATEX 1987 (21)		2.09 ± 0.43	3.6 ± 0.05	0.4 ± 0.03	0.45 ± 0.28	4.34 ± 0.32
MOHAVE 1992 (16)		6.29 ± 0.59	4.91 ± 0.30	0.56 ± 0.06	0.64 ± 0.62	
ETEX, Austria, 1994 (37)	0.63 ± 0.18	5.24 ± 1.03	5.9 ± .64	0.98 ± 0.48	0.59 ± 0.60	5.37 ± 1.85
ETEX, Europe, 1994 (38)		4.6 ± 0.3	4.6 ± 0.8	0.6 ± 0.31		6.1 ± 0.8
1996, New Jersey, Rural (39)		4.15 ± 0.05	3.84 ± 0.10	0.34 ± 0.10	0.07 ± 0.10	
2001, Korea (40)			7.4 ± 0.80	1.12 ± 0.25		
2001, Ireland, UK (35)	2.7 ± 0.2	6.3 ± 0.2	5.5 ± 0.2	0.7 ± 0.1		4.88 ± 0.03
2001, Europe urban (6)	3.0 ± 1.5	8.1 ± 1.8	6.3 ± 1.1			
2001, Europe remote (6)	2.5 ± 0.4	6.8 ± 1.0	5.2 ± 1.3			
BRAVO, 2001, suburban (41)	2 ± 0.4			0.6 ± 0.1		7 ± 1.2
this study						
2005, NY, Urban	2 ± 0.9	7 ± 1.2	7 ± 1.3	1 ± 0.4	2 ± 1.3	7 ± 1.2
2005, NY, Suburban	2 ± 0.6	8 ± 1.9	7 ± 1.5	1 ± 0.3	1 ± 0.9	7 ± 0.3
2006, Florida, Remote	3 ± 0.4	8 ± 0.6	8 ± 0.9	1 ± 0.4	1 ± 0.9	8 ± 0.8

Figure 27: Estimated and rounded background concentrations of PFCs chosen for CCS MMV purposes; above: generalized background values in ppqv; below: complementary measured data from various past years and atmospheric monitoring campaigns (adapted from Watson & Sullivan (2011); Watson et al. (2007))

A recent estimation of atmospheric PFC backgrounds was used in the diffusive transport calculations of [45] Watson & Sullivan (2011). They used 10 ppqv (lower parts of quadrillion(10^{15})) as the background value for the heavy PFC compounds of PMCP and PMCH and 1,3 PDCH (Fig.26). Other PFCs considered so far as potential tracer for CCS range in the order of 1 to 3 ppqv (Fig.27).

6.3. Greenhouse Gas Potential of PFCs

The Greenhouse Gas Potential, i.e. Global Warming Potential (GWP), of PFCs is about 10000 times higher than CO₂ (Fig.28).

Species	Lifetime [yr]	Radiative Efficiency [W m ⁻² ppb ⁻¹]	Global Warming Potential (GWP)		
			20-yr horizon	100-yr horizon	500-yr horizon
CF ₄ ^a	50000	0.10	5210	7390	11200
C ₂ F ₆ ^a	10000	0.26	8630	12200	18200
C ₃ F ₈ ^a	2600	0.26	6310	8830	12500
c-C ₄ F ₈ ^a	3200	0.32	7310	10300	14700
C ₄ F ₁₀ ^a	2600	0.33	6330	8860	12500
C ₅ F ₁₂ ^a	4100	0.41	6510	9160	13300
C ₆ F ₁₄ ^a	3200	0.49	6600	9300	13300
C ₇ F ₁₆ ^b	(3000)	0.45	–	–	–
C ₇ F ₁₆ ^c	(3000)	0.48	–	–	–
C ₈ F ₁₈ ^b	(3000)	0.50	5280	7390	10500
C ₈ F ₁₈ ^c	(3000)	0.57	–	–	–
C ₁₀ F ₁₈ ^d	> 1000	0.56	> 5500	> 7500	> 9500

^a Forster et al. (2007)

^b Bravo et al. (2010)

^c Ivy et al. (2012)

^d Shine et al. (2005)

Figure 28: Global Warming Potential of PFCs (adapted from [44])

However, due to the very low amounts of PFCs in the atmosphere, the corresponding mass of CO₂ has been calculated normalized to all PFC mass in the atmosphere. In total, all heavy PFCs (>C-4 backbone) have a GWP equivalent of 750 million tonnes of CO₂. Here, a linear increase is reflected which is potentially an overestimation as seen in Fig.29 in which the PFC concentration reflects an asymptotic behavior in the recent years with decreasing additions of heavy PFCs.

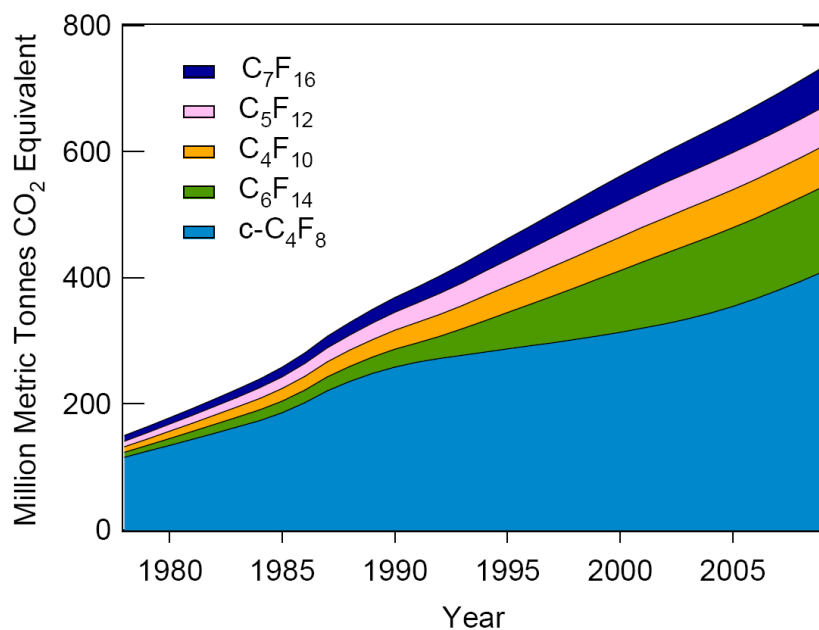


Figure 29: Corresponding cumulative GWP of all heavy PFCs reflected in mass of CO₂ (adapted from [43])

6.4. Solubility of PFCs

Generally, it is important to distinguish between the absolute solubility of a solute, which is defined by a K_{sp} value (solubility constant) or similar parameter, and the relative solubility, which reflects the equilibrium distribution of the solute between two solvents and is defined by a partition coefficient. Partition coefficients therefore quantify the equilibrium distribution of a solute between two immiscible phases, which are most often but not necessarily liquids.

For sufficiently dilute solution conditions (i.e. the concentration of the chemical species in each phase is much lower than the solubility limit), it is defined as the ratio of the chemical concentrations in each of the two phases. Partition coefficients of CO₂ vs. water are generally reported as:

$$K_{C/W}^C = \left(\frac{C_i^{(C)}}{C_i^{(W)}} \right) = \left(\frac{C_{i,GC}^{(C)}}{C_{i,GC}^{(W)}} \right) \left(\frac{V_{D,C}/V_{S,C}}{V_{D,W}/V_{S,W}} \right) \quad K_{C/W}^x = K_{C/W}^C \frac{\rho_W}{\rho_C} \frac{MW_C}{MW_W}$$

Figure 30: Partition coefficient on molar basis on the left side measured by GC counts and taking into account different sample volume correction vs. conversion to mole fraction based units on the right side using densities and molecular weights of the solvents (from[46])

As tracers are typically utilized at low concentrations (i.e. ppm or lower concentration), partition coefficients are essential for accurately characterizing their behaviour in multi-phase systems. Both theory and practice have demonstrated that partition coefficients often exhibit Arrhenius type temperature dependence which can be illustrated in a van't Hoff plot (Fig. 31).

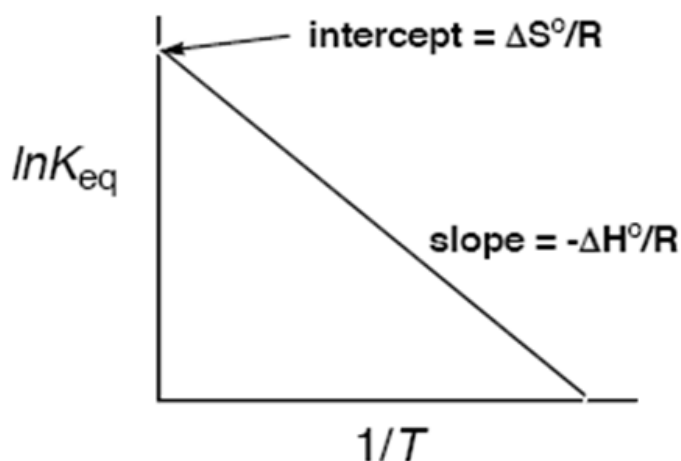
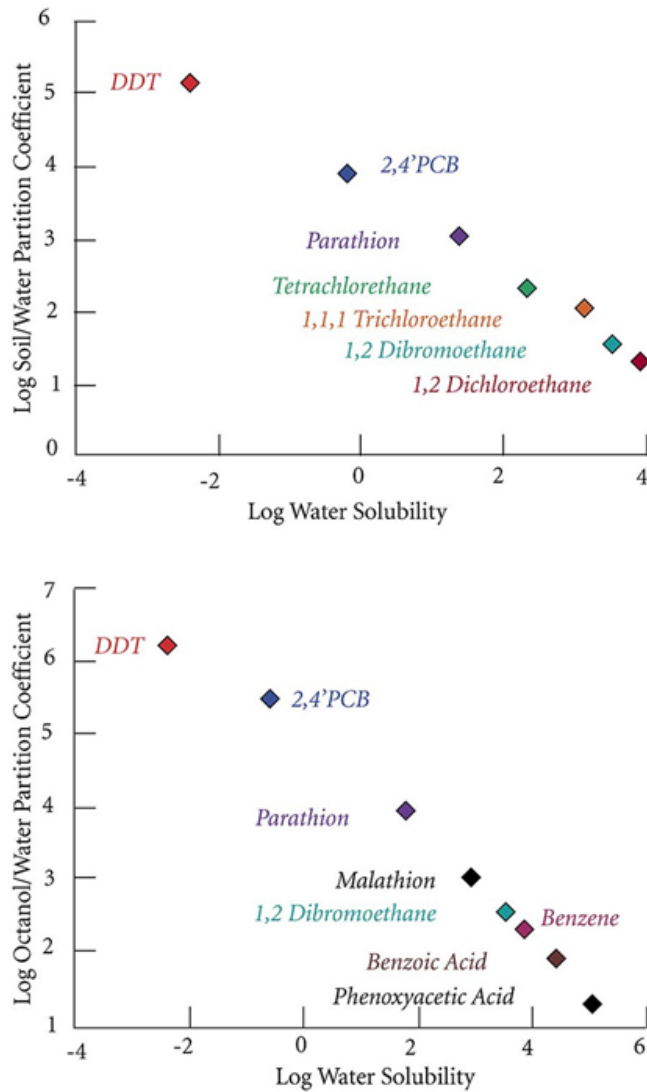


Figure 31: Van't Hoff plot – illustration of temperature dependency of an equilibrium constant/partition coefficient

Apart from direct partition data, for organic compounds, octanol-water partition coefficients have been used extensively in understanding and predicting the bioaccumulation and environmental fate of organic species ([47] [48] Chiou and coworkers 1982; Chiou 2002).

The octanol/water partition coefficient $K_{(o/w)}$ is regarded as a measure of hydrophobicity. Octanol is a largely non polar solvent which exhibits no ordering between the molecules as for water. $K_{(o/w)}$ is linked to another partition coefficient called $K_{(o/m)}$: partitioning between organic solids and water. Both coefficients are linked to each other by an empirical relationship: $K_{(o/m)} = b(K_{(o/w)})^a$, “a” has an approx. value of 0.8. The relationship is negatively correlated with respect to the solubility in water (Fig.32).



Geochemistry, First Edition. William M. White.
© 2013 John Wiley & Sons, Ltd. Published 2013 by John Wiley & Sons, Ltd.

Figure 32: Octanol/water vs. solid organics/water partitioning of organic compounds (from [49])

To describe vapour liquid equilibria or solubility of gases in liquids, Henry’s law coefficients (otherwise known as air/water partition coefficients) have been generally used. However, Henry’s law might only be applicable in a narrow range of concentrations as it uses vapour pressures

instead of fugacities. Therefore, if activity or fugacity coefficients are close to one, Henry's law is a useful approximation of the vapour liquid behavior. However, we focus in the interim report on the partitioning of liquid PFCs in liquid solvents, i.e. supercritical CO₂ and water/brine as the vapour/liquid equilibria are covered in the future experiments mimicking gaseous CO₂/PFC and interaction with fluids in the shallow subsurface.

For CCS projects, the two most dominant phases within the formation are typically supercritical CO₂ and water. There is currently limited fundamental information available on the scCO₂/water partitioning behaviour for organic compounds ([46] Timko et al., 2004). Notably, there is no existing supercritical CO₂/water partition coefficient data for any PFC used in the referenced CCS tracer test applications. Octanol compared to supercritical CO₂ have different dielectric constants and solvent properties (polarizability) and therefore may not be representative or indicative of actual subsurface behaviour of CO₂ – PFC systems. Correlation of $K_{(c/w)}$ vs. $K_{(o/w)}$ for perfluorohexane was determined in Timko et al. (2004)[46] having a correlation coeff. of AAD= 0.2.

Clearly, there is a need to determine the partition coefficients of tracers in regards to their partitioning behaviour between supercritical CO₂ and H₂O or formation fluids for CCS projects. Timko et al. (2004)[46] measured the supercritical CO₂/water partition coefficients for a variety of organic compounds (e.g. aldehydes, ketones, esters, halides, phenols, alkanes and aromatic hydrocarbons) and showed that there is no adequate correlation with octanol/water partition coefficients.

Solubility of halogenated compounds serves as a comparable example for perfluorinated chemicals. A short summary of the state of the art of contaminant geochemistry is given to reflect on perfluorocarbon behavior (see [2] Berkowitz et al 2008 for an overview). Partly fluorinated chemicals which consist of a more hydrophilic region in their structure serve as surfactants and have been extensively monitored due to the high pollution risk coupled to the long residence time of these compounds. Prominent representatives of this class of compounds are the perfluorooctane sulfonate (PFOS) and the perfluorooctanoate (PFOA) groups which are studied in much more detail due to the environmental hazard associated with them ([50] Saikat et al 2013).

Analytically, it has been a challenge to experimentally derive CO₂/water or octanol/water coefficients for the straight chain and cyclic compounds due to their very high hydrophobicity which is better termed high fluorophilicity according to [27] Gladysz et al. (2012).

Perfluorinated compounds with measured $K_{(o/w)}$ from the academic literature are listed as follows :

- perfluorodecalin – see Tsai (2011)[51]
- perfluorobenzene – see Freire et al. (2005)[52] , Oliveira et al. (2007)[1] , Schroeder et al. (2011)[53]
- perfluorotributylamine – see 3M Company -HPV EPA-GOV report (2001)[54]

Modeled and calculated partition coefficients rely on the various association theories derived parameters. In the following summary of literature based partition data, straight chain and cyclic PFCs were assigned a partition coefficient for octanol/water and for some specific PFCs also for scCO₂/water.

Freire et al. (2010)[55] and Oliveira et al. (2007)[1] tried to measure perfluorocarbon concentrations in water and vice versa using pure phases. However, they failed in reporting a partition coefficient for the PFC dissolution in water. Only modeled partition coefficients were

reported. The theoretically determined PFC solubility in water was only calculated so far by Oliveira et al. (2007)[1] . The mutual solubilities of perfluorohexane in the hydrocarbon and in the water phase are shown in Fig.34.

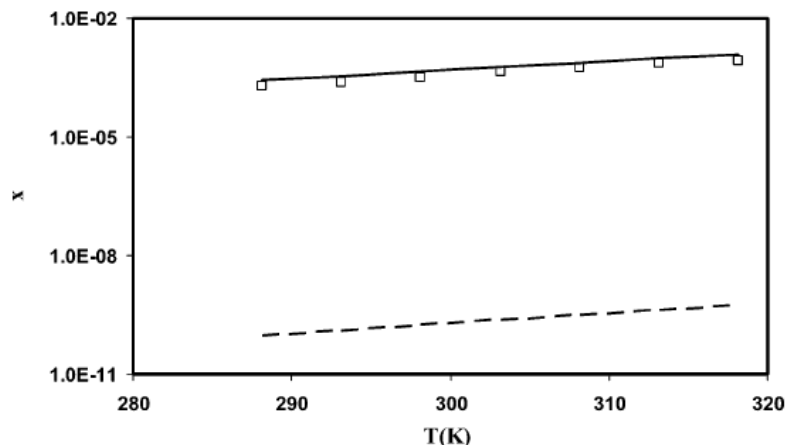


Figure 33: Solubility of perfluorohexane in the hydrocarbon phase as open squares for measured data and a solid line for the CPA predicted values; Perfluorohexane solubility in the water phase as stippled line – calculated (from [1]).

Tsai (2011)[51] report on the calculated $\log K_{(o/w)}$ on perfluorodecalin after data from Meylan & Howard(1995)[56] and compares perfluorodecalin with the corresponding hydrocarbons using the same approach. Perfluorodecalin was assigned a $K_{(o/w)} = 2.85$ compared with similar structured hydrocarbons: naphthalene ($K_{(o/w)} = 3.17$), decalin ($K_{(o/w)} = 4.88$), decane ($K_{(o/w)} = 5.25$). The corresponding experimental values for the hydrocarbons were in a range of 20% within the calculated values.

Tsai (2011)[51] adapted a method of Lyman et al (1982)[57] to estimate octanol water partition coefficients for liquid perfluoroalkanes. He found an empirical equation to describe their water partitioning:

$$\log K_{(o/w)} = 0.229 + 0.2676 \times (n+2) + (-0.00316) \times (2n+6); \text{ for } n=3-7$$

$$\begin{aligned} \log K_{ow} &= 0.229 + 0.2676 \times (n+2) + (-0.00316) \times (2n+6), n=3 \sim 7 \\ &= 1.53(\text{perfluoropentane}, n=3) \\ &= 1.79(\text{perfluorohexane}, n=4) \\ &= 2.05(\text{perfluoroheptane}, n=5) \\ &= 2.31(\text{perfluorooctane}, n=6) \\ &= 2.57(\text{perfluorononane}, n=7) \end{aligned}$$

That corresponds to water solubility (mol/l):

$$\begin{aligned} S &= 1.9 \times 10^{-5} \text{ mol/L or } 3.4 \times 10^{-7} \text{ in mole fraction (perfluoropentane)} \\ &= 1.0 \times 10^{-5} \text{ mol/L or } 1.9 \times 10^{-7} \text{ in mole fraction (perfluorohexane)} \\ &= 5.7 \times 10^{-6} \text{ mol/L or } 1.0 \times 10^{-7} \text{ in mole fraction (perfluoroheptane)} \\ &= 3.1 \times 10^{-6} \text{ mol/L or } 5.6 \times 10^{-8} \text{ in mole fraction (perfluorooctane)} \\ &= 1.7 \times 10^{-6} \text{ mol/L or } 3.1 \times 10^{-8} \text{ in mole fraction (perfluorononane)} \end{aligned}$$

Figure 34: Octanol/water constants calculated after Lyman 1982 and water solubility estimated; taken from [51]

In an EPA-GOV HPV document (no. 201-13244) additional PFC-octanol/water partition constants were calculated using QSAR - quantitative structure–activity relationship (Fig.35). See Yee et al. (2012)[58] for introduction of the QSAR method and Cronin & Schultz 2003[59] for pitfalls of the method.

Test Substance:	C₅-C₁₈ straight chain perfluoroalkanes	
Method:	Quantitative Structure Activity Relationship (QSAR) calculations utilizing US EPA KowWin version 1.66.	
Test Type:	Estimation	
GLP:	No	
Year:	2003	
Results:	Structure	Predicted LogKow
	C5F12	>4.90
	C6F14	>5.86
	C7F16	>6.83
	C8F18	>7.79
	C9F20	>8.76
	C10F22	>9.73
	C11F24	>10.69
	C12F26	>11.66
	C13F28	>12.62
	C14F30	>13.59
	C15F32	>14.56
	C16F34	>15.52
	C17F36	>16.49
	C18F38	>17.46
Test Remarks:	This study utilized a logP value generated under a GLP study of perfluorobutane as a reference value within KOWWIN™ to allow for an adjustment of the calculations for the study compounds. The actual study did not result in a definitive value for perfluorobutane. It only concluded that the logP was >3.93. Hence, the values for the study compounds were assigned “greater than” values.	

Figure 35: Calculated logK for octanol/water of straight chain PFC (from [54] EPA GOV report No. 201-13244)

The molar polar perfluorobenzene and its solubility in water was determined and modeled with several association theory approaches by Schroeder et al. (2011)[53] (Fig.36).

	Experimental (this work)	COSMO-RS	SPARC	EPISuite	ALOGPS
Solubility of C ₆ F ₆ (mol dm ⁻³)	0.00325 ± 0.00003	0.00128	0.00056	0.00736 ^a	0.00118
Henry's law constant, H (Pa m ³ mol ⁻¹)	3465 ^d	8798 ^d	26 200	1380 ^b 272000 ^c	9544 ^d
log K _{OW}	-	2.93	3.83	3.2 ^e	2.33
		3.67 ^f			
		3.72 ^f			
log K _{OC}	-	2.92 ^h	-	3.45 ⁱ	-
				2.20 ^j	

^a WATERNT.

^b HENRYWIN/EPISuite – bond estimation.

^c HENRYWIN/EPISuite – group estimation.

^d From experimental vapor pressure data (considering a liquid vapor pressure of 11 262 Pa, at T = 298.15 K, as derived from the DIPPR database

^e BP-TZVP-COSMO QSPR mix (wet octanol/water).

^f logPOW.prop (QSPR included in COSMOtherm, for BP-SVP-AM1).

^g KOWWIN.

^h log K_{OC}.prop (QSPR included in COSMOtherm, for BP-SVP-AM1).

ⁱ KOCWIN v2.00 MCI (estimate from Molecular Connectivity Index).

^j KOCWIN v2.00 (estimate from recommended log K_{OW} = 2.54).

Figure 36: Perfluorobenzene solubility estimates using various modelling approaches ([53])

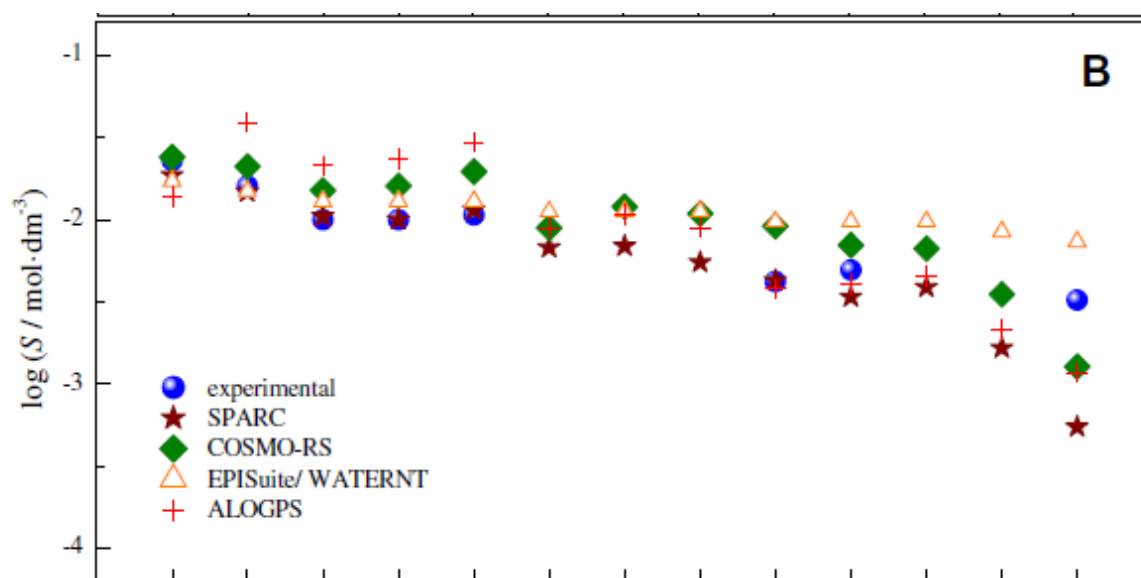


Figure 37: Water solubility of fluorobenzenes (C₆H_(6-y)F_y) calculated and experimentally determined, from left to right fluorination increases, from [53]

In comparison of the modelled data with the experimental derived solubility, there is a good match (Fig.37). This marks a good understanding and an almost complete capture of all relevant interaction parameters in the modelling approach. With higher fluorination, the data diverges over a spread of two log scales which reflects on the difficulty of characterizing these systems.

Ethylbenzene in water		Hexafluorobenzene in water	
<i>T</i> / (K)	$10^{-3} (x \pm \sigma^a)$	<i>T</i> / K	$10^{-3} (x \pm \sigma^a)$
280.25	3.02 ± 0.07	281.46	7.54 ± 0.04
290.09	2.95 ± 0.07	291.36	6.48 ± 0.04
299.90	3.07 ± 0.07	300.97	5.97 ± 0.03
309.71	3.25 ± 0.02	310.82	5.76 ± 0.04
319.65	3.59 ± 0.02	320.51	5.67 ± 0.06
329.89	3.99 ± 0.02	329.77	5.78 ± 0.04
339.80	4.61 ± 0.04	339.76	6.16 ± 0.03

^aStandard deviation

Figure 38: Water solubility of perfluorobenzene vs. ethylbenzene, from [52] Freire et al. (2005)

Freire et al (2005) experimentally determined solubility constants of C₆F₆ in water which is in the order of one magnitude lower compared to the data of Schroeder et al (2011).

FC-43 – Perfluorotributylamine, C₁₂F₂₇N was tabulated for octanol/water partition coefficient as well in an addition to the EPA-GOV report from 2001, no. 201-13244. Experimental data was acquired by the company 3M, one of the biggest organofluorine chemicals producers, in 1981. The corresponding value is $K_{(o/w)} = 557$, equals a rounded $\log K_{(o/w)} = 2.75$ and corresponds in the report to a measured solubility of 0.68mg/l. However, the result is criticized by the EPA-GOV in terms of inconsistent $\log K$ vs. solubility relationship. A value of 1mg/kg of water should have a $\log K_{(o/w)}$ in the order of 5 to 6 instead of 2.75. A measured solubility down to 1ppb is the threshold of the EPA-GOV for experimental accuracy. That corresponds to a $\log K$ of about 9. The EPA-GOV also complains about the vague solubility of the perfluorohexane products. The result is confirmed in an update letter from 2007. Water solubility data was collected for perfluorohexane as well by 3M. The document is an additional document to the above report, no. 201-14684B. Perfluorhexane water solubility was determined in two attempts using NMR and GC methods. Attempt one was using a 50/50 mixture of the PFC and water which was constantly mixed for 16hrs. After 7 days detection of PFCs in the water phase was conducted using NMR. The measured solubility was 33mg/l at 25°C. The second attempt a 50/50 mixture of perfluorhexane and distilled water was in static contact for 16 hrs. Analysis was conducted using FR-NMR. Measured solubility was <5mg/l.

6.4.1. Synopsis

The summary of in literature reported values addresses quite a variation in partition coefficients being determined with various experimental and modeling approaches. The very low solubility is best reflected in the $K_{(o/w)}$ calculations of EPA-GOV/3M which corresponds to ppm to ppt concentrations of PFCs in the water and is reproduced by [1] Oliveira et al. (2007) in the low partitioning of perfluorohexane into the water phase. Perfluorobenzene water partition data which could be measured in the lab is up to 2-3 orders of magnitude higher than the corresponding straight chain perfluoroalkane.

6.5. Detection of PFCs

The detection methods of perfluorocarbons relate back to their high affinity to attract electrons due to the high electronegativity of fluorine. Therefore, using an electron capture detector in combination with a GC is a simple and very effective technique to trace these compounds (see Dietz et al. (1986)[60] for an introduction). An electron capture detector consists of an electron source which emits electrons. The capture of these electrons results in a certain current. If a compound with high affinity to electrons enters the chamber, the current is reduced. This reduction can be measured very accurately. The negative aspect of the method is that it is relatively “blind” and will detect multiple electron capturing compounds. Especially the tremendous variations in halogenated compounds in the atmosphere are encountered as being problematic for the method. Therefore, a much more defined pre-purification method needs to be used in order to reduce any interference in the chromatographic determination of PFCs. Such a method relies on the choice of GC column, desorption temperature program and a clever choice of multi-desorption steps.

Mass spectrometry detection is another detector option and will be discussed later in this chapter. In general, the detection limits and sampling strategies have to be split between atmospheric and soil gas detection. Atmospheric detection was the initial application as researchers recognized increasing pollution levels highlighted in the Montreal and Kyoto protocols on ozone layer depletion and greenhouse gas potential. An immediate atmospheric application was to study atmospheric dispersion models using PFCs (see Watson et al (2007)[61] for an overview). Soil gas detection is an application which was promoted by the CCS business and since then the methodology was optimized in terms of easiness of detection and field based suitability. The two very different environments of PFC samples play a role in the analytical protocol and associated levels of detection (LOD).

Perfluorocarbons are best “captured” with an adsorbent based method. Capillary adsorption tubes (CATS) introduced earlier in this report are the sampling devices which have been found most successful to detect perfluorocarbons. After a certain time of exposure and flow through of air/soil gas mixture, PFCs with other pollutants are adsorbed onto the sorbent which belongs to the class of activated charcoal or resin type coatings. Thermal desorption methods follow subsequently and serve two purposes:

- reduction of background interfering compounds due to a selection of desorption temperatures
- full capture of very low amounts of perfluorocarbons

Low amounts of perfluorocarbons means sensitivity down to parts per quadrillion (ppq) or femtoliter/litre. The detection limits for soil gas and atmosphere differ only slightly and are in the range of ppq to ppt. Highlighted here is the conventional way of detecting PFCs using GC-ECD and a more advanced mass spectrometry method using negatively ion chemical ionization (NICI).

6.5.1. GC-ECD – electron capture detection method

Nazzari et al. (2013)[64] used the most recently applied GC-ECD method to distinguish between the various perfluorocyclopentane and-hexanes. Former application for petroleum reservoir samples and atmospheric sampling was studied by Galdiga et al. (1997)[62] and Lagomarsino et al. (1996)[63].

Atmospheric detection PFCs needs an additional purification step to get rid of chlorofluorocarbons (CFCs) using a Palladium containing catalytic reduction technique.

In general, PFCs were desorbed from the former Amborsorb[®] containing CATS and flushed onto a Florisil column. Using ohmic heating, PFCs were desorbed again and flushed onto a pre-cut column. With a thoroughly tested temperature program, low boiling and high boiling impurities were removed due to the variation in desorption temperatures. The PFCs entered the GC column, a DB-Petro 100 (fused-silica column (100 m × 0.25-mm i.d., 0.5- μ m film thickness, J&W Scientific, Folsom, CA), which here was replaced from a former packed column as the general choice. The co-eluting CFCs were destroyed using the above mentioned catalytic reduction. A multi-purification step, temperature programming with desorption temperatures ranging from 200 to 400 °C and a valve switching protocol, is the method of choice to extract the PFCs efficiently from the adsorbent.

For detailed temperature program and carrier gas flow rates please refer to [63] Lagomarsino et al. (1996).

Galdiga et al. (1997)[62] used a Carbopack column, 6ft long, 1.8” diameter, 0.5 μ m thickness filled with 0.1% SP-1000, 80/100 mesh grain size in combination with a 5 Angstrom molecular sieve column, 2 meters long for the separation of multiple PFCs and SF₆ (molecular sieve).

Nazzarini et al. (2013)[64] used Carbotrap 100 adsorbent tubes for the capture of PFCs out of 2 liters of soil gas flushed through the tubes. They used a two step purification method before injecting onto an Al₂O₃/Na₂SO₄ PLOT column (50 m × 0.32 mm × 8 μ m) supplied from Agilent Technologies (Torino, Italy). The two step process included the Carbotrap desorption process at 330°C for 10 min and a narrow bore Carbotrap/Carbosieve cold trap at -20°C before injecting onto the GC column.

Carbotrap columns were checked with a sequentially connected second adsorption tube for full adsorption verification. The separation of the Nazzarini et al. (2013)[64] reached limits of detection for the PFCs in a range of 0.2 to 3 pg which corresponds to soil gas sample detection limits of 1.3 to 6 fl/l at an signal to noise (S/N) = 3. The method was able to detect perfluoropentane and cyclohexanes. Isomers of perfluorodimethylhexane were not analysed. The full separation of all perfluorodimethylhexane isomers was not successful with TD-GC-ECD. Galdiga et al. (1997)[62] tested for PDMCB, PMCP, PMCH, 1,2 PDMCH and 1,3 PDMCH. Lagomarsino et al. (1996)[63] with a more sophisticated purification and an extra long capillary column was able to reach a sufficient separation of the various dimethylated perfluorocyclohexanes (Fig.39).

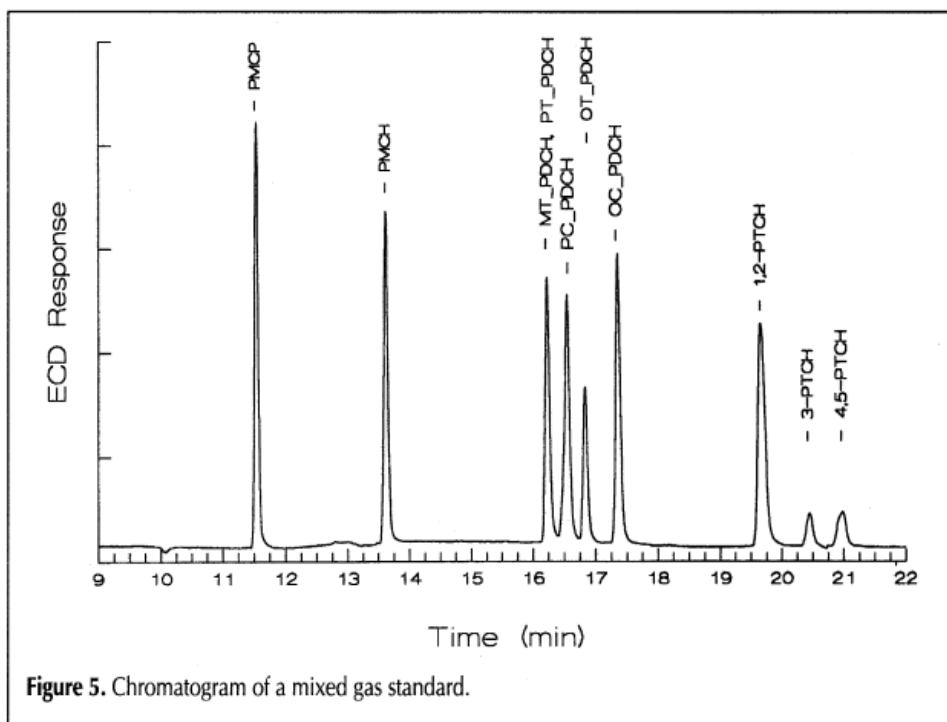


Figure 39: Gas standard used with TD-GC-ECD methodology by [63]

6.5.2. GC-MS - Mass spectrometry detection technique

A better precision but lack of full quantification was achieved by mass spectrometry detection: GC-MS.

The sensitivity to distinguish the PFCs from each other using negative ion chemical ionization mass spectrometry is related to the high molecular weights and the low vapour pressure of the PFCs (Cooke et al 2001[65]). Their quick elution time makes it suitable to generate a stable and indicative high mass ion to be measured.

The combination of cryogenic adsorbent-filled micro traps, thick film coated capillary columns and single ion monitoring mass spectrometry mode makes this technique suitable to detect PFCs in the sub ppq levels (sub fl/l). The microtrap is equipped with a Peltier cooling device and cooled at a temperature of -50°C. It is filled with 10 mg of Carboxen 569, 40-50 mesh (Supelco, Bellafonte, PA) to enrich the PFCs mainly from atmospheric sampling devices. The trap is thermally desorbed at 255°C in 4 s onto the capillary GC column.

Simmonds et al (2002)[66] reported as well on the achievement of chromatographic separation of all six perfluorodimethylcyclohexane isomers using a PLOT column coated with activated carbon. Previous studies like the one by Lagomarsino et al. (1996)[63] were only able to distinguish four out of six isomers.

However, the PLOT column is no longer commercially available. Instead, a gas-liquid wall-coated open tubular (WCOT) CP-Sil 5 CB methyl silicone column (0.32 mm, 100 m, 5-µm film thickness, Varian Inc.) was used by the research group. A typical temperature profile for the GC acquisition consists of an isothermal period at 30 °C followed up by a ramp up at 20°C/min to

150 °C. Carrier gas for the elution is ultragrade helium. For the chemical ionization method, methane is used as ionization gas.

The main advantage of the method is also that halocarbons like chlorofluorocarbons (CFCs) undergo rather dissociation under electron capture unlike the PFCs and therefore are not forming the same high mass molecular anions as the PFCs. The catalytic scrubbing facility can be therefore discarded in this setup and adds to the higher sensitivity of this method. It was highlighted that the system was found to be linear over 5 orders of magnitude with respect to the PFCs compared to the much smaller dynamic range of the ECD method (Cooke et al. 2001[65]).

The most recent study using TD-NICI-MS detection is by Ren et al (2013)[67] . Operating conditions of the Mass spectrometer are at 70eV in negative ionization mode with methane (N55 quality, Air Liquide) as reagent gas with a flow rate of 1.5 mL/min and in either SIM (selected ion monitoring) mode: ion detection at 300, 350 and 400 amu (atomic mass units), or SCAN mode with a range of 50–550 amu. The GC/MS interface and the source temperature were set to 190 °C.

The focusing trap contained about 100mg Carboxen 569 and is used for PFC enrichment. All sampling tubes and the cold trap were conditioned at 260°C for at least 5 h under high-purity helium flow to clean before use. Each CATS sample tube was heated at 250°C for typically 20 min, and adsorbed PFCs were flushed through a 4-port valve onto the cold trap which is held at -30°C. The second desorption step was done with an instant heating step up to 260°C and a subsequent desorption in about 3 seconds onto the GC column. An Al₂O₃-PLOT-S column was selected for trace analysis of PFCs, because of its good separation capability and its commercial availability. This column could separate out PECH from PDCH occurrences very effectively. The characteristics of the PFC are taken from Ren et al. (2013)[67] :

Table 5: Characteristics of TD-GC-NICI detection of PFCs (after[67])

PFC names	Acronyms	Molecular formula	Molecular weight	Melting point (°C)	Boiling point (°C)	Density (g mL ⁻¹ at 25 °C)	Purity (%) (F ₂ Chemicals)
Perfluorodimethylcyclobutane	PDCB	C ₆ F ₁₂	300	-32.0	45.0	1.67	
Perfluoromethylpentane	PMCP	C ₆ F ₁₂	300	-50.0	48.0	1.707	94.7
Perfluoromethylcyclohexane	PMCH	C ₇ F ₁₄	350	-37.0	76.0	1.788	95.3
Perfluoro- <i>o</i> -dimethylcyclohexane	<i>o</i> -PDCH ^a	C ₈ F ₁₆	400	-22.0	102.0	1.828	88.8
Perfluoro- <i>m</i> -dimethylcyclohexane	<i>m</i> -PDCH ^b	C ₈ F ₁₆	400	-70.0	102.0	1.828	96.6
Perfluoro- <i>p</i> -dimethylcyclohexane	<i>p</i> -PDCH ^c	C ₈ F ₁₆	400	<-80.0	102.0	1.828	96.8
Perfluoroethylcyclohexane	PECH	C ₈ F ₁₆	400	<-80.0	101.7	1.829	93.7

^a The cis and trans isomers of *o*-PDCH are *oc*- and *ot*-PDCH
^b The cis and trans isomers of *m*-PDCH are *mc*- and *mt*-PDCH
^c The cis and trans isomers of *p*-PDCH are *pc*- and *pt*-PDCH

A characteristic single ion monitoring trace chromatogram of PFC detection given in Table 5 is shown in Figure 40.

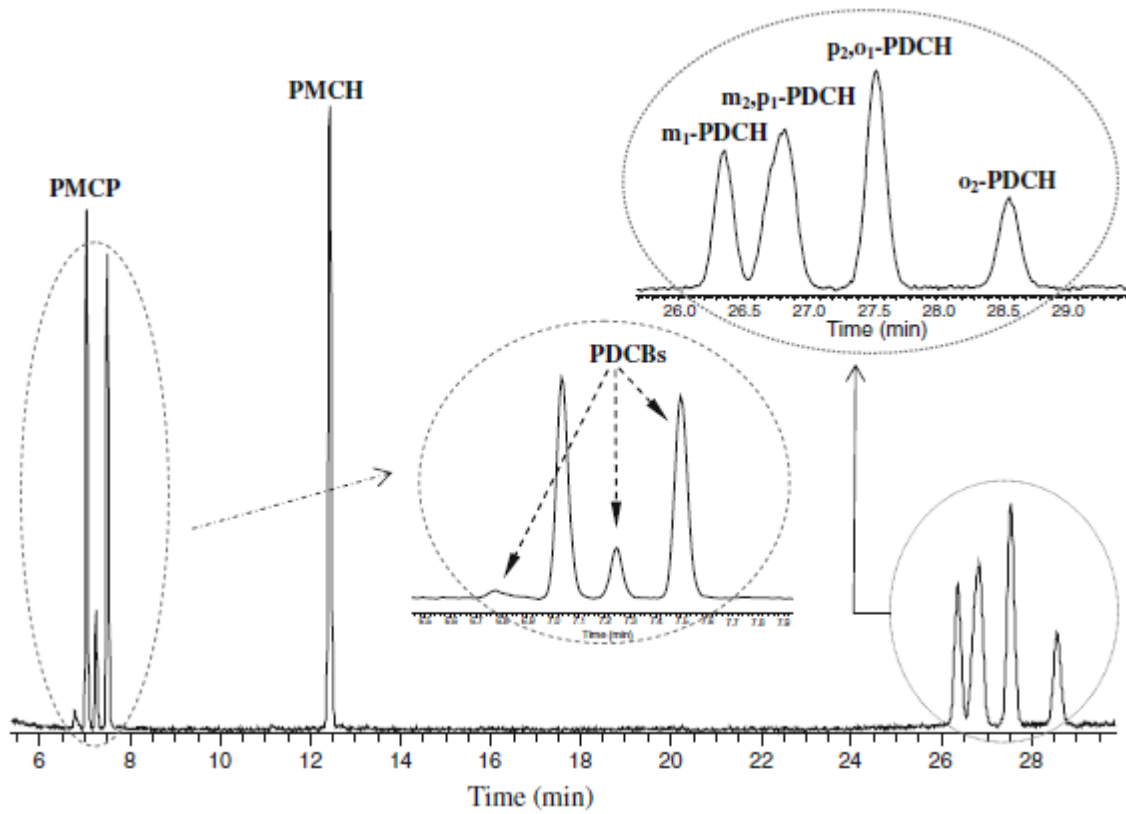


Figure 40: Conceptual chromatogram with elution time of major PFCs reported in [67]

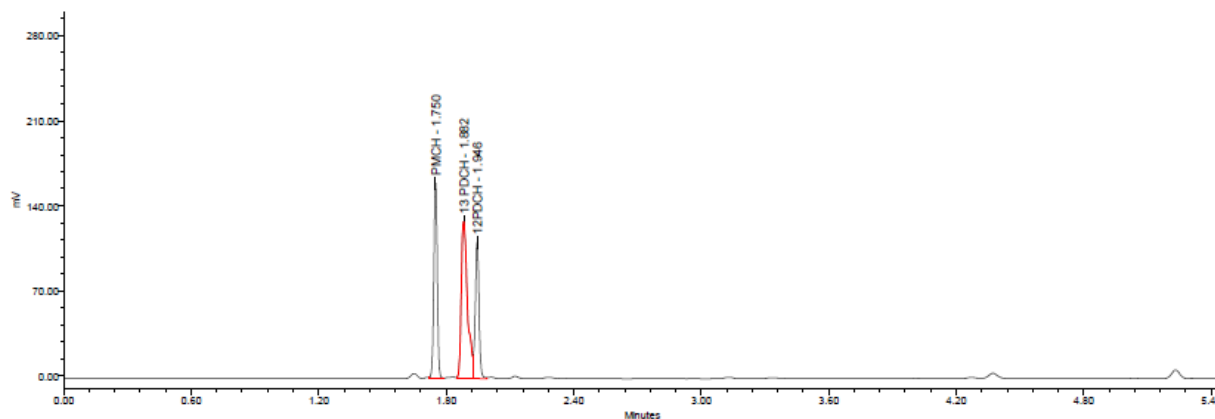


Figure 41: Corresponding GC-ECD trace from CSIRO experiments – first PFC batch

In Fig.41 the three perfluorohexanes with different methylation are detected in close proximity to each other. The not complete separation of 1,3 PDCH and 1,2 PDCH is here compensated with a dominated areal contribution towards the 1,3 PDCH which indicated a more skewed, non symmetrical peak pattern. This needs to be taken into account in the calibration. Different peak height is also reflecting the electron capture affinity of the various compounds which is included in the quantification.

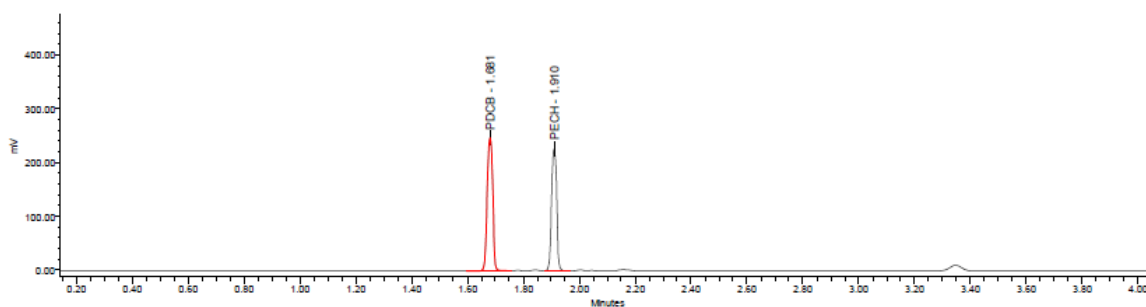


Figure 42: Corresponding GC-ECD trace from CSIRO experiments – second lower boiling PFC mix

A much better split of the lower boiling PFCs used so far in the CSIRO experiments are demonstrated here with PDCB and PECH. The two compounds are used in combination and do not suffer from interferences of each other. Electron capture affinity is similar for both compounds demonstrated by similar peak heights.

7. Laboratory study to understand subsurface behavior of Perfluorocarbon Tracers

7.1. Laboratory setup of batch and slim tube experiments

The laboratory setup of batch and slim tube experiments needed to accommodate for an effective extraction technique of the PFCs from the liquids in which they were dissolved. Second analytical difficulty is related to do this step in-situ and online in relation to the slim tube efforts. Therefore, one needed to accommodate for back pressure regulation and sampling using an autosampler device.

The setup contains a pre-conditioning of the fluids and loading procedure to equilibrate the fluids prior to injection into the batch reactor. Syringe pumps (ISCO, up to 3000 psi, incl. Pressure relief valve and pressure gauge) are used to fill and pressurize the reactor as well as providing the opportunity to mix the CO₂ and aqueous fluids. All valves beyond the use of CO₂ are made out of SuperDuplex. The aqueous phase is sampled from the bottom of the reactor due to its higher density. Sampling can be done under the reactor's pressure conditions. Pressure release to ambient conditions is done once the sample is connected to the CATs tube and liquid/gas separation took place. A carrier gas flow of pure nitrogen is flushed through the CATS tube and remaining PFC will be adsorbed. Here also a suite of test experiments have been conducted to proof the quantitative desorption of the tracer onto the Carboxen 1000 loaded column using a sequential setup of two CATs. The second one is measured to verify full adsorption onto the first column.

7.1.1. Loading procedure

2.5 µL of a 1:1000 dilution of PFC mixture in hexane was added with 1200 mL of water into a 1.65 L pressure vessel. The vessel is heated to the required temperature and pressurized with CO₂ to the required pressure (CO₂ was added via another pressure vessel with a piston installed and operated with a high pressure syringe pump). To achieve equilibrium conditions, a high-pressure circulation pump (Eldex B-100-S-2 CE) was operated over night at full speed. The supercritical CO₂ fluids from the top of the vessel were circulated into water phase at the bottom of the vessel.

7.1.2. Sampling procedures

A glass tube containing approximately 500 mg of a 50:50 mixture of Carbopack B/Carboxen 1000 is used. The sorbent material in the glass tubes is recycled after quantitative desorption at 350 °C. Repeated runs of the same glass tube on the GC show that there is no residual material left on the sorbent after initial desorption. Ultra-Torr fittings from Swagelok were used to connect the glass tube to the low pressure side of the pressure regulator. Sampled volume is passed through the Carbopack tube and PFC amounts are adsorbed onto the Carboxen1000.

7.1.3. Gas Phase sampling

A 2 mL volume of supercritical CO₂ from the top of the pressure vessel is de-pressurized using a 2-stage pressure reducing regulator (to less than 0.1 MPa) over approximately 5 minutes. After de-pressurizing the sample loop, nitrogen gas is passed through the sample loop to ensure that any residual PFCs are captured with the packed glass tube.

7.1.4. Water phase sampling

A volume of water from the bottom of the pressure vessel is de-pressurized using a 2-stage pressure reducing regulator (to less than 0.1 MPa). A water trap is used to prevent direct contact of the water with the glass tube. After de-pressurizing the sample loop, nitrogen gas is passed through the sample loop to ensure that any residual PFCs are captured with the packed glass tube.

7.2. Slim tube experimental setup description

The slim tube experimental setup contains a fluid mixing setup which is able to provide two different fluids to the slim tube. Here, this is mainly the supercritical CO₂ phase and an aqueous phase which can contain various amounts of NaCl wt%. Maximum concentration is 20 wt% NaCl (200000ppm).

The compression chambers are pressurizing the various fluids again using syringe pumps (ISCO). The tracer is added in a sampling loop device using a split of a n-hexane and PFC containing solution (1 ul out of 1000 fold dilution with n-hexane).

In the beginning, the setup was tested with a slim tube of 1/2" tubing with a wall thickness of 0.049" and a length of 6 meters. The slim tube is equipped with two fritted filters as end caps.

The tubing was slowly packed with sand (Aldrich, 50-70 mesh, 560 mL) in a vertical arrangement. After complete filling with sand, the tubing was bent into a helix approximately 50 cm in diameter. The previously determined pore volume under ambient conditions with water was approximately 40 to 41%. The tubing ends were then connected to the ends of the system and placed into an oven and heated to 80°C. The inlet side fluids pass through a flow/density meter (vertical arrangement with fluids flowing upwards) immediately after the tracer injection sampling manifold and before entering the slim tube. On the outlet side, the slim tube fluids enter another flow/density meter (vertical arrangement with fluids flowing upwards) immediately after exiting the oven and before the back pressure regulator. The tubing was then filled with CO₂ and pressurized to 214bar and slim tube flow was commenced at 2mL/min using a high pressure syringe pump with a back pressure regulator at the tubing end maintaining column pressure (variation of less than 1.5 % in pressure over the entire run, no pulsation observed). The back pressure regulator is a needle-type regulator and was set to 210bar. The inlet column pressure was approximately 207bar throughout the run.

After slim tube was conditioned with scCO₂ at 2ml/min flow rate, the slim tube was then prepared with filling of water/brine which is the displaced fluid phase in an original experiment. Later on, due to pressure fluctuations the diameter was narrowed to 1/4" tubing and extended onto 12 meters. General flow rate in the experiments were 0.15ml/min.

7.2.1. Sampling procedure

Intervals of gas samples eluting from the back pressure regulator connected to the slim tube were de-pressurized to low pressure using a two-stage pressure regulator and passed through the packed glass tube. A water trap is used here as well in line with the flow to ensure that no water enters the glass tube.

7.2.2. GC Sample Injection Procedure Using Packed Glass Tube

A Varian CP-3800 GC is used with a ECD detector with a WCOT CP-Sil CB5 column. The packed glass tube is attached to a EST Encon Concentrator. The packed glass tube is heated to 350 °C and desorbed species are concentrated onto a Vocarb 3000 trap (Carbopack B, Carboxen 1000 and Carboxen 1001, Supelco Cat. No. 24920-U). Repeated analysis of the same packed glass tube shows that this desorption process is quantitative. EST Encon Concentration is used to introduce PFC samples in a concentrated form onto the column for analysis.

Sampling of the tracers was conducted using an autosampler, purge gas and CATS tubes.

Volumetrics of the 1/2 " slim tube determined a total volume of 185 to 195 ml which is roughly a 30% open pore volume in a 560ml total volume slim tube.

For the 1/4" tubing, 12 meters, a total volume of 241ml and a total pore volume of around 80ml was determined which resembles a porosity of around 30%. These setup conditions were verified to be able to limit pressure fluctuations and an ideal immiscible displacement of the water/brine with scCO₂.

8. Batch reactor experimental results

The first batch reactor results generated in June-August 2013 need to be explained in the light of testing the procedure of equilibrating the vessel fluid mixture. Having in mind the only theoretically robust determined dissolution/partitioning behavior of cyclic and straight chain PFCs in water/brine in the literature, the attempt to sample PFCs in the water phase is a challenge. For long term sequestration projects, even an incremental fraction of PFCs scavenged into the water phase would be important due to the very large amounts of CO₂ (up to 20 million tons over 25 years) injected into the reservoir. Losses of the tracer to the stationary water wetted matrix plays a crucial role also for designing the appropriate amounts in the MMV program..

During the the initial design of the experiments in the batch reactor, a tracer partitioning value was determined by CSIRO for the following intermediate to high boiling PFC compounds (see Table 6 below):

- Perfluorooctane (PO)
- Perfluoromethylhexane (PMCH)
- Perfluorodimethylbutane (PDCB)
- 1,3 Perfluorodimethylhexane (1,3 PDCH)

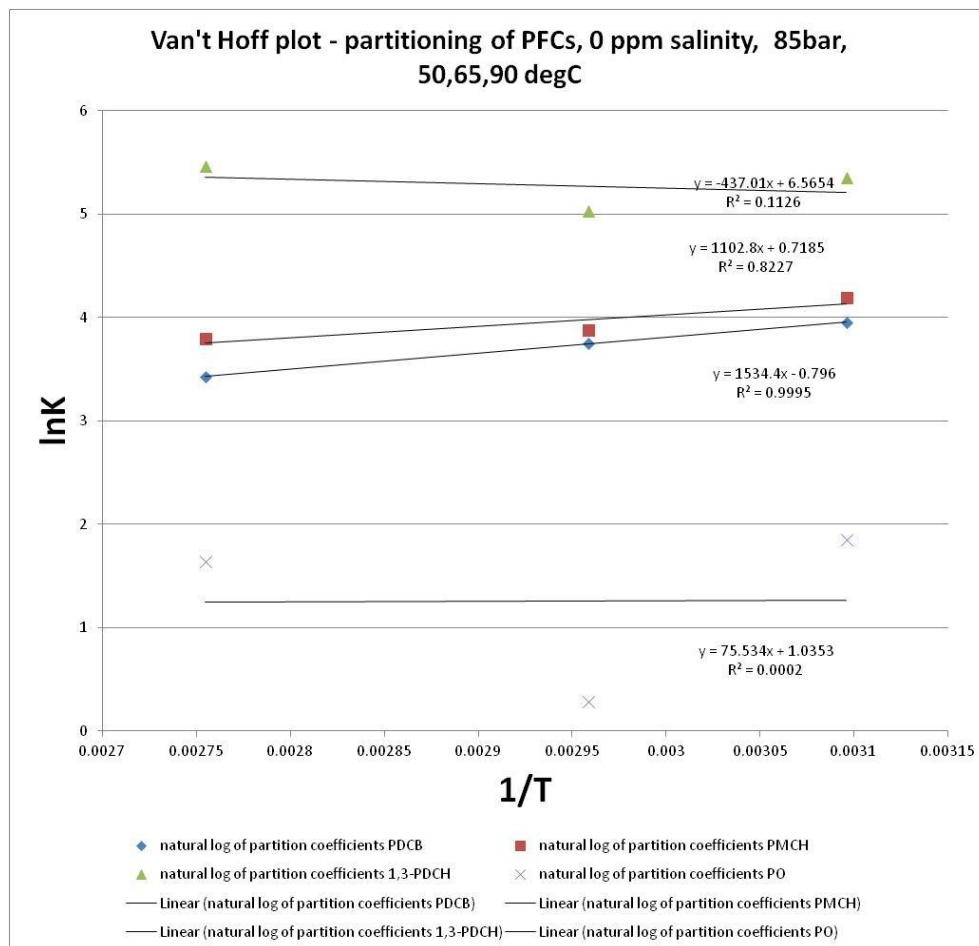


Figure 43: Partitioning of PFCs into the water/brine phase – van't Hoff plot

Table 6: Data acquired for scCO₂/H₂O partitioning of various PFC compounds (first attempt)

#	Sample Name	Time & Date	Measured concentrations of tracer compounds				density corrected mole fraction basis partition coefficients				natural log of partition coefficients				GC area counts					
			PDCB	PMCH	1,3-PDCH	PO	abs T[K]	PDCB	PMCH	1,3-PDCH	PO	1/T[K]	PDCB	PMCH	1,3-PDCH	PO	PDCB	PMCH	1,3-PDCH	PO
1	CO ₂ 15min 18/6/13 split 100	18/06/2013 12:51:18 PM	1	1	1	1	323	51.961724	66.21933	212.0254	6.369673	0.003096	3.950507	4.192972	5.356706	1.851548	739536	664068	1370422	394
2	H ₂ O 1 15min 18/6/13 split 100	18/06/2013 3:02:00 PM	0.187379	0.147035	0.045922	1.528579											138574	97641	62932	404
3	CO ₂ 1 15min 19/6/13 split 100	19/06/2013 2:32:24 PM	1	1	1	1	338	42.549599	48.44378	153.0565	1.328097	0.002959	3.75067	3.880404	5.030807	0.283747	978749	795337	1641813	406
4	H ₂ O 1 15min 19/6/13 split 100	19/06/2013 3:50:50 PM	0.102351	0.089898	0.028454	3.279124											100176	71499	46715	391
5	CO ₂ 15min 20/6/13 split 100	20/06/2013 2:41:52 PM	1	1	1	1	363	30.826245	44.57334	234.8137	5.135128	0.002755	3.428366	3.797136	5.458793	1.636105	940143	827693	1691893	375
6	H ₂ O 15min 20/6/13 split 100	20/06/2013 3:21:03 PM	0.12884	0.089104	0.016914	0.77343											121128	73751	28617	404

$K_{(c/w)}$ partition coefficients so far were in between $K_{(c/w)} = 1.4$ to 250 for the corresponding perfluorocarbons (Table 6). The van't Hoff plot describes the temperature dependence of the enthalpy of mixing and is a good quality control for measured data as pointed out before (Fig.43).

Reported values did not match expected differences between the cyclic and the straight chain PFCs with lower $K_{(c/w)}$ partition coefficients for the cyclic compounds. Within the cyclic compounds, the lower boiling PDCB also was expected to partition more into the water phase than the PDCH one, e.g. having a lower partition coefficient, because of its lower molecular weight and its more compact conformation. The lower total amount of “fluorination”, i.e. carbon vs. fluorine content, is less compared to the high boiling PFCs.

Comparable organic compound partition coefficients for CO₂/water systems were reported by Timko et al. (2004) for 80 bars and 50 °C. For comparison, straight chain alkanes have partition coefficients in between 4900 +/- 600 for the cyclohexane and 9000 +/- 3000 for the straight chain hexane. PFCs are expected to report even higher $K_{(c/w)}$ partition coefficients in the range of 10⁴ to 10⁶ according to its low Hildebrandt parameters. Therefore, the initial data was not trusted and the reason for this observation was investigated.

The result which was agreed on was that the erroneous data may be due to the injection approach. The data shown in Table 6 are based on a sequential injection of the PFC tracer, and did not include prior full dispersion within the supercritical CO₂ phase. The subsequent result of this separate injection of the two fluids affected their behavior in the multiphase fluid environment. PFCs likely formed a separate phase and due to the density contrast was not able to be fully dispersed back in the scCO₂. As a consequence, the PFC fluid phase was sampled together with the water phase as it would attach at the bottom of the reactor or simply sink to the bottom of the reactor.

As partition coefficients were discovered to be much higher between CO₂ and the brine phase (exceeding 10⁵), former lower partitioning coefficients in Table 6 were discarded. Currently, a pre-mixing of the PFCs into the scCO₂ is used prior to the equilibrating procedure of the scCO₂ with water/brine. A good peak representation for the PFC in supercritical CO₂ are reported as predicted, but no peaks represented the PFC in the water phase. Subsequently, the split ratio was increased to a 20:1 split for the water phase and a 500:1 split ratio for the CO₂ phase to increase the detection of traces of PFCs in the water phase. Sample loop size for the water was increased from 2mL to 150 mL in an attempt to measure PFCs in the water phase. But the partitioning could not be determined. To ensure that the detection and sample transfer to the GC happens without heavy losses, it was recommended to use perfluorobenzene, an aromatic PFC, which has three orders of magnitude higher water solubility and which can be compared to benchmark values highlighted in chapter 6.4. CSIRO was able to detect the perfluorobenzene in measureable amounts. Partition coefficients are currently being evaluated for comparison with existing literature values.

9. Slim tube experimental results

In classic applications in the oil industry, slim tube apparatus have been used to study miscible displacement for EOR purposes. Minimum miscible pressure including dispersion effects is determined in such experiments as an important parameter to study phase behaviour in miscible gas injection EOR.

However, a well characterized slim tube experiment can also be used for immiscible fluid displacement to focus on the interactions of solutes within the matrix. In that sense, slim tube experiments are regarded to mimic transport behavior and interactions of solutes with the porous media. Here, PFC tracers dissolved in scCO₂ or mixed in subcritical CO₂ conditions interact with various fluids and solid matrices. The different interactions which are governed by surface chemistry and wettability of the solid surfaces can influence travel times of the various dissolved components in the parent fluid. The retention and/or scavenging/trapping behavior of sorbates vs. different adsorbents (i.e. organic solids, clays, quartz, feldspars, and carbonate minerals) are of special interest. Adsorption can be subdivided into surface complex formation, i.e. chemical bonding to surface structures, electrostatic interactions and hydrophobic adsorption. Hydrophobic compounds like organics and PFCs are repelled by water, and therefore surface interaction is not solely governed by surface affinity but also on solution energies.

The retention of the tracer in comparison to its parent solvent and or other solvents in multiphase displacements is one desired outcome.

The total recovery of the tracer in comparison to different fluid saturations in the slim tube is the second important parameter determined in these experiments.

The proven very low water solubility of the PFC tracers and their very low surface tension indicates a strong potential to interact with the matrices and wet especially free organic surfaces.

Various matrices have been selected in order to reflect tracer transport properties over a wide range of potential lithologies. The experiments started with synthetic glass beads, sintered quartz and admixtures of clays (up to 5 wt.%). Clay admixtures to quartz sand have been studied before by Dugstad et al. (1993)[4]. However, instead of using supercritical CO₂, methane was used in Dugstad's experiments. His group reported on tracer retentions wrt. methane gas using triated methane as ideal co-injected tracer. No densitometers were used to determine breakthrough in such experiments. A potential threat of PFCs to be fully scavenged and extracted from the parent CO₂ phase by organic matrices is of major concern in the ultimate applicability of PFCs in the subsurface. That links back to the general way PFCs are detected using activated charcoal matrices.

9.1. GC response curves for PFC concentration ranges

To be able to measure quantitatively the tracer retentions and total recovery, fully quantified mass balances are necessary. To derive such mass balances, a proper detection response vs. concentration of the compound needs to be calibrated. The detection of PFCs is done via offline GC-ECD measurements. Below is the summary of the GC-ECD responses of the various PFCs used to calibrate the GC-ECD detection. Reported are μl of PFC injected onto the GC directly vs. their response as counts. The data has very good RSQ values in between 0.95 to 0.99 over a concentration interval which resembles the ranges of reported PFCs in the experiments (Fig.44). However, above 1 μl injected PFC, the linearity seems to be less prominent and at 3 μl injected

volume, the non linearity especially for the 1,2 PDCH is apparent (Fig.45). To link the calibration curve to the slim tube experiment, an injected volume of 2 ul of PFCs added in the slim tube experiments is initially out of calibration range. However, the volumes sampled at the outlet of the slim tube are always in the range of an equivalent of 0.2 to 0.5 ul of PFC.

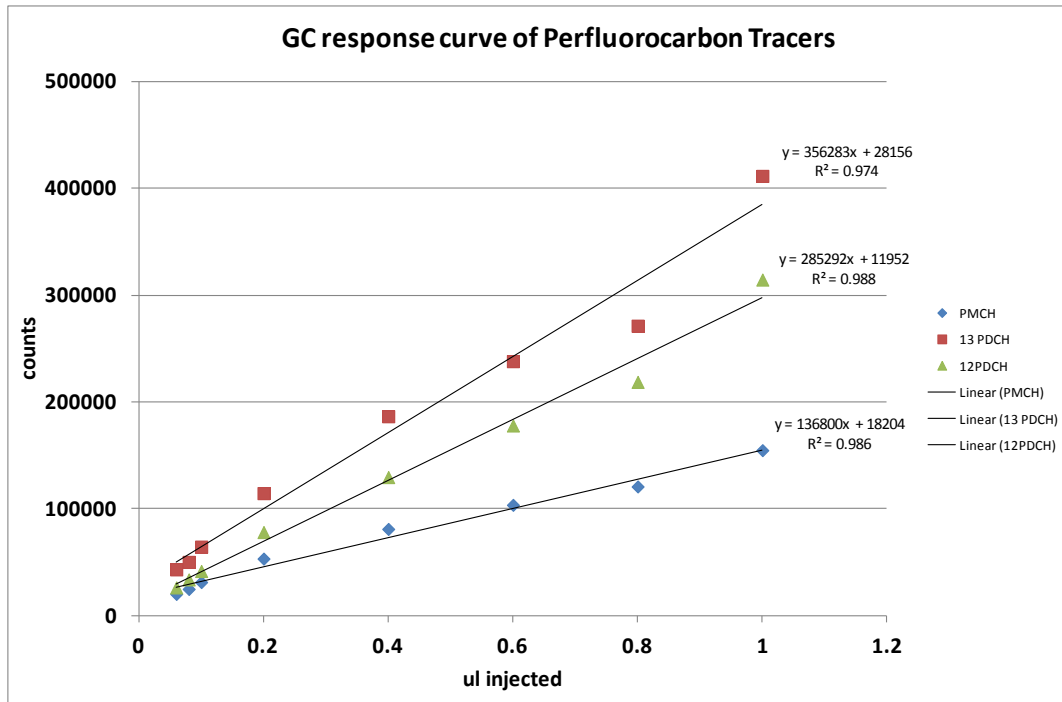


Figure 44: GC-desorption method related response of PFCs used in the experiments in a linear interval

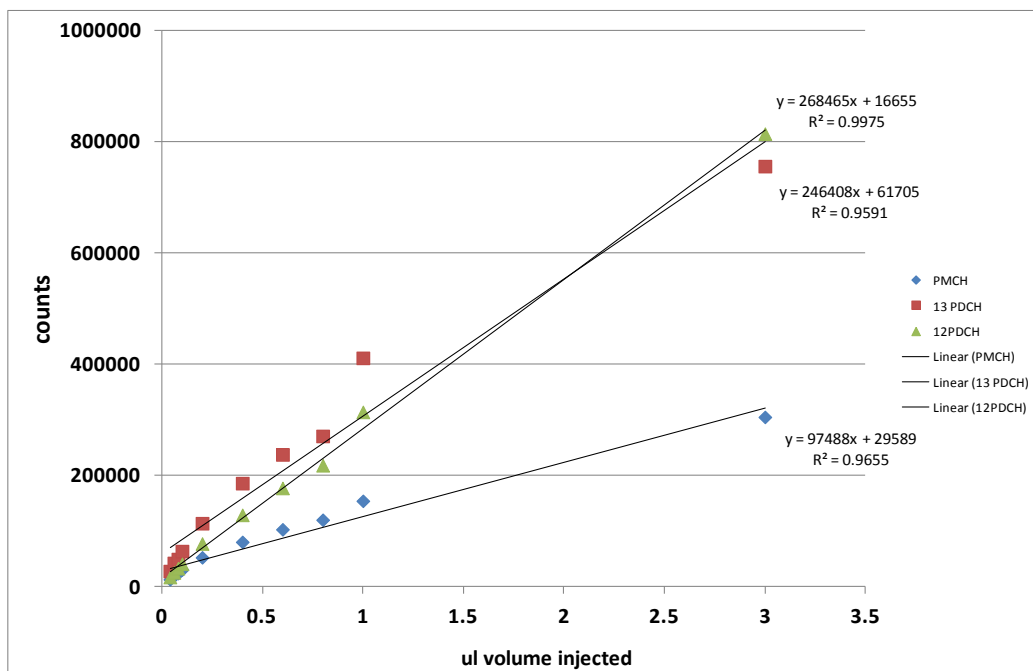


Figure 45: GC-desorption method related response of PFCs used in the experiments in a linear interval

The Table 7 highlights the response and concentration data visualized in Fig. 44 and 45. The concentration interval of interest, is indicated as injected pure PFC tracer liquid volume and converted according to the 1:500 split ratio.

Table 7: Summary of GC response calibration curves for multiple PFCs in a concentration range from 0.08 to 6 nl

vol injected[ul]	split	total PFC vol[nl]	amount	SampleName	Area counts		
					PMCH	13 PDCH	12PDCH
0.04	500	0.08	0.04	0.04uL358PMCH1312split500 6/12/2013	13725	28458	17737
0.06	500	0.12	0.06	0.06uL358PMCH1312split500 6/12/2013	20046	43059	26139
0.08	500	0.16	0.08	0.08uL358PMCH1312split500 6/12/2013	24700	50052	33640
0.1	500	0.2	0.1	0.1uL358PMCH1312split500 6/12/2013	31138	64346	41527
0.2	500	0.4	0.2	0.2uL358PMCH1312split500 6/12/2013	53133	114465	78004
0.4	500	0.8	0.4	0.4uL358PMCH1312split500 6/12/2013	80916	186519	129513
0.6	500	1.2	0.6	0.6uL358PMCH1312split500 6/12/2013	103494	238110	177869
0.8	500	1.6	0.8	0.8uL358PMCH1312split500 6/12/2013	120718	271350	218692
1	500	2	1	1uL358PMCH1312split500 6/12/2013	154722	411706	314580
3	500	6	3	3uL358PMCH1312split500 6/12/2013	305519	756428	814804
				full range RSQ value	0.965494	0.959131	0.997466
				0.06-1ul RSQ value	0.986048	0.974036	0.988047

During the first phase of the slim tube experiments, the focus was on sintered quartz and sandstone matrices packed in the slim tube. The sandstone matrix contained certain amounts of clays/feldspars. The influence of temperature, pressure, salinity and different matrices were investigated, as summarized in Table 8, to determine its dependency on the partitioning of PFC in the studied systems.

Table 8: Scheduled slim tube experiments under supercritical CO₂ conditions

No	Rock	Tracers	Temperature	Pressure	Salinity
1	Sandstone/silica	PB, PCB	80 °C	20.7 MPa	0 ppm
2	Sandstone/silica	PB, PCB	80 °C	20.7 MPa	100000 ppm
3	Sandstone/silica	PB, PCB	80 °C	20.7 MPa	300000 ppm
4	Sandstone/silica	PECH, PMEP, PH, PMCP, 1,4-PDCH	80 °C	20.7 MPa	0 ppm
5	Sandstone/silica	PECH, PMEP, PH, PMCP, 1,4-PDCH	80 °C	20.7 MPa	100000 ppm
6	Sandstone/silica	PECH, PMEP, PH, PMCP, 1,4-PDCH	80 °C	20.7 MPa	300000 ppm
7	Sandstone/silica	PMCH, 1,3-PDCH, PDCB, PO, 1,2-PDCH	80 °C	20.7 MPa	0 ppm
8	Sandstone/silica	PMCH, 1,3-PDCH, PDCB, PO, 1,2-PDCH	80 °C	20.7 MPa	100000 ppm
9	Sandstone/silica	PMCH, 1,3-PDCH, PDCB, PO, 1,2-PDCH	80 °C	20.7 MPa	300000 ppm
10	Sandstone/silica	PB, PCB	65 °C	12 MPa	0 ppm
11	Sandstone/silica	PB, PCB	65 °C	12 MPa	100000 ppm
12	Sandstone/silica	PB, PCB	65 °C	12 MPa	300000 ppm
13	Sandstone/silica	PECH, PMEP, PH, PMCP, 1,4-PDCH	65 °C	12 MPa	0 ppm
14	Sandstone/silica	PECH, PMEP, PH, PMCP, 1,4-PDCH	65 °C	12 MPa	100000 ppm
15	Sandstone/silica	PECH, PMEP, PH, PMCP, 1,4-PDCH	65 °C	12 MPa	300000 ppm
16	Sandstone/silica	PMCH, 1,3-PDCH, PDCB, PO, 1,2-PDCH	65 °C	12 MPa	0 ppm
17	Sandstone/silica	PMCH, 1,3-PDCH, PDCB, PO, 1,2-PDCH	65 °C	12 MPa	100000 ppm
18	Sandstone/silica	PMCH, 1,3-PDCH, PDCB, PO, 1,2-PDCH	65 °C	12 MPa	300000 ppm
19	Coal	PB, PCB	80 °C	20.7 MPa	0 ppm
20	Coal	PB, PCB	80 °C	20.7 MPa	100000 ppm
21	Coal	PB, PCB	80 °C	20.7 MPa	300000 ppm
22	Coal	PECH, PMEP, PH, PMCP, 1,4-PDCH	80 °C	20.7 MPa	0 ppm
23	Coal	PECH, PMEP, PH, PMCP, 1,4-PDCH	80 °C	20.7 MPa	100000 ppm
24	Coal	PECH, PMEP, PH, PMCP, 1,4-PDCH	80 °C	20.7 MPa	300000 ppm
25	Coal	PMCH, 1,3-PDCH, PDCB, PO, 1,2-PDCH	80 °C	20.7 MPa	0 ppm
26	Coal	PMCH, 1,3-PDCH, PDCB, PO, 1,2-PDCH	80 °C	20.7 MPa	100000 ppm
27	Coal	PMCH, 1,3-PDCH, PDCB, PO, 1,2-PDCH	80 °C	20.7 MPa	300000 ppm
28	Sandstone	PB, PCB	80 °C	20.7 MPa	0 ppm
29	Sandstone	PB, PCB	80 °C	20.7 MPa	100000 ppm
30	Sandstone	PB, PCB	80 °C	20.7 MPa	300000 ppm
31	Sandstone	PECH, PMEP, PH, PMCP, 1,4-PDCH	80 °C	20.7 MPa	0 ppm
32	Sandstone	PECH, PMEP, PH, PMCP, 1,4-PDCH	80 °C	20.7 MPa	100000 ppm
33	Sandstone	PECH, PMEP, PH, PMCP, 1,4-PDCH	80 °C	20.7 MPa	300000 ppm
34	Sandstone	PMCH, 1,3-PDCH, PDCB, PO, 1,2-PDCH	80 °C	20.7 MPa	0 ppm
35	Sandstone	PMCH, 1,3-PDCH, PDCB, PO, 1,2-PDCH	80 °C	20.7 MPa	100000 ppm
36	Sandstone	PMCH, 1,3-PDCH, PDCB, PO, 1,2-PDCH	80 °C	20.7 MPa	300000 ppm
37	Sandstone	PB, PCB	65 °C	12 MPa	0 ppm
38	Sandstone	PB, PCB	65 °C	12 MPa	100000 ppm
39	Sandstone	PB, PCB	65 °C	12 MPa	300000 ppm
40	Sandstone	PECH, PMEP, PH, PMCP, 1,4-PDCH	65 °C	12 MPa	0 ppm
41	Sandstone	PECH, PMEP, PH, PMCP, 1,4-PDCH	65 °C	12 MPa	100000 ppm
42	Sandstone	PECH, PMEP, PH, PMCP, 1,4-PDCH	65 °C	12 MPa	300000 ppm
43	Sandstone	PMCH, 1,3-PDCH, PDCB, PO, 1,2-PDCH	65 °C	12 MPa	0 ppm
44	Sandstone	PMCH, 1,3-PDCH, PDCB, PO, 1,2-PDCH	65 °C	12 MPa	100000 ppm
45	Sandstone	PMCH, 1,3-PDCH, PDCB, PO, 1,2-PDCH	65 °C	12 MPa	300000 ppm
46	carbonate	PB, PCB	80 °C	20.7 MPa	0 ppm
47	carbonate	PB, PCB	80 °C	20.7 MPa	100000 ppm
48	carbonate	PB, PCB	80 °C	20.7 MPa	300000 ppm
49	carbonate	PECH, PMEP, PH, PMCP, 1,4-PDCH	80 °C	20.7 MPa	0 ppm
50	carbonate	PECH, PMEP, PH, PMCP, 1,4-PDCH	80 °C	20.7 MPa	100000 ppm
51	carbonate	PECH, PMEP, PH, PMCP, 1,4-PDCH	80 °C	20.7 MPa	300000 ppm

During execution of the various experiments, adjustments to the pressure, temperature and salinity conditions and PFC mixes needed to be made. The salinity range was reduced due to

technical difficulties regarding clogging and corrosion. Salinity was reduced from initially 300000 ppm to a maximum of 200g NaCl/kg H₂O. Tracer mixes first focus on the medium to high boiling PFC mixes. The straight chain perfluoroalkanes – perfluorohexane and –octane were excluded in the runs due to their limit of detection in the GC-ECD compared to their cyclic counterparts.

9.2. Retention behavior – scCO₂ vs. water/brine

The retention behavior of scCO₂ spiked with perfluorocarbon tracer (1ul of PFC in 1ml hexane sample loop corresponding to a 1:1000 split ratio) has been studied for pure silica matrix at 65 °C and 12 MPa with changing salinity conditions at 0 ppm, 100000ppm and 200000 ppm. The two tracer mixes included perfluoroethylcyclohexane, perfluorodimethylcyclobutane (Mix1) and 1, 2 dimethylcyclohexane, 1,3 dimethylcyclohexane and methylcyclohexane (Mix2).

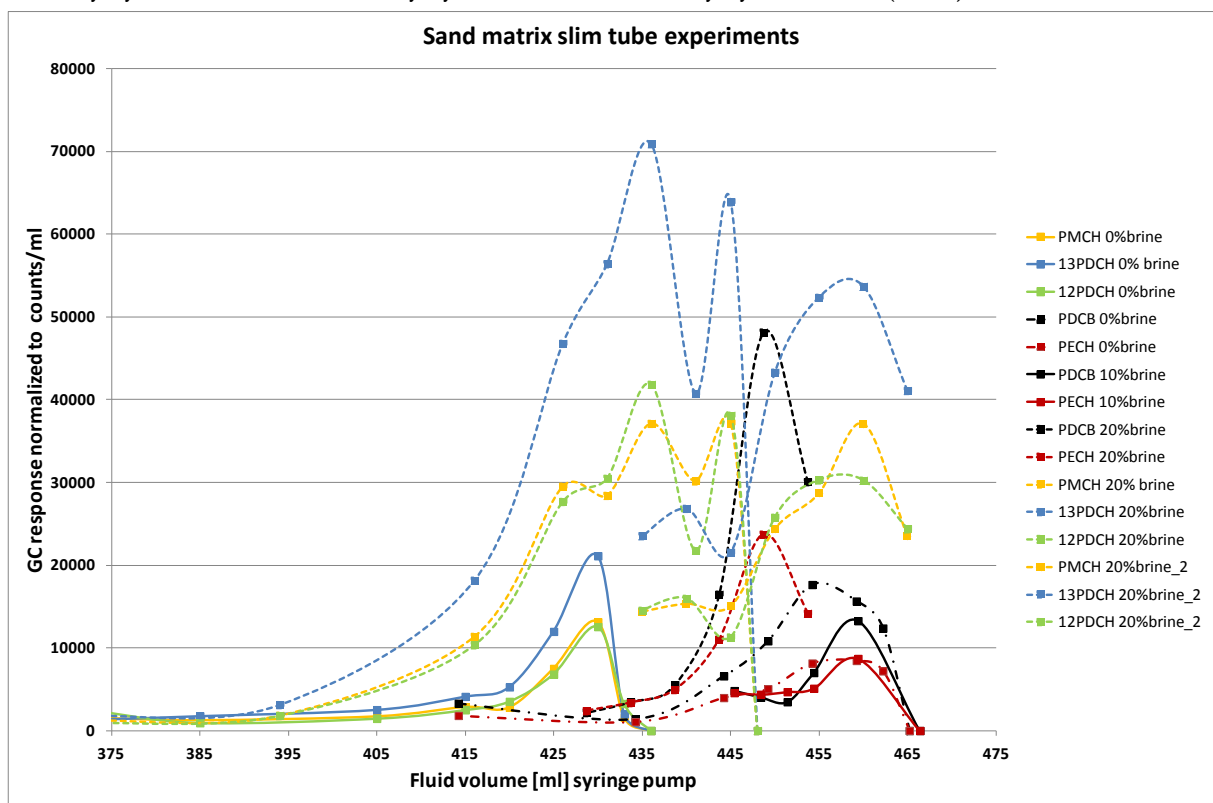


Figure 46: Summary plot of tracer response from all experiments listed in Table 8 except 10% brine of PMCH and PDCH; focus is on the variation regarding the different PFC tracer

The response curves have to be interpreted from right to left in Fig. 46 and onwards. Sample acquisition was linked to CO₂ breakthrough indicated by densitometer measurements. The summary tracer response plot is given in Fig.46. The two runs at 20% brine conditions have been both marked with stippled lines for the Mix2. The plot in Fig. 46 indicates a reasonable good fit on the capture of the various PFC tracers during water displacement by scCO₂ which enables to differentiate their different retention and response behaviours. The validity of the data is indicated by the volume of CO₂ displacing the water/brine (i.e. equivalent of CO₂ volume left in the syringe pump reservoir) ranging from 465ml down to 385 ml and the response of the tracers

highlighted in the peak shape. The peak shape of the tracer response in the slim tube experiments resembles a tailed Gaussian type with various modes ranging from bi-/multimodal to unimodal. The difference in response for the various tracers still needs to be normalized to the GC response curves (see Fig. 44/45) in order to have correct mass balances. The 1,3 PDCH has the highest ECD response in the GC compared to 1,2 PDCH and PMCH which is also indicated in the slim tube runs. The 10% brine sand matrix run with PMCH and PDCH tracers had a different breakthrough time and is just discussed in relation to the shape of the tracer breakthrough(Fig. 47).

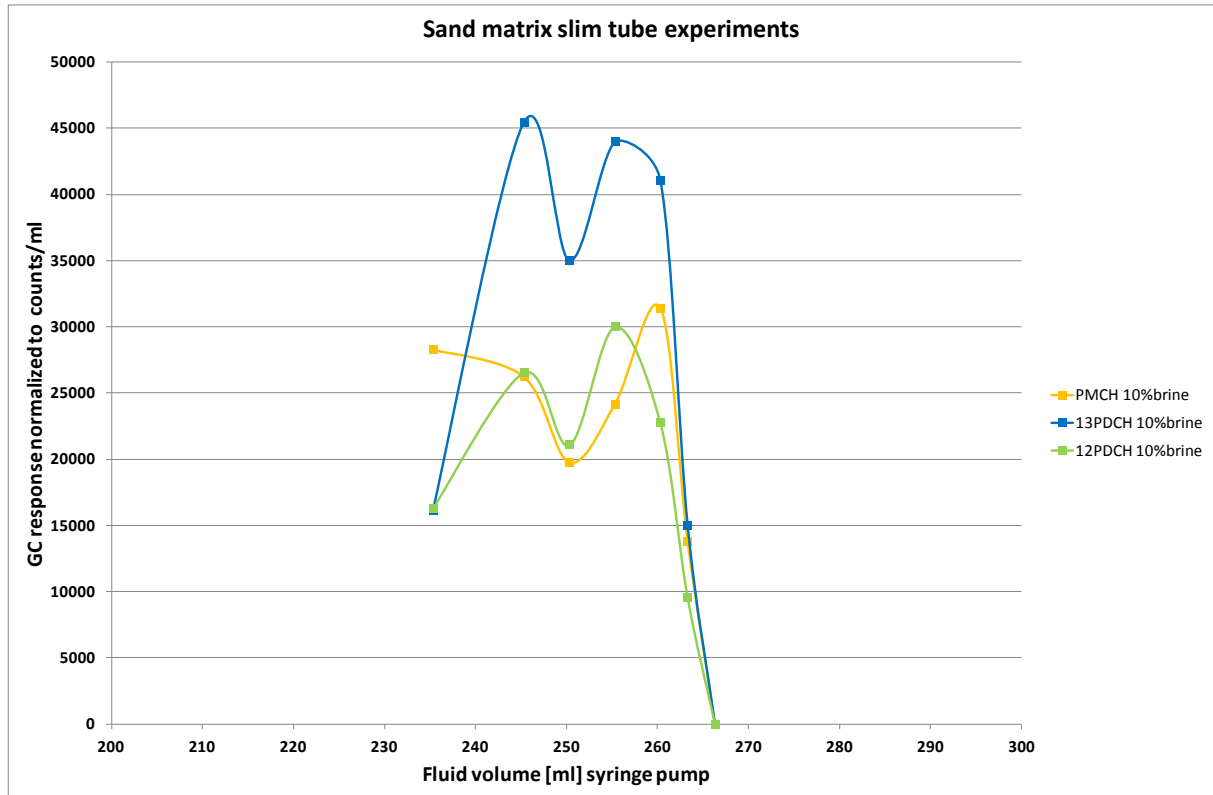


Figure 47: Slim tube tracer response curve for 10% brine of PMCH, 1,2 PDCH and 1,3 PDCH

The 10% brine run of PDCH and PMCH indicate the same broad response like the 20% brine runs. This is interpreted as retention of the tracer due to higher interactions with the matrix and solutes. The flow path of the CO₂ might be different. Although, the CO₂ is less soluble in the high salinity brines, residual CO₂ pockets might remain in the slim tube. To assess the overall mass balance of the tracer, nitrogen gas (N₂) was flushed through the slim tube after the displacement to recover tracer losses on residual CO₂/water saturations. The aim is to proof quantitatively the link between CO₂ saturations and overall tracer recovery as the throughput of tracers in the brine runs is much higher than in the pure water one.

The following plots (Fig. 48 and 49) will focus on the more detailed the split up of the tracer response curves to the two mixes applied and the various salinities covered.

In Fig.48, the higher boiling PFC tracer mixes were split by salinity. Neglecting the different GC response of the various tracers, it is demonstrated that with increased salinity from 0 ppm to 200 000 ppm, the PFC tracer recovery increased by 100 to 200%. A more pronounced tailing of the response of the tracer, especially the 1,3 PDCH is shown. The higher salinity runs are characterized also by a plateau of tracer response indicated by fluctuating responses over a broader interval regarding volume recovered.

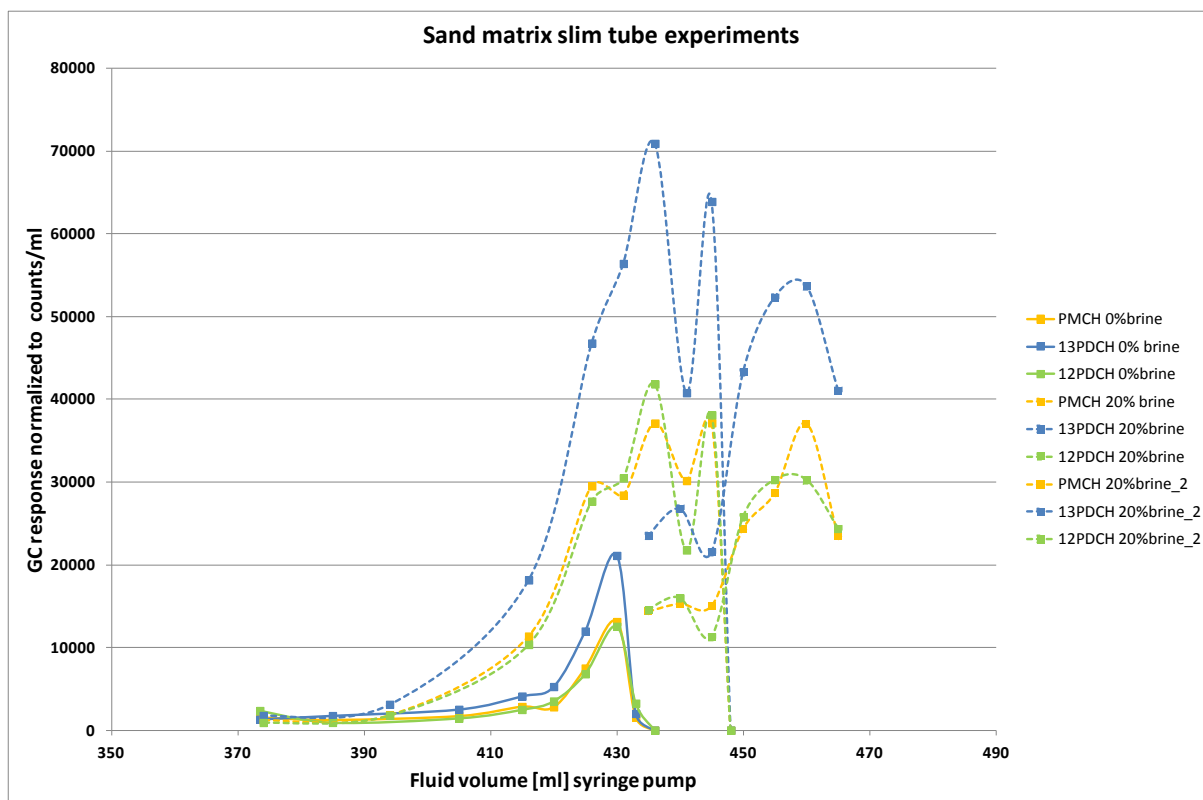


Figure 48: Comparison of 20% salinity vs. 0% salinity of high boiling tracer mix

As a summary of the results shown in Fig. 48, two observations can be made with regards to the effects of salinity on the PFC tracer response:

1. The recovery of the tracer is higher with higher salinities.
2. The retention and bleed off (tailing of the response curve) of the tracer is also more prolonged with higher salinities.

Point 1) is apparent as higher salinity means less residual CO₂ saturations, therefore lower amount of trapping of PFCs with the residual CO₂. The earlier CO₂ breakthrough at higher salinity conditions is also accompanied immediately with a tracer response.

Point 2) The broader peaks and fluctuating peaks can be due to higher interactions with solutes and a potential salt precipitation and blocking of flow with small evaporation of NaCl. That would also influence tortuosity and flow pathways of the CO₂, pocket formation etc. Higher dispersion in the brine runs is potentially linked to residence time of the CO₂. Dispersion also depends on flow rate which is 0.15ml/min for all runs and should therefore not account for the discrepancies in the brine runs compared to the pure water one.

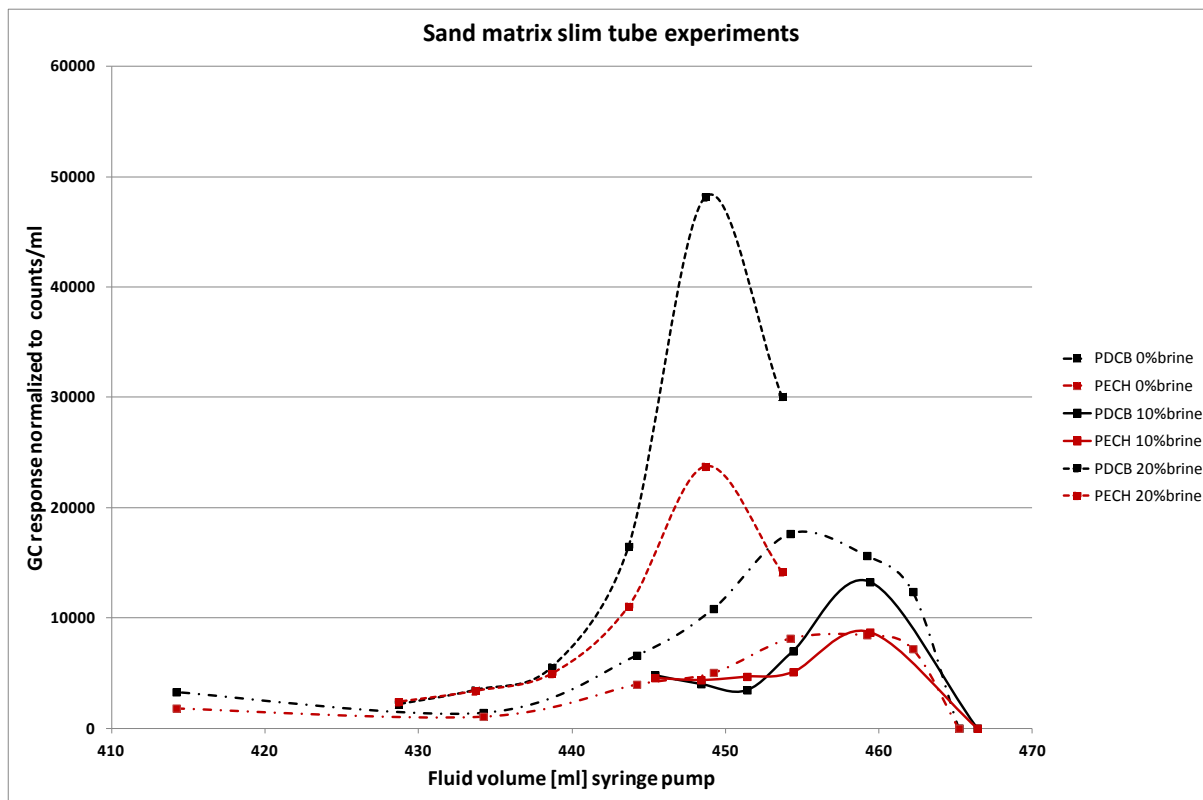


Figure 49: Comparison of low boiling tracer mix with sand matrix

In comparison to the perfluoromethylhexanes, the PDCB and PECH indicate a different behavior with regards to salinity (Fig.49). The 0 wt. % NaCl salinity runs show two fold higher concentrations of the tracer at breakthrough compared to the 10 and 20 wt.% NaCl salinity runs. Peak shape broadening is similar compared to the high boiling tracer mixes which can be again related to retention behaviour of the tracers. The heavier compound, i.e. ethylated perfluorohexane (PECH), has a much lower response compared to PDCB due to its lesser “mobility” and velocity (see Fig.49). At the moment potential retention or adsorption of PECH cannot be fully assessed due to the missing full mass balance calculations which are in progress.

9.3. Retention behavior – synthetic quartz vs. clay content

To test on more pronounced retention behaviour of PFCs, synthetic silica matrix with additions of kaolinite clays (5 wt.%) were used as packing material for the slim tube. Clays were mixed prior to the packing procedure with the quartz. The clay should adhere to the quartz grains to ensure potential surface coating. Clays therefore should have even a bigger impact as they should account for more than 5% of surface coating area of the overall matrix. Surface area mineralogy/ using sophisticated spectroscopy methods like XPS – X Ray Photoabsorption Spectroscopy were not applied to further characterize the surface of the material.

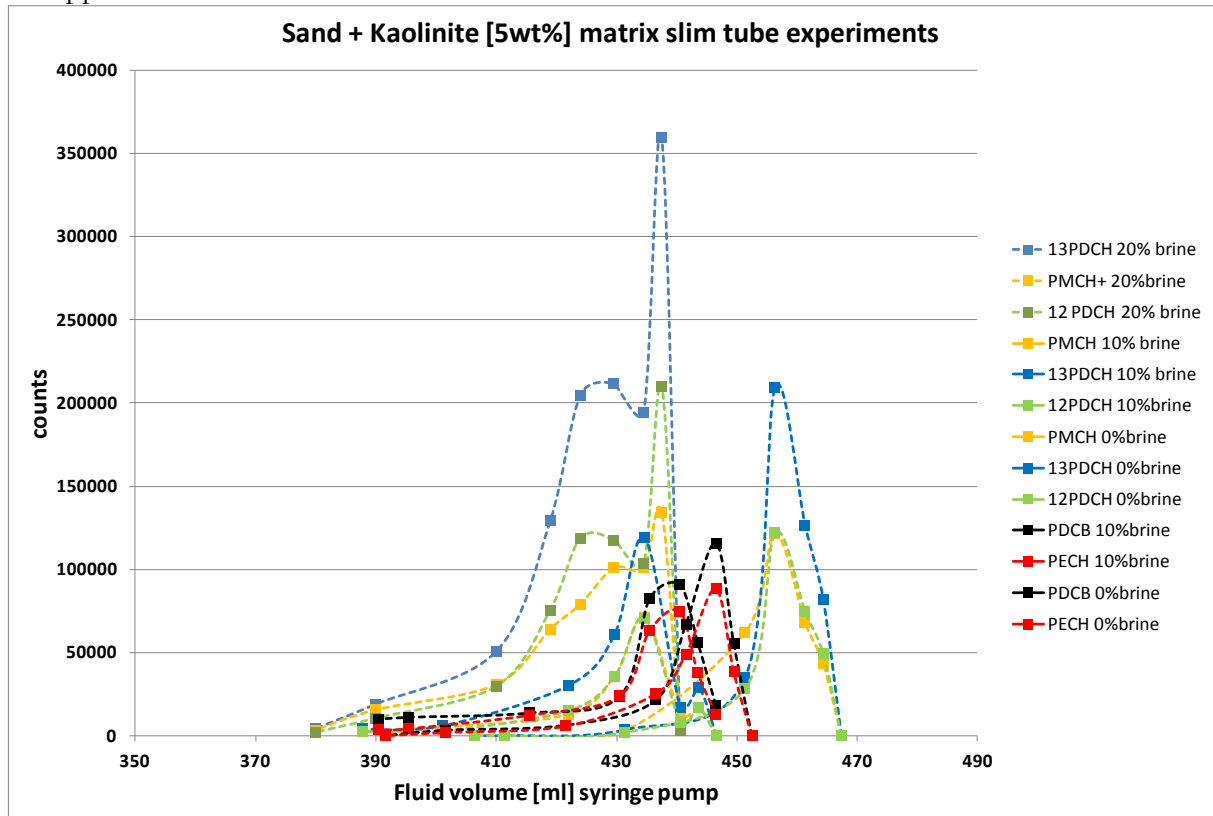


Figure 50: Summary of High and low boiling tracer mix response curves, sand + clay (kaolinite matrix)

In Fig. 50, the summary of sand + clay runs indicate a very good consistency in terms of breakthrough and the relationships of tracer concentrations within the two mixes used – PMCH and PDCH vs. PDCB and PECH.

The pure water (0% brine) response curves show a single Gaussian type curve for the PDCB mix with a sharp first maximum which declines in a skewed Gaussian manner (refer to Figs. 50/51). The 10% brine run indicates similar as in the sand matrix a much broader peak response. This is best explained with a prolonged retention and potential more contact to surface due to the difference in flow path/tortuosity for the brine run.

The PMCH/PDCH runs in Figs. 50/52 are represented with a more peculiar response as they show a bimodal peak shape for the brine runs and the usual skewed Gaussian only dispersion influenced peak shape for the pure water (0% brine).

The bimodality of the peaks in the more saline brine runs of Mix2 (PDCH compounds) is even more pronounced with increasing salinity.

Differentiating the two mixes, the higher boiling, heavier PFCs of PDCH and PMCH have a much higher interaction with the matrix and are more influenced by sorption than the lower boiling ones, i.e. PDCB and PECH. This fits with the fact that polarity and molecular conformation is slightly increased for the heavier PFCs. Retention of the PDCH and PMCH with regards to salinity is best shown in Fig. 51. The Mix2-10% brine run expresses a slight tailing of the peak which is more pronounced on the 20% brine run. A skewed peak on the 10% brine one indicate broadening, however the reduction of the tracer after the peak maximum is rapid except for the PMCH which is smeared along the column and more fading out until after 40ml of volume are recovered. The broadening and a double peak in the 20% brine run potentially indicates two separate pathways/ “fingers” of CO₂ breaking through and recombined in the last part of the slim tube. That would explain the bimodality coupled to a more vigorous interaction of the PDCH molecules with the matrix due to increased tortuosity of the flow path. The salinity impact on the PFC response might be of two reasons: a) it decreases the CO₂/water interactions and b) it might influence clays surface area, wettability and therefore increased interactions of tracers with the matrix resulting in higher retention. The pure water run indicates a response curve for PDCH and PMCH tracers as expected for the main peak. The earlier breakthrough of a small amount of tracer might be due to fluctuations again in the flow paths which need to be further investigated.

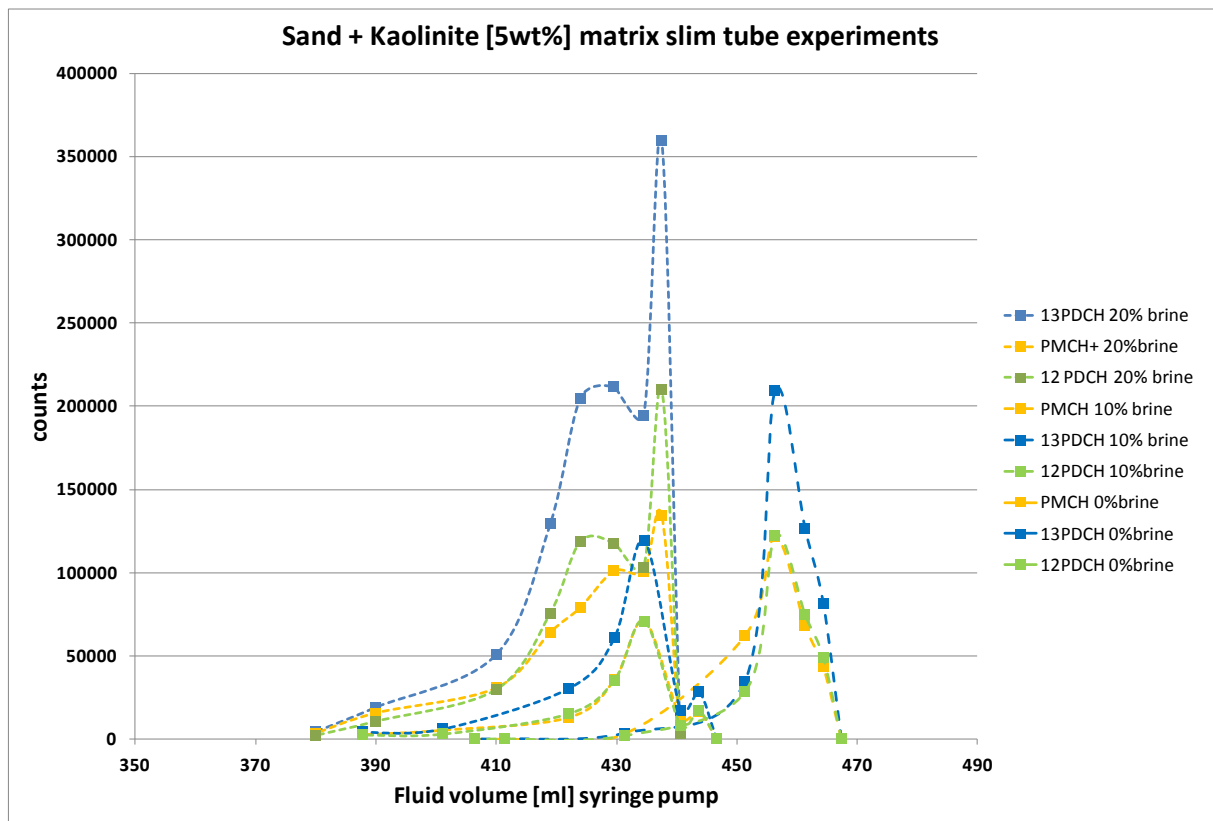


Figure 51: Summary of High Boiling PFC Mix vs. sand+clay (kaolinite) matrix response curves

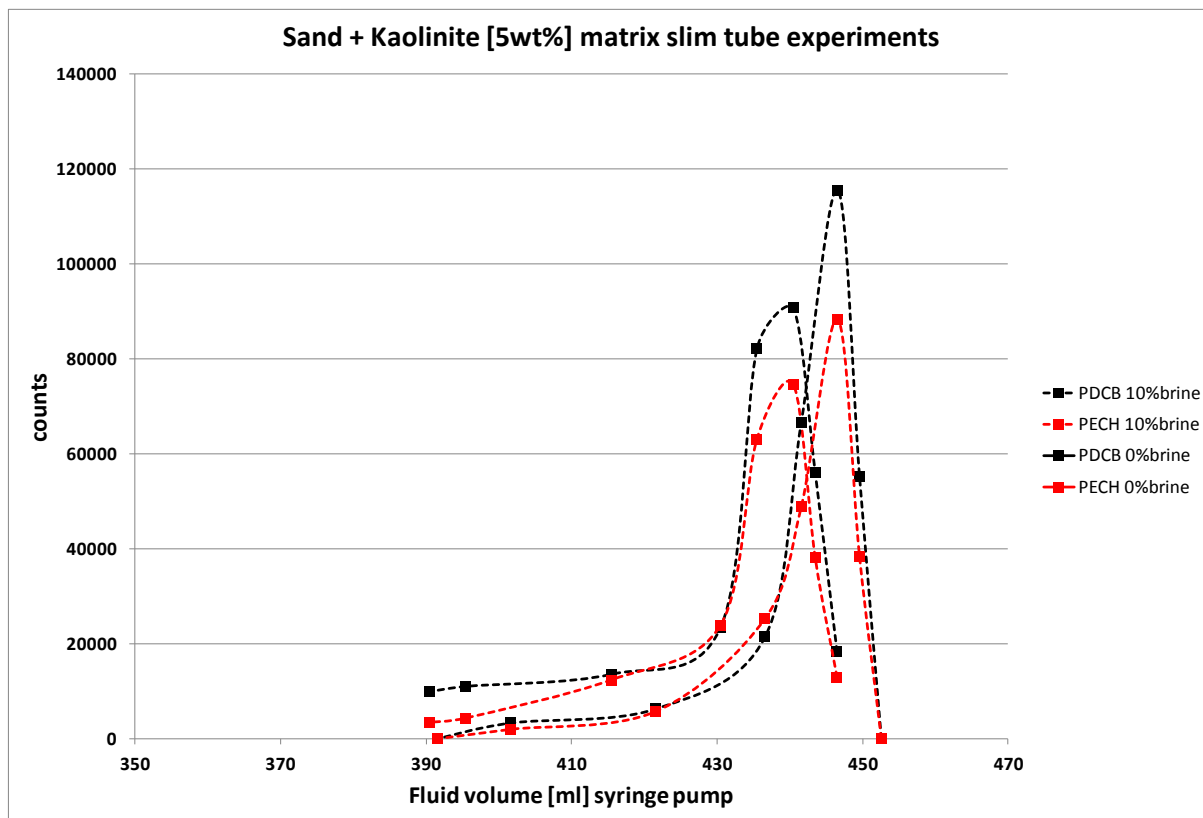


Figure 52: Summary of “Low” Boiling tracer Mix vs. sand + clay (kaolinite) response curves

The PDCB and PECH runs are not so much affected by the salinity (Fig.52). The slight retention and peak broadening for the 10% brine run is consistent with a higher interaction of the tracer with the matrix promoted by the salinity and again a potentially longer flow path also indicated by the slightly later occurrence of the CO₂ and the tracer. Compared to pure quartz at 0 ppm salinity (Fig.49), the tracer indicate a slight retention in the sand+clay run. Still it expresses a unimodal peak maximum, but not as pronounced as shown in the runs before that indicated a very rapid and almost contemporaneous occurrence of CO₂ and the tracer. The CO₂ breakthrough is always related to the first sample taken as it is determined by the densitometer detection.

10. Preliminary Conclusion

The preliminary conclusion is that PFCs may remain in sufficient detectable amounts in its parent CO₂ phase at shallow depth in the hydrostratigraphic column. The preliminary data results confirm that PFCs dissolved in supercritical CO₂ have very low solubility in water and are not retained at significant/critical amounts during migration by matrices prone to adsorb organic compounds like clays. Hence, experimental data obtained so far suggest that PFCs are a suitable reliable passive/conservative tracer of injected CO₂ under supercritical conditions. Experimental measurements are continuing to explore the behavior of organic substrate adsorption and CO₂/water/hydrocarbons partitioning expanded also to gaseous CO₂ (subcritical conditions).

From a conceptual point of view, taking into account the physical behavior of PFCs, it was noted that the most critical moment for retention or even full adsorption of PFCs within supercritical CO₂ is linked to the evaporation of existing water into the scCO₂ (potential dry out zone).

11. Outstanding experimental work

Batch Reactor Experiments:

- Outstanding PFC compounds to be investigated using batch reactor experiments include the following low to mid boiling:
 - Perfluorobutane
 - Perfluorocyclobutane
 - Perfluoroethylcyclopentane.
- The relationship of pressure, temperature and salinity are expected to be investigated for sub-critical conditions. This depends upon assessment of the sensitivity of the experimental setup using slightly more soluble perfluorinated tracers like perfluorobenzene and perfluorodecalin for aromatic and cyclic perfluoroalkanes.
- No solubility measurements and hence full passive behavior of the tracer has been shown so far for the supercritical fluid realm. A final attempt at measuring the solubility of perfluorohexane in the water phase will be done using pure phases instead of tracer amounts in a miscible phase like scCO₂.

Slim Tube Experiments:

- Outstanding slim tube experiments will contain more complex matrices, such as coal, higher amounts of clay and feldspars and reactive matrices like carbonates.
- Experimental conditions will also address subcritical conditions, which mimic a more shallow compartment along the stratigraphic column. Hence, outstanding slim tube experiments will investigate the liquid to gas phase boundary for the parent CO₂ phase.
- Apart from scCO₂ vs. water/brine phase systems, outstanding experiments will also account for partitioning of multiple fluids comprising hydrocarbons, scCO₂ and brine in a siliciclastic environment.

References

- [1] Oliveira, M. B., et al. (2007). "Modeling the liquid-liquid equilibria of water + fluorocarbons with the cubic-plus-association equation of state." *Industrial and Engineering Chemistry Research* 46(4): 1415-1420.
- [2] Berkowitz, B., et al. (2008). "Contaminant Geochemistry – Interactions and Transport in the Subsurface Environment." Heidelberg, New York, Springer, 412p.
- [3] Brunauer, S. et al. (1938). "Adsorption of Gases in Multimolecular Layers". *J.Am.Chem.Soc.* 60(2): 309-319
- [4] Dugstad, O., et al. (1993). "Measurements of gas tracer retention under simulated reservoir conditions." *Journal of Petroleum Science and Engineering*, 10: 17-25.
- [5] Vandeweyer, V., et al (2011). "Monitoring the CO2 injection site: K12-B." *Energy Procedia* 4: 5471–5478.
- [6] McCallum, S.D., Phelps, T.J., Riestenberg, D.E., Friefeld, B.M., and Trautz, R.C. (2004). "Interpretation of perfluorocarbon tracer data collected during the Frio carbon dioxide sequestration test". American Geophysical Union Fall Meeting, San Francisco, California, December 5–9, 2005, paper GC13A-1214. GCCC Digital Publication Series #05-03f, pp. 1-2.
- [7] Trautz, R., Friefeld, B., and Doughty, C. (2004). "Comparison of single and multiphase tracer test results from the Frio CO2 Pilot Study, Dayton, Texas." National Energy Technology Laboratory Fourth Annual Conference on Carbon Capture and Sequestration, Alexandria, Virginia, May 2-5, 2005. GCCC Digital Publication Series #05-04t, pp. 1-11.
- [8] Wells, A.W., et al. (2013). "Atmospheric and soil-gas monitoring for surface leakage at the San Juan Basin CO2 pilot test site at Pump Canyon New Mexico, using perfluorocarbon tracers, CO2 soil-gas flux and soil-gas hydrocarbons". *International Journal of Greenhouse Gas Control* 14: 227–238.
- [9] Strazisar, B., et al. (2009). "Near-surface monitoring for the ZERT shallow CO2 injection project". *International Journal of Greenhouse Gas Control* 3: 736–744.
- [10] Wells, A.W. (2010). "Atmospheric tracer monitoring and surface plume development at the ZERT pilot test in Bozeman, Montana, USA". *Environ Earth Sci* 60: 299–305.
- [11] Pruess, K., Friefield, B., Kennedy, M., Oldenburg, C., Phelps, T.J., and van Soest, M.C.,(2005). "Use of gas phase tracers for monitoring CO2 injection at the Frio Test Site". National Energy Technology Laboratory Fourth Annual Conference on Carbon Capture and Sequestration, Alexandria, Virginia, May 2-5, 2005. GCCC Digital Publication Series #05-04r, pp. 1-17.
- [12] McCallum et al (2005). "Monitoring Geologically Sequestered CO2 during the Frio Brine Pilot Test using Perfluorocarbon Tracers". FOURTH ANNUAL CONFERENCE ON CARBON CAPTURE AND SEQUESTRATION DOE/NETL Proceedings
- [13] Siriwardane, H.J. et al. (2012). "Modeling of CBM production, CO2 injection, and tracer movement at a field CO2 sequestration site". *International Journal of Coal Geology* 96-97: 120–136.
- [14] Wilson, T.H., et al. (2005). "Ground-penetrating radar survey and tracer observations at the West Pearl Queen carbon sequestration pilot site, New Mexico". *The Leading Edge* 24(7): 718-722.
- [15] Dugstad, O., et al. (1992). "Construction of a Slim-tube Equipment for Gas Tracer Evaluation at Simulated Reservoir Conditions." *Appl. Radiat. Isot.* 43(4): 521-535

- [16] Dugstad, O., et al. (1999). "Application of Tracers to Monitor Fluid Flow in the Snorre Field: A Field Study". – SPE Paper 56427.
- [17] Huseby, O., et al. (2008). "Improved Understanding of reservoir Fluid Dynamics in The North Sea Snorre Field by Combining Tracers, 4D Seismic and Production Data". SPE Paper 105288.
- [18] Senum, G.I., et al. (1992). "Petroleum Reservoir Characterization by Perfluorocarbon Tracer". SPE/DOE Paper No. 24137
- [19] Chatzichristos, C., (2000). "Application of Partitioning Tracers for Remaining Oil Saturation Estimation: An Experimental and Numerical Study". SPE Paper 59369
- [20] Jang, S. S., et al. (2003). "The source of helicity in perfluorinated N-alkanes." *Macromolecules* 36(14): 5331-5341.
- [21] Dunitz, J. D., et al. (2003). "Molecular Shape and Intermolecular Liaison: Hydrocarbons and Fluorocarbons." *Helvetica Chimica Acta* 86(12): 4073-4092.
- [22] Gladysz, J. A. and C. Emnet (2004). "Fluorous Solvents and Related Media." *Handbook of Fluorous Chemistry*: 11-23.
- [23] Smart, B. E. (1994). Characteristics of C-F systems. *Organofluorine Chemistry: Principles and Commercial Applications*. R. E. Banks, B. E. Smart and J. C. Tutlow. New York, Plenum Press: 57-88.
- [24] Smart, B. E. (1995). "Properties of fluorinated compounds, physical and physicochemical properties." *Chemistry of Organic Fluorine Compounds II* 187: 979-1010.
- [25] Smart, B. E. (2001). "Fluorine substituent effects (on bioactivity)." *Journal of Fluorine Chemistry* 109(1): 3-11.
- [26] Dunitz, J. D. (2004). "Organic fluorine: Odd man out." *ChemBioChem* 5(5): 614-621.
- [27] Gladysz, J. A. and M. Jurisch (2012). Structural, physical, and chemical properties of fluorous compounds. 308: 1-24.
- [28] Krafft, M. P. and J. G. Riess (2009). "Chemistry, physical chemistry, and uses of molecular fluorocarbon- hydrocarbon diblocks, triblocks, and related compounds-unique "apolar" components for self-assembled colloid and interface engineering." *Chemical Reviews* 109(5): 1714-1792.
- [29] Sandford (2003). "Perfluoroalkanes". *Tetrahedron* 59: 437-454.
- [30] Hunter, L. (2010). "The C-F bond as a conformational tool in organic and biological chemistry." *Beilstein Journal of Organic Chemistry* 2010, 6, No. 38. doi:10.3762/bjoc.6.38
- [31] O'Hagan, D. (2008). "Understanding organofluorine chemistry. An introduction to the C-F bond." *Chem. Soc. Rev.* 37: 308-319.
- [32] Tsai, W. T. (2009). "Environmental hazards and health risk of common liquid perfluoro-n-alkanes, potent greenhouse gases." *Environment International* 35(2): 418-424.
- [33] Varanda, F. R., et al. (2008). "Liquid-liquid equilibrium of substituted perfluoro-n-octane + n-octane systems." *Fluid Phase Equilibria* 268(1-2): 85-89.
- [34] Dias, A. M. A., et al. (2006). "Vapor - Liquid equilibrium of carbon dioxide - Perfluoroalkane mixtures: Experimental data and SAFT modeling." *Industrial and Engineering Chemistry Research* 45(7): 2341-2350.
- [35] Dias, A. M. A., et al. (2009). "Thermodynamic characterization of pure perfluoroalkanes, including interfacial and second order derivative properties, using the crossover soft-SAFT EoS." *Fluid Phase Equilibria* 286(2): 134-143.

- [36] Morgado, P., et al. (2011). "Viscosity of liquid perfluoroalkanes and perfluoroalkylalkane surfactants." *Journal of Physical Chemistry B* 115(29): 9130-9139.
- [37] Potoff, J. J. and D. A. Bernard-Brunel (2009). "Mie potentials for phase equilibria calculations: Application to alkanes and perfluoroalkanes." *Journal of Physical Chemistry B* 113(44): 14725-14731.
- [38] Hallewell, G., et al. (2010). "Properties of saturated fluorocarbons: Experimental data and modeling using perturbed-chain-SAFT." *Fluid Phase Equilibria* 292: 64-70.
- [39] Rabai, J. et al. (2006).: "Fluorous chemistry and its application perspectives in the field of fluoroorganic and fluoroinorganic compounds". The Second International Siberian Workshop -Advanced Inorganic Fluorides 'INTERSIBFLUORINE-2006' June 11-16, 2006. Tomsk, Russia. Proceedings of ISIF-2006: 245-249
- [40] Funk, E.E. & Prausnitz, J. M. (1971). "Entropies of Vaporization for Fluorocarbons and Hydrocarbons from the Hildebrand Rule". *The Journal of Physical Chemistry* 75(16): 2530-2532.
- [41] Amii, H. and K. Uneyama (2009). "C-F bond activation in organic synthesis.". *Chemical Reviews* 109(5): 2119-2183.
- [42] Murphy, C. D. (2010). "Biodegradation and biotransformation of organofluorine compounds." *Biotechnology Lett.* 32: 351-359.
- [43] Laube, J.C., (2012). "Distributions, long term trends and emissions of four perfluorocarbons in remote parts of the atmosphere and firn air". *Atmos. Chem. Phys.*, 12: 4081–4090.
- [44] Ivy, D.J., (2012). "Atmospheric histories and growth trends of C4F10, C5F12, C6F14, C7F16 and C8F18". *Atmos. Chem. Phys.*, 12: 4313–4325.
- [45] Watson, T. & Sullivan, T., (2011). "Design of a perfluorocarbon tracer based monitoring network to support monitoring verification and accounting of sequestered CO2". EPJ Web of Conferences 50, 04003, DOI: 10.1051/epjconf/20135004003
- [46] Timko, M.T., Nicholson, B.F., Steinfeld, J.I., Smith, K.A. and Tester, J.W., 2004. Partition coefficients of organic solutes between supercritical carbon dioxide and water: Experimental measurements and empirical correlations. *Journal of Chemical and Engineering Data*, 49(4): 768-778.
- [47] Chiou, C. T.; Schmedding, D. W.; Manes, M. (1982). "Partitioning of organic compounds in octanol-water systems". *Environ. Sci. Technol.*, 16: 4-10.
- [48] Chiou, C. T. (2002). "Partition and Adsorption of Organic Contaminants in Environmental Systems"; Wiley-Interscience: Hoboken, NJ.
- [49] White, W. (2013). "Geochemistry" - Oxford, UK: Blackwell-Wiley, 672p.
- [50] Saikat, S., et al. (2013). "The impact of PFOS on health in the general population: a review." *Environ. Sci.: Processes Impacts* 15: 329-335.
- [51] Tsai, W.T. (2011). "Environmental Property Modeling of Perfluorodecalin and its Implications for Environmental Fate and Hazards". *Aerosol and Air Quality Research*, 11: 903–907.
- [52] Freire, M.G., et al. (2005). "PHASE EQUILIBRIA AND INTERFACIAL PROPERTIES OF WATER + PERFLUOROCARBONS". ENPROMER, 4th Mercosur Congress on Process Systems Engineering Conf. Proc.
- [53] Schroeder, B., et al. (2011). "Aqueous solubility, effects of salts on aqueous solubility, and partitioning behavior of hexafluorobenzene: Experimental results and COSMO-RS predictions". *Chemosphere* 84: 415–422

- [54] 3M Company (2001). "HPV Robust Summaries - CAS# 86508-42 Perfluoro compounds C5-C 18, including CAS#3 Perfluorotributyl amine". EPA-GOV report, no. 201-13244
- [55] Freire, M.G., et al. (2010). "Solubility of water in fluorocarbons: Experimental and COSMO-RS prediction results". *J. Chem. Thermodynamics* 42: 213–219.
- [56] Meylan, W.M. and Howard, P.H. (1995). Atom/fragment Contribution Method for Estimating Octanol-water Partition Coefficients. *J. Pharm. Sci.* 84: 83–92.
- [57] Lyman WJ, Reehl WF, Rosenblatt DH. Handbook of chemical property estimation methods: environmental behavior of organic compounds. Washington, DC: American Chemical Society; 1982.
- [58] Yee, L.C. & Wei, Y.C. (2012). "Current Modeling Methods Used in QSAR/QSPR" in: "Statistical Modelling of Molecular Descriptors in QSAR/QSPR". First Edition. Published 2012 by Wiley-VCH Verlag GmbH & Co. KGaA.
- [59] Cronin, M. T.D. & Schultz, T. W., (2003) "Pitfalls in QSAR". *Journal of Molecular Structure* 622: 39–51
- [60] Dietz, R.N., (1986). "Perfluorocarbon Tracer Technology".-Regional and Long Range Transport of Pollution, Lecture; BNL report38847: 215-247.
- [61] Watson, T. B., et al. (2007). "The Atmospheric Background of Perfluorocarbon Compounds Used as Tracers". *Environmental Science & Tech.* 41(20):6909-6913
- [62] Galdiga, C.T. & Greibock, T. (1997). "Simultaneous Determination of Trace Amounts of Sulphur Hexafluoride and Cyclic Perfluorocarbons in Reservoir Samples by Gas Chromatography". *Chromatographia* 46 (7/8): 440-443.
- [63] Lagomarsino, R. (1996). "An Improved Gas Chromatographic Method for the Determination of Perfluorocarbon Tracers in the Atmosphere". *Journal of Chromatographic Science* 34: 405-412.
- [64] Nazzari, M., et al. (2013). "A simple and sensitive gas chromatography–electron capture detection method for analyzing perfluorocarbon tracers in soil gas samples for storage of carbon dioxide". *International Journal of Greenhouse Gas Control* 14: 60–64.
- [65] Cooke, K.M., et al. (2001). "Use of Capillary Gas Chromatography with Negative Ion-Chemical Ionization Mass Spectrometry for the Determination of Perfluorocarbon Tracers in the Atmosphere". *Anal. Chem.* 73: 4295-4300.
- [66] Simmonds, P.G., et al (2002). "The backgroundatmospheric concentrations of cyclic perfluorocarbon tracers determined by negative ion-chemical ionization mass spectrometry". *Atmospheric Environment* 36: 2147–2156.
- [67] Ren, Y., et al. (2013). "The Application of TD/GC/NICI–MS with an Al₂O₃-PLOT-S Column for the Determination of Perfluoroalkylcycloalkanes in the Atmosphere". *Chromatographia* DOI 10.1007/s10337-013-2584-6
- [68] Chiou, C.T., et al. (1979). "A physical concept of soil-water equilibria for nonionic organic compounds". *Science* 206: 831-832.
- [69] Freed, B.K. et al. (1990). "Spectral Polarity Index; A new Method for determining the relative polarity of solvents." *J. of Fluorine Chemistry* 48: 63-75.
- [70] Freire, M.G. et al. (2006). "Surface Tension of Perfluorocompounds." *J.Chem.Eng.Data* 51: 1820-1824.

Bibliographic information

Classification Unrestricted

Report Number SR.14.

Title Interim Report

Perfluorocarbon Tracers Technology applied

to

CCS Quest Project

Author(s) H.Peters (PTI/RC)

Keywords Perfluorocarbon, Quest, Tracer, CCS, Carbon Sequestration

Date of Issue January 2014

Period of Work March 2013 - March 2014

US Export Control Non US - No disclosure of Technology

Approved by Luc Rock (SCAN)

Mauri Smith (SCAN)

Sean McFadden (SCAN)

Sponsoring
Company /
Customer Shell Canada Ltd

Issuing Company Shell Global Solutions International B.V.

P.O. Box 60

2280 AB Rijswijk

The Netherlands

APPENDIX E – GOLDR HBMP RESULTS FALL 2012 TO END 2013



January 23, 2014

2012-2013 HBMP SUMMARY REPORT

Shell Quest CCS Hydrosphere Biosphere Monitoring Program

Submitted to:
Shell Canada Limited
400 4th Avenue SW
Calgary, AB
T2P 2H5

REPORT



Report Number: 1213510001_RP013_V2_2013AER

Distribution:

Shell - 1 ecopy
Golder -1 ecopy





Table of Contents

1.0 INTRODUCTION..... 1

2.0 ATMOSPHERE..... 1

 2.1 Methods..... 2

 2.1.1 Discrete Laboratory Atmospheric Samples 2

 2.1.2 In Situ Atmospheric Measurements in Real Time 2

 2.1.3 Independent Greenhouse Gas Measurements 3

 2.2 Results..... 3

 2.2.1 National Oceanic and Atmospheric Administration’s Earth System Research Laboratory Results 3

 2.2.2 Discrete Laboratory Atmospheric Samples 4

 2.2.3 In Situ Measurements in Real Time 5

 2.3 Summary of Key Findings..... 12

3.0 BIOSPHERE 13

 3.1 Land Classification..... 13

 3.2 Plot Selection..... 18

 3.3 Vegetation 20

 3.3.1 Methodology 20

 3.3.2 Results 22

 3.3.2.1 Annual Crops 22

 3.3.2.2 Pasture 25

 3.3.2.3 Broadleaf Forests 27

 3.3.2.4 Coniferous Forests 30

 3.3.2.5 Wetlands..... 32

 3.3.3 Summary of Key Findings 35

 3.4 Soils..... 36

 3.4.1 Soil Profile Characterization Program 36

 3.4.1.1 Field Methods 37

 3.4.1.2 Soil Sampling..... 39

 3.4.1.3 Laboratory Analytical Methods 39



2012-2013 HBMP SUMMARY REPORT

3.4.3	Summary of Key Findings	41
3.4.4	Shallow Surface Soil Sampling Program	41
3.4.4.1	Field Methods	41
3.4.4.2	Laboratory Analytical Methods	42
3.4.4.3	Results.....	42
3.4.4.4	Summary of Key Findings.....	46
3.5	EM38	47
3.5.1	Methodology and Quality Assurance/Quality Control	47
3.5.2	Results	48
3.5.2.1	Annual Crops	51
3.5.2.2	Pastures	51
3.5.2.3	Broadleaf Forest	51
3.5.2.4	Coniferous Forests	52
3.5.2.5	Wetlands.....	52
3.5.3	Summary of Key Findings	52
3.6	Soil Gas and Surface Flux	53
3.6.1	Fluxnet Literature Review	53
3.6.1.1	Background	53
3.6.1.2	Boreal Forests	56
3.6.1.3	Western Canadian Wetlands	57
3.6.1.4	Northern Temperate Grasslands	58
3.6.1.5	Fluxnet-Canada Research Network Summary and Recommendations	59
3.6.2	Soil Gas and Surface CO ₂ Flux Sampling Methods	60
3.6.2.1	Soil Gas Sampling	60
3.6.2.2	Surface CO ₂ Flux Sampling	62
3.6.3	Soil Gas Results.....	63
3.6.4	Surface CO ₂ Flux Results	69
3.6.5	Summary of Key Findings	72
3.7	Remote Sensing	73
3.7.1	Methodology and Field Program	73
3.7.2	Data Collected	74



3.7.3 Empirical Line Calibration Analytical Results 74

3.7.4 Spectral Data Analytical Results 74

3.7.4.1 Background on Spectral Signatures 75

3.7.4.2 Annual Crops 76

3.7.4.3 Pastures 77

3.7.4.4 Wetlands..... 77

3.7.5 Summary of Key Findings 78

4.0 HYDROSPHERE 78

4.1 Baseline Monitoring Well Network 79

4.1.1 Landowner Wells..... 79

4.1.2 Project Wells 80

4.1.3 Laboratory Analyses 80

4.1.3.1 Groundwater Analyses 80

4.1.3.2 Wellhead Gas Analyses..... 81

4.1.3.3 2012-2013 Sampling Schedule..... 82

4.2 Methodology 82

4.2.1 Groundwater Sampling 83

4.2.1.1 Landowner Wells 83

4.2.1.2 Project Wells..... 83

4.2.2 Gas Sampling 83

4.2.2.1 Wellhead Gas Sampling 83

4.2.2.2 Flow-Through Gas Sampling 84

4.2.3 Water Quality Data Loggers..... 84

4.2.4 Quality Assurance/Quality Control 84

4.3 Results..... 85

4.3.1 Groundwater 85

4.3.1.1 Laboratory Results..... 87

4.3.1.2 Data Logger Results 96

4.3.2 Wellhead Gas Results..... 98

4.3.2.1 Wellhead Gas Composition 98

4.3.3 Quality Assurance/Quality Control 100



5.0 REFERENCES..... 101

6.0 ABBREVIATIONS 105

TABLES

Table 2.2-1: Atmospheric Gas Sample Location and Number Summary 8

Table 2.2-2: Laboratory Results for Atmospheric Gases Measured at 1.0 meter Elevation 9

Table 2.2-3: *In-situ* Results for Atmospheric Gases Measured at 0.1 and 1.0 meter Elevations 9

Table 3.1-1: Summary of Land Cover and Plot Distribution Within the Project Area 13

Table 3.2-1: Names and Locations of the 2012 Transient Plots and 2012/2013 Semi-Permanent Plots 18

Table 3.3-1: Plant Vigour Descriptions 21

Table 3.3-5: Species Richness Values Within Coniferous Forests 32

Table 3.3-6: Species Richness Values Within Wetlands 35

Table 3.4-1: Exova Soil Analytical Methods 39

Table 3.4-2: Soil Characteristics Within Monitoring Plots Sorted by Soil Correlation Area and Vegetation Type 40

Table 3.4-3: Exova and Golder Edmonton Material Testing Laboratory Soil Analytical Methods 42

Table 3.4-4: Soil Moisture Contents by Vegetation Type – October 2012 42

Table 3.6-1: Fluxnet Canada Research Network Data Availability 55

Table 3.6-2: Comparison of Lethbridge Data to Global Data 59

Table 3.6-3: Soil Gas Sampling Summary 64

Table 3.6-4: Surface CO₂ Flux Statistics Grouped by Sampling Event 69

Table 3.6-5: Seasonal Surface CO₂ Flux Statistics Grouped by Land Cover Type 70

Table 4.1-1: Project Injection Wells 80

Table 4.1-2: Laboratory Analyses – Groundwater 81

Table 4.1-3: Laboratory Analyses – Wellhead Gas 81

Table 4.1-4: 2012-2013 Groundwater and Wellhead Gas Sampling Schedule 82

Table 4.3-1: 2012-2013 Groundwater Sampling Summary 87

Table 4.3-2: 2012-2013 Groundwater Chemical Analysis Summary 88

Table 4.3-2: 2012-2013 Groundwater Isotopic Analysis Summary (to Dec. 2013) 96

Table 4.3-3: 2013 Troll 9500 Data Logger Summary 97

Table 4.3-4: 2012-2013 Wellhead Gas Sampling Summary 98

Table 4.3-5: 2012-2013 Wellhead Gas Chemical Analysis Summary 99

Table 4.3-6: 2012-2013 Wellhead Gas Isotopic Analysis Summary (to Dec. 2013) 99

Table 4.3-6: 2012-2013 Quality Assurance/Quality Control Sampling 100



FIGURES

Figure 1-1: Project Location Map 1
Figure 2.1-1: Atmospheric Measurements of CO2, CH4 and H2O..... 3
Figure 2.2-1: Annual Trends in Atmospheric Carbon Dioxide 6
Figure 2.2-2: Annual Trends in Atmospheric Methane 7
Figure 2.2-3: Greenhouse Gas Analyzer Atmospheric Carbon Dioxide Concentrations by Sampling Event (rows), Sampling Height (columns) and Land Use Type (subplot-columns) 10
Figure 2.2-4: Greenhouse Gas Analyzer Atmospheric Methane Concentrations by Sampling Event (rows), Sampling Height (columns) and Land Use Type (subplot-columns) 10
Figure 2.2-5: Greenhouse Gas Analyzer Atmospheric Water Vapour Concentrations by Sampling Event (rows), Sampling Height (columns) and Land Use Type (subplot-columns) 11
Figure 3.1-1: Land Classification 14
Figure 3.1-2: Landsat 5 Land Cover Classification..... 15
Figure 3.1-3: Landsat 5 Land Cover Classification: Detail 1 (Northeastern Sampling Plots)..... 16
Figure 3.1-4: Landsat 5 Land Cover Classification: Detail 2 (Central Sampling Plots)..... 17
Figure 3.2-1: Plot Design for Annual Crops and Perennial Vegetation Plots (Non-Annual Croplands) 20
Figure 3.3-1: Average Percent Cover by Strata for Each Vegetation Survey Period in the Annual Crop Vegetation Class: Living and Senesced and/or Non-Living 23
Figure 3.3-2: Example of the Annual Crop Vegetation Class (Plot 08-21) 23
Figure 3.3-3: Average Percent Cover by Strata for Each Vegetation Survey Period in the Pasture Vegetation Class: Living and Senesced and/or Non-Living 26
Figure 3.3-4: Example of the Pasture Vegetation Class (Plot 13-35b) 26
Figure 3.3-5: Average Percent Cover by Strata for Each Vegetation Survey Period in the Broadleaf Vegetation Class: Living and Senesced and/or Non-Living 28
Figure 3.3-6: Example of the Broadleaf Forest Vegetation Class (Plot 13-35a) 29
Figure 3.3-7: Average Percent Cover by Strata for Each Vegetation Survey Period in the Coniferous Forests Vegetation Class: Living and Senesced and/or Non-Living 31
Figure 3.3-8: Example of the Coniferous Forest Vegetation Class (Plot 04-33b) 31
Figure 3.3-9: Average Percent Cover by Strata for Each Vegetation Survey Period in the Wetland Vegetation Class: Living and Senesced and/or Non-Living 33
Figure 3.3-10: Example of the Wetlands Vegetation Class (Plot 16-08) 34
Figure 3.4-1: Map of Area of Review Boundary Showing Soil Correlation Areas and Monitoring Plot Locations. 38
Figure 3.4-2: Mean Soil Moisture content by Plot Vegetation Type for Spring 2013 Sampling Period 43
Figure 3.4-3: Mean Soil Moisture Content by Plot Vegetation Type for Summer 2013 Sampling Period 43
Figure 3.4-4: Mean Soil Moisture Content by Plot Vegetation Type for Fall (October) 2013 Sampling Period..... 44
Figure 3.4-5: Mean Soil Percent Saturation by Vegetation Type for Fall (October) 2013 Sampling Period 44



Figure 3.4-6: Mean Soil Electrical Conductivity by Vegetation Type for Fall (October) 2013 Sampling Period	45
Figure 3.5-1: EM38-MK2 Instrument	47
Figure 3.5-2a: Example Colour Conductivity Map 0.75 m Depth.....	49
Figure 3.5-3b: Example Colour Conductivity Map 1.5 m Depth.....	50
Figure 3.6-1: Fluxnet-Canada Research Network Measurement Locations (Source: Margolis et al. 2006.)	54
Figure 3.6-2: Modelling Simulation of Net Ecosystem Productivity for (left) a 73-year-old Aspen Stand, and (right) a 121-year-old Black Spruce Stand (Source: Chen et al. 2003.)	56
Figure 3.6-3: Simultaneous Measurements of Moss-Surface Net Exchange (solid lines) and Whole-Forest Net Exchange (dashed lines) in a Black Spruce Forest in Saskatchewan (Source: Goulden and Crill 1997).	57
Figure 3.6-4: Leak Test (left photo) – Flushmount Vault (right photo)	61
Figure 3.6-5: LiCor Model 8100A – Green Gas Analyzer	62
Figure 3.6-6: Seasonal Oxygen Deficit Plotted versus CO ₂ Enrichment for Soil Gases Samples	65
Figure 3.6-7: Keeling Plot for Soil Gas CO ₂ Measured Seasonally	66
Figure 3.6-8: Vertical Profiles of Hydrosphere and Biosphere Monitoring Program Atmospheric and Soil Gas CO ₂ (left) and CH ₄ (right).....	67
Figure 3.6-9: Seasonal Atmospheric and Soil Gas CO ₂ Profiles Separated by Land Cover Type	68
Figure 3.6-10: Seasonal Atmospheric and Soil Gas CH ₄ Profiles Separated by Land Cover Type.....	68
Figure 3.6-11: Seasonal Surface CO ₂ Fluxes for all Land Cover Types.....	70
Figure 3.6-12: Seasonal Surface CO ₂ Fluxes Grouped by Land Cover Type	71
Figure 3.7-1: Linear Regression for the RapidEye Green Band, July 2013 Image.....	74
Figure 3.7-2: Spectral Signatures of Common Land Cover Types	75
Figure 4.3-1: Well Sampling Locations.....	86
Figure 4.3-2: PH Values for Regional Wells Completed in the Foremost Formation – Quarter 4, 2012.....	90
Figure 4.3-3: PH Values for Regional Wells Completed in the Foremost Formation – Quarter 1, 2013.....	91
Figure 4.3-4: PH Values for Regional Wells Completed in the Foremost Formation – Quarter 2, 2013.....	92
Figure 4.3-5: PH Values for Regional Wells Completed in the Foremost Formation – Quarter 3, 2013.....	93
Figure 4.3-6: PH Values for Regional Wells Completed in the Foremost Formation – Quarter 4, 2013.....	94
Figure 4.3-7: Piper Plot – 2012-2013 Groundwater Samples.....	95



1.0 INTRODUCTION

The purpose of the Shell Canada Limited (Shell) Quest Carbon Capture and Sequestration Project (the Project) is to capture up to 1.2 million tonnes (Mt) of carbon dioxide (CO₂) per year from the Scotford Upgrader, and to compress and then transport the CO₂ by pipeline to the proposed injection and storage facility located north of Scotford where it will be injected.

The cumulative injected mass of CO₂ is forecast to be 27 Mt over the 25-year projected life of the Project. To allow for verification of the storage performance and containment of CO₂ within the Basal Cambrian Sand (BCS) aquifer and the BCS storage complex, Shell submitted a pre-baseline Measurement, Monitoring and Verification (MMV) Plan for the Project on October 15, 2012 in accordance with AERCB Approval 11837A Conditions. The purpose of the MMV Plan is to develop a proactive verification program to ensure that the storage complex is operating as expected and to provide a verification of the absence of leaks. The MMV Plan outlines the Sequestration Lease Area (the Project area) (Figure 1-1) located north of Fort Saskatchewan, Alberta, Canada. To help achieve the objectives of the MMV Plan, a Hydrosphere and Biosphere Monitoring Program (HBMP) was developed to assess the variability of current environmental conditions before the CO₂ injection begins. The main purpose of the Biosphere portion of the HBMP program is to calibrate the remote sensing (satellite) data proposed to be used for monitoring during injection.

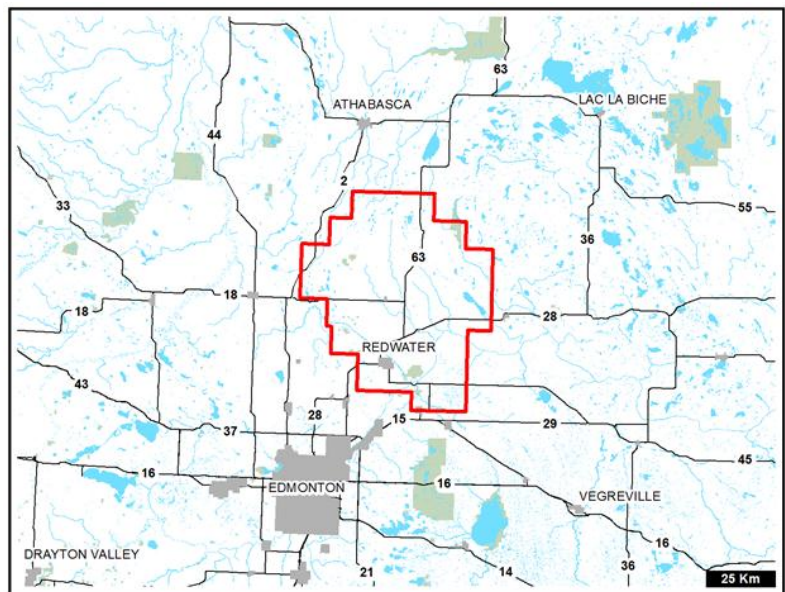


Figure 1-1: Project Location Map

From September 2012 to November 2013, Atmosphere and Biosphere field programs were conducted within the Project area to characterize pre-injection conditions based on a vegetation land classification for the Sequestration Lease Area. The programs included surveys of vegetation communities, spectral signatures, soil electromagnetic conductivity (EM38), soil CO₂, surface flux and soil assessment. The Hydrosphere field programs included sampling over 145 wells from Q4 2012 to Q4 2013 on five sampling events. This report outlines the sampling methodologies, field activities and results for each of these programs.

2.0 ATMOSPHERE

Measurements of atmospheric gas composition are required to understand the exchange of gases between the land and the atmosphere in the Shell Quest Project Area. The atmospheric gases of interest can vary spatially and temporally on diurnal, seasonal, and inter-annual time scales. Quantifying atmospheric gas concentrations as part of the HBMP requires the use of field instruments and/or laboratory methods with analytical accuracy greater than the observed or predicted natural variations in their concentrations. The following section outlines the methods and preliminary results from the measurements of atmospheric gases from fall 2012 to fall 2013.



2.1 Methods

Two types of atmospheric gas samples are being collected and analyzed as part of the Shell Quest HBMP. These types are discrete flask samples that are collected and sent off-site for laboratory analysis, and in situ real time measurements using a field deployable Greenhouse Gas Analyzer (GGA). The measured concentrations were also compared to a third independent dataset collected by Environment Canada, and analyzed by the United States National Oceanic and Atmospheric Administration's Earth System Research Laboratory (NOAA/ESRL).

2.1.1 Discrete Laboratory Atmospheric Samples

Discrete atmospheric samples were obtained using three different sampling media between fall 2012 and fall 2013. In fall 2012, six pre-evacuated 125 millilitre (mL) glass vials were used to collect each atmospheric gas sample. The glass vials were sent for offsite analysis by a commercial laboratory. High reportable detection limits, the inability to monitor glass vial vacuum before sampling, and the requisite use of sampling syringes necessitated the selection of an alternate sampling media and new commercial laboratory in 2013.

In spring, summer and fall 2013, discrete atmospheric samples were collected using three pre-evacuated 250 mL glass bottles. In summer 2013, laboratory samples returned anomalously high soil gas concentrations of carbon monoxide (CO), methane (CH₄) and C₁-C₇₊ hydrocarbons, as well as anomalously low concentrations of soil gas CO₂. These results indicated possible sample contamination.

In fall 2013, 1.4 litre (L) pre-evacuated SUMMA canisters were used to collect an additional atmospheric gas sample at each location. Results from sampling using glass bottles and SUMMA canisters are being compared in order to select the best sampling media for the HBMP in 2014 and beyond.

Each soil gas sample was analyzed by a commercial laboratory for the following compounds and isotopes:

- hydrogen (H₂), helium (He), oxygen (O₂), nitrogen (N₂), CO₂, CH₄, CO, hydrogen sulphide (H₂S);
- non-methane hydrocarbons (C₁ – C₇₊);
- halogenated hydrocarbons;
- stable carbon isotope ratios, δ¹³C of CO₂, and δ¹³C of CH₄; and
- stable hydrogen isotope ratio, δ²H of CH₄.

2.1.2 In Situ Atmospheric Measurements in Real Time

Atmospheric concentrations of carbon dioxide, methane and water vapour were measured in situ in real time using a Model 915-0011 ultra-portable Greenhouse Gas Analyzer (GGA) (Los Gatos Research, California). Though external calibrations are periodically required, the GGA instrument is typically accurate to within 1% over the following range of gas concentrations:

- CO₂: 0 to 200,000 parts per million by volume (ppmv);



- CH₄: 0 to 100,000 ppmv; and
- H₂O: 0 to 70,000 ppmv (0% to 100% relative humidity).

Atmospheric measurements were collected in spring, summer and fall 2013 at two elevations, 0.1 metres (m) and 1.0 m above the ground surface. A valve was used to alternate the sampling between tubing installed at the two elevations. Measurements were collected facing into the wind, and tubing was held in place by attaching it to a piece of rebar driven into the ground (Figure 2.1-1). Measurements were collected consecutively over two 300-second periods, and at a rate of 1 sample per second (1-hertz [Hz]). For each location, statistics including mean, median, standard deviation, minimum and maximum concentrations were calculated from the 1-Hz data.

Figure 2.1-1: Atmospheric Measurements of CO₂, CH₄ and H₂O

2.1.3 Independent Greenhouse Gas Measurements

The Global Monitoring Division of the United States National Oceanic and Atmospheric Administration's Earth System Research Laboratory (NOAA/ESRL) conducts sustained observations of atmospheric constituents that are capable of forcing change in the Earth's climate through a worldwide co-operative air sampling network. The measurements are considered of the highest quality and accuracy possible, and document global changes in key atmospheric gas species (NOAA 2013). Environment Canada collected, and NOAA/ESRL analyzed, flask samples for atmospheric CO₂ and CH₄ approximately bi-weekly at Lac La Biche, Alberta (54.9500°N, 112.45°W, 540 metres above sea level [masl]) beginning in January 2008. In January 2013 the flask sample collection program at Lac La Biche (LLB) was terminated by Environment Canada.

The next closest NOAA/ESRL vetted measurement station is at East Trout Lake, Saskatchewan (54.3501°N, 104.9834°W, 492 masl). Measurements of CO₂ and CH₄ at East Trout Lake began in October of 2005 and are ongoing. However, none of the East Trout Lake data are available via the NOAA/ESRL website.

Results of the measurements of atmospheric gases from the Shell Quest HBMP are compared to Environment Canada and NOAA/ESRL results from LLB using the full January 2008 to December 2012 data set.

2.2 Results

2.2.1 National Oceanic and Atmospheric Administration's Earth System Research Laboratory Results

The NOAA/ESRL measurements of greenhouse gases at LLB indicate that CO₂ concentrations in north-central Alberta can be expected to vary seasonally and interannually between approximately 370 and 430 ppmv (Figure 2.2-1). Atmospheric concentrations of methane also vary seasonally and diurnally between approximately 1.8 and 2.2 ppmv (Figure 2.2-2). Thus, techniques used to measure seasonal variations in atmospheric CO₂ require analytical accuracy at least greater than 2.5% (i.e., 10 ppmv), and preferably better than 1% (i.e., 4 ppmv). Techniques used to measure seasonal variations in atmospheric CH₄ require analytical accuracy at least greater than 5% (i.e., approximately 0.1 ppmv), and preferably better than 1% (i.e., 0.02 ppmv).



2.2.2 Discrete Laboratory Atmospheric Samples

The locations of discrete atmospheric samples collected for offsite laboratory analysis are summarized in Table 2.2-1. In fall 2012, a single sample was collected at injection well site IW-05-35. In spring 2013 no atmospheric sample was collected due to a miscommunication with the field technicians. In summer 2013 two discrete samples were collected; one at injection well site IW05-35, and one at vegetation plot site TP13-35a.

In fall 2013 four atmospheric samples were collected, two at each location. One glass bottle and one SUMMA canister sample were collected at injection well site IW07-11, and one glass bottle and one SUMMA canister sample were collected at vegetation plot site TP13-35a.

The chemical and isotope ratios for each of these discrete atmospheric samples are summarized in Table 2.2-2. The results are plotted graphically along with annual mean and plus/minus one standard deviation for the time series of the NOAA/ESRL data on Figure 2.2-1 (CO₂) and Figure 2.2-2 (CH₄).

The Reportable Detection Limit (RDL) for CO₂ in the fall 2012 atmospheric sample analyzed by a commercial lab was 100 ppmv; the accuracy of the estimate was unknown. Thus, the results were expected to be one of 300, 400 or 500 ppmv. The recorded concentration was 500 ppmv, well above the annual or interannual variability observed by NOAA/ESRL over a 6-year period. Partially due to this result, a new analytical laboratory with lower RDLs for CO₂ was sought for the 2013 program. In spring and summer 2013, the RDL for CO₂ analyzed by the new commercial laboratory was 10 ppmv. Carbon dioxide concentrations reported by the commercial laboratory for summer and fall 2013 ranged from 420 to 570 ppmv. These values are all greater than one standard deviation of the CO₂ concentrations measured by NOAA/ESRL for the LLB samples.

The reportable detection limit for CH₄ concentrations measured in the fall 2012 atmospheric sample was 10 ppmv. The reported methane concentration was expected, and observed, to be below the analytical method's RDL (Table 2.2-2). The elevated RDL for CH₄ necessitated the use of a new analytical laboratory, with lower reportable detection limits, for the 2013 HBMP. In spring and summer 2013, the RDL for glass bottle samples analyzed for CH₄ was 1.0 ppmv. As a result of the high RDL for methane, only four 2013 samples sent for laboratory analysis returned quantitative results (i.e., 2.0 to 2.3 ppmv). The fall 2013 atmospheric CH₄ concentrations are close to one standard deviation of the concentrations observed by NOAA/ESRL at the LLB site. During 2014, further work will be undertaken to assess measured versus expected atmospheric concentration data.

The results of the isotopic analysis for Shell Quest HBMP atmospheric gas samples are also summarized in Table 2.2-2. The $\delta^{13}\text{C}$ ratio for CO₂ for the Shell Quest laboratory samples ranged from -7.43‰ to -17.06‰. The range in these values is unusually high. There are no $\delta^{13}\text{C}$ measurements of atmospheric CO₂ at the LLB site. However, mean $\delta^{13}\text{C}$ ratio for atmospheric CO₂ (+/- 1 standard deviation) measured between January 2008 and December 2012 at the NOAA/ESRL Mauna Loa, Hawaii Observatory is -8.35‰ (+/- 0.31‰). The glass vial samples in fall 2012 (-9.06‰ and -9.36‰) are comparable to the fall SUMMA canister results (-7.43‰ and -9.66‰), and both differ significantly from the summer and fall glass bottle values (-10.23‰ to -17.06‰). The contrasting isotope results for the atmospheric samples potentially indicate fractionation of CO₂ is occurring while the samples are being held in the glass bottles, and/or that sample contamination may be occurring.

The concentrations of methane in the 2013 Shell Quest samples were too low for a reliable determination of the $\delta^{13}\text{C}$ ratio for CH₄ and the $\delta^2\text{H}$ ratio of CH₄. The mean and standard deviation of the monthly averaged $\delta^{13}\text{C}$ ratio for CH₄ recorded by NOAA/ESRL at LLB is -47.70 +/- 0.33‰ (January 2008 to December 2012).



2.2.3 In Situ Measurements in Real Time

The locations and number of atmospheric CO₂, CH₄ and H₂O measurements collected during the 2013 HBMP are summarized in Table 2.2-1. Two sample numbers are provided at each location because measurements were collected at 0.1 and 1.0 metres elevation above the ground surface. Each sample is the average of (typically) 300 seconds of data collected at a rate of 1-Hz.

The GGA instrument was acquired after the fall 2012 sampling event, but prior to spring 2013. As a result, there are no in situ measurements listed in fall 2012. Instrument failure in the field led to no in situ samples being collected at vegetation plot TP04-05 in either spring or summer of 2013. Measurements collected at 0.1 m elevation at vegetation site TP01-11 in spring 2013 were found to contain poor quality data during post-collection quality assurance and quality control. These data have been removed from further analysis.

Statistics summarizing the results for pooled *in-situ* atmospheric samples collected during the 2013 Shell Quest HBMP are provided in Table 2.2-3, and are separated by sample elevation (i.e., either 0.1 or 1.0 m above ground surface). Figure 2.2-1 and Figure 2.2-2 include the individual values of *in-situ* CO₂ and CH₄ concentrations measured using the GGA during the 2013 HBMP. Mean and one standard deviation of the results are plotted as open circles with whiskers. When compared to the 6-year NOAA/ESRL record for the corresponding period in 2013, the in situ HBMP results for CO₂ appear to be accurate and precise (Figure 2.2-1).

The concentration range over which the GGA instrument is expected to measure CH₄ to within an accuracy of 1% is 0 to 100,000 ppmv (i.e., 0.0000% to 10%). Compared to the mean concentrations measured by NOAA/ESRL, the HBMP results appear to be low by approximately 20% (spring and summer 2013) to 30% (fall 2013) (Figure 2.2-2). This difference may be due to errors in the methane calibration for the GGA instrument. A three-point calibration verification using Certified Master¹ grade (Praxair Canada Inc.) methane concentrations of 0.100, 10.0 and 20,000 ppmv is scheduled for January 2013.

Results from the in situ atmospheric gas measurements for the 2013 HBMP are plotted on Figure 2.2-3, Figure 2.2-4, and 2.2-5. In each plot the columns correspond to measurements at 0.1 m (left) and 1.0 m (right) elevation above the ground surface. Rows in each plot correspond to the spring (Q2), summer (Q3) and fall (Q4) 2013 measurements. The red line in each box plot corresponds to the median concentration, the box the 25th to 75th percentiles, the whiskers the 95% confidence interval of the arithmetic mean, and any red crosses are considered statistical outliers at $\alpha=0.05$.

In general, CO₂ concentrations were highest in spring, lowest in summer and intermediate in fall; observations consistent with the seasonal drawdown of CO₂ in Earth's Northern hemisphere. Median concentrations among the four land surface types were comparable in spring and fall, but differed in summer. Land under cultivation showed the lowest concentrations at both elevations, whereas CO₂ concentrations were highest in summer within broadleaf forests.

Methane concentrations were little changed between the spring and summer HBMP measurements, but were lowest in fall 2013. The NOAA/ESRL measurements indicate that CH₄ concentrations typically begin dropping in spring, are lowest in summer and begin climbing again in fall (Figure 2.2-1). Methane concentrations appear

¹ Routine calibration mixtures prepared by either gravimetric, volumetric or partial pressure methods and analyzed against US National Institute of Standards and Technology traceable reference materials.



somewhat higher at the cultivated sites in spring, but were comparable to CH₄ concentrations above other land surface types in summer and fall.

In situ concentrations of water vapour were highest in summer and lowest in the spring, consistent with water vapour's dependence on ambient air temperature. Water vapour concentrations appeared highest within the broadleaf forests in spring, but were highest above annual crops in summer. Little difference in water vapour was observed among the land cover types in fall.

Figure 2.2-1: Annual Trends in Atmospheric Carbon Dioxide

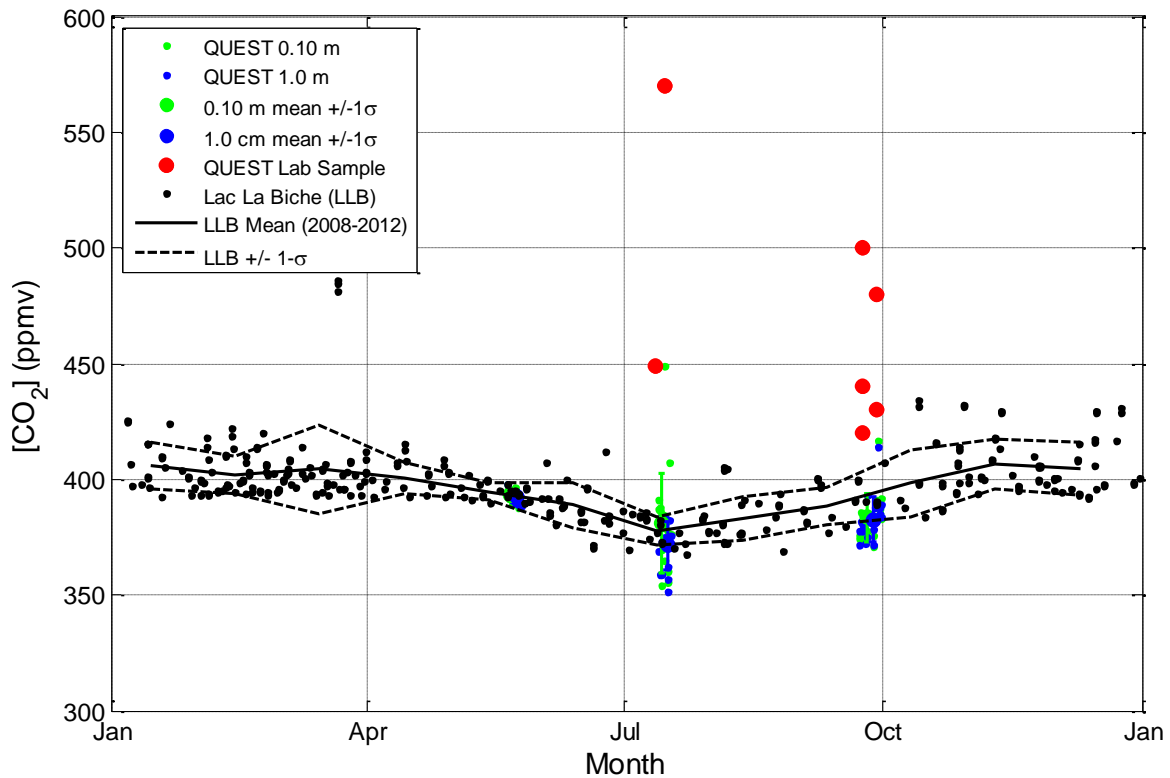
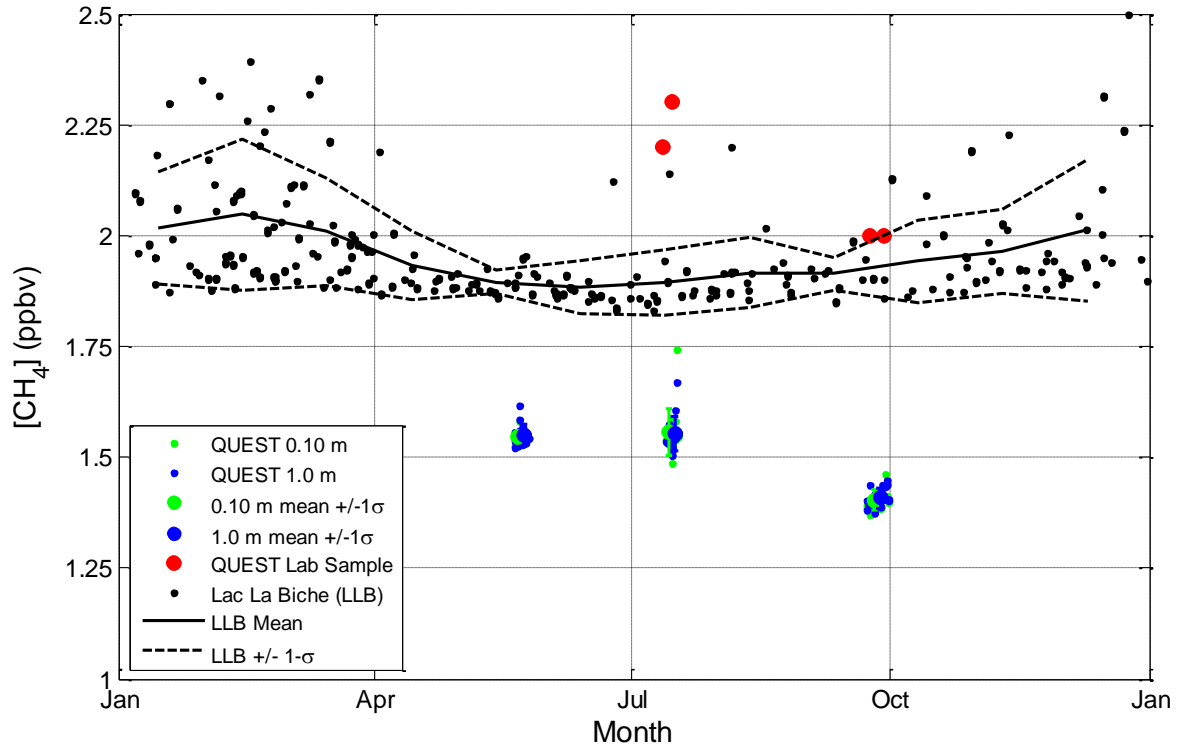




Figure 2.2-2: Annual Trends in Atmospheric Methane





2012-2013 HBMP SUMMARY REPORT

Table 2.2-1: Atmospheric Gas Sample Location and Number Summary

Sample Location ID	Fall 2012 (Q4)		Spring 2013 (Q2)		Summer 2013 (Q3)		Fall 2013 (Q4)	
	Laboratory Sample	In Situ Sample ^(a)	Laboratory Sample	In Situ Sample ^(a)	Laboratory Sample	In Situ Sample ^(a)	Laboratory Sample	In Situ Sample ^(a)
IW05-35	1	n/a	n/a	2	1	2	n/a	2
IW07-11	n/a	n/a	n/a	2	n/a	2	2	2
IW08-19	n/a	n/a	n/a	2	n/a	2	n/a	2
TP01-11	n/a	n/a	n/a	1	n/a	2	n/a	2
TP02-34	n/a	n/a	n/a	2	n/a	2	n/a	2
TP03-36a	n/a	n/a	n/a	2	n/a	2	n/a	2
TP03-36b	n/a	n/a	n/a	2	n/a	2	n/a	2
TP04-05	n/a	n/a	n/a		n/a		n/a	2
TP04-33a	n/a	n/a	n/a	2	n/a	2	n/a	2
TP04-33b	n/a	n/a	n/a	2	n/a	2	n/a	2
TP06-36	n/a	n/a	n/a	2	n/a	2	n/a	2
TP08-21	n/a	n/a	n/a	2	n/a	2	n/a	2
TP12-20	n/a	n/a	n/a	2	n/a	2	n/a	2
TP12-24	n/a	n/a	n/a	2	n/a	2	n/a	2
TP13-08	n/a	n/a	n/a	2	n/a	2	n/a	2
TP13-35a	n/a	n/a	n/a	2	1	2	2	2
TP13-35b	n/a	n/a	n/a	n/a	n/a	2	n/a	2
TP16-08	n/a	n/a	n/a	n/a	n/a	2	n/a	2

^(a) Sample numbers includes those collected at both 0.1 and 1.0 metre elevations.

n/a – not available.



2012-2013 HBMP SUMMARY REPORT

Table 2.2-2: Laboratory Results for Atmospheric Gases Measured at 1.0 meter Elevation

Sample Location ID	Sample ID	Sample Media	Sample Date	He ppm v	H ₂ ppm v	CH ₄ ppm v	CO ppm v	CO ₂ ppm v	O ₂ %	N ₂ %	H ₂ S ppm v	C1-C7+ ppmv	C1-C10+ ppmv	Halogenated C1-C7+ ppmv	d13C of CO ₂ ‰	d13C of CO ₂ ‰	d13C of CH ₄ ‰	d2 H of CH ₄ ‰
05-35	ATM01-0912	Glass Vial	9/23/2012	<10	<10	<10	n/a	500	21.830	78.120	<10	<100	n/a	n/a	-9.06	-9.36	b.d.	b.d.
05-35	ATM01-0713	Glass Bottle	7/17/2013	40	80	2.3	2.4	570	21.800	78.200	1.0	25.5	n/a	<5	-11.71	n/a	b.d.	b.d.
13-35a	ATM02-0713	Glass Bottle	7/14/2013	<10	130	2.2	12	449	21.200	78.700	<1.0	16.2	n/a	<5	-14.87	n/a	b.d.	b.d.
07-11	ATM01-0913	Glass Bottle	9/24/2013	40	70	2	8	420	21.700	78.300	<1.0	n/a	<10	n/a	-10.23	n/a	b.d.	b.d.
07-11	ATM01-0913	SUMMA	9/24/2013	10	20	<1	5	440	21.376	78.578	<1.0	n/a	<10	n/a	-7.43	n/a	b.d.	b.d.
13-35a	ATM03-0913	Glass Bottle	9/29/2013	40	60	2	<2	480	21.700	78.200	<1.0	n/a	<10	n/a	-17.06	n/a	b.d.	b.d.
13-35a	ATM03-0913	SUMMA	9/29/2013	<10	<10	<1	<2	430	21.760	78.198	<1.0	n/a	<10	n/a	-9.66	n/a	b.d.	b.d.

n/a = not applicable (i.e., not analyzed)

b.d. = below detection

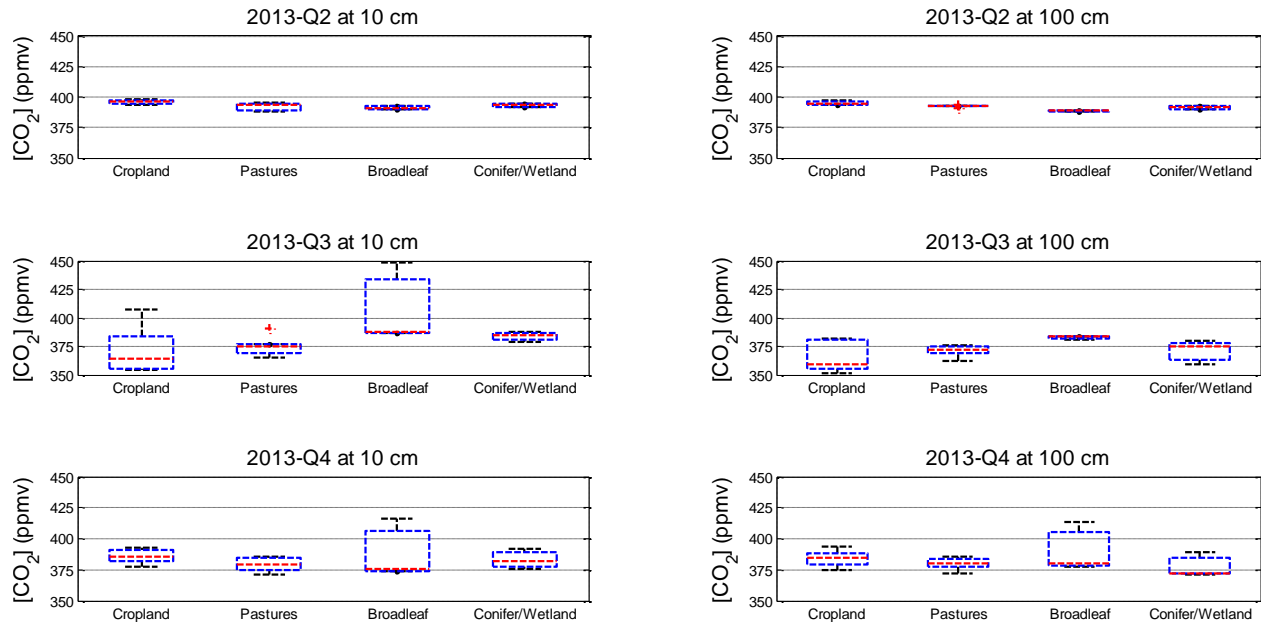
Table 2.2-3: In-situ Results for Atmospheric Gases Measured at 0.1 and 1.0 meter Elevations

Elevation	Summary Statistic	Spring 2013 (Q2)				Summer 2013 (Q3)				Fall 2013 (Q4)			
		Temp. (°C)	CO ₂ (ppmv)	CH ₄ (ppmv)	H ₂ O (ppmv)	Temp. (°C)	CO ₂ (ppmv)	CH ₄ (ppmv)	H ₂ O (ppmv)	Temp. (°C)	CO ₂ (ppmv)	CH ₄ (ppmv)	H ₂ O (ppmv)
(m)	-	(°C)	(ppmv)	(ppmv)	(ppmv)	(°C)	(ppmv)	(ppmv)	(ppmv)	(°C)	(ppmv)	(ppmv)	(ppmv)
0.1	mean	23.9	393.1	1.55	6923	24.9	380.9	1.56	14973	15.1	383.6	1.40	7684
	median	27.1	393.5	1.55	6355	25.0	377.6	1.54	14011	15.8	382.4	1.40	7604
	stdev	5.2	2.8	0.01	1664	4.8	21.6	0.05	3048	4.9	10.6	0.02	1117
1.0	mean	23.3	392.5	1.55	6343	24.3	371.6	1.55	11892	14.8	382.7	1.41	7597
	median	25.0	392.6	1.54	6344	23.1	374.8	1.54	11421	15.1	380.8	1.40	7183
	stdev	5.0	2.4	0.02	1449	4.9	10.4	0.04	1799	4.8	9.9	0.02	1489



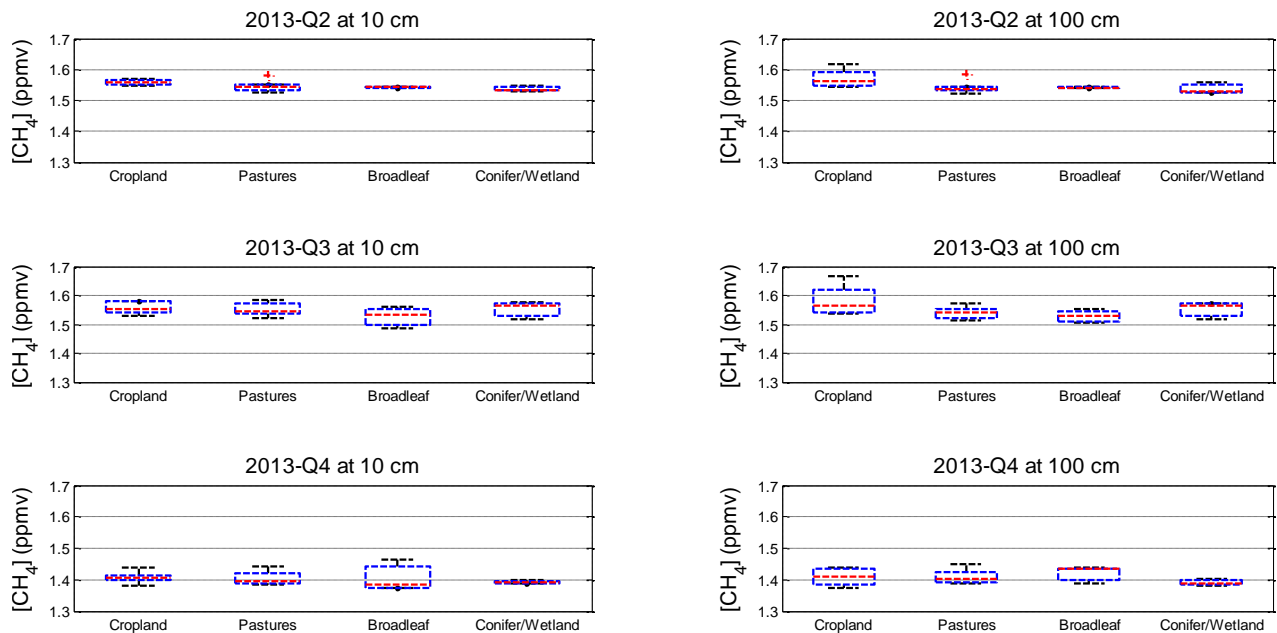
2012-2013 HBMP SUMMARY REPORT

Figure 2.2-3: Greenhouse Gas Analyzer Atmospheric Carbon Dioxide Concentrations by Sampling Event (rows), Sampling Height (columns) and Land Use Type (subplot-columns)



QUEST_ATM_6panelCO2_LandType.fig, 2013_AnnualReport_AnalysisFigures.m, CMc, 2013-11-08

Figure 2.2-4: Greenhouse Gas Analyzer Atmospheric Methane Concentrations by Sampling Event (rows), Sampling Height (columns) and Land Use Type (subplot-columns)

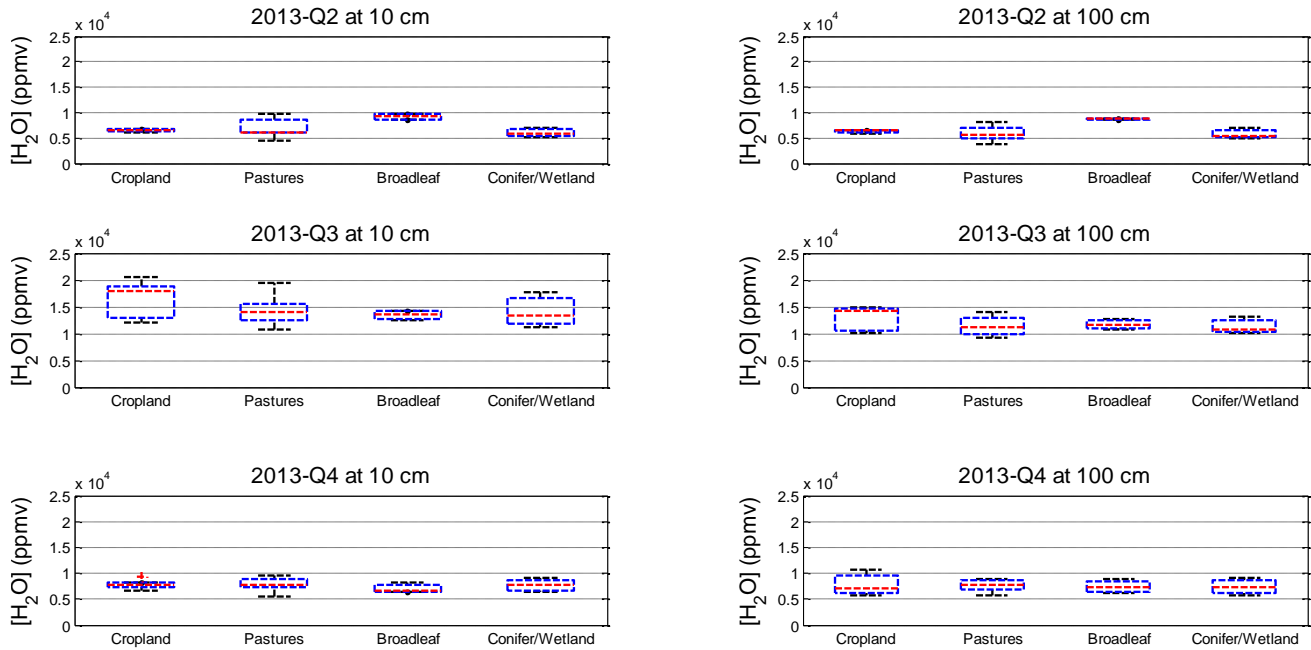


QUEST_ATM_6panelCH4_LandType.fig, 2013_AnnualReport_AnalysisFigures.m, CMc, 2013-11-08



2012-2013 HBMP SUMMARY REPORT

Figure 2.2-5: Greenhouse Gas Analyzer Atmospheric Water Vapour Concentrations by Sampling Event (rows), Sampling Height (columns) and Land Use Type (subplot-columns)



QUEST_ATM_6panelH2O_LandType.fig, 2013_AnnualReport_AnalysisFigures.m, CM*c, 2013-11-08



2.3 Summary of Key Findings

Key findings related to sampling methods for atmospheric gases sampled during the 2013 Shell Quest HBMP include the following:

- Reportable detection limits of less than 10 ppmv for CO₂, and of less than 1.0 ppmv for CH₄, are required for the quantification of the atmospheric concentrations of these gases.
- Analytical accuracy of better than 2.5% (i.e., approximately 10 ppmv), and preferably better than 1% (i.e., approximately 4 ppmv), is required for measurements of atmospheric CO₂.
- Analytical accuracy of better than 5% (i.e., approximately 0.1 ppmv), and preferably better than 1% (i.e., approximately 0.02 ppmv), is required for the measurement of atmospheric CH₄.
- High concentrations of CO and non-methane hydrocarbons together with low concentrations of CO₂ in glass bottle samples collected in summer 2013 indicate possible sample contamination.
- Unusual enrichment in $\delta^{13}\text{C}$ of CO₂ from atmospheric samples collected in glass bottles in summer and fall 2013 suggest that the integrity of the sample bottles may have been compromised during those field campaigns.

Key scientific findings from the 2013 Shell Quest HBMP include the following:

- Commercial laboratory results for discrete samples of atmospheric gases are biased high compared to the NOAA/ESRL measurements at Lac La Biche, Alberta.
- In situ measurements of atmospheric CO₂ using a portable greenhouse analyzer were both accurate and precise compared to NOAA/ESRL measurements at Lac La Biche, Alberta.
- In situ measurements of atmospheric CH₄ using a portable greenhouse analyzer were precise, but were biased low compared to NOAA/ESRL measurements at Lac La Biche, Alberta. Planned external calibration of the GGA in January 2013 could eliminate the CH₄ discrepancy.
- Atmospheric CO₂ concentrations in the Project area were highest in spring, lowest in summer and intermediate in fall.
- Median CO₂ concentrations among the four land surface types were comparable in spring and fall, but showed significant differences in summer.
- In summer, land under cultivation showed the lowest CO₂ concentrations at both elevations, whereas broadleaf forests showed the highest concentrations.
- CH₄ concentrations were little changed between the spring and summer, and were lowest in fall 2013.
- CH₄ concentrations appear somewhat higher at the cultivated sites in spring, but cultivated sites CH₄ concentrations were comparable to concentrations above other land surface types in summer and fall.



3.0 BIOSPHERE

The biosphere program is responsible for collection, processing and analysis of baseline environmental data to calibrate the remotely sensed imagery and characterize pre-injection environmental conditions. There are five components involved in the biosphere program: vegetation, soils, soil conductivity (EM38), soil gas and surface flux, and remote sensing. Each of these components' data were built around a regional land classification developed for the Shell Quest Carbon Capture and Storage Project. Seasonal data are collected three times a year for each component in conjunction with a scheduled satellite flyover. The following sections describe the development of the land classification, the field plot selection and design, the methodology, and a brief summary of the results for each component. Results presented in the following sections represent data collected during the September 2012, May 2013, July 2013, and September 2013 field programs.

3.1 Land Classification

Land cover classification was conducted using 2011 Landsat 5 satellite imagery to identify the dominant land cover classes in the Project area, and establish a representative distribution of vegetation plots to be used in this Project. An object-oriented image analysis approach was used for the classification. This two-step process segments the image into many polygons (or "objects") depending on the values of the pixels in the image, their "groupings", and relative location to each other. Once the objects are generated, they are assigned class values based on spectral, relational and contextual indicators by an analyst using knowledge of the land cover and available field data. Using this approach, seven classes were identified within the Project area (Table 3.1-1). The classification was assessed for accuracy using a subset of 39 field points and 11 points identified from visual interpretation of the imagery. Based on these 50 points, the overall classification accuracy was calculated to be 87.2%. This classification was conducted on Landsat 5 imagery due to the unavailability of sufficient RapidEye scenes at the time. However, a more detailed classification, employing the same methods, is currently being finalized using summer 2013 RapidEye imagery, and will be verified using field data collected in the Project area with the May, July and September 2013 field programs.

Table 3.1-1: Summary of Land Cover and Plot Distribution Within the Project Area

Class	Area [ha]	Percentage of Total Project Area	Number of Field Plots (2013)	Percentage of Field Plots (2013)
Annual Crop	132,400	34.8%	5	33.3%
Broadleaf Forest	86,700	22.8%	3	20.0%
Pasture	85,300	22.5%	3	20.0%
Coniferous Forest	37,400	9.8%	2	13.3%
Wetland	27,000	7.1%	2	13.3%
Developed	6,500	1.7%	0	0%
Water	4,600	1.2%	0	0%
Total	380,000	100.0%	15	100.0%

An overview of the land classification is provided on Figure 3.1-1 and detail maps for each of the plots are provided in Figure 3.1-2 to Figure 3.1-4.



2012-2013 HBMP SUMMARY REPORT

Figure 3.1-1: Land Classification

